H_∞ Control of Acoustic Noise

by

Janet R. Grad

A thesis
presented to the University of Waterloo
in fulfilment of the
thesis requirement for the degree of
Doctor of Philosophy
in
Applied Mathematics

Waterloo, Ontario, Canada, 1997

The University of Waterloo requires the signatures of all persons using or photocopying this thesis. Please sign below, and give address and date.

Abstract

The application of H_∞ control techniques to study global acoustic noise reduction in a one-dimensional duct is considered. The acoustic problem is formulated as an unbounded control system on an infinite-dimensional Hilbert space. A sequence of approximating finite-dimensional control systems is shown to converge to the solution of the well-posed infinite-dimensional problem under certain conditions. The finite-dimensional control problem is solved using Nevanlinna-Pick interpolation. The question of the achievable level of global acoustic noise reduction in the one-dimensional duct is then addressed. Both feedback and feedforward design are examined. Optimal placement of the controller actuator location and controller sensor location is discussed, as well as the effect of the number and location of performance points in relation to the actuator and sensor. Numerical results indicate that uniform stabilizability of approximations is not necessary for controller design. Results also indicate that behaviour of the zeros of the approximations, as well as the poles, is important for H_∞ controller design.

Acknowledgements

I would like to thank Dr. Kirsten Morris for many years of support, enthusiasm, many enlightening discussions, and for always encouraging me and allowing me to speak my mind. I would also like to thank the readers of this thesis, Dr.'s Chun-ming Wang, David Wang, Stanley Lipshitz, and Peter Forsyth, for their interesting comments and suggestions. I am also extremely grateful to Dr. Joseph Paldus for providing me with wonderful computing resources, without which I'd surely still be waiting for some results.

Some odd years ago, I hopped into my little Horizontal, drove from Manitoba, down the 401, and into Waterloo. I then ventured into the the Math Building and so began, unknown to me at the time, years of many headaches and tears and long phone calls home, but also much laughter and great times with some people I will never forget. Debbie, you've been an amazing officemate. I hope your next officemate curls, isn't prone to spaz-attacks, and doesn't smell. Nat, you've been a great friend and my reality check. I'll keep on passing out naked in public places if you keep up with the broom closet stories. Ada, oh great provider of yummy goodies, boy did we have some lovely discussions on stuff I will never mention on the beach. Jason, thanks for being my Coffee Buddy. Erik and Ryan, my happy dance is better than your happy dance! Serge, you're nowhere close to being a turd. Rhonda, don't you think our hair looks great?! May, thank you for walking through the Waterloo years with me. I would also like to thank the awesome people at Tim's, the Second Cup, Blue Dog, the makers of Strongbow, and whoever built my favourite place in Waterloo, the Grad House patio. Here's to goobers, nutcases, weirdos, muppets, cows, and rice-crispies.

I would like to run out to the parking lot and thank my little Horizontal for "making it" and my nice mechanic for keeping her happy. Of course, the nice mechanic doesn't accept peanuts, so I must thank my Dad for ultimately keeping Horizontal purring like a kitten. When Horizontal's happy, I feel good and the world is mine. Thanks to my sister Anna for, once upon a time, learning her multiplication tables and for providing me with sundried tomatoes. Kelvin, how's this for grabbing a life? Denise, you will always always be my pal.

Wiesia, thank you for listening to me go on and on and never once failing to make me feel better about everything. Thanks to you, I will always be my same "gum-dropping" self.

Mom, you watched me choose my path and then followed me with both ears always ready, a cup of tea, and some truly huge care-packages. I hope I didn't give you an ulcer. Guess what? Not only have I crossed the back lane, but I'm also eating those crabapples!

Dear Lord:

So far today, God, I've done all right.
I haven't gossiped, haven't lost my temper,
haven't been greedy, grumpy, nasty,
selfish, over-indulgent, coveted my neighbor's
spouse or taken your name in vain.

I'm very thankful for that.

But, in a few minutes, God,
I'm going to get out of bed.
And from then on, everyone
that I encounter will probably
need a lot of help from you.

Amen

Contents

List of Figures

List of Tables

Chapter 1

Introduction

Acoustic noise is a source of pollution that has unfavourable effects on people. Passive noise control has been shown to be effective at frequencies higher than 500 Hertz (e.g., [TL92]). Unfortunately, passive noise control techniques such as the use of sound absorbers do not work well at lower frequencies. For lower frequencies, active noise control techniques are required. This is because the wavelength of the acoustic wave becomes large compared to the dimension of the absorptive material. Furthermore, adding material for sound absorption increases the weight. This is especially of concern when designing noise control systems for airplanes and automobiles.

An active noise control system generally consists of one or more control speakers (sources of sound) driven by a signal determined by the undesirable acoustic noise measured through sensors and processed by a controller. The waves are superimposed and destructively interfere with each other to produce a reduction in noise. This concept is of increasing interest in a variety of applications such as noise reduction in air conditioning ducts, airplane cabins, the interior of automobiles, as

well as exterior exhaust and motor noise.

Active noise control systems have been studied since the 1930's. In 1936, Lueg (referred to by [EN93] and [TL92]) first described the basic concepts of active noise control. In 1953, Olson and May (referred to by [EN93] and [TL92]) introduced an "electronic sound absorber". In this paper, Olson and May proposed applying the effect of noise cancellation at a microphone to create a quiet area in an enclosed space. Both Tokhi and Leitch [TL92] and Nelson and Elliott [NE92] give extensive historical reviews of the development of active noise control.

Over the last 25 years, a number of different noise suppression techniques have been developed. Several examples referred to by Tokhi and Leitch [TL92] include the work of Swinbanks in 1973, Roure in 1985, Manjal and Eriksson in 1988, and Elliott and Nelson in 1987. Tokhi and Leitch [TL92] provide a detailed account of the research undertaken to date. The controller techniques in these past studies have not used classical feedback control theory. Instead adaptive filters have been used to reduce acoustic noise. Adaptive systems modify their characteristics in an attempt to conform to changing properties of signals and systems. In other words, an adaptive controller is one that is capable of "self-tuning" itself. In essence, design of a self-tuning controller involves recursive parameter estimation based on the current input and output to the system.

However, as already noted, these approaches do not fully explore the applicability of modern feedback control theory. In particular, these techniques have no systematic analysis of the closed loop stability and performance. As a result, in more recent years, attempts have been made at incorporating modern control techniques in acoustic noise reduction design. Hull *et al.* [HRS93] use a pole placement feedback control algorithm to reduce noise levels. Pole placement modifies the eigenstructure of the system to increase the dissipation in the duct and attenuate duct noise.

Hu [Hu95] [Hu96] undertakes a complete analysis of the transfer function and then uses the internal model principle in the controller design. This approach requires an accurate internal model of the noise (for example, the frequency) and can also only deal with narrow-band noise. Another approach is to consider "optimal" controller design using linear quadratic control theory. Hong *et al.* [HAV+96] use feedback control and linear quadratic Gaussian (LQG) synthesis to study the acoustic noise reduction problem with a single input and a single output. In recent years, more attention has been given to applying "smart materials" to control acoustic noise in a cavity. In a paper by Banks, Fang, Silcox, and Smith [BFSS91], piezoceramic patches embedded in a beam are used to excite the beam and produce bending moments which lead to acoustic noise reduction in the adjacent cavity. Banks, Demetriou, and Smith [BDS97] also study two-dimensional structural acoustic systems and the use of coupling effects between two adjacent media. In these latter two cases, the authors employ an "optimal" controller design approach by solving a linear quadratic regulator (LQR) problem.

In this thesis, we consider a different approach to solving the problem of achievable noise reduction. The problem of acoustic noise reduction can be expressed as the problem of minimizing the transfer of acoustic energy through the application of some controller. This method is known as H_∞ controller design. We shall use this concept to formulate the problem of acoustic noise reduction in a duct.

The duct is the simplest acoustic cavity that we may consider. If the cross-section of a three-dimensional duct is small compared to the wavelengths of interest, then we may think of this three-dimensional duct or cavity as being a one-dimensional duct. Studying a problem involving a one-dimensional duct is beneficial since the problem is simple enough that both theoretical and numerical analysis is possible. To explore the advantage of feedback control in active sound cancellation, we need

an appropriate model that describes the dynamics of the duct and completely qualifies the interaction between the noise in the duct and cancellation signal. Most importantly, we need a transfer function that shows the system zeros, which, as we shall see, are important in designing feedback controllers.

Acoustic noise is best modeled using partial differential equations. These equations are just one example of *infinite-dimensional* systems. We shall attempt to use the infinite-dimensional model rather than a *finite-dimensional* approximation since it better represents the dynamics of the system, and therefore provides more accurate results in the controller design.

It seems logical that an infinite-dimensional controller could be used to stabilize an infinite-dimensional system or *plant*, or to achieve certain performance specifications. The difficulty in this approach is in the design and implementation of such a controller. The other approach is to approximate the plant by a finite-dimensional system, and then to design a controller using this approximation. The initial benefit of such a design strategy is the usefulness of the large wealth of theory and software that exists for such systems. However, by introducing finite-dimensional approximations we open the door to questions of convergence of the approximations to the exact solution, as well as to problems of determination and appropriateness of the approximations to the plant. It is well known that zeros in the transfer function of a plant play an important role in the controller design and achievable performance. Therefore, the chosen approximations must somehow represent the zeros of the original infinite-dimensional system. We consider in some detail the question of what makes one approximating scheme better than another. We keep in mind that any methodology or strategy should be practical when extended to acoustic noise reduction in a three-dimensional cavity.

We also address the following question: Is it possible to reduce acoustic noise

everywhere in an enclosure by applying a feedback controller at a finite number of sensing points? This is the problem of *global* noise reduction. In particular, we consider the one-dimensional duct with one noise disturbance and one sensor, where the noise is measured and used in the controller design. The controller produces some controller signal which is introduced to the duct at some actuating point. Now suppose there are m performance or observation points in the duct at which we would like to reduce the noise level. This leads to a "tall" problem where the number of outputs (m) of our system is greater than the number of inputs (one in this case). This problem is numerically sensitive and not easily solved. The tall problem H_∞ optimal control problem is solved exactly, hence providing results on the optimal placement of sensors and actuators for global noise reduction.

Chapter 2

The One-Dimensional Duct

Acoustics is the general name given to the study of the production, transmission, effect, and control of sound. Sound, on the other hand, is the impression left by energy transmitted by longitudinal pressure waves. These waves are modeled using the wave equation. Realistically, the acoustic response in an enclosure may be a combination of standing and propagating wave components, caused by some non-idealized partially reflective / partially absorptive boundary condition. Physically, a partially absorptive boundary would allow acoustic waves to pass through the boundary. A partially reflective condition would allow some acoustic energy to be dissipated through the boundary while the remainder of the energy is reflected back into the enclosure or cavity. This would create both standing and propagating waves.

The simplest cavity we consider is the one-dimensional duct. Studying this problem is constructive since it is simple enough that both theoretical and numerical analysis is possible. In addition, we may think of the duct as modeling a long and narrow cavity so that it is also physically realistic and important in applications.

$z(x,t)$	particle displacement (m)
x	position of the particle along the duct (m)
t	time (s)
L	length of duct (m)
c	wave speed (m/s)
ρ	density of the medium in the duct (kg/m^3)
x_d	position where the disturbance is applied $(0 \leq x_d \leq L)$
x_s	position where the pressure is sensed or measured and fed back through the controller $(0 \leq x_s \leq L)$
x_a	position where the pressure generated by the controller is applied to duct $(0 \leq x_a \leq L)$
$P_c(t)$	control pressure applied at $x = x_a$
$P_d(t)$	disturbance pressure applied at $x = x_d$

Table 2.1: One-dimensional duct: variable definitions

2.1 Modeling

2.1.1 Time Domain

The system model we use is as follows [Doa73a], [Doa73b], [HRMM90], [HAV+96].

All variable definitions are given in Table 2.1. Suppose we have a duct of length L (m). The partial differential equation governing the motion of waves in the duct is given by

$$\frac{\partial^2 z}{\partial t^2}(x,t) = c^2 \frac{\partial^2 z}{\partial x^2}(x,t) + \delta(x - x_a)\frac{P_c(t)}{\rho} + \delta(x - x_d)\frac{P_d(t)}{\rho} \tag{2.1}$$

with zero initial conditions

$$z(x,0) = 0, \quad 0 \leq x \leq L$$
$$\frac{\partial z}{\partial t}(x,0) = 0, \quad 0 \leq x \leq L.$$

Assume that all forces and measurements in the duct are pressure. The term "$\delta(x - x_a)\frac{P_c(t)}{\rho}$" represents a control pressure $P_c(t)$ applied at the point $x = x_a$ in the duct. Similarly, the term "$\delta(x - x_d)\frac{P_d(t)}{\rho}$" represents point application of a disturbance pressure $P_d(t)$ at $x = x_d$. Assume that we are modeling a hard-walled duct so that there is dissipation only at the ends of the duct. In addition, assume that there is no mean flow in the duct and air viscosity is negligible.

Consider a completely reflective end at $x = 0$, so that

$$\frac{\partial z}{\partial x}(0,t) = 0. \tag{2.2}$$

At $x = L$, consider a partially reflective boundary condition. By conservation of mass, we find that this condition is a relationship between the spatial gradient and the time gradient of the wave displacement. Let $K \in \mathbb{R}$ be the impedance of the end (dimensionless). Then the boundary condition may be expressed as [SR88]

$$\frac{\partial z}{\partial x}(L,t) = -\frac{K}{c}\frac{\partial z}{\partial t}(L,t), \quad K \neq 0, \ 1, \ \infty. \tag{2.3}$$

When K is zero or infinity, the end of the duct reflects all the acoustic energy and the acoustic response in the duct is composed only of standing waves. When $K = 1$, the end of the duct absorbs all the acoustic energy and the acoustic response in the duct is composed only of propagating waves. All other values of K result in some combination of standing and propagating waves. The value of K is associated with energy dissipation. Experimental evidence in [HR92] and [SR88] supports this choice of boundary condition.

In addition, the acoustic pressure $P(x,t)$ at some point $0 \leq x \leq L$ and time $t \geq 0$ is related to the spatial gradient of the wave displacement by (given in [Set71], referred to in [HRS93])

$$P(x,t) = -\rho c^2 \frac{\partial z}{\partial x}(x,t).$$

2.1.2 Frequency Domain: The Transfer Function

Taking the Laplace transform of equations (2.1), (2.2), and (2.3), and assuming zero initial conditions we obtain,

$$s^2 \hat{z}(x,s) = c^2 \frac{\partial^2 \hat{z}}{\partial x^2}(x,s) + \delta(x - x_a)\frac{\hat{P}_c(s)}{\rho} + \delta(x - x_d)\frac{\hat{P}_d(s)}{\rho}, \tag{2.4}$$

$$\frac{\partial \hat{z}}{\partial x}(0,s) = 0, \tag{2.5}$$

and

$$\frac{\partial \hat{z}}{\partial x}(L,s) = -\frac{K}{c} s \hat{z}(L,s) \tag{2.6}$$

where

$$\begin{aligned} \hat{z}(x,s) &= \mathcal{L}(z(x,t)), \\ \hat{P}_c(s) &= \mathcal{L}(P_c(t)), \\ \hat{P}_d(s) &= \mathcal{L}(P_d(t)). \end{aligned}$$

The solution to (2.4) with $\hat{P}_c(s) = \hat{P}_d(s) = 0$ is

$$\hat{z}(x,s) = Ae^{\frac{xs}{c}} + Be^{-\frac{xs}{c}} \tag{2.7}$$

for $A,\ B \in \mathbb{R}$. Define $\alpha = \frac{1+K}{1-K} \in \mathbb{R}$, where $1 < |\alpha| < \infty$.

In the duct, we have possible forces applied at x_a and x_d, and possible measurements at x and x_s. Let $P(x,s)$ (or simply $P(x)$) indicate the Laplace transform of pressure $P(t)$ applied at x. Since it is obvious whether a function is in the time or frequency

domain, the hats over all frequency domain functions are dropped. Let $G(x_1, x_2)$ be the transfer function relating the pressure measured at x_1 to the pressure applied at x_2, so that

$$\frac{P(x_1)}{P(x_2)} = \frac{\text{pressure at } x_1}{\text{disturbance pressure at } x_2} = G(x_1, x_2).$$

Solving for the Green's function of (2.4), (2.5), and (2.6) [Hu95] [YT92] we find

$$G(x_1, x_2) = \begin{cases} e^{\frac{s}{c}(x_1 - x_2)} \left(\frac{e^{\frac{2s}{c}(x_2 - L)} + \alpha}{e^{-\frac{2s}{c}L} - \alpha} \right) \left(\frac{1 - e^{-\frac{2s}{c}x_1}}{2} \right), & x_1 < x_2 \\ e^{\frac{s}{c}(x_2 - x_1)} \left(\frac{e^{\frac{2s}{c}(x_1 - L)} - \alpha}{e^{-\frac{2s}{c}L} - \alpha} \right) \left(\frac{1 + e^{-\frac{2s}{c}x_2}}{2} \right), & x_1 > x_2. \end{cases} \tag{2.8}$$

We will use this transfer function to formulate the problem of minimizing noise in the duct.

2.2 Stability

Control systems are designed to meet certain performance specifications. We would like to formulate a control problem that gives us a formal definition of what we mean by acoustic noise reduction. Before doing so, we first provide a brief review of some important background concepts in feedback control theory.

2.2.1 Definitions

Consider the basic feedback configuration in Figure 2.1. The plant being controlled is represented by its transfer function $G(s)$ and the controller by its transfer function $C(s)$. The signals labeled in Figure 2.1 have the following interpretations:

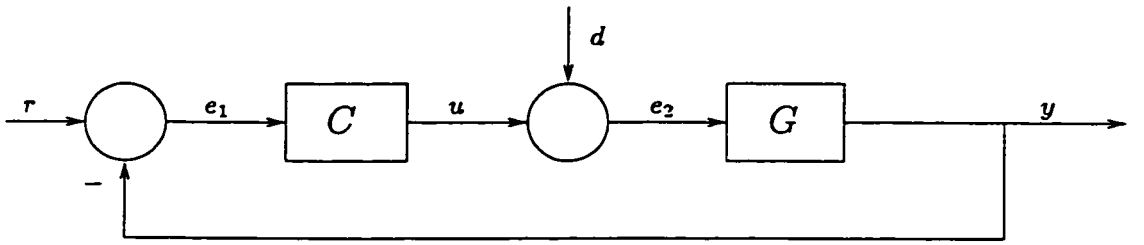

Figure 2.1: Basic feedback control system

r - reference input

u - actuating signal or plant input

d - external disturbance

y - plant output.

We consider only linear time-invariant systems. As well, the energy of all signals is assumed to be finite, i.e., all signals belong to $L_2[0,\infty)$. These signals are called *L_2-stable.*

Definition 2.1

A system is L_2-stable if inputs $u \in L_2[0,\infty)$ map to outputs $y \in L_2[0,\infty)$. Furthermore, there is a maximum ratio

$$\sup_{u \neq 0} \frac{\|y\|_2}{\|u\|_2} < \infty. \tag{2.9}$$

This is called the L_2-gain.

Thus, $G(s)$ is stable if the maximum energy amplification from all finite energy input signals u to all output signals y is finite.

Definition 2.2 *(H_∞ transfer functions)*

The Hardy space H_∞ consists of all complex-valued functions $F(s)$ which are analytic and bounded in the right half plane, $\Re(s) > 0$. The H_∞ norm of $F(s)$ is the least such bound; that is,

$$\|F\|_\infty = \sup_{\Re(s)>0} |F(s)| < \infty.$$

Theorem 2.1 *(e.g., [Fra87])*

The maximum energy amplification in (2.9) is the norm of $G(s)$, i.e.,

$$\sup_{u\neq 0} \frac{\|y\|_2}{\|u\|_2} = \|G\|_\infty.$$

Thus, H_∞ can be thought of as the set of all stable transfer functions.

The H_∞ norm of a system represents a physically meaningful quantity, namely the ratio of the energy of the output signal over the energy of the input signal.

Example We shall show that the transfer function for the one-dimensional duct (2.8) is in H_∞. We first find the poles of $G(x_s, x_a)$ and show that the function is analytic in the right half plane. We then show that $G(x_s, x_a)$ is bounded in the right half plane.

The poles of $G(x_s, x_a)$ are solutions of

$$e^{-\frac{2sL}{c}} - \alpha = 0.$$

This implies the poles are

$$p_n = -\frac{c}{2L}[\ln \alpha + 2n\pi\jmath], \quad n = 0, \pm 1, \pm 2, \ldots. \tag{2.10}$$

Since $1 < |\alpha| < \infty$, the poles of $G(x_s, x_a)$ lie in the left half plane. Therefore $G(x_s, x_a)$ is analytic in the right half plane. Now, obviously, $G(x_s, x_a)$ is bounded on closed, bounded subsets in the right half plane. All exponential terms have negative real parts for $\Re(s) > 0$. Since $|\alpha| > 1$, it follows that $G(x_s, x_a)$ is uniformly bounded in the right half plane. Thus, $G(x_s, x_a) \in H_\infty$.

Definition 2.3 *(Closed Loop Stability)*

The transfer functions from the exogenous inputs r and d to the outputs of the summing junctions e_1 and e_2 are given by

$$\begin{bmatrix} e_1 \\ e_2 \end{bmatrix} = \frac{1}{1+GC} \begin{bmatrix} 1 & -G \\ C & 1 \end{bmatrix} \begin{bmatrix} r \\ d \end{bmatrix}.$$

The feedback system is closed loop stable if and only if all four of these transfer functions are in H_∞.

We now introduce a method of parametrizing the set of all possible controllers C for which the feedback system in Figure 2.1 is stable.

Theorem 2.2 *(e.g., [Vid85, page 364])*

Let $G(s) \in H_\infty$. The set of all controllers C for which the feedback system (Figure 2.1) is stable is

$$\left\{ \frac{Q}{1-GQ} : Q \in H_\infty \right\}.$$

The function $Q(s)$ is known as the *Youla* parameter. Since any $Q \in H_\infty$ yields a stable closed loop, Q is free to be chosen so that performance specifications are satisfied.

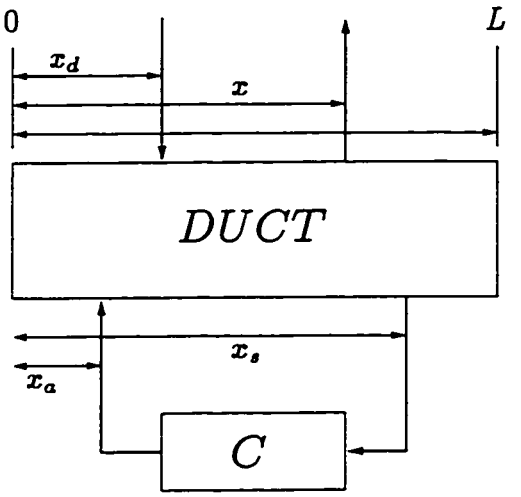

Figure 2.2: One-dimensional duct with controller

2.3 Simple Control Problem

Consider the duct and controller configuration in Figure 2.2. A basic control problem can be stated as follows.

> Given a disturbance at x_d and a measurement at x_s, can we determine the best control pressure to be applied at x_a so that the effect of the disturbance is minimized at some arbitrary location x?

The plant we are controlling has transfer function $G(x_s, x_a)$. When $x_s > x_a$, we say the system is a *feedback* system (since the output at x_s is further away from $x = 0$ than the input at x_a). Similarly, when $x_s < x_a$, we say the system is a *feedforward* system. Both systems are illustrated in Figure 2.3.

The pressure $P(x)$ at an arbitrary location x is due to the disturbance P_d and the control pressure P_c. (Here we are working entirely with Laplace transforms, and

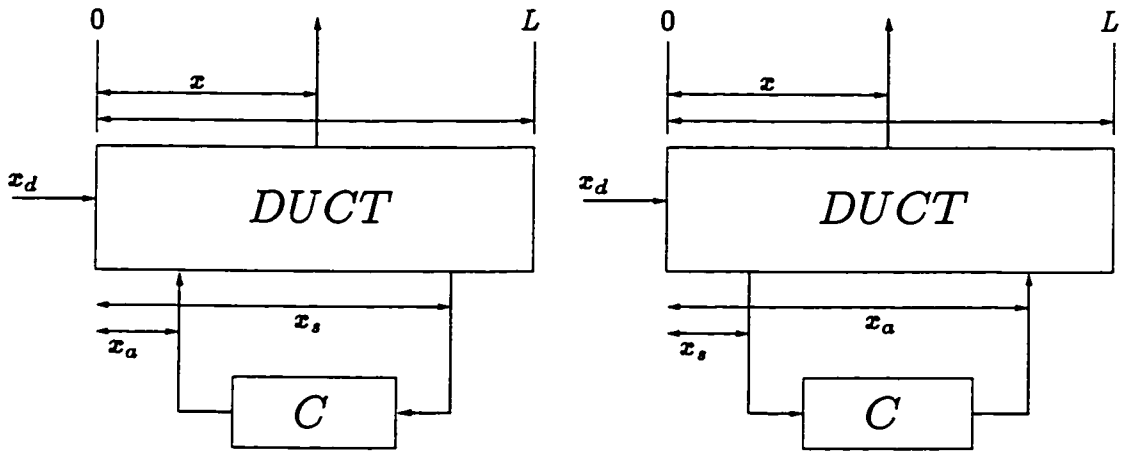

(a) Feedback (b) Feedforward

Figure 2.3: Feedback and feedforward systems

so the $\hat{\cdot}$ notation is not used.) Suppose all disturbance signals are in $L_2[0,\infty)$. The L_2-gain γ between the norm of the output $P(x)$ and the disturbing P_d is the maximum ratio such that

$$\|P(x)\|_2 \leq \gamma \|P_d\|_2.$$

To minimize this gain over all frequencies in some range we find the infimum of

$$\left\| W_1 \frac{P(x)}{P_d} \right\|_\infty \tag{2.11}$$

over all stable, stabilizing controllers. At higher frequencies, acoustic noise may be effectively suppressed using passive methods [TL92]. We therefore design the controller to reduce the response to low frequencies. We choose the simplest low pass weighting function

$$W_1(s) = \frac{1}{1 + s/\omega_c}$$

where ω_c is the cut-off frequency.

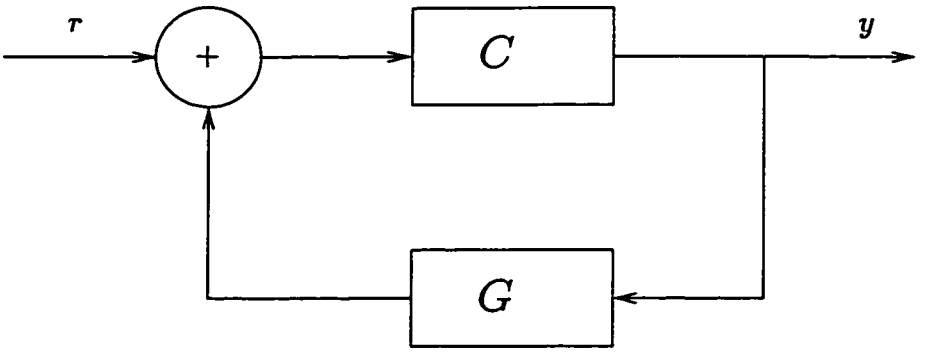

Figure 2.4: Block diagram of simple duct control system

We now calculate $P(x)$ explicitly. Consider the block diagram in Figure 2.4. Suppose C is stabilizing. Then

$$\frac{y}{r} = -Q$$

for some $Q \in H_\infty$. Also,

$$\frac{y}{r} = \frac{C}{1 - CG}.$$

Now,

$$P(x) = G(x, x_d)P_d + G(x, x_a)P_c \tag{2.12}$$

and

$$P_c = CG(x_s, x_d)P_d + CG(x_s, x_a)P_c$$

so

$$P_c[1 - CG(x_s, x_a)] = CG(x_s, x_d)P_d$$

which yields

$$P_c = \frac{CG(x_s, x_d)}{1 - CG(x_s, x_a)}P_d. \tag{2.13}$$

We need a controller C so that the closed loop due to feedback from x_a to x_s is stable. Since $G(x_s, x_a) \in H_\infty$, any stabilizing controller is given by

$$C(s) = \frac{-Q(s)}{1 - G(x_s, x_a)Q(s)} \tag{2.14}$$

for some $Q(s) \in H_\infty$ (see Theorem 2.2). Thus, substituting (2.14) into (2.13) we obtain,

$$P_c = \left[\frac{\frac{-Q}{1-G(x_s,x_a)Q} G(x_s, x_d)}{1 + \frac{Q}{1-G(x_s,x_a)Q} G(x_s, x_a)} \right] P_d$$

so that

$$P_c = -QG(x_s, x_d)P_d.$$

Substituting this into (2.12) we obtain

$$P(x) = G(x, x_d)P_d - G(x, x_a)QG(x_s, x_d)P_d.$$

That is,

$$\frac{P(x)}{P_d} = G(x, x_d) - G(x, x_a)G(x_s, x_d)Q,$$

so that (2.11) becomes

$$\gamma_{opt} = \inf_{Q \in H_\infty} \left\| W_1(s) \Big[G(x, x_d) - G(x, x_a)G(x_s, x_d)Q \Big] \right\|_\infty. \tag{2.15}$$

2.3.1 Noise Reduction at a Point

In this section, we consider the simplest problem of noise reduction at a single point. This problem was analyzed by Morris [Mor97a]. Both feedforward ($x_a > x_s$) and feedback ($x_a < x_s$) are considered. The results provide insight as well as a framework for further study of the global noise reduction problem.

We write

$$G(x_1, x_2) = G_i G_o$$

where

$$G_i = e^{-\frac{s}{c}|x_1 - x_2|}$$

and

$$G_o = \begin{cases} \left(\frac{e^{\frac{2s}{c}(x_2 - L)} + \alpha}{e^{\frac{-2s}{c}L} - \alpha}\right)\left(\frac{1 - e^{-\frac{2s}{c}x_1}}{2}\right), & \text{for } x_1 < x_2, \\ \left(\frac{e^{\frac{2s}{c}(x_1 - L)} - \alpha}{e^{-\frac{2s}{c}L} - \alpha}\right)\left(\frac{1 + e^{-\frac{2s}{c}x_2}}{2}\right), & \text{for } x_1 > x_2. \end{cases}$$

Note that $|G_i(jw)| = 1$ and G_o has no right half plane zeros. The performance measure (2.15) may be rewritten as

$$\gamma_{opt} = \inf_{Q \in H_\infty} \left\| W_1 \left[G_o(x, x_d) e^{-\frac{s}{c}[|x - x_d| - |x - x_a| - |x_s - x_d|]} - G_o(x, x_a) G_o(x_s, x_d) Q \right] \right\|_\infty . \tag{2.16}$$

Feedforward ($x_s < x_a$)

In all cases analyzed in [Mor97a], the disturbance is at $x_d = 0$.

Case 1: $x > x_a$

Consider (2.16) with x_d=0:

$$\gamma_{opt} = \inf_{Q \in H_\infty} \left\| W_1 \left[G_o(x, 0) e^{-\frac{s}{c}(x_a - x_s)} - G_o(x, x_a) G_o(x_s, 0) Q \right] \right\|_\infty .$$

Clearly, the choice

$$Q_{opt} = G_o(x, 0) e^{-\frac{s}{c}(x_a - x_s)} G_o(x_s, 0)^{-1} G_o(x, x_a)^{-1}$$

will give a zero response at any frequency. The "optimal" controller is then

$$C_{opt} = \frac{Q_{opt}}{I - G(x_s, x_a) Q_{opt}}$$

(see also [HB95], [Rou85]). However there are several problems with this choice of controller. The controller C_{opt} may be improper. Since $G_o(x, x_a)^{-1} \notin H_\infty$,

$Q_{opt} \notin H_\infty$ so that the closed loop is unstable. Thus, it is possible to reduce the effect of a disturbance to zero at the point x only if the disturbance frequency is not equal to a zero of $G(x, x_a)$. That is, if ω_d is the frequency of the disturbance then any $Q \in H_\infty$ such that $Q(j\omega_d) = Q_{opt}(j\omega_d)$ will work. However, this is not usually practical since this controller will only reduce noise at one point and few disturbances are purely harmonic. As well, if the feedback gain $|G(x, x_a)|$ is large, the controller may become unstable. This results in implementation problems.

Morris also shows the following. Let

$$G_o(x, x_a) = G_o(x, 0) f_r(x_a)(s)$$

where

$$f_r(x_a)(s) = \frac{1 + e^{-\frac{2s}{c} x_a}}{2}.$$

The closed right half plane zeros of f_r are $s = \pm j\omega_n$ where $\omega_n = \frac{(2n+1)c\pi}{2x_a}$, $n = 0, \pm 1, \pm 2, \ldots$. Thus,

$$\gamma_{opt} \geq \sup_n |(W_1 G_o(x, 0))(j\omega_n)|.$$

If $K < 1$,

$$\sup_\omega |G_o(x, 0)(j\omega)| \leq \frac{|-1-\alpha|}{|1-\alpha|} = \frac{1}{K}$$

and

$$\inf_\omega |G_o(x, 0)(j\omega)| \geq \frac{|1-\alpha|}{|-1-\alpha|} = K.$$

If $K > 1$,

$$\sup_\omega |G_o(x, 0)(j\omega)| \geq \frac{|-1-\alpha|}{|1-\alpha|} = K$$

and

$$\inf_\omega |G_o(x, 0)(j\omega)| \leq \frac{|1-\alpha|}{|-1-\alpha|} = \frac{1}{K}.$$

If the control actuator point x_a satisfies $\frac{x_a}{L} = \frac{1}{2m}$, for m some positive integer, and $\frac{x}{L} = 1 + \frac{1}{2m} - \frac{k}{m}$ where k is some integer chosen so that $x > 0$, then

$$G_o(x,0)(j\omega_n) = \frac{|-1-\alpha|}{|1-\alpha|},$$

i.e., the supremum is achieved. These values of x_a and x are "bad".

If the control actuator point x_a satisfies $\frac{x_a}{L} = \frac{1}{2m+1}$, for m some positive integer, and $\frac{x}{L} = 1 - \frac{2k}{2m+1}$ where k is some integer chosen so that $0 < k < \frac{2m+1}{2}$, then

$$G_o(x,0)(j\omega_n) = \frac{|1-\alpha|}{|-1-\alpha|},$$

i.e., the infimum is achieved. These values of x_a and x are "good". In either case, the sensing point x_s does not affect the achievable performance. The above analysis is for $x_s < x_a < x$. Thus, the performance point is further removed from the sensing point. The actuating point is an intermediate point that directly affects the disturbance seen at x.

Results for both "good" and "bad" choices of x_a show a phenomenon referred to as the "spatial waterbed effect": an improvement in performance for $x > x_a$ comes with a worsening of performance for $x < x_a$.

Case 2: $x < x_a$

In this case, (2.16) becomes

$$\gamma_{opt} = \inf_{Q \in H_\infty} \left\| W_1 \left[G_o(x,0) e^{\frac{s}{c}(x_a + x_s - 2x)} - G_o(x,x_a) G_o(x_s,0) Q \right] \right\|_\infty .$$

Morris shows the following. The closer x is to $\frac{x_s + x_a}{2}$, the better the performance. Also, note that since again $G_o(x,x_a) \notin H_\infty$, the optimal performance cannot be achieved by a stabilizing controller. Let $j\omega_n$ be the imaginary axis zeros of $G_o(x,x_a)$.

Then $|G_o(x,0)(j\omega_n)| = 1$ regardless of Q. Thus, performance better than the uncontrolled performance can only be achieved on frequency ranges that exclude the points $j\omega_n$.

Feedback ($x_s > x_a$)

Consider the case where $x_d = 0$, $x_a = 0$, and $x_s > x_a$, . With these choices (2.16) becomes

$$\begin{aligned} \gamma_{opt} &= \inf_{Q\in H_\infty} \left\| W_1 \Big[G_o(x,0) - e^{-\frac{x_s s}{c}} G_o(x,0) G_o(x_s,0) Q \Big] \right\|_\infty \\ &= \inf_{\tilde{Q}\in H_\infty} \left\| W_1 G_o(x,0) - e^{-\frac{x_s s}{c}} \tilde{Q} \right\|_\infty \end{aligned} \tag{2.17}$$

where

$$\tilde{Q} = W_1 G_o(x,0) G_o(x_s,0) Q.$$

However, here the function $W_1 G_o(x,0)$ in (2.17) is not rational. The case where $W_1 G_o(x,0)$ is a rational function has been studied by a number of groups [ZK87], [LST88], [FTZ87].

In the case where this weight is not rational, the problem may be manipulated until the weight is rational. Consider the following. Recall (2.15) is

$$\gamma_{opt} = \inf_{Q\in H_\infty} \left\| W_1(s) \Big[G(x,x_d) - G(x,x_a) G(x_s,x_d) Q \Big] \right\|_\infty .$$

Let

$$W = W_1(s) G(x,x_d).$$

We will assume for simplicity of the discussion that $x_d = x_a$. Then

$$G(x,x_d)^{-1} G(x,x_a) G(x_s,x_d) = G(x_s,x_d)$$

and

$$\gamma_{opt} = \inf_{Q\in H_\infty} \left\| W(s) \Big[1 - G(x_s,x_d) Q(s) \Big] \right\|_\infty .$$

Suppose we write a factorization of $G(x_s, x_d)$

$$G(x_s, x_d) = G_i G_o$$

where

$$G_i = e^{-\frac{s}{c}|x_s - x_d|} \tag{2.18}$$

and G_o has no zeros in $\Re(s) > 0$. Let $\tilde{Q} = G_o Q$ so that

$$\gamma_{opt} = \inf_{\tilde{Q} \in H_\infty} \left\| W\left(1 - G_i \tilde{Q}\right) \right\|_\infty . \tag{2.19}$$

If W is of the form

$$W = \frac{p}{1 - G_i q} \tag{2.20}$$

where p and q are rational functions and $1/(1 - G_i q) \in H_\infty$, then

$$\gamma_{opt} = \inf_{\tilde{Q} \in H_\infty} \left\| p\left(1 - q\frac{\tilde{Q} - s}{1 - qs}\right) \right\|_\infty .$$

Let $\bar{Q} = \frac{\tilde{Q} - s}{1 - qs}$. Then

$$\gamma_{opt} = \inf_{\bar{Q} \in H_\infty} \left\| p\left(1 - q\bar{Q}\right) \right\|_\infty .$$

This is in the form of a problem with rational weight and irrational plant. The solution to this problem has been studied by several authors [Ö93], [ZK87], [LST88], [FTZ87]. However, in our case, this method is not practical. Firstly, the above discussion assumes that $x_d = x_a$, which is not a realistic assumption. Secondly, the above discussion also assumes that the weight $W(s)$ is of the form given in (2.20). This special form restricts our choice of W_1. Again this is not a realistic assumption since we would like to choose W_1 so that low frequencies are weighted.

Case 1: $2(L - x) \geq x_s$

In this case, the problem in (2.17) becomes

$$\gamma_{opt} = \inf_{\tilde{Q} \in H_\infty} \left\| W_1 - e^{-\frac{x_{sa}}{c}} \tilde{Q} \right\|_\infty .$$

This is the rational weight case solved by Zhou and Khargonekar [ZK87]. The main result is summarized in the following theorem.

Theorem 2.3 *[ZK87]*

Let $W_1(s) = C(sI - A)^{-1}B$ *be a stable rational minimal realization, and let* $\phi = e^{-\frac{x_s s}{c}}$. *Define*

$$F_\lambda = \begin{bmatrix} A & BB^T/\lambda \\ -CC^T/\lambda & -A^T \end{bmatrix}.$$

Then

$$\gamma_{opt} = max\left\{\lambda \;\middle|\; det\{[\phi^*(F_\lambda)]_{(2,2)}\} = 0\right\},$$

where $[H]_{(2,2)}$ *denotes the* $(2,2)$ *block of the block matrix* H. *If* $W_1(s) = \frac{1}{1+s/a}$, *then*

$$\gamma_{opt} = \frac{1}{\sqrt{1 + \left(\frac{rc}{ax_s}\right)^2}}$$

where $r \in (\pi/2, \pi)$ *is the unique solution to*

$$\tan(r) + \frac{rc}{ax_s} = 0.$$

Case 2: $2(L - x) < x_s$

Because these is no method to compute γ_{opt} in (2.17) exactly, a numerical technique to calculate γ_{opt} to within arbitrary accuracy is given.

Case 3: $x = L$

Let $w_1(t) = \mathcal{L}^{-1}(W_1(s))$. In this case $w_1(t)$ is replaced by $w(t)$ where $w(t) = (1 - \frac{1}{a})w_1(t)$. Thus, the method in [ZK87] can be used where W_1 has the minimal

realization $[A, B, C, 0]$ and W has the realization $[A, fB, fC, 0]$ for $f = \sqrt{1 - 1/\alpha}$. In this case, Morris shows that

$$\gamma_{opt} = \left|1 - \frac{1}{\alpha}\right| \gamma_o$$

where γ_o is the optimal performance for Case 1 when $2(L - x) > x_s$.

Results

The results obtained for the feedback case are summarized as follows.

- The feedback sensor x_s should be placed as close as possible to $x_d = 0$.
- For $2(L - x) > x_s$, the optimal performance $\gamma_{opt} = \gamma_1$ depends only on the location of x_s and the weight W_1.
- For $x = L$, the optimal performance $\gamma_{opt} = \gamma_2$ depends on x_s, W_1, and K.
- For intermediate points x, the optimal performance varies continuously from γ_1 to γ_2.

These results as well as those obtained for the feedforward case will influence our choices for x_a, x_d, x_s, and K when we consider the solution of the global noise reduction problem in Chapters 4 and 6.

2.4 Global Noise Reduction

The control problem formulated in the last section considers the effect of the disturbance at x_d on one arbitrary location x in the duct. We would like to extend this to considering the problem of global noise reduction. We are interested in the following questions.

- Is it possible to reduce acoustic noise everywhere in the duct by applying a control pressure at a finite number of points?
- What is the best location for the sensor?

This problem of "optimal global noise reduction" may be mathematically formulated as follows.

Problem 1:

Find

$$\gamma_{opt} = \inf_{x_s \in [0,L]} \left[\inf_{Q \in H_\infty} \left[\sup_{x \in [0,L]} \left\| W_1(s) \Big(G(x, x_d) - G(x, x_a) G(x_s, x_d) Q \Big) \right\|_\infty \right] \right]. \quad (2.21)$$

In other words, we minimize the maximal output pressure everywhere in the duct by choosing a Youla parameter $Q(s)$. Then we determine the optimal position of the sensor x_s such that the acoustic noise is again minimized everywhere in the duct. We minimize the maximum output pressure by choosing the best Youla parameter $Q(s)$ for each sensing point x_s. This problem is very difficult. We consider the following simplifications to this problem.

Suppose we let the sensor location x_s be fixed. This yields the following.

Problem 2:

$$\gamma_{opt} = \inf_{Q \in H_\infty} \left[\sup_{x \in [0,L]} \left\| W_1(s) \Big(G(x, x_d) - G(x, x_a) G(x_s, x_d) Q \Big) \right\|_\infty \right]. \quad (2.22)$$

In simplifying from Problem 1 to Problem 2, we lose any information regarding the optimal placement of the sensor at x_s. However, because there are still an uncountable number of performance points x, the problem is still intractable.

As a further simplification to Problem 2, let $\mathcal{X} = \{x_1, x_2, \ldots, x_m\}$ be some appropriate discrete partition of the duct, spanning the length of the duct. Then we have the following.

Problem 3:

$$\gamma_{opt} = \inf_{Q \in H_\infty} \left\| \tilde{T}_1 - \tilde{T}_2 Q \right\|_\infty \tag{2.23}$$

where

$$\tilde{T}_1 = \begin{bmatrix} W_1(s)G(x_1, x_d) \\ W_1(s)G(x_2, x_d) \\ \vdots \\ W_1(s)G(x_m, x_d) \end{bmatrix}, \quad \tilde{T}_2 = \begin{bmatrix} W_1(s)G(x_1, x_a)G(x_s, x_d) \\ W_1(s)G(x_2, x_a)G(x_s, x_d) \\ \vdots \\ W_1(s)G(x_m, x_a)G(x_s, x_d) \end{bmatrix}.$$

In Problems 1 and 2, we are concerned with reducing acoustic noise everywhere in the duct. In Problem 3, we consider whether it is possible to reduce the acoustic noise at some fixed points given by $\mathcal{X}$. If only one point is considered, then (2.23) is precisely the problem discussed in Section 2.3.

However, because the matrices $\tilde{T}_1$ and $\tilde{T}_2$ have irrational elements, we again cannot solve the problem. A further simplification to the global noise reduction problem is to approximate each infinite-dimensional plant $G(x_1, x_2)$ with some *appropriate* sequence of finite-dimensional plants $G_n(x_1, x_2)$.

Definition 2.4

The space RH_∞ is the subset of H_∞ consisting of all real rational functions which are stable and proper. Matrices are indicated by $RH_\infty^{m \times n}$ or $M(RH_\infty)$.

This results in a problem of the following form.

Problem 4:

$$\gamma_n = \inf_{Q \in RH_\infty} \left\| T_1 - T_2 Q \right\|_\infty \tag{2.24}$$

where

$$T_1 = \begin{bmatrix} W_1(s)G_n(x_1, x_d) \\ W_1(s)G_n(x_2, x_d) \\ \vdots \\ W_1(s)G_n(x_m, x_d) \end{bmatrix} \quad T_2 = \begin{bmatrix} W_1(s)G_n(x_1, x_a)G_n(x_s, x_d) \\ W_1(s)G_n(x_2, x_a)G_n(x_s, x_d) \\ \vdots \\ W_1(s)G_n(x_m, x_a)G_n(x_s, x_d) \end{bmatrix}. \tag{2.25}$$

Here $T_1 \in RH_\infty^{m\times 1}$, $T_2 \in RH_\infty^{m\times 1}$, and $Q \in RH_\infty$. In addition, T_1 and T_2 are strictly proper. We will refer to (2.24) as the "tall problem".

In the scalar-valued case ($m = 1$), solution to this problem is straightforward. In the matrix-valued case ($m > 1$), the solution is much more involved. However, because T_1 and T_2 are rational, a solution can be obtained. Details are in Chapter 5. This problem is the most easily solvable of the four problems discussed. However, the approximations G_n to the irrational transfer function G must be chosen so that $\gamma_n \to \gamma_{opt}$. This problem is not straightforward and will be discussed in Chapter 3.

Chapter 3

Control and Approximation of Systems

Systems whose dynamics are described by linear ordinary differential equations can be described by linear maps on linear function spaces. We shall refer to such systems as *finite-dimensional* since the states lie in a finite-dimensional function space. Many problems with physical applications have delays in the dynamics of the system, or dynamics best described by partial differential equations. For systems described by partial differential equations (distributed parameter systems) or by delay equations, the appropriate state-space is an infinite-dimensional function space. Such systems are generally called *infinite-dimensional.* In addition, infinite-dimensional systems can be classified as *bounded* or *unbounded* control systems, depending on the control and observation used.

It is generally very difficult if not impossible to solve control problems involving infinite-dimensional systems. Finite-dimensional approximations are usually required.

In this chapter, we present an overview of finite-dimensional control systems theory and the linear quadratic regulator (LQR) problem. The LQR problem is an optimal control problem which has a very simple elegant solution. The solution to this problem is also key to determining, for example, stabilizability and detectability of control systems.

Unlike the solution to the H_∞ optimal sensitivity problem, the solution to the infinite-dimensional LQR problem via finite-dimensional approximations for bounded control systems is well-known. These results have also been extended to some unbounded control problems. We will use the solution of the LQR problem as our benchmark problem. Approximations to the infinite-dimensional LQR problem will provide us with some general criteria which ensure convergence to the infinite-dimensional solution.

We conclude this chapter by considering approximations to the H_∞ optimal control problem given by Problems 3 and 4 (see page 26 and page 27, respectively) and requirements for the approximations to converge to the actual solution.

3.1 Finite-Dimensional Theory

In this section, we restrict ourselves to systems which are governed by linear time invariant ordinary differential equations with a given initial state. These systems can be written in *state-space form*,

$$\begin{aligned} \dot{w}(t) &= Aw(t) + Bu(t), \quad w(0) = w_0 \\ y(t) &= Cw(t) \end{aligned} \tag{3.1}$$

where $w \in \mathbb{R}^n$ is the state, $w_0 \in \mathbb{R}^n$, $u(t) \in \mathbb{R}^m$, $A \in \mathbb{R}^{n\times n}$, $B \in \mathbb{R}^{n\times m}$, and $C \in \mathbb{R}^{p\times n}$. The control function is $u(t)$, and $y(t) = Cw(t)$ is known as the observation

equation. The unique solution of (3.1) is

$$y(t) = Ce^{At}w_0 + C\int_0^t e^{A(t-\tau)}Bu(\tau)\,d\tau.$$

In general, the purpose of a control system is to maintain or create stability in a system while meeting certain performance criteria. To discuss the development of control systems further, we require concepts of stability, stabilizability, and detectability.

Definition 3.1

The group of operators e^{At} is exponentially stable if there exist $M, \sigma > 0$ such that

$$\|e^{At}\| \leq Me^{-\sigma t} \quad \text{for all } t \geq 0.$$

Definition 3.2

The matrix A is Hurwitz if and only if the real parts of all its eigenvalues are negative.

Definition 3.3

Equation (3.1) (or equivalently (A, B)) is stabilizable if there exists $K \in \mathbb{R}^{m\times n}$ such that $A - BK$ is Hurwitz.

Definition 3.4

Equation (3.1) (or equivalently (A, C)) is detectable if there exists $F \in \mathbb{R}^{n\times p}$ such that $A - FC$ is Hurwitz.

If we design our control system such that it is stabilizable and detectable, we may consider the question of optimal control.

3.1.1 Linear Quadratic Regulator Problem

The linear quadratic regulator (LQR) problem consists of finding an optimal control to a linear system by minimizing a quadratic cost function. Consider the cost functional,

$$J(u, w_0) = \int_0^\infty \Big[\langle w(t), Qw(t) \rangle + \langle u(t), Ru(t) \rangle \Big] \, dt \tag{3.2}$$

where Q and R are real symmetric $n \times n$ and $m \times m$ matrices, respectively, with $Q \geq 0$ and $R > 0$. The problem of minimizing (3.2) subject to (3.1) is called the *linear quadratic regulator problem.* The matrix Q may be thought of as a penalty or weight on the states and similarly, the matrix R as a weight on the control. One possible choice for Q is $Q = C^*C$. In effect, this introduces a weight on the output y of the system. The conditions imposed on the definiteness of the matrices Q and R ensure that the cost functional has positive values. The form of the solution to the linear regulator problem is strongly associated with the solution to the algebraic Riccati equation

$$Q + \Pi A + A^*\Pi - \Pi B R^{-1} B^* \Pi = 0, \tag{3.3}$$

which is solved for the nonnegative definite self-adjoint matrix Π. If $\tilde{\Pi}$ is a solution to (3.3) and $\tilde{\Pi} \leq \Pi$ for all other solutions Π, then $\tilde{\Pi}$ is called the *minimal solution* of (3.3).

Theorem 3.1 *[Zab92, page 138]*

If there exists a nonnegative self-adjoint solution Π *of (3.3), then there exists a unique minimal solution* $\tilde{\Pi}$ *of (3.3) and the control* $\tilde{u}$ *in feedback form,*

$$\tilde{u}(t) = -R^{-1} B^* \tilde{\Pi} w(t), \quad t \geq 0$$

minimizes the cost functional (3.2). The minimal value of the cost functional is

$$\langle \tilde{\Pi} w, w \rangle.$$

If we consider the case when $Q = C^*C$, then we have the following result.

Theorem 3.2 *[Zab92, page 138]*

If (A, B) is stabilizable and (A, C) is detectable, then (3.3) has a unique nonnegative self-adjoint solution and the matrix $A - BR^{-1}B^*\Pi$ is Hurwitz.

Theorem 3.2 gives a way to determine whether a system can be stabilized by finding the solution to an associated linear quadratic regulator problem.

3.2 Motivating Examples

In the sections that follow, we will consider both "bounded" and "unbounded" control systems, as well as approximations to the LQR problem for such systems. Before doing so, we present two examples of control systems which illustrate the difference between "bounded" and "unbounded" control systems. The first example is a heated metal rod. The second example is the one-dimensional duct model presented in Chapter 2.

Example 1 Consider a metal rod of length one heated along its length according to

$$\frac{\partial z}{\partial t}(x,t) = \frac{\partial^2 z}{\partial x^2}(x,t) + b(x)u(t)$$
$$z(x,0) = f(x)$$
$$y(t) = \int_0^1 c(x)z(x,t)\ dx$$

for $x \in [0,1]$ and $t > 0$, with boundary conditions

$$\frac{\partial z}{\partial x}(0,t) = \frac{\partial z}{\partial x}(1,t) = 0, \quad t > 0$$

where $z(x,t)$ is the temperature at time t and position x, $u(t)$ is the control function representing the addition of heat in the rod, and $y(t)$ is the observation. Suppose $b(x)$ and $c(x)$ represent "functions" around the points x_0 and x_1, respectively, given by,

$$b(x) = \frac{1}{2\epsilon_b} 1_{[x_0-\epsilon_b, x_0+\epsilon_b]}(x),$$

and

$$c(x) = \frac{1}{2\epsilon_c} 1_{[x_1-\epsilon_c, x_1+\epsilon_c]}(x),$$

where

$$1_{[\alpha,\beta]} = \begin{cases} 1, & \text{for } \alpha \leq x \leq \beta, \\ 0, & \text{elsewhere.} \end{cases}$$

For fixed, small, positive constants ϵ_b and ϵ_c, $b(x)$ and $c(x)$, respectively, are both elements of $L_2(0,1)$, which is a suitable state-space for the heat equation without input (e.g., [CZ95, Example 2.3.7]). Thus, the above partial differential equation can be formulated in state-space form,

$$\dot{z}(t) = \mathcal{A}z(t) + \mathcal{B}u(t)$$
$$y(t) = \mathcal{C}z(t)$$

where $\mathcal{H} = L_2(0,1)$, $\mathcal{U} = \mathbb{R}$, $\mathcal{A} : D(\mathcal{A}) \subset \mathcal{H} \to \mathcal{H}$ is given by $\mathcal{A} = \frac{d^2}{dx^2}$, and $\mathcal{B}u := b(x)u$ for $\mathcal{B} \in \mathcal{L}(\mathbb{R}, \mathcal{H})$. In addition,

$$\mathcal{C}z(t) := \int_0^1 c(x)z(x)\,dx.$$

We will refer to systems which fit the above framework as *bounded control systems.*

The operators $\mathcal{B}$ and $\mathcal{C}$ approximate point actuators and point sensors, respectively. As well, for ϵ_b, $\epsilon_c > 0$, $\mathcal{B}$ and $\mathcal{C}$ are bounded. However, a point

actuator is usually modeled as a delta distribution. Thus a point actuator is not represented as a bounded operator on $L_2(0,1)$. We will refer to such systems as *unbounded control systems.* Curtain and Zwart [CZ95, Section 3.3] give some examples of control systems that can be reformulated on an extended state-space with bounded $\mathcal{B}$.

Example 2 Consider the one-dimensional acoustic duct model given in Chapter 2 (see (2.1), (2.2), and (2.3)). Note that the one-dimensional duct model is both infinite-dimensional and unbounded. Suppose $P_c(t) = 0$ and the input $u(t)$ is the disturbance $P_d(t)$ at x_d. These equations may be written as an abstract differential equation of the form

$$\dot{w}(t) = \mathcal{A}w(t) + \mathcal{B}u(t).$$

Let

$$H_1(0,L) = \left\{ \zeta \in L_2(0,L), \frac{\partial \zeta}{\partial x} \in L_2(0,L) \right\}.$$

We endow $H_1(0,L)$ with the inner product

$$\langle \zeta, \xi \rangle = \int_0^L \zeta(x)\overline{\xi(x)}\, dx + \int_0^L \frac{\partial \zeta}{\partial x}\overline{\frac{\partial \xi}{\partial x}}\, dx.$$

Similarly, define the quotient space $\overline{H}_1(0,L)$ by

$$\overline{H}_1(0,L) = H_1(0,L) \setminus k$$

for k some constant, with inner product

$$\langle \zeta, \xi \rangle = \int_0^L \frac{\partial \zeta}{\partial x}\overline{\frac{\partial \xi}{\partial x}}\, dx.$$

Let the state-space for $w = (z, z_t)$ be $\mathcal{H} = \overline{H}_1(0,L) \times L_2(0,L)$ with inner product

$$\langle \zeta, \xi \rangle_{\mathcal{H}} = c^2 \int_0^L \frac{\partial \zeta_1}{\partial x}\overline{\frac{\partial \xi_1}{\partial x}}\, dx \; + \int_0^L \zeta_2 \overline{\xi_2}\, dx. \tag{3.4}$$

Then,

$$\mathcal{A}w(t) = \begin{bmatrix} 0 & I \\ c^2 \frac{d^2}{dx^2} & 0 \end{bmatrix} w(t), \tag{3.5}$$

and

$$\mathcal{B}u(t) = \begin{bmatrix} 0 \\ \frac{\delta(x-x_d)}{\rho} \end{bmatrix} u(t). \tag{3.6}$$

In the following sections, we will describe both bounded and unbounded infinite-dimensional control systems. We will also discuss the linear quadratic regulator problem for both of these systems, as well as results for approximating these problems on finite-dimensional spaces.

3.3 Semigroup Operators and Control Systems

In order to use existing state-space techniques for infinite-dimensional systems, we would like to be able to take any linear control system and write it in state-space form. The purpose of this section is to describe an abstract state-space formulation

$$\dot{w}(t) = \mathcal{A}w(t) + \mathcal{B}u(t), \;\; w(0) = w_0 \tag{3.7}$$

on a Hilbert space $\mathcal{H}$ that will enable us to present a unified approach to both finite and infinite-dimensional systems. Let $\mathcal{H}$ be a (possibly infinite-dimensional) Hilbert space. Let $w_0 \in \mathcal{H}$ be the initial state of the dynamical system defined on $\mathcal{H}$ and let $w(t)$ be the state at any future time t. We will assume that the dynamics governing the evolution from w_0 to w are linear and time invariant. Let I denote the identity operator on $\mathcal{H}$; that is, $Iw = w$, for $w \in \mathcal{H}$. Define a linear operator $S(t)$ for some time t such that,

$$S(t) : \mathcal{H} \to \mathcal{H}; \;\; S(0) = I$$
$$w(t) = S(t)w_0.$$

The operator $S(t)$ on $\mathcal{H}$ maps the state of the system at time 0 to its state at time t. We also assume that the state of our system satisfies the Hadamard well-posedness conditions, namely:

(1) it is unique;

(2) it varies continuously with the initial state.

Because the state is unique, we have

$$w(t+s) = S(t+s)w_0 = S(t)w(s) = S(t)S(s)w_0,$$
$$S(t+s) = S(t)S(s).$$

Since we are assuming the state varies continuously with the initial state w_0, we know $S(t)$ is a bounded map on $\mathcal{H}$. We also impose smoothness on $w(t)$ and assume $w(t) \to w_0$ as $t \to 0^+$ for all $w_0 \in \mathcal{H}$. $S(t)$ is called a *semigroup of bounded linear operators*, formally defined as follows.

Definition 3.5

Let $\mathcal{H}$ be a Hilbert space. A one parameter family $S(t)$, $0 \leq t < \infty$, of bounded linear operators from $\mathcal{H}$ into $\mathcal{H}$ is a semigroup of bounded linear operators on $\mathcal{H}$ if

(i) $S(0) = I$;

(ii) $S(t+s) = S(t)(s)$ *for every* $t, s \geq 0$ *(the semigroup property).*

Definition 3.6

A semigroup $S(t)$, $0 \leq t < \infty$, of bounded linear operators on $\mathcal{H}$ is a strongly continuous (C_0) semigroup of bounded linear operators if

$$\lim_{t \to 0^+} S(t)w = w \quad \text{for every } w \in \mathcal{H}.$$

If $S(t)$ is a C_0 semigroup, then there exist constants $\sigma \geq 0$ and $M \geq 1$ such that

$$\|S(t)\| \leq Me^{\sigma t}, \quad \text{for } 0 \leq t \leq \infty.$$

Example Let $A \in \mathcal{L}(\mathcal{H})$. Then

$$S(t) = e^{At} = \sum_{n=0}^{\infty} \frac{(At)^n}{n!}$$

is a C_0 semigroup and is uniformly continuous.

We would like to relate the operator $S(t)$ to the operator $\mathcal{A}$ in (3.7).

Definition 3.7

The infinitesimal generator $\mathcal{A}$ of a strongly continuous semigroup $S(t)$ on a Hilbert space $\mathcal{H}$ is defined by

$$\mathcal{A}w = \lim_{t \to 0^+} \frac{1}{t}\Big(S(t) - I\Big)w$$

whenever the limit exists. The domain of $\mathcal{A}$, $\mathcal{D}(\mathcal{A})$, is the set of elements in $\mathcal{H}$ for which the limit exists.

Let $\mathcal{A}$ be the infinitesimal generator of $S(t)$. Then, $\dot{w}(t) = \mathcal{A}w(t)$, $w(0) = w_0 \in \mathcal{D}(\mathcal{A})$, has the solution $w(t) = S(t)w(0)$. Thus, the conditions under which an operator $\mathcal{A}$ is the infinitesimal generator of a semigroup are of utmost importance. The following theorem provides a necessary and sufficient condition under which this requirement is met.

Theorem 3.3 *(Hille-Yosida Theorem [Paz83, page 8])*

A linear (unbounded) operator $\mathcal{A}$ on a Banach space $\mathcal{H}$ is the infinitesimal generator of a C_0 semigroup $S(t)$, $t \geq 0$ if and only if

(i) $\mathcal{A}$ *is closed and* $\overline{\mathcal{D}(\mathcal{A})} = \mathcal{H}$.

(ii) *There exist real numbers* M, σ, *such that for all real* $\lambda > \sigma$, $\lambda \in \rho(\mathcal{A})$, *the resolvent set of* $\mathcal{A}$,

$$\|R(\lambda : \mathcal{A})\| \leq \frac{M}{(\lambda - \sigma)}$$

or equivalently,

$$\|(\lambda I - \mathcal{A})\| \geq \frac{(\lambda - \sigma)}{M},$$

where $R(\lambda : \mathcal{A}) = (\lambda I - \mathcal{A})^{-1}$ *is the resolvent.*

In this case,

$$\|S(t)\| \leq Me^{\sigma t}. \tag{3.8}$$

In general, it is difficult to check the conditions of the Hille-Yosida theorem. Below, we state a result derived from the Hille-Yosida theorem which involves the adjoint operator $\mathcal{A}^*$. This leads to conditions which are in general easier to verify on a Hilbert space.

Definition 3.8

Let $\mathcal{A}$ *be a closed, densely defined, linear operator with domain* $\mathcal{D}(\mathcal{A})$ *on a Hilbert space* $\mathcal{H}$, *which is identified with its adjoint space. The adjoint* $\mathcal{A}^*$ *of* $\mathcal{A}$ *is a transformation whose domain* $\mathcal{D}(\mathcal{A}^*)$ *consists of all* $g \in \mathcal{H}$ *for which there exists a* $g^* \in \mathcal{H}$ *such that*

$$\langle \mathcal{A}w, g \rangle = \langle w, g^* \rangle \text{ for all } w \in \mathcal{D}(\mathcal{A}).$$

In this case, $g^* = \mathcal{A}^* g$.

Theorem 3.4 *[CP78, page 22]*

Let $\mathcal{A}$ be a closed, densely defined, linear operator on a Hilbert space $\mathcal{H}$. Then $\mathcal{A}$ generates a semigroup $S(t)$ on $\mathcal{H}$ satisfying $\|S(t)\| \leq e^{\sigma t}$ for all $t \geq 0$ if and only if for all $\lambda > \sigma$, where $\sigma \in \mathbb{R}$,

$$\|(\lambda I - \mathcal{A})w\|_{\mathcal{H}} \geq (\lambda - \sigma)\|w\|_{\mathcal{H}}, \quad w \in \mathcal{D}(\mathcal{A}) \tag{3.9}$$

$$\|(\lambda I - \mathcal{A}^*)w^*\|_{\mathcal{H}^*} \geq (\lambda - \sigma)\|w^*\|_{\mathcal{H}^*}, \quad w^* \in \mathcal{D}(\mathcal{A}^*). \tag{3.10}$$

The conditions in (3.9) and (3.10) can be rewritten as

$$\langle (\lambda I - \mathcal{A})w, (\lambda I - \mathcal{A})w \rangle \;\; \geq \;\; (\lambda - \sigma)^2 \langle w, w \rangle$$

for $\lambda > \sigma$, $w \in \mathcal{D}(\mathcal{A})$ and

$$\langle (\lambda I - \mathcal{A}^*)w^*, (\lambda I - \mathcal{A}^*)w^* \rangle \;\; \geq \;\; (\lambda - \sigma)^2 \langle w^*, w^* \rangle$$

for $\lambda > \sigma$, $w^* \in \mathcal{D}(\mathcal{A}^*)$, respectively, and these equations can in turn be rewritten as

$$2\lambda\Big(\sigma\|w\|^2 - \Re\langle \mathcal{A}w, w\rangle\Big) + \langle \mathcal{A}w, \mathcal{A}w\rangle - \sigma^2\|w\|^2 \geq 0, \quad w \in \mathcal{D}(\mathcal{A}) \tag{3.11}$$

and

$$2\lambda\Big(\sigma\|w^*\|^2 - \Re\langle \mathcal{A}^*w, w\rangle\Big) + \langle \mathcal{A}^*w, \mathcal{A}^*w\rangle - \sigma^2\|w^*\|^2 \geq 0, \quad w^* \in \mathcal{D}(\mathcal{A}^*), \tag{3.12}$$

respectively. The inequality in (3.11) holds with a suitable choice for w if there exists a β such that

$$\beta\|w\|^2 \geq \Re\langle \mathcal{A}w, w\rangle, \quad w \in \mathcal{D}(\mathcal{A}). \tag{3.13}$$

Similarly, the inequality in (3.12) holds if

$$\beta\|w^*\|^2 \geq \Re\langle \mathcal{A}^*w^*, w^*\rangle, \quad w^* \in \mathcal{D}(\mathcal{A}^*). \tag{3.14}$$

These results can be summarized in the following corollary.

Corollary 3.5 *[CP78]*

If for a suitable choice of w there exists a β such that

$$\beta\|w\|^2 \geq \Re\langle \mathcal{A}w, w\rangle, \quad w \in \mathcal{D}(\mathcal{A})$$
$$\beta\|w^*\|^2 \geq \Re\langle \mathcal{A}^*w^*, w^*\rangle, \quad w^* \in \mathcal{D}(\mathcal{A}^*),$$

then the operator $\mathcal{A}$ satisfies the Hille-Yosida theorem with semigroup $S(t)$.

The conditions of the corollary are easier to check that those given in the Hille-Yosida theorem.

Thus far we have seen that if $\mathcal{A}$ generates a strongly continuous semigroup $S(t)$, then $\dot{w}(t) = \mathcal{A}w(t)$, $w(0) = w_0$ has solution $w(t) = S(t)w(0)$. We now extend this concept to

$$\begin{aligned} \dot{w}(t) &= \mathcal{A}w(t) + f \\ w(0) &= w_0 \end{aligned} \tag{3.15}$$

where $f : [0,T] \to \mathcal{H}$.

Definition 3.9

Any continuous function $w : [0,T] \to \mathcal{H}$ such that

(i) $w(0) = w_0$, $w(t) \in \mathcal{D}(\mathcal{A})$, $t \in [0,T]$,

(ii) *w is differentiable at any time $t \in [0,T]$ and*

$$\dot{w}(t) = \mathcal{A}w(t) + f(t), \quad t \in [0,T]$$

is called a strong solution of (3.15) on $[0,T]$.

If $f(\cdot)$ is a function with continuous first derivatives on $[0,\infty)$ and $w \in \mathcal{D}(\mathcal{A})$, then (3.15) has a strong solution [Paz83]. The strong solution is

$$w(t) = S(t)w_0 + \int_0^t S(t-s)f(s)\,ds, \quad t \geq 0. \tag{3.16}$$

If the function $w(t)$, $t \geq 0$, given in (3.16) is well-defined for an arbitrary integrable function $f(\cdot)$, then (3.16) is called a *weak or mild solution* of (3.7). In general, we have the following definition.

Definition 3.10 *[CP78]*

If $f \in L_p(0, t_1; \mathcal{H})$, $p \geq 1$, we say that

$$w(t) = S(t)w_0 + \int_0^t S(t-s)f(s)\,ds \tag{3.17}$$

is a mild solution of

$$\dot{w}(t) = \mathcal{A}w(t) + f \tag{3.18}$$

on $[0, t_1]$. That is, $w(t)$ is the only function such that for all $v^* \in \mathcal{D}(\mathcal{A}^*)$,

(1) $\langle w(t), v^* \rangle$ *is absolutely continuous and*

(2) $\frac{d}{dt}\langle w(t), v^* \rangle = \langle w(t), \mathcal{A}^* v^* \rangle + \langle f, v^* \rangle$.

In general, for $\mathcal{B} \in \mathcal{L}(\mathcal{U}, \mathcal{H})$ and the state-space system,

$$\begin{aligned} \dot{w}(t) &= \mathcal{A}w(t) + \mathcal{B}u(t), \;\; w(0) = w_0 \\ y(t) &= \mathcal{C}w(t), \end{aligned} \tag{3.19}$$

we use the mild solution

$$w(t) = S(t)w_0 + \int_0^t S(t-s)\mathcal{B}u(s)\,ds$$

almost everywhere on $[0, T]$.

3.4 Infinite-Dimensional Bounded Control Systems

In this section, we consider the optimal control problem for (possibly) infinite-dimensional, bounded, linear time invariant systems with quadratic cost criteria.

The corresponding problem for finite-dimensional systems leads to feedback control. A similar result holds for the infinite-dimensional case.

3.4.1 Linear Quadratic Regulator Problem

Consider a semigroup control system defined on a Hilbert space $\mathcal{H}$,

$$\begin{aligned} \dot{w}(t) &= \mathcal{A}w(t) + \mathcal{B}u(t), \;\; w(0) = w_0 \\ y(t) &= \mathcal{C}w(t) \end{aligned} \tag{3.20}$$

where $\mathcal{A}$ and $\mathcal{B}$ are operators and $\mathcal{A} : \mathcal{D}(\mathcal{A}) \subset \mathcal{H} \to \mathcal{H}$ is the infinitesimal generator of a strongly continuous semigroup $S(t)$ on $\mathcal{H}$, $\mathcal{B} \in \mathcal{L}(\mathcal{U}, \mathcal{H})$, with control space $\mathcal{U}$, and $\mathcal{C} \in \mathcal{L}(\mathcal{H}, \mathcal{Y})$. For controls in $\mathcal{U}$, the mild solution of (3.20) is

$$w(t) \;=\; S(t)w_0 + \int_0^t S(t-\tau)\mathcal{B}u(\tau)\, d\tau. \tag{3.21}$$

Let $Q = \mathcal{C}^*\mathcal{C}$ and R be operators such that $Q \in \mathcal{L}(\mathcal{H}, \mathcal{H}), R \in \mathcal{L}(\mathcal{U}, \mathcal{U})$ are self-adjoint and $R > 0$. This effectively establishes a weight on the output y of the system. The associated cost functional is

$$J(u, w_0) = \int_0^\infty \Big[\langle w(t), Qw(t) \rangle \;+\; \langle u(t), Ru(t) \rangle \Big]\, dt. \tag{3.22}$$

The abstract linear optimal regulator problem is

$$\text{Minimize} \Big\{ J(u, w_0) \text{ where } u \;\in\; L_2(0, \infty; \mathcal{U}) \Big\} \tag{3.23}$$

subject to w satisfying (3.21). A function $u \in L_2(0, \infty; \mathcal{U})$ is an *admissible control* if (3.22) is finite.

As in the corresponding finite-dimensional case, the algebraic Riccati equation plays a very important role in the solution of (3.23). For our abstract semigroup system, an operator $\Pi \in \mathcal{L}(\mathcal{H}, \mathcal{H})$ is a solution of the algebraic Riccati equation if

$\Pi : \mathcal{D}(\mathcal{A}) \rightarrow \mathcal{D}(\mathcal{A}^*)$ and Π satisfies

$$\mathcal{A}^*\Pi + \Pi\mathcal{A} - \Pi\mathcal{B}R^{-1}\mathcal{B}^*\Pi + Q = 0 \tag{3.24}$$

on $\mathcal{H}$. Similarly to its counterpart, $\mathcal{A}^*$ is the generator of a strongly continuous semigroup of operators $S^*(t)$ which is adjoint to $S(t)$.

In control theory, we are often concerned with the question of stabilizability. Earlier we presented definitions and results for finite-dimensional control systems. Here, we introduce similar results for semigroup control systems.

Definition 3.11

The C_0 semigroup $S(t)$ is (uniformly) exponentially stable if there exist positive constants M and σ such that $\|S(t)\| \leq Me^{-\sigma t}$, for all $t \geq 0$.

Definition 3.12

Let $\mathcal{A}$ be the infinitesimal generator of a strongly continuous semigroup $S(t)$ on a Hilbert space $\mathcal{H}$, and $\mathcal{B} \in \mathcal{L}(\mathcal{U}, \mathcal{H})$, where $\mathcal{U}$ is a Hilbert space. If there exists $K \in \mathcal{L}(\mathcal{H}, \mathcal{U})$ such that $\mathcal{A} - \mathcal{B}K$ generates a strongly continuous semigroup $T(t)$ with

$$\|T(t)\| \leq Me^{-\sigma t}, \ \omega > 0, \tag{3.25}$$

then the pair $(\mathcal{A}, \mathcal{B})$ is said to be exponentially stabilizable.

Definition 3.13

$(\mathcal{A}, \mathcal{C})$ is detectable if there exists an operator $F \in \mathcal{L}(\mathcal{Y}, \mathcal{H})$ such that $\mathcal{A} - F\mathcal{C}$ generates a uniformly exponentially stable semigroup on $\mathcal{H}$.

The solution of (3.24) is summarized in the following theorem [Gib79, Theorem 4.11].

Theorem 3.6 *(Algebraic Riccati Equation Solution)*

Let $\mathcal{A}, \mathcal{B}, R, Q$ be as above. There exists a nonnegative self-adjoint solution Π of

$$\mathcal{A}^*\Pi + \Pi\mathcal{A} - \Pi\mathcal{B}R^{-1}\mathcal{B}^*\Pi + Q = 0 \tag{3.26}$$

if and only if for each $w_0 \in \mathcal{H}$, there exists an admissible control. If this is true, then the unique optimal control and corresponding trajectory for (3.23) are given by

$$u(t) = -R^{-1}\mathcal{B}^*\Pi w(t)$$

and

$$w(t) = T(t)w_0$$

respectively, where Π is the unique minimal nonnegative self-adjoint solution of (3.26) and $T(t)$ is the strongly continuous semigroup generated by $\mathcal{A} - \mathcal{B}R^{-1}\mathcal{B}^*\Pi$. If $\|w(t)\| \to 0$ as $t \to \infty$ for any admissible control, then Π is the unique nonnegative self-adjoint solution of the algebraic Riccati equation and $T(t)$ is uniformly exponentially stable.

Assuming the special form $Q = \mathcal{C}^*\mathcal{C}$ we have the following useful result.

Theorem 3.7 *(e.g., [CP78, page 111])*

If $(\mathcal{A}, \mathcal{B})$ is stabilizable and $(\mathcal{A}, \mathcal{C})$ is detectable, then the algebraic Riccati equation has a unique nonnegative self-adjoint solution Π.

3.4.2 Approximation of the LQR Problem

Solution of the bounded infinite-dimensional LQR problem, denoted by $(\mathcal{A}, \mathcal{B}, Q, R)$, requires the solution of an infinite-dimensional algebraic Riccati equation. Such

a Riccati equation cannot usually be solved. A sequence of finite-dimensional problems will be shown to converge to the solution of the infinite-dimensional problem provided certain criteria are met. We begin by formulating a sequence of approximate finite-dimensional regulator problems, which will be denoted by $(A_n, B_n, Q_n, \mathbb{R}^n)$.

For $n = 1, 2, \ldots$, consider a sequence $\mathcal{H}_n$ of finite-dimensional linear subspaces of $\mathcal{H}$. Let $(\mathcal{H}_n, A_n, B_n)$ be the corresponding problem. Let P_n be the orthogonal projection of $\mathcal{H}$ onto $\mathcal{H}_n$. Also, $A_n : \mathcal{H}_n \to \mathcal{H}_n$, $B_n \in \mathcal{L}(\mathcal{U}, \mathcal{H}_n)$, $Q_n \in \mathcal{L}(\mathcal{H}_n, \mathcal{H}_n)$, and $R \in \mathcal{L}(\mathcal{U}, \mathcal{U})$.

Consider the sequence of finite-dimensional regulator problems:

$$\text{Minimize} \left\{ J_n(u, w_n(0)) \text{ where } u \in L_2(0, \infty; \mathcal{U}) \right\} \tag{3.27}$$

subject to

$$\begin{aligned} \dot{w}_n(t) &= A_n w_n(t) + B_n u(t), \quad t > 0 \\ w_n(0) &= w_{n_0} \equiv P_n w_0 \end{aligned} \tag{3.28}$$

where

$$J_n(u, w_n(0)) = \int_0^\infty \Big[\langle w_n(t), Q_n w_n(t) \rangle + \langle u(t), Ru(t) \rangle \Big] \, dt. \tag{3.29}$$

The solution of (3.28) is given by

$$w_n(t) = S_n(t) P_n w_0 + \int_0^t S_n(t - \tau) B_n u(\tau) \, d\tau$$

where $S_n(t)$ is a sequence of C_0 semigroups on $\mathcal{H}_n$ with infinitesimal generators A_n. If there exists an admissible control $u_n \in L_2(0, \infty; \mathcal{U})$, then the optimal control for (3.27) is given by

$$u_n(t) = -R^{-1} B_n^* \Pi_n w_n(t) \tag{3.30}$$

where $\Pi_n \in \mathcal{L}(\mathcal{H}_n, \mathcal{H}_n)$ is the unique minimal nonnegative self-adjoint solution of the algebraic Riccati equation

$$A_n^* \Pi_n + \Pi_n A_n - \Pi_n B_n R^{-1} B_n^* \Pi_n + Q_n = 0 \tag{3.31}$$

for the approximating system, and $w_n(t)$ is the corresponding solution of (3.28) with $u(t)$ given in (3.30). As before, A_n^* is the infinitesimal generator of a strongly continuous semigroup of operators $S_n^*(t)$ adjoint to $S_n(t)$.

We require several assumptions on the approximations for simulation and control. The following assumptions are necessary for the simulation of approximations to bounded control systems.

(S1b) For each $w \in \mathcal{H}$, we have

$$S_n(t) P_n w \to S(t) w$$

where the convergence is uniform in t on bounded subsets of $[0, \infty)$.

(S2b) For each $v \in \mathcal{U}$, $B_n v \to \mathcal{B} v$, and for each $w \in \mathcal{H}$, $B_n^* w \to \mathcal{B}^* w$.

(S3b) For each $w \in \mathcal{H}$, $Q_n P_n w \to Q w$.

The following assumptions are sufficient for controller design using the approximating control systems.

(C1b) For each $w \in \mathcal{H}$, we have

$$S_n(t)^* P_n w \to S^*(t) w$$

where the convergence is uniform in t on bounded subsets of $[0, \infty)$.

(C2b) If $(\mathcal{A}, \mathcal{B})$ is exponentially stabilizable, then $\{(A_n, B_n)\}$ is uniformly exponentially stabilizable by some $\{K_n\}$, where $\|K_n\| \leq M$.

Theorem 3.8 *[BK84]*

Assume (S1b)–(S3b) and (C1b) hold. Let Π_n be the unique nonnegative self-adjoint solution to the Riccati equation on $\mathcal{H}_n$ for the approximating formulation (3.29). Assume $(\mathcal{A}, \mathcal{B})$ and (A_n, B_n) are uniformly exponentially stabilizable by some operators K and $K_n = KP_n$, respectively. Let M_1, M_2, $\sigma > 0$. Let $T_n(t)$ indicate the semigroups generated by $A_n - B_n R^{-1} B_n^* \Pi_n$ on $\mathcal{H}_n$. Then

$$\|T_n(t)\|_{\mathcal{H}_n} \leq M_1 e^{-\sigma t} \quad \text{for } t \geq 0,\ n = 1, 2, \ldots, \tag{3.32}$$

$$\|\Pi_n\|_{\mathcal{H}_n} \leq M_2, \tag{3.33}$$

and (A_n, B_n) is uniformly exponentially stabilizable by the operator $K_n = R^{-1} B_n^* \Pi_n$.

Thus, an approximating scheme is suitable for LQR controller design if (S1b)–(S3b) and (C1b)–(C2b) are satisfied. These include conditions on

(1) the existence of an admissible control in the approximating system,

(2) the convergence of the approximating semigroups $S_n(t)$ and approximating adjoints of semigroups $S_n^*(t)$,

(3) the convergence of the approximating control operators B_n and adjoints of control operators B_n^*, and

(4) the uniform stabilizability of the approximations (A_n, B_n).

Ito and Morris [IM98] study approximations to the solution to operator Riccati equations for H_∞ control. The authors make the same assumptions required in the approximation of the LQR problem and show that the sequence of solutions to the finite-dimensional (H_∞) Riccati equations converge to the solution of the corresponding infinite-dimensional (H_∞) Riccati equation.

In the following section, we will consider the analogous unbounded control case. We will look for similar conditions for suitability of the finite-dimensional approximations for controller design.

3.5 Infinite-Dimensional Unbounded Control Systems

Consider the state-space representation in (3.20). For bounded linear operators $\mathcal{B}$ and $\mathcal{C}$, the input/output map is given by

$$y(t) = \mathcal{C} \int_0^t S(t-\tau)\mathcal{B}u(\tau)\, d\tau.$$

When $\mathcal{B}$ and $\mathcal{C}$ are unbounded operators, this map is no longer well-defined.

In this section, we will consider the case of point observation and control, as in the one-dimensional duct model in Chapter 2. In the standard state-space representation,

$$\dot{w}(t) = \mathcal{A}w(t) + \mathcal{B}u(t), \quad w(0) = w_0, \tag{3.34}$$

and

$$y(t) = \mathcal{C}w(t), \tag{3.35}$$

this leads to unbounded operators $\mathcal{C}$ and $\mathcal{B}$. Let $\mathcal{W}$, $\mathcal{H}$, and $\mathcal{V}$ be Hilbert spaces such that $\mathcal{W} \hookrightarrow \mathcal{H} \hookrightarrow \mathcal{V}$. Suppose $\mathcal{A} \in \mathcal{L}(\mathcal{W}, \mathcal{H})$, $\mathcal{B} \in \mathcal{L}(\mathcal{U}, \mathcal{V})$ and $\mathcal{C} \in \mathcal{L}(\mathcal{W}, \mathcal{Y})$. We assume that $\mathcal{A}$ is the infinitesimal generator of a strongly continuous semigroup $S(t)$ on all three spaces $\mathcal{W}$, $\mathcal{H}$, and $\mathcal{V}$. Then for $u \in H_1(0,t;\mathcal{U})$, the solution to (3.34) is

$$w(t) = S(t)w_0 + \int_0^t S(t-\tau)\mathcal{B}u(\tau)\, d\tau$$

where S is in $\mathcal{V}$. However, $w(t)$ may not be in the domain of the operator C. For $\mu \in \rho(\mathcal{A})$ and $u \in H_2(0,t;\mathcal{U})$, (3.34) may be written as

$$w(t) = (\mu I - \mathcal{A})^{-1}\Big(\mu w(t) - \dot{w}(t)\Big) + (\mu I - \mathcal{A})^{-1}\mathcal{B}u(t).$$

This suggests defining

$$y(t) = C(\mu I - \mathcal{A})^{-1}\Big(\mu w(t) - \dot{w}(t)\Big) + G_\mu u(t)$$

for some $G_\mu \in \mathcal{L}(\mathcal{U},\mathcal{Y})$. To summarize, the state-space realization on $\mathcal{H}$ is

$$\begin{aligned} \dot{w}(t) &= \mathcal{A}w(t) + \mathcal{B}u(t), \quad w(0) = w_0, \\ y(t) &= C(\mu I - \mathcal{A})^{-1}\Big(\mu w(t) - \dot{w}(t)\Big) + G_\mu u(t). \end{aligned} \tag{3.36}$$

This system is said to be *well-posed* if both the state $w(t)$ and the output $y(t)$ depend continuously on the initial state w_0 and the input $u(t)$. The formal definition is as follows.

Definition 3.14 *(Well-posedness of an unbounded control system (e.g., [Sal87]))*

The state-space realization given in (3.36) is said to be well-posed if the following four conditions hold for all $t \geq 0$:

(WP1) *The operator $\mathcal{A}$ with domain $D(\mathcal{A})$ generates a strongly continuous semigroup on all three spaces $\mathcal{W}$, $\mathcal{H}$, and $\mathcal{V}$.*

(WP2) *There exists a constant c_1 such that for all $u \in H_1(0,t;\mathcal{U})$*

$$\left\| \int_0^t S(t-\tau)\mathcal{B}u(\tau)\, d\tau \right\|_{\mathcal{H}} \leq c_1 \|u\|_{L_2(0,t;\mathcal{U})}.$$

(WP3) *There exists a constant c_2 such that for all $w \in \mathcal{W}$*

$$\|CS(\cdot)w_0\|_{L_2(0,t;\mathcal{Y})} \leq c_2 \|w_0\|_{\mathcal{H}}.$$

(WP4) *There exists a constant c_3 such that for all $u \in H_2(0,t;\mathcal{U})$ with $u(0) = 0$*

$$\|y\|_{L_2(0,t;\mathcal{Y})} \leq c_3 \|u\|_{L_2(0,t;\mathcal{U})}.$$

The above conditions essentially ensure that the mappings from the input to the output, the input to the state, and the state to the output are bounded and continuous in some sense. When the transfer function $G(s)$ from u to y is known, condition (WP4) may be established using the following result.

Theorem 3.9 *[CW89]*

Suppose $(\mathcal{A},\mathcal{B},\mathcal{C})$ satisfies conditions (WP1)-(WP3). Condition (WP4) is satisfied if and only if there exists a real number δ such that the transfer function G satisfies

$$\sup_{\Re(s)>\delta} \|G(s)\|_{\mathcal{L}(\mathcal{U},\mathcal{Y})} < \infty.$$

We now consider the well-posedness of the one-dimensional duct model described in Chapter 2.

3.5.1 Well-posedness of the One-Dimensional Duct Model

We first formulate the state-space representation of the one-dimensional duct model first presented in Chapter 2 (see (2.1), (2.2), and (2.3)).

The state-space for the state (z, z_t) is $\mathcal{H} = \overline{H}_1(0,L) \times L_2(0,L)$ (see page 34). Then $\mathcal{A} : D(\mathcal{A}) \subset \mathcal{H} \to \mathcal{H}$ is given by

$$\mathcal{A}\begin{bmatrix} \zeta \\ \xi \end{bmatrix} = \begin{bmatrix} 0 & I \\ c^2\frac{d^2}{dx^2} & 0 \end{bmatrix}\begin{bmatrix} \zeta \\ \xi \end{bmatrix} \tag{3.37}$$

where

$$D(\mathcal{A}) = \left\{(\zeta,\xi) \in \mathcal{H} \mid \xi \in \overline{H}_1(0,L), \zeta_{xx} \in L_2(0,L), \zeta_x(0) = 0, \zeta_x(L) = -\frac{K}{c}\xi(L)\right\}.$$

The eigenvalues λ_n of $\mathcal{A}$ are

$$\lambda_n = -\frac{c}{2L}\ln\alpha + \frac{n\pi cj}{L}, \quad n = 0, \pm 1, \pm 2, \ldots. \tag{3.38}$$

The eigenfunctions ϕ_n of $\mathcal{A}$ are

$$\phi_n = \begin{bmatrix} \frac{1}{\lambda_n}(e^{\frac{\lambda_n x}{c}} + e^{\frac{-\lambda_n x}{c}}) \\ e^{\frac{\lambda_n x}{c}} + e^{\frac{-\lambda_n x}{c}} \end{bmatrix}. \tag{3.39}$$

The adjoint operator $\mathcal{A}^*$ of $\mathcal{A}$ is

$$\mathcal{A}^* \begin{bmatrix} y_1 \\ y_2 \end{bmatrix} = \begin{bmatrix} 0 & -I \\ -c^2\frac{d^2}{dx^2} & 0 \end{bmatrix} \begin{bmatrix} y_1 \\ y_2 \end{bmatrix} \tag{3.40}$$

where

$$D(\mathcal{A}^*) = \left\{(y_1,y_2) \in \mathcal{H} \mid y_2 \in \overline{H}_1(0,L), y_{1_{xx}} \in L_2(0,L), y_{1_x}(0) = 0, y_{1_x}(L) = \frac{K}{c}y_2(L)\right\}.$$

The eigenvalues μ_n of $\mathcal{A}^*$ are

$$\mu_n = \overline{\lambda_n}. \tag{3.41}$$

The eigenfunctions ψ_n of $\mathcal{A}^*$ are

$$\psi_n = \begin{bmatrix} \frac{a_n}{\mu_n}(e^{\frac{\mu_n x}{c}} + e^{\frac{-\mu_n x}{c}}) \\ -a_n(e^{\frac{\mu_n x}{c}} + e^{\frac{-\mu_n x}{c}}) \end{bmatrix} \tag{3.42}$$

where a_n are constants determined so that $\langle\phi_n,\psi_n\rangle_{\mathcal{H}} = \delta_{mn}$. It is easy to show that $a_n = -\frac{1}{4L}$. For simplicity of exposition, consider a single control input at x_d

and a single output measurement at x_s. The control space is then $\mathcal{U} = \mathbb{R}$. Define $\mathcal{W} = [D(\mathcal{A})]$ to be the domain of $\mathcal{A}$ equipped with the graph norm, i.e.,

$$\|w\|_{D(\mathcal{A}^*)} = \|w\|_{\mathcal{H}} + \|\mathcal{A}^* w\|_{\mathcal{H}}.$$

Also let $\mathcal{V} = [D(\mathcal{A}^*)]'$ where $\mathcal{X}'$ indicates the dual space of $\mathcal{X}$. Thus, $[D(\mathcal{A})] \hookrightarrow \mathcal{H} \hookrightarrow [D(\mathcal{A}^*)]'$. The control operator $\mathcal{B} \in \mathcal{L}(\mathcal{U}, \mathcal{V})$ is

$$\mathcal{B} = \begin{bmatrix} 0 \\ \frac{\delta(x-x_d)}{\rho} \end{bmatrix}. \tag{3.43}$$

Consider an observation (output) at x_s with observation space $\mathcal{Y} = \mathbb{R}$. The observation operator $\mathcal{C} \in \mathcal{L}(\mathcal{W}, \mathcal{Y})$ is

$$\mathcal{C} = -\rho c^2 \begin{bmatrix} \frac{d}{dx}\Big|_{x=x_s} & 0 \end{bmatrix}. \tag{3.44}$$

Spectral Representation of Semigroups

To show that (WP2) and (WP3) hold, we need a representation for $S(t)$. To find this representation, we use its spectral expansion. We will first find the spectral expansion when the states are in $\mathcal{H}_e = L_2(0, L) \times L_2(0, L)$. We will then use this result to show that $S(t)$ defined on $\mathcal{H}$ has a spectral expansion.

We begin with some mathematical preliminaries concerning the definition of a Riesz basis and Riesz spectral operator.

Definition 3.15 *(e.g., [CZ95, page 38])*

A sequence of vectors $\{\phi_n,\ n \geq 1\}$ in a Hilbert space $\mathcal{X}$ forms a Riesz basis for $\mathcal{X}$ if

(a) $\overline{span}_{n\geq 1}\{\phi_n\} = \mathcal{X}$, *and*

(b) *there exist positive constants* m *and* M *such that for arbitrary* $N \in \mathbb{N}$ *and arbitrary scalars* α_n, $n = 1, \ldots, N$,

$$m \sum_{i=1}^{N^*} |\alpha_n|^2 \leq \left\| \sum_{i=1}^{N^*} \alpha_n \phi_n \right\|^2 \leq M \sum_{i=1}^{N^*} |\alpha_n|^2.$$

Alternatively, we have the following result.

Theorem 3.10 *(e.g., [CZ95, Exercise 2.21(a), page 89])*

Let $\{e_n, n \geq 1\}$ *be an orthonormal basis for the Hilbert space* $\mathcal{X}$. *The set* $\{\phi_n, n \geq 1\}$ *forms a Riesz basis for* $\mathcal{X}$ *if and only if there exists a bounded invertible operator* $T \in \mathcal{L}(\mathcal{X})$ *such that* $\phi_n = Te_n, n \geq 1$.

Definition 3.16

Two sequences $\{\phi_n\}$ *and* $\{\psi_n\}$ *are* biorthogonal *if*

$$\langle \phi_m, \psi_n \rangle = \delta_{mn}.$$

The next theorem shows that any element in $\mathcal{X}$ can be uniquely represented as a linear combination of the Riesz basis elements ϕ_n by means of a biorthogonal sequence.

Theorem 3.11 *[CZ95, Lemma 2.3.2, page 38]*

Suppose that the closed, linear operator $\mathcal{A}$ *on the Hilbert space* $\mathcal{X}$ *has simple eigenvalues* $\{\lambda_n\}$, *for* $n = 1, 2, \ldots$, *and that its corresponding eigenfunctions* $\{\phi_n\}$ *for* $n = 1, 2, \ldots$, *form a Riesz basis for* $\mathcal{X}$.

(a) *If* $\{\psi_n\}$ *for* $n = 1, 2, \ldots$, *are the eigenfunctions of the adjoint of* $\mathcal{A}$ *corresponding to the eigenvalues* $\{\overline{\lambda_n}\}$ *for* $n = 1, 2, \ldots$, *then the* $\{\psi_n\}$ *can be suitably scaled so that* $\{\phi_n\}$ *and* $\{\psi_n\}$ *are biorthogonal.*

(b) *Every* $z \in \mathcal{X}$ *can be represented uniquely by*

$$z = \sum_{n=1}^{\infty} \langle z, \psi_n \rangle \phi_n$$

and there exist positive constants m *and* M *such that*

$$m \sum_{n=1}^{\infty} |\langle z, \psi_n \rangle|^2 \leq \|z\|^2 \leq M \sum_{n=1}^{\infty} |\langle z, \psi_n \rangle|^2.$$

In order to show that $S(t)$ has a spectral representation we need the following definition.

Definition 3.17 *(Riesz Spectral Operator, e.g., [CZ95, page 41])*

Suppose that $\mathcal{A}$ *is a linear, closed operator on a Hilbert space* $\mathcal{H}$ *with simple eigenvalues* $\{\lambda_n,\ n \geq 1\}$ *and suppose that the corresponding eigenfunctions* $\{\phi_n,\ n \geq 1\}$ *form a Riesz basis in* $\mathcal{H}$. *If the closure of* $\{\lambda_n,\ n \geq 1\}$ *is totally disconnected, then we call* $\mathcal{A}$ *a* Riesz spectral operator.

The following theorem provides a way of obtaining the spectral expansion of the semigroup $S(t)$ for a Riesz spectral operator.

Theorem 3.12 *[CZ95, Theorem 2.3.5(c), page 41]*

Suppose that $\mathcal{A}$ *is a Riesz-spectral operator with simple eigenvalues* $\{\lambda_n,\ n \geq 1\}$ *and corresponding eigenfunctions* $\{\phi_n,\ n \geq 1\}$. *Let* $\{\psi_m,\ m \geq 1\}$ *be the eigenfunctions of* $\mathcal{A}^*$ *such that* $\langle \phi_n, \psi_m \rangle = \delta_{nm}$. *Then* $\mathcal{A}$ *is the infinitesimal generator of a* C_0

semigroup if and only if $\sup_{n\geq 1} \Re(\lambda_n) < \infty$ *and* $S(t)$ *is given by*

$$S(t)\cdot = \sum_{n=1}^{\infty} e^{\lambda_n t}\langle \cdot, \psi_n\rangle \phi_n. \tag{3.45}$$

Let us now return to the one-dimensional duct model. In [MRH91], the authors define a "virtual duct" on $[-L, 0]$ and then use this model to define an inner product under which the eigenfunctions form an orthogonal basis. The following argument was inspired by this idea. Let $\mathcal{H}_e = L_2(0, L) \times L_2(0, L)$ with weighted norm

$$\|\cdot\|_e^2 = \langle \cdot, \cdot \rangle_e$$

where

$$\langle \zeta, \xi \rangle_e = c^2 \int_0^L \zeta_1 \overline{\xi_1}\, dx \; + \; \int_0^L \zeta_2 \overline{\xi_2}\, dx.$$

Consider the one-dimensional duct model with states $w = (z_x, z_t) \in \mathcal{H}_e$. The partial differential equation (2.1) with no control terms (i.e., $P_c(t) = 0$ and $P_d(t) = 0$) can be written as

$$\dot{w}(t) = \mathcal{A}_e w(t)$$

where

$$\mathcal{A}_e \begin{bmatrix} \zeta \\ \xi \end{bmatrix} = \begin{bmatrix} 0 & \frac{d}{dx} \\ c^2 \frac{d}{dx} & 0 \end{bmatrix} \begin{bmatrix} \zeta \\ \xi \end{bmatrix} \tag{3.46}$$

and the domain of $\mathcal{A}_e$ is

$$D(\mathcal{A}_e) = \left\{ (\zeta_1, \zeta_2) \in \mathcal{H} \mid \zeta_{1_x} \in L_2(0, L),\ \zeta_{2_x} \in L_2(0, L),\ \zeta_1(0) = 0,\ \zeta_1(L) = -\frac{K}{c}\zeta_2(L) \right\}.$$

The eigenvalues λ_n of $\mathcal{A}_e$ are the same as those of $\mathcal{A}$ (see (3.38)). The eigenfunctions ϕ_{n_e} of $\mathcal{A}_e$ are

$$\phi_{n_e} = \begin{bmatrix} \frac{1}{c}(e^{\frac{\lambda_n x}{c}} - e^{\frac{-\lambda_n x}{c}}) \\ e^{\frac{\lambda_n x}{c}} + e^{\frac{-\lambda_n x}{c}} \end{bmatrix}. \tag{3.47}$$

The adjoint $\mathcal{A}_e^*$ of $\mathcal{A}_e$ is given by

$$\mathcal{A}_e^* = \begin{bmatrix} 0 & -\frac{d}{dx} \\ -c^2\frac{d}{dx} & 0 \end{bmatrix}$$

and the domain of $\mathcal{A}_e^*$ is

$$D(\mathcal{A}_e^*) = \left\{(y_1, y_2) \in \mathcal{H}_e \mid y_{1x}, y_{2x} \in L_2(0, L), y_1(0) = 0, y_1(L) = \frac{K}{c}y_2(L)\right\}.$$

The eigenvalues μ_n of $\mathcal{A}_e^*$ are the same as those of $\mathcal{A}^*$ (see (3.41)). The eigenfunctions ψ_{n_e} of $\mathcal{A}_e^*$ are

$$\psi_{n_e} = \begin{bmatrix} \frac{a_n}{c}(e^{\frac{\mu_n x}{c}} - e^{\frac{-\mu_n x}{c}}) \\ -a_n(e^{\frac{\mu_n x}{c}} + e^{\frac{-\mu_n x}{c}}) \end{bmatrix} \tag{3.48}$$

where $a_n = -\frac{1}{4L}$.

Lemma 3.1 *[Mor97b]*

The functions $\{\phi_{n_e}\}$ defined in (3.47) form a Riesz basis for $\mathcal{H}_e$.

Proof:

The set

$$e_n = \begin{bmatrix} \frac{1}{c}\sqrt{\frac{2}{L}}\cos(\frac{n\pi x}{L}) \\ \sqrt{\frac{2}{L}}\sin(\frac{n\pi x}{L}) \end{bmatrix}, \quad n = 0, 1, \ldots,$$

form an orthonormal basis for $\mathcal{H}_e$. Let $r = -\frac{1}{2L}\ln\alpha$. Defining,

$$T_1 = \begin{bmatrix} \frac{1}{c} & -\frac{1}{c} \\ 1 & 1 \end{bmatrix}, \; T_2 = \begin{bmatrix} e^{-rx} & 0 \\ 0 & e^{rx} \end{bmatrix}$$

$$T_3 = \begin{bmatrix} \frac{1}{2} & \frac{1}{2} \\ \frac{1}{2j} & -\frac{1}{2j} \end{bmatrix}, \; T_4 = \begin{bmatrix} \frac{1}{c}\sqrt{\frac{2}{L}} & 0 \\ 0 & \sqrt{\frac{2}{L}} \end{bmatrix},$$

and finally

$$T = T_1T_2T_3T_4,$$

we have that

$$\phi_{n_e} = Te_n.$$

Thus, by Theorem 3.10, $\{\phi_{n_e}\}$ form a Riesz basis for $\mathcal{H}_e$. □

We now need to show that $\mathcal{A}_e$ is a closed linear operator. Clearly, $\mathcal{A}_e$ is linear. By [CZ95, Theorem A.3.46, page 596], we need to show that $\mathcal{A}_e$ is invertible with $\mathcal{A}_e^{-1} \in \mathcal{L}(\mathcal{H}_e, \mathcal{H}_e)$. Let

$$T = \begin{bmatrix} 0 & \frac{1}{c^2}Q^{-1} \\ Q^{-1} & 0 \end{bmatrix}$$

where $Q = \frac{d}{dx}$ and $Q^{-1}f = \int f(x)\,dx$. Clearly, T is bounded on $\mathcal{H}_e$, $\mathcal{A}_e T = I$, and $T\mathcal{A}_e = I$. Hence, $\mathcal{A}_e$ is a closed linear operator. Thus, by Theorem 3.11, every $w_e \in \mathcal{H}_e$ can be represented uniquely by

$$w_e = \sum_{n=1}^{\infty} \langle w_e, \psi_{n_e} \rangle_{\mathcal{H}_e} \phi_{n_e}$$

where convergence is in the $\mathcal{H}_e$ norm.

Theorem 3.13 *[Mor97b]*

The set $\{\phi_n\}$ of eigenfunctions in (3.39) form a Riesz basis for $\mathcal{H}$.

Proof:

Define $P \in \mathcal{L}(\mathcal{H}, \mathcal{H}_e)$

$$P = \begin{bmatrix} \frac{d}{dx} & 0 \\ 0 & I \end{bmatrix}.$$

Note that $P\phi_n = \phi_{n_e}$, $P\psi_n = \psi_{n_e}$ and that $\langle Pw, Pz \rangle_{\mathcal{H}_e} = \langle w, z \rangle_{\mathcal{H}}$ for any $w, z \in \mathcal{H}$. Choose any $w \in \mathcal{H}$. Since ϕ_{n_e} forms a Riesz basis on $\mathcal{H}_e$,

$$\begin{aligned} w &= P^{-1}Pw \\ &= P^{-1} \sum_{n=1}^{\infty} \langle Pw, \psi_{n_e} \rangle_{\mathcal{H}_e} \phi_{n_e}. \end{aligned}$$

Now since

$$P^{-1}f = \begin{bmatrix} \int f(x)\,dx & 0 \\ 0 & I \end{bmatrix}$$

is bounded from $\mathcal{H}_e$ to $\mathcal{H}$,

$$w = \sum_{n=1}^{\infty} \langle Pw, \psi_{n_e} \rangle_{\mathcal{H}_e} P^{-1}\phi_{n_e}$$

where convergence is now in $\mathcal{H}$. Thus,

$$\begin{aligned} w &= \sum_{n=1}^{\infty} \langle Pw, P\psi_n \rangle_{\mathcal{H}_e} \phi_n \\ &= \sum_{n=1}^{\infty} \langle w, \psi_n \rangle_{\mathcal{H}} \phi_n. \end{aligned}$$

Thus, $\overline{span(\phi_n)} = \mathcal{H}$. Now, for any scalars $\alpha_n, n = 1, 2, \ldots, N$, where N is arbitrary,

$$\begin{aligned} \left\| \sum_{n=1}^{N} \alpha_n \phi_n \right\|^2 &= \left\| P^{-1} P \sum_{n=1}^{N} \alpha_n \phi_n \right\|^2 \\ &= \left\| P^{-1} \sum_{n=1}^{N} \alpha_n \phi_{n_e} \right\|^2 \\ &= \left\| \sum_{n=1}^{N} \alpha_n \phi_{n_e} \right\|_e^2. \end{aligned}$$

But $\{\phi_{n_e}\}$ form a Riesz basis for $\mathcal{H}_e$. Therefore, there exist positive constants m and M such that

$$m \sum_{n=1}^{N} |\alpha_n|^2 \leq \left\| \sum_{n=1}^{N} \alpha_n \phi_{n_e} \right\|_e^2 \leq M \sum_{n=1}^{N} |\alpha_n|^2.$$

Thus, by Definition 3.15, the sequence $\{\phi_n\}$ form a Riesz basis for $\mathcal{H}$. □

We must finally show that $\mathcal{A}$ is a linear closed operator. Clearly, $\mathcal{A}$ is linear. By [CZ95, Theorem A.3.46, page 596], we need to show that $\mathcal{A}$ is invertible with $\mathcal{A}^{-1} \in \mathcal{L}(\mathcal{H}, \mathcal{H})$. Define

$$\tilde{T} = \begin{bmatrix} 0 & \frac{1}{c^2} Q^{-1} \\ I & 0 \end{bmatrix}$$

where $Q = \frac{d}{dx}$ and $Q^{-1}f = \int f(x)\,dx$. Now, for P defined by

$$P = \begin{bmatrix} Q & 0 \\ 0 & I \end{bmatrix},$$

we have

$$\mathcal{A}^{-1} = P^{-1}\tilde{T}.$$

Since P^{-1} and $\tilde{T}$ are bounded in $\mathcal{H}$, $\mathcal{A}$ is bounded in $\mathcal{H}$. Thus, $\mathcal{A}$ is a linear closed operator. Therefore, $\mathcal{A}$ is a Riesz spectral operator.

We now show that the one-dimensional duct model is well-posed.

Theorem 3.14

The system in (3.37), (3.43), and (3.44) is well-posed on $\mathcal{H}$.

Proof:

To show well-posedness, we must verify (WP1)–(WP4).

(WP1) We have shown that $\mathcal{A}$ is a Riesz spectral operator on $\mathcal{H}$ with simple eigenvalues $\{\lambda_n, n \geq 1\}$ and eigenfunctions $\{\phi_n, n \geq 1\}$ which form a Riesz basis in $\mathcal{H}$. By Theorem 3.12, we know that if $\sup_{n\geq 1} \Re(\lambda_n) < \infty$, then $\mathcal{A}$ is the infinitesimal generator of a C_0 semigroup. Since $\Re(\lambda_n) = -\frac{c}{2L}\ln\alpha$, this result follows trivially. The semigroup $S(t)$ defined on $\mathcal{H}$ can be extended to $\mathcal{W} = [D(\mathcal{A})]$ and $\mathcal{V} = [D(\mathcal{A}^*)]'$ [Sal84]. Thus, (WP1) holds.

(WP2) [Mor97b] First note that $\mathcal{B} \in \mathcal{L}(\mathcal{U}, \mathcal{V})$. Now, since S has an expansion in terms of the Riesz basis

$$\begin{aligned} \int_0^T S(T-s)\mathcal{B}u(s)\,ds &= \int_0^T \sum_{n=1}^{\infty} e^{\lambda_n(T-s)}\langle \mathcal{B}u, \psi_n\rangle_{\mathcal{V},\mathcal{V}^*}\phi_n\,ds \\ &= \int_0^T \sum_{n=1}^{\infty} e^{\lambda_n(T-s)}u(s)\mathcal{B}^*\psi_n\phi_n\,ds \end{aligned}$$

where convergence is in $\mathcal{V}$. This convergence is independent of s and so

$$\int_0^T S(T-s)\mathcal{B}u(s)\,ds = \sum_{n=1}^{\infty} \int_0^T e^{\lambda_n(T-s)}u(s)\,ds\mathcal{B}^*\psi_n\phi_n,$$

where convergence is guaranteed in $\mathcal{V}$.

If

$$\sum_{n=1}^{\infty}\left[\int_0^T e^{\lambda_n(T-s)}u(s)\,ds\mathcal{B}^*\psi_n\right]^2 \leq M_1^2\|u\|^2_{L_2(0,T;\mathcal{U})}, \tag{3.49}$$

then

$$B(T)u := \int_0^T S(T-s)\mathcal{B}u(s)\,ds \in \mathcal{H}$$

and $B(T) \in \mathcal{L}(L_2(0,T);\mathcal{H})$ for each T. Thus, in order to show (WP2), we need to prove (3.49).

First

$$\mathcal{B}^*\psi_n = -\frac{1}{4L}(e^{\frac{\mu_n x_d}{c}} - e^{-\frac{\mu_n x_d}{c}})$$

and

$$M_2 := \sup_n |\mathcal{B}^*\psi_n| < \infty.$$

Also,

$$\left|\int_0^T e^{\lambda_n(T-s)}u(s)\,ds\right| \leq \left|\int_0^T u(s)e^{-\frac{jn\epsilon\pi s}{L}}\,ds\right|.$$

By standard results in Fourier series theory,

$$\sum_{n=1}^{\infty}\left[\int_0^T u(s)e^{-\frac{jn\epsilon\pi s}{L}}\,ds\right]^2 \leq M_3^2\|u\|^2_{L_2(0,T;\mathcal{U})}$$

for some constant M_3. Therefore, (3.49) is true with $M_1 = M_2M_3$ and (WP2) holds.

(WP3) [Mor97b] We now prove (WP3) or, equivalently, that

$$\left\|\int_0^T S^*(T-s)\mathcal{C}^*u(s)\,ds\right\|_{\mathcal{H}} \leq M\|u\|_{L_2(0,T;\mathcal{U})}. \tag{3.50}$$

The spectral expansion of $S^*(t)$ is

$$S^*(t)z = \sum_{n=1}^{\infty} e^{\mu_n t}\langle z, \phi_n\rangle\psi_n$$

and

$$\int_0^T S^*(T-s)C^*u(s)\,ds = \int_0^T \sum_{n=1}^{\infty} e^{\mu_n(T-s)}u(s)C\phi_n\psi_n\,ds.$$

As for the proof of (WP2), in order to prove (3.50) we need to prove

$$\sum_{n=1}^{\infty}\left(\int_0^T e^{\mu_n(T-s)}u(s)\,ds\,C\phi_n\right)^2 < \infty.$$

But

$$\sup_n |C\phi_n| = \sup_n |\rho c(e^{\frac{\lambda_n x_s}{c}} - e^{\frac{\lambda_n x_s}{c}})| < \infty$$

and $\mu_n = \overline{\lambda_n}$. The proof is identical to that of (WP2). Thus, (WP3) holds.

(WP4) In Chapter 2, Section 2.3, we showed that $G(x_1, x_2)$ is bounded in the right half plane for all feasible inputs at x_1 and outputs at x_2. Thus, by Theorem 3.9, (WP4) holds.

Therefore, since (WP1)-(WP4) hold, we conclude that the one-dimensional duct model is well-posed. □

3.5.2 Linear Quadratic Regulator Problem

In Section 3.4.1 we considered the LQR problem for bounded control systems. We showed that under certain assumptions including uniform stabilizability of the approximations, the optimal feedback control for the approximations converges to the infinite-dimensional solution.

In this section, we will look at the analogous LQR problem for unbounded systems and review the existing results. We will show that under certain assumptions the approximating optimal state feedback operators converge to the infinite-dimensional solution. These results are similar to those for bounded control systems. We will review the results of Ito and Tran [IT89] which apply to Pritchard-Salamon systems (defined below), and Banks and Ito [BI97] which apply to unbounded systems that generate analytic semigroups. First we consider the work of Ito and Tran.

The Pritchard-Salamon conditions [PS87] for well-posedness are similar to but more restrictive than conditions (WP1)-(WP4).

Definition 3.18

A control system of the form

$$w(t) = S(t)w_0 + \int_0^t S(t-\tau)\mathcal{B}u(\tau)\,d\tau$$
$$y(t) = \mathcal{C}w(t)$$

where $w_0 \in \mathcal{V}$ and $t \geq 0$ is called a Pritchard-Salamon system if, for $\mathcal{W} \hookrightarrow \mathcal{H} \hookrightarrow \mathcal{V}$, the following four conditions hold.

(WP1) ' *The operator $\mathcal{A}$ with domain $D(\mathcal{A})$ generates a strongly continuous semigroup $S(t)$ on all three spaces $\mathcal{W}$, $\mathcal{H}$, and $\mathcal{V}$.*

(WP2) ' *There exists a constant c_1 such that for all $u \in L_2(0,t;\mathcal{U})$*

$$\left\| \int_0^t S(t-\tau)\mathcal{B}u(\tau)\,d\tau \right\|_{\mathcal{W}} \leq c_1 \|u\|_{L_2(0,t;\mathcal{U})}.$$

(WP3) ' *There exists a constant c_2 such that for all $w \in \mathcal{W}$*

$$\|\mathcal{C}S(\cdot)w\|_{L_2(0,t;\mathcal{Y})} \leq c_2 \|w\|_{\mathcal{V}}.$$

(WP4) ′ *There exists a constant* c_3 *such that for all* $u \in L_2(0,t;\mathcal{U})$ *with* $u(0) = 0$

$$\|y\|_{L_2(0,t;\mathcal{Y})} \leq c_3 \|u\|_{L_2(0,t;\mathcal{U})}.$$

It is more difficult to determine whether a system is Pritchard-Salamon than well-posed. Norms on the spaces $\mathcal{W}$ and $\mathcal{V}$ enter as part of conditions (WP2) ′ and (WP3) ′, and the choice of these spaces is generally not obvious. Curtain [Cur88] gives conditions for systems to belong to this class. The following are required assumptions.

Assumptions:

As shown in Section 3.5.1, our system satisfies the following.

(1) The operator $\mathcal{A}$ has eigenvalues $\{\lambda_n\}_{n=1}^{\infty}$ and corresponding eigenfunctions $\{\phi_n\}_{n=1}^{\infty}$ which form a Riesz basis.

(2) The operator $\mathcal{A}^*$ has eigenvalues $\{\overline{\lambda_n}\}_{n=1}^{\infty}$ and corresponding eigenfunctions $\{\psi_n\}_{n=1}^{\infty}$ which form a biorthogonal sequence on $\mathcal{H}$.

(3) The semigroup $S(t)$ generated by $\mathcal{A}$ has the spectral representation

$$S(t)\cdot = \sum_{n=1}^{\infty} e^{\lambda_n t}\langle \cdot, \psi_n\rangle \phi_n.$$

(4) Define

$$\begin{aligned} c_n &= C\phi_n \\ b_n &= B^*\psi_n \end{aligned}$$

for $n = 1, 2, \ldots, \infty$.

We then have the following result.

Theorem 3.15 *[Cur88]*

Suppose

(i) $b_n = 0$, $c_n \neq 0$, $\Re\lambda_n \neq 0$, $n^2\|c_n\|_{\mathcal{Y}}|\Re\lambda_n| < 1$, *for sufficiently large* n;

(ii) $c_n = 0$, $b_n \neq 0$, $\Re\lambda_n \neq 0$, $n^2\|b_n\|_{\mathcal{U}} < |\Re\lambda_n|$, *for sufficiently large* n; *and*

(iii) $\sup_n |\Re\lambda_n| \geq \epsilon > 0$.

Then conditions (WP2)' and (WP3)' are satisfied if

$$\sum_{n\in I} \frac{\|c_n\|_{\mathcal{Y}}\|b_n\|_{\mathcal{U}}}{|\Re\lambda_n|^{1/2}} < \infty \tag{3.51}$$

where $I = \{n \in \boldsymbol{N} : \ \Re\lambda_n < 0\}$.

In our system,

$$c_n = C\phi_n = -\rho c\left(e^{\frac{\lambda_n x_s}{c}} - e^{\frac{-\lambda_n x_s}{c}}\right)$$

and

$$b_n = \mathcal{B}^*\psi_n = -\frac{a_n}{\rho}\left(e^{\frac{\mu_n x_d}{c}} + e^{-\frac{\mu_n x_d}{c}}\right).$$

Thus, for $\mathcal{Y} = \mathbb{R}$,

$$n^2\|c_n\|_{\mathbb{R}} = n^2\rho c\left|e^{\frac{\lambda_n x_s}{c}} - e^{\frac{-\lambda_n x_s}{c}}\right|$$

which grows without bound as n gets large. Therefore condition (i) of Theorem 3.15 fails. It is unlikely that the one-dimensional duct model is Pritchard-Salamon. Nevertheless, reviewing the results of Ito and Tran still provides some insight into approximating infinite-dimensional systems.

Let $\mathcal{H}$, $\mathcal{U}$, $\mathcal{V}$, and $\mathcal{Y}$ be Hilbert spaces such that $\mathcal{W} \hookrightarrow \mathcal{H} \hookrightarrow \mathcal{V}$. Consider a semigroup control system defined on a Hilbert space $\mathcal{H}$,

$$\begin{aligned} \dot{w}(t) &= \mathcal{A}w(t) + \mathcal{B}u(t), \ w(0) = w_0 \\ y(t) &= Cw(t) \end{aligned} \tag{3.52}$$

where $\mathcal{A}$ is the infinitesimal generator of a strongly continuous semigroup $S(t)$ on $\mathcal{H}$. Also suppose $\mathcal{B} \in \mathcal{L}(\mathcal{U}, \mathcal{V})$ and $\mathcal{C} \in \mathcal{L}(\mathcal{W}, \mathcal{Y})$. To allow for solutions in all three spaces $\mathcal{W}$, $\mathcal{H}$, and $\mathcal{V}$, Ito and Tran [IT89] make several assumptions on the semigroup $S(t)$, the details of which may also be found in Pritchard and Salamon [PS87]. Let $D(\mathcal{A}) \subset \mathcal{W}$ be restricted to $\mathcal{V}$ with a continuous dense embedding and let $D(\mathcal{A})$ be endowed with the graph norm of $\mathcal{A}$ on $\mathcal{V}$. For controls in $\mathcal{U}$, the weak solution of (3.52) is

$$w(t) = S(t)w_0 + \int_0^t S(t-\tau)\mathcal{B}u(\tau)\, d\tau. \tag{3.53}$$

Consider the special case when $Q = C^*C$. Then the associated cost functional is

$$J(u, w_0) = \int_0^\infty \Big[\langle Cw(t), Cw(t) \rangle + \langle u(t), Ru(t) \rangle \Big]\, dt. \tag{3.54}$$

For simplicity, we let the penalty on control $R = 1$. As in the bounded input/output case, the abstract linear optimal regulator problem is

$$\text{Minimize} \Big\{ J(u, w_0) \text{ where } u \in L_2(0, \infty; U) \Big\} \tag{3.55}$$

subject to w satisfying (3.53).

Similarly to the bounded input/output case we have the following definitions.

Definition 3.19 *(Stabilizability)*

The pair $(\mathcal{A}, \mathcal{B})$ is <u>stabilizable</u> if there exists an operator $K \in \mathcal{L}(\mathcal{V}, \mathcal{U})$ such that the operator $\mathcal{A} - \mathcal{B}K$ generates an exponentially stable semigroup on $\mathcal{V}$.

Definition 3.20 *(Detectability)*

The pair $(\mathcal{A}, \mathcal{C})$ is <u>detectable</u> if there exists an operator $F \in \mathcal{L}(\mathcal{Y}, \mathcal{V})$ such that the operator $\mathcal{A} - F\mathcal{C}$ generates an exponentially stable semigroup on $\mathcal{V}$.

The solution of the infinite-dimensional unbounded input/output LQR problem is summarized in the following theorem.

Theorem 3.16 *[PS87]*

Suppose $(\mathcal{A}, \mathcal{B})$ *is stabilizable and* $(\mathcal{A}, \mathcal{C})$ *is detectable. Then there exists a unique solution* $\Pi \in \mathcal{L}(\mathcal{V}, \mathcal{W})$ *where* $\Pi = \Pi^* \geq 0$ *to the algebraic Riccati equation*

$$(\mathcal{A}^*\Pi + \Pi\mathcal{A} - \Pi\mathcal{B}\mathcal{B}^*\Pi + \mathcal{C}^*\mathcal{C})w = 0$$

for all $w \in D(\mathcal{A})$. *The optimal control* u^* *that minimizes (3.54) is*

$$u^*(t) = -\mathcal{B}^*\Pi w(t).$$

3.5.3 Approximation of the LQR Problem

Consider a sequence of approximations $(A_n, B_n, C_n; i_n, j_n)$ such that $A_n \in \mathcal{L}(\mathbb{R}^n)$, $B_n \in \mathcal{L}(\mathcal{U}, \mathbb{R}^n)$, $C_n \in \mathcal{L}(\mathbb{R}^n, \mathcal{Y})$, and i_n and j_n are injective linear maps defined as follows:

$$i_n : \mathbb{R}^n \to \mathcal{H}$$
$$j_n : \mathbb{R}^n \to \mathcal{V}^*.$$

Let H_n be a sequence of finite-dimensional linear subspaces of $\mathcal{H}$ such that $H_n = image(i_n)$. The norm is induced from the $\mathcal{H}$ norm; that is, $\|z\|_N^2 = \|i_n z\|_{\mathcal{H}}^2$ for $z \in \mathbb{R}^n$. Also let $W_n = image(j_n)$ where $W_n \subset \mathcal{V}^*$. In general, $W_n \not\subset H_n$. The norm $\|\cdot\|_{\tilde{N}}$ on $\mathbb{R}^n$ is induced from one on $\mathcal{V}^*$; that is, $\|z\|_{\tilde{N}}^2 = \|j_n z\|_{\mathcal{V}^*}^2$ for $z \in \mathbb{R}^n$. Define the linear map k_n by $\langle k_n w, z\rangle_{\tilde{N}} = \langle w, j_n z\rangle_{\mathcal{V}^*}$ for $z \in \mathbb{R}^n$ and $w \in \mathcal{V}^*$.

Consider the following. The output equation $y(t) = Cw(t)$ can be written as [Gib83]

$$y(t) = Mw_0 + Lu$$

where

$$(Mw_0)(t) = CS(t)w_0 \qquad \text{for } w_0 \in \mathcal{W} \tag{3.56}$$

$$(Lu)(t) = C\int_0^t S(t-\tau)\mathcal{B}u(\tau)\,d\tau \qquad \text{for } u \in L_2(0,\infty;\mathcal{U}). \tag{3.57}$$

The cost functional (3.54) can be written as

$$J(u,w_0) = \|Mw_0 + Lu\|^2_{L_2(0,\infty;\mathcal{Y})} + \|u\|^2_{L_2(0,\infty;\mathcal{U})}.$$

The n^{th}-dimensional approximation of the cost functional is

$$J_n(u,w_0) = \|M_nw_0 + L_nu\|^2_{L_2(0,\infty;\mathcal{Y})} + \|u\|^2_{L_2(0,\infty;\mathcal{U})}$$

where

$$(M_nw_0)(t) = Ci_ne^{tA_n}(j_n)^*w_0, \qquad w_0 \in \mathcal{V} \tag{3.58}$$

and

$$(L_nu)(t) = Ci_n\int_0^t e^{(t-\tau)A_n}(i_n)^*\mathcal{B}u(\tau)\,d\tau, \qquad u \in L_2(0,\infty;\mathcal{U}). \tag{3.59}$$

With the above results, we have the following definition.

Definition 3.21

An approximation is consistent if, as $n \to \infty$, the following hold:

$$\begin{aligned}
\|M_nw_0 - Mw_0\|_{L_2(0,\infty;\mathcal{Y})} &\to 0, \quad \textit{for all } w_0 \in \mathcal{V} \\
\|L_nu - Lu\|_{L_2(0,\infty;\mathcal{Y})} &\to 0, \quad \textit{for all } u \in L_2(0,\infty;\mathcal{U}) \\
\|(M_n)^*y - M^*y\|_{\mathcal{V}^*} &\to 0, \quad \textit{for all } y \in L_2(0,\infty;\mathcal{Y}) \\
\|(L_n)^*y - L^*y\|_{\mathcal{V}^*} &\to 0, \quad \textit{for all } y \in L_2(0,\infty;\mathcal{Y}).
\end{aligned}$$

That is, an approximation is consistent if the output maps M_n, the input/output maps L_n, and their adjoints converge. For bounded control systems, this condition follows from the convergence of the semigroups S_n and their adjoints S_n^*. Let $P_{\mathcal{H}}^n$

be the orthogonal projection of $\mathcal{H}$ onto H_n. We also assume that $C_n(i_n)^* = CP_{\mathcal{H}}^n$ and $i_n B_n = P_{\mathcal{H}}^n \mathcal{B}$.

We have the following main convergence result.

Theorem 3.17 *[IT89, Theorem 2.6]*

Suppose that for some positive constant N,

(1) *the approximation is consistent,*

(2) *(A_n, B_n) is uniformly stabilizable; that is, there exist constants $M_1 \geq 1$, $\sigma_1 > 0$ independent of n and a sequence of operators $K_n \in \mathcal{L}(\mathbb{R}^n, \mathcal{U})$ such that*

$$\sup \|j_n(K_n)^*\|_{\mathcal{L}(\mathcal{U},\mathcal{V}^*)} < \infty,$$

$$\|j_n e^{t(A_n - B_n K_n)^*} k_n \phi\|_{\mathcal{V}^*} \leq M_1 e^{-\sigma_1 t} \|\phi\|_{\mathcal{V}^*},$$

and

(3) *(A_n, C_n) is uniformly detectable; that is, there exist constants $M_2 \geq 1$, $\sigma_2 > 0$ independent of n and a sequence of operators $F_n \in \mathcal{L}(\mathcal{Y}, \mathbb{R}^n)$ such that*

$$\sup \|(F_n)^* k_n\|_{\mathcal{L}(\mathcal{V}^*,\mathcal{Y})} < \infty,$$

$$\|j_n e^{t(A_n - F_n C_n)^*} k_n \phi\|_{\mathcal{V}^*} \leq M_2 e^{-\sigma_2 t} \|\phi\|_{\mathcal{V}^*},$$

for $n \geq N$ and $\phi \in \mathcal{V}^*$. Then, as $n \to \infty$,

$$\|j_n \Pi_n (j_n)^* w_0 - \Pi w_0\|_{\mathcal{V}^*} \to 0$$

for all $w_0 \in \mathcal{V}$, where Π is as in Theorem 3.16, and $\Pi_n = \Pi_n^* \geq 0$ is the unique solution to the approximate algebraic Riccati equation in $\mathbb{R}^n$

$$A_n^* \Pi_n + \Pi_n A_n - \Pi_n B_n B_n^* \Pi_n + C_n^* C_n = 0.$$

In addition, for each $u \in \mathcal{U}$,

$$\|j_n \Pi_n B_n u - \Pi \mathcal{B} u\|_{\mathcal{V}^*} \to 0$$

as $n \to \infty$.

We can see the recurrence of the following requirements of an approximating scheme for controller design:

(1) consistency of the approximations, and

(2) uniform stabilizability and detectability of the approximations.

We now consider the work of Banks and Ito [BI97] which applies to a different class of systems. Let $\mathcal{W}$, $\mathcal{H}$, and $\mathcal{V}$ be Hilbert spaces such that $\mathcal{W} \hookrightarrow \mathcal{H} \hookrightarrow \mathcal{V}$. There are not always the same spaces as in the definition of a well-posed system (see Definition 3.14). Consider a sesquilinear form σ on $\mathcal{W}$, i.e., $\sigma : \mathcal{W} \times \mathcal{W} \to \mathbb{C}$ such that

$$|\sigma(\phi, \psi)| \leq c\|\phi\|_{\mathcal{W}}\|\psi\|_{\mathcal{W}} \quad \text{for } \phi, \psi \in \mathcal{W} \tag{3.60}$$

and

$$\Re\sigma(\phi, \phi) \geq \omega\|\phi\|_{\mathcal{W}}^2 - \rho\|\phi\|_{\mathcal{H}}^2 \quad \text{for } \phi \in \mathcal{W} \tag{3.61}$$

where $\omega > 0$. If $\mathcal{A}$ is defined by

$$\sigma(\phi, \psi) = \langle -\mathcal{A}\phi, \psi\rangle_{\mathcal{V},\mathcal{W}} \quad \text{for all } \phi, \psi \in \mathcal{W}$$

and the adjoint operator $\mathcal{A}^* \in \mathcal{L}(\mathcal{W}, \mathcal{V})$ is defined by

$$\sigma(\phi, \psi) = \langle \phi, -\mathcal{A}^*\psi\rangle_{\mathcal{W},\mathcal{V}} \quad \text{for all } \phi, \psi \in \mathcal{W},$$

then $\mathcal{A}$ generates an analytic semigroup [Paz83] $S(t)$ on $\mathcal{H}$, $\mathcal{W}$, and $\mathcal{V}$ where $\mathcal{W} \hookrightarrow \mathcal{H} \hookrightarrow \mathcal{V}$ and

$$D_{\mathcal{H}}(\mathcal{A}) = \Big\{\phi \in \mathcal{W} : \ |\sigma(\phi, \psi)| \leq k_\phi\|\psi\|_{\mathcal{H}} \text{ for all } \psi \in \mathcal{W}\Big\}.$$

Thus, the sesquilinear form generates an analytic semigroup which implies the uniform stabilizability of $(\mathcal{A}, \mathcal{B})$. As we shall see, using these sesquilinear forms in the approximations also generates stable analytic semigroups which again are automatically uniformly stabilizable. Since the eigenvalues of $\mathcal{A}$ for the one-dimensional duct (see (2.10)) lie on a vertical line, the semigroup $S(t)$ generated by $\mathcal{A}$ is not analytic [Paz83]. Thus, the one-dimensional duct model does not fit the framework outlined by Banks and Ito. However, for completeness, we review the main existence and convergence results of Banks and Ito.

We need the following additional definitions. Define the sesquilinear forms σ_0 and σ_1 on $\mathcal{W}$ by

$$\sigma_0 = \frac{\sigma(\phi,\psi) + \overline{\sigma(\psi,\phi)}}{2}$$

and

$$\sigma_1 = \frac{\sigma(\phi,\psi) - \overline{\sigma(\psi,\phi)}}{2}$$

for $\phi, \psi \in \mathcal{W}$. Let $\mathcal{A}_0$ be a self-adjoint operators on $\mathcal{H}$ defined by

$$\begin{aligned} D(\mathcal{A}_0) &= \left\{ u \in \mathcal{W} : \ |\sigma_0(u,v)| \leq k_u \|v\|_{\mathcal{H}} \text{ for all } v \in \mathcal{W} \right\} \\ \langle \mathcal{A}_0 u, v \rangle &= \sigma_0(u,v) + \rho \langle u, v \rangle_{\mathcal{H}} \text{ for all } u, v \in \mathcal{W}, \end{aligned}$$

where

$$\sigma_0(u,u) + \rho\langle u,u\rangle_{\mathcal{H}} \geq \omega \|u\|^2_{\mathcal{W}} \text{ for } u \in \mathcal{W}.$$

Let $\Lambda = A_0^{1/2}$ with $D(\Lambda) = \mathcal{W}$. Also for $0 \leq \theta \leq 1$, let $\mathcal{W}_\theta = [\mathcal{W}, \mathcal{H}]_\theta = D(\Lambda^{1-\theta})$. Then $[\mathcal{W}, \mathcal{V}]_{1/2} = \mathcal{H}$ and

$$\begin{aligned} \|\phi\|_{\mathcal{W}_0} &\leq c\|\phi\|^{\theta}_{\mathcal{H}} \|\phi\|^{1-\theta}_{\mathcal{W}} \\ &\leq c\|\phi\|^{\theta/2}_{\mathcal{V}} \|\phi\|^{\theta/2}_{\mathcal{W}} \|\phi\|^{1-\theta}_{\mathcal{W}} \\ &\leq c\|\phi\|^{\theta/2}_{\mathcal{V}} \|\phi\|^{1-\theta/2}_{\mathcal{W}}. \end{aligned}$$

Let $C \in \mathcal{L}(\mathcal{W}, \mathcal{Y})$ and $B \in \mathcal{L}(\mathcal{U}, \mathcal{V})$. As in the bounded control case, we are concerned with minimizing the cost functional

$$J(u, w_0) = \int_0^\infty \Big[\langle Cw(t), Cw(t) \rangle + \langle u(t), u(t) \rangle \Big] \, dt.$$

The optimal feedback solution is given by the following theorem.

Theorem 3.18 *[BI97, Theorem 5.4]*

Suppose the sesquilinear form σ satisfies

$$|\sigma_1(\phi, \psi)| \leq \tilde{M} \|\phi\|_{\mathcal{W}_\theta} \|\psi\|_{\mathcal{W}}$$

for some $\tilde{M} > 0$ and $0 \leq \theta < 1$ for all ϕ, $\psi \in \mathcal{W}$, as well as (3.60) and (3.61). If $(\mathcal{A}, \mathcal{B})$ is stabilizable and $(\mathcal{A}, \mathcal{C})$ is detectable, then the algebraic Riccati equation

$$\sigma(x, \Pi y) + \sigma(y, \Pi x) + \langle B^* \Pi x, B^* \Pi y \rangle - \langle Cx, Cy \rangle = 0, \quad \text{for all } x, y \in \mathcal{W} \tag{3.62}$$

has a unique non-negative solution $\Pi = \Pi^* \in \mathcal{L}(\mathcal{W})$ and $A - BB^*\Pi$ generates a stable analytic semigroup $T(t)$, $t \geq 0$ on $\mathcal{H}$. The optimal control u^* is given by

$$u^*(t) = -B^* \Pi T(t) w, \quad t \geq 0, \text{ for } w \in \mathcal{H}.$$

Let W_n be a sequence of finite-dimensional subspaces of $\mathcal{W} \subset \mathcal{H}$. Let $A_n : W_n \to W_n$ be such that

$$\langle -A_n \phi, \psi \rangle = \sigma(\phi, \psi) \quad \text{for all } \phi, \psi \in W_n.$$

For $B \in \mathcal{L}(\mathcal{U}, \mathcal{V})$ define $B_n \in \mathcal{L}(\mathcal{U}, W_n)$ by

$$\langle B_n u, \psi \rangle = \langle u, B^* \psi \rangle \quad \text{for all } \psi \in W_n$$

and let $C_n = C|_{W_n}$.

Let P_n denote the usual orthogonal projection of $\mathcal{H}$ onto W_n; i.e., for $\phi \in \mathcal{H}$, $P_n \phi \in W_n$, and $\langle P_n \phi_n, \psi_n \rangle = \langle \phi, \psi \rangle$ for all $\psi \in W_n$. We have the following result for the approximating systems.

Theorem 3.19 *[BI97, Theorem 5.5]*

Suppose the assumptions of Theorem 3.18 hold. Also suppose that

(i) for any $\phi \in \mathcal{W}$, there exists a sequence $\phi_n \in W_n$ such that $\|\phi_n - \phi\|_{\mathcal{W}} \to 0$ as $n \to \infty$, and

(ii) there exists a constant $\tilde{c} > 0$ such that $\|P_n\phi\|_{\mathcal{W}} \leq \tilde{c}\|\phi\|_{\mathcal{W}}$ for all $\phi \in \mathcal{W}$.

Then, for n sufficiently large, there exists a unique non-negative solution $\Pi_n = \Pi_n^* \in \mathcal{L}(\mathcal{W}) \cap \mathcal{L}(\mathcal{H})$ to the algebraic Riccati equation in W_n

$$\sigma(x, \Pi_n y) + \sigma(y, \Pi_n x) + \langle B^*\Pi_n x, B^*\Pi_n y\rangle - \langle Cx, Cy\rangle = 0, \quad \text{for all } x, y \in W_n,$$

and there exist constants $\tilde{M} \geq 1$ and $\tilde{\omega} > 0$ such that

$$\|e^{t(A_n - B_n B_n^* \Pi_n)} P_n\phi\|_{\mathcal{H}} \leq \tilde{M} e^{-\tilde{\omega}t}\|\phi\|_{\mathcal{H}}, \quad t \geq 0. \tag{3.63}$$

In addition,

$$\Pi_n P_n \phi \to \Pi\phi \quad \text{strongly in } \mathcal{H} \text{ for each } \phi \in \mathcal{H},$$

$$\Pi_n P_n \phi \to \Pi\phi \quad \text{weakly in } \mathcal{W} \text{ for each } \phi \in \mathcal{W},$$

and $B^*\Pi_n P_n \to B^*\Pi$ strongly in $\mathcal{L}(\mathcal{W}, \mathcal{U})$ is the unique non-negative solution to (3.62). Also, for n sufficiently large, $\mathcal{A} - \mathcal{B}B_n^*\Pi_n$ generates a stable analytic semigroup on $\mathcal{H}$.

The inequality in (3.63) and the assumptions in the theorem statement imply that the approximations are uniformly stabilizable if the original system is stabilizable. As well, for all $\phi \in \mathcal{H}$,

$$\|S_n(t)P_n\phi - S(t)\phi\|_{\mathcal{H}} \to 0$$

and

$$\|S_n^*(t)P_n\phi - S^*(t)\phi\|_{\mathcal{H}} \to 0$$

as $n \to \infty$, where convergence is uniform on bounded t-intervals [BI97].

In the next section, we will discuss general requirements of an approximating scheme for guaranteed convergence of the closed loop system.

3.6 General Conditions for Approximating Systems

Consider the following differential equation defined on a (possibly infinite-dimensional) Hilbert space $\mathcal{H}$:

$$\begin{aligned} \dot{w}(t) &= \mathcal{A}w(t) + \mathcal{B}u(t), \quad w(0) = w_0, \\ y(t) &= \mathcal{C}w(t). \end{aligned} \tag{3.64}$$

The operator $\mathcal{A}$ generates a strongly continuous semigroup of operators $S(t)$ on $\mathcal{H}$ so that $\mathcal{A}$ is closed with domain $D(\mathcal{A})$ dense in H, i.e., $\mathcal{A} : D(\mathcal{A}) \subset \mathcal{H} \to \mathcal{H}$. In general $\mathcal{B}$ and $\mathcal{C}$ may be unbounded.

Practical design and simulation involving (3.64) is generally very difficult and in most cases it is impossible to determine a closed form solution. Thus, it is necessary to approximate (3.64) on some finite-dimensional subspace $\mathcal{H}_n \subset \mathcal{H}$. Let P_n denote the orthogonal projection of $\mathcal{H}$ onto $\mathcal{H}_n$. Also, $A_n : D(A_n) \to \mathcal{H}_n$, $B_n := P_n\mathcal{B}$ and $C_n := \mathcal{C}|_{\mathcal{H}_n}$. This approximation is given by a system of n ordinary differential equations,

$$\begin{aligned} \dot{w}_n(t) &= A_n w_n(t) + B_n u(t), \quad w_n(0) = w_{n_0}, \\ y(t) &= C_n w_n(t). \end{aligned} \tag{3.65}$$

For $u(t) \in L_2(0, \infty; \mathbb{R}^p)$, (3.65) has the mild solution

$$y(t) = C_n S_n(t) w_{n_0} + C_n \int_0^t S_n(t-\tau) B_n u(\tau)\, d\tau.$$

The transfer function from u to y is given by $C_n(sI - A_n)^{-1}B_n$. We would like to use the above finite-dimensional system for both controller design and simulation. The designed controller should behave as predicted by computer simulation when implemented with the original infinite-dimensional system.

A scheme that is good for simulation may not be appropriate for controller design. In particular, although sufficient for simulation, convergence of the approximating semigroups $S_n(t)$ for the open loop response is not sufficient to ensure that the approximating scheme is compatible for controller design. Consider the following assumptions, standard in schemes for simulation (e.g., [BK84], [Ito87], [Mor96]).

(S1) For all $w \in \mathcal{H}$, $\lim_{n\to\infty} \|P_n w - w\| = 0$.

(S2) Let $\mathcal{H} \subset \mathcal{V}$ so that $\mathcal{B} \in \mathcal{L}(\mathcal{U}, \mathcal{V})$. Then, as $n \to \infty$,

$$\|B_n u - \mathcal{B}u\|_{\mathcal{V}} \to 0, \quad \text{for all } u \in \mathcal{U}$$

and

$$\|B_n^* u - \mathcal{B}^* u\|_{\mathcal{U}} \to 0, \quad \text{for all } w \in \mathcal{H}.$$

(S3) For all $w \in \mathcal{H}$, $S_n(t)P_n w \to S(t)w$.

(S4) The semigroups $S_n(t)$ are uniformly bounded, i.e., there exist real numbers M, k, and an integer N such that

$$\|S_n(t)\| \leq Me^{kt}, \quad \text{for all } n \geq N$$

where the convergence is uniform in t on bounded subsets of $[0, \infty)$.

Morris [Mor96] gives an example of an approximation scheme for a bounded control system that meets assumptions (S1)–(S4), but is not suitable for controller design.

The following assumptions appear in all existing results on LQR controller design using approximations. Similar assumptions on the approximating systems for non-singular H_∞ state-feedback control problems are made in [IM98].

(C1) For all $w \in \mathcal{H}$, $S_n^*(t)P_n w \to S^*(t)w$ where the convergence is uniform in t on bounded subsets of $[0, \infty)$.

(C2) If the original system $(\mathcal{A}, \mathcal{B})$ is stabilizable, then the approximations (A_n, B_n) are uniformly stabilizable.

(C3) If the original system $(\mathcal{A}, \mathcal{C})$ is detectable, then the approximations (A_n, C_n) are uniformly detectable.

We shall see that not all of these conditions appear necessary for controller design in finite dimensions. Morris [Mor96] proves that assumptions (S1)–(S4) plus (C2) or (C3) imply convergence of the transfer functions. The common factor in all assumptions is the importance of the convergence of transfer functions. Suppose we have a linear system with transfer function G and a controller C. Let $\Delta(G, C)$ denote the closed loop system (see Figure 2.1 in Chapter 2) and suppose this system is stable. Let G_n be the n^{th}-dimensional approximation of G. Suppose that for all sufficiently small neighbourhoods B of G, $G_n \in B$ implies that

(1) the closed loop $\Delta(G_n, C)$ of G_n and C is externally stable, and

(2) the closed loop response $\Delta(G_n, C)$ of G_n and C is close to the closed loop response $\Delta(G, C)$ of G and C.

If G and G_n are stable, then $\|G_n - G\|_\infty \to 0$ as $n \to \infty$ implies (1) and (2) above. Thus, we are justified in considering convergence in the H_∞ norm.

3.7 Approximating the H_∞ Optimal Sensitivity Problem

Recall that we would like to solve an H_∞ optimal control problem (see page 26) via approximations (see page 27). The following definitions are required.

Definition 3.22 *(Inner Functions and Matrices)*

A scalar-valued function $f \in RH_\infty$ is inner if it has magnitude one on the $j\omega-$axis.

A matrix $\Phi \in M(RH_\infty)$ is inner if $\Phi^*(s)\Phi(s) = I$, i.e., $\Phi^*(s) = \Phi^T(-s)$.

Definition 3.23 *(Outer Functions and Matrices)*

A scalar-valued function $f \in RH_\infty$ is outer if it has no zeros in $\Re(s) > 0$.

A matrix $\Phi \in M(RH_\infty)$ is outer if, for every $\Re(s) > 0$, $\Phi(s)$ has a right-inverse which is analytic in $\Re(s) > 0$.

Definition 3.24 *(Blashke Product)*

A function $B(s)$ of the form

$$B(s) = \prod_{i=1}^{n} \frac{s - a_i}{s + a_i}$$

where $a_i \in \mathbb{C}$ is called a (finite) Blashke product.

Definition 3.25 *(Inner/Outer Factorization, e.g., [Vid85])*

An inner/outer factorization of a matrix $F \in M(RH_\infty)$ is a factorization

$$F = F_i F_o$$

where F_i is inner and F_o is outer. Every matrix in $M(RH_\infty)$ has an inner/outer factorization. If F has no zeros on the $jw-$axis, then $F = BF_o$, where B is a matrix whose elements are a finite Blashke product.

As we shall see, convergence of the approximating transfer functions G_n as well as convergence of the approximating inner factors G_{n_i} in a weighted semi-norm is sufficient for convergence of the H_∞ optimal sensitivity problem.

Let

$$\gamma_n = \inf_{Q \in H_\infty} \|T_1 - T_2 Q\|_\infty$$

(see Problem 4 on page 27), where we require that $\gamma_n \to \gamma$ (see Problem 3 on page 26).

The general H_∞ weighted sensitivity minimization problem is to find γ such that

$$\gamma(G) = \inf_{Q \in H_\infty} \|W_1(1 - GQ)\|_\infty$$

where $G \in H_\infty$, and $W_1(s) \in H_\infty$ is outer and strictly proper. Let $G_n(s)$ be the n^{th}-dimensional approximation to an infinite-dimensional system $G(s)$. Smith [Smi90] considers the following problem. Does $\|G_n - G\| \to 0$ imply $\gamma(G_n) \to \gamma(G)$? The answer is no. This is illustrated by the following two examples.

Example 1

Let

$$G(s) = \frac{s}{s+1}, \quad W(s) = \frac{1}{s+1}.$$

Then $\gamma(G) \geq |W(0)| = 1$. Let

$$G_\epsilon(s) = \frac{s+\epsilon}{s+1}.$$

Then $\|G_\epsilon - G\|_\infty \to 0$ as $\epsilon \to 0$ and $\gamma(G_\epsilon) = 0$ for all $\epsilon > 0$. Thus, $\gamma(\cdot)$ is discontinuous at G. In this example, $G(s)$ has a zero on the imaginary axis. The approximations $G_\epsilon(s)$ are all invertible outer functions.

Example 2

Let

$$G(s) = \frac{e^{-s}}{s+1}, \quad W(s) = \frac{1}{s+1}.$$

Then

$$\begin{aligned} \gamma(G) &= \inf_{Q \in H_\infty} \|W(1 - GQ)\|_\infty \\ &= \inf_{Q \in H_\infty} \|W - e^{-s}Q\|_\infty \\ &= \frac{1}{\sqrt{1+a^2}} \end{aligned}$$

where a is the unique root of the equation

$$\tan a + a = 0$$

lying between $\pi/2$ and π [FTZ86]. Let

$$G_n(s) = \frac{1}{(s+1)(1+s/n)^n}.$$

Then $\|G_n - G\|_\infty \to 0$ as $n \to \infty$ and $\gamma(G_n) = 0$ for all n. Thus, $\gamma(\cdot)$ is discontinuous at G. In this example, $G(s)$ has a pure time delay which is an inner function. The approximations $G_n(s)$ are all outer functions.

The one-dimensional acoustic duct model which we study in this thesis also has an inner factor which is a pure time delay. Thus, we must be careful in our approximations.

Let $G = G_i G_o$ and $G_n = G_{n_i} G_{n_o}$ be inner/outer factorizations of G and G_n, respectively. Then we have the following result.

Theorem 3.20 *[Smi90]*

If there exists a sequence $\{G_n\}$ *such that* $\|G_n - G\|_\infty \to 0$ *as* $n \to \infty$ *and furthermore if* $\|W_1(G_{n_i} - G_i)\|_\infty \to 0$ *and* $n \to \infty$, *then* $\gamma(G_n) \to \gamma(G)$.

Thus, the H_∞ problem is well-posed provided that the G_{n_i} are chosen appropriately.

Rodriguez and Dahleh [RD90] show that by approximating the inner factor G_{n_i} on compact sets and ensuring that the approximation of the outer factor G_{n_o} is well-behaved, one can obtain a near optimal finite-dimensional solution.

Theorem 3.21 *[RD90]*

Let $W_1(s) \in RH_\infty$. *Let*

$$X_\Omega := \begin{cases} 1, & \text{for } w \in [-\Omega, \Omega] \\ 0, & \text{elsewhere.} \end{cases}$$

If

1) $|(G_n(jw) - G(jw))X_\Omega| \to 0$ *as* $n \to \infty$, *and*
2) $|W_1(jw)(G_{n_i}(jw) - G_i(jw))X_\Omega| \to 0$ *as* $n \to \infty$,

then $\gamma(G_n) \to \gamma(G)$ *as* $n \to \infty$.

Thus, in general, the inner factor of the infinite-dimensional system must be approximated by a sequence of finite-dimensional inner functions. However, not all approximations of an inner factor have right half plane zero locations that are similar. This phenomenon was studied by Lindner *et al.* [LRT93]. In their paper, the authors study the zeros of the modal approximations of a flexible beam. The authors show that in some instances the zero placement may change significantly with model order.

This is one reason we must use extreme caution when using a finite-dimensional plant to approximate the infinite-dimensional plant. The location and number of right half plane zeros generated by a particular scheme is important because, for a scheme to be a viable choice for solving the optimal sensitivity problem, the inner factors (which contain the right half plane zeros) of the transfer function must converge. The reason for this will become clear when we discuss the solution to the optimal sensitivity problem in Chapter 5. The effect of the right half plane zeros is further studied when looking at the convergence of the inner factor of the transfer function in Chapter 7.

Thus, given an approximating scheme, if the transfer functions converge and the inner factors converge over increasingly larger frequency subintervals then we know that $\gamma_n \to \gamma$. Note that these approximation results are centred on convergence of the transfer functions.

Chapter 4

Approximating the Acoustic Model

In Chapter 2, the problem of global acoustic noise reduction was formulated (see (2.21)). Through successive simplifications of this problem, we arrived at two problems, Problems 3 and 4 (see page 26 and page 27, respectively). In Chapter 3, Section 3.7, we provided criteria under which the solution of Problem 4 is guaranteed to converge to that of Problem 3. We also considered general conditions for approximating systems.

In this chapter, we examine several approximating schemes. We pay particular attention to the margin of stability generated by the approximation methods studied.

One of the goals of this research was to obtain a method for studying the global noise reduction problem in three dimensions. Because of this, it is not appropriate to use some simple approximation method such as Padé approximants to formulate finite-dimensional approximations to our problem. We want a method suitable for studying the three-dimensional problem. With this in mind, we consider the

following popular approximation schemes.

Method I Legendre polynomial based Galerkin approximation method with states (z, z_t).

Method II Linear spline based Galerkin approximation method with states (z, z_t).

Method III Finite difference method with states (z, z_t).

All numerical examples used $c = 331\ m/s$ (the speed of sound in air), $\rho = 1.29\ kg/m^3$, and $K = 0.7$. The impedance K was chosen so that the end of the duct is partially reflective/absorptive. The length L of the duct is 4 m. The transfer function studied is for the single-input/single-output case with the input at $x_d = 0$ and the output at $x = 2$. The weight W_1 was chosen to be a simple low-pass filter

$$W_1(s) = \frac{1}{\frac{s}{1000} + 1}.$$

In the results that follow we will determine

1) the margin of stability of the approximations,
2) whether $|G_n(jw) - G(jw)| \to 0$ over any compact interval Ω as n increases, and
3) whether $|W_1(jw)(G_{n_i}(jw) - G_i(jw))| \to 0$ over any compact interval Ω as n increases.

These latter two points will establish whether or not an approximation method is suitable for our purpose of determining optimal weighted sensitivity (see Section 3.7).

We begin by showing the general variational approach to finding the finite-dimensional state-space representation of the one-dimensional duct problem. This approach is used to calculate the Galerkin approximations (Methods I and II).

4.1 Semi-Discrete Galerkin Approximations

If z solves (2.1), then for $\psi(x) \in L_2(0, L)$,

$$\int_0^L z_{tt}\psi(x)\,dx = \int_0^L c^2 z_{xx}\psi(x)\,dx + \frac{P_c(t)\psi(x_a)}{\rho} + \frac{P_d(t)\psi(x_d)}{\rho}.$$

Using integration by parts we obtain,

$$\int_0^L z_{tt}\psi(x)\,dx = c^2\left[\psi(L)z_x(L) - \int_0^L z_x\psi_x(x)\,dx\right] + \frac{P_c(t)\psi(x_a)}{\rho} + \frac{P_d(t)\psi(x_d)}{\rho}.$$

Substituting in the boundary conditions we get,

$$\int_0^L z_{tt}\psi(x)\,dx + Kc\psi(L)z_t(L) + c^2\int_0^L z_x\psi_x(x)\,dx = \frac{P_c(t)\psi(x_a)}{\rho} + \frac{P_d(t)\psi(x_d)}{\rho}. \quad (4.1)$$

If z satisfies (4.1) for all $\psi(x) \in L_2(0, L)$, we say that it is the *weak solution* of the partial differential equation (2.1). Consider now a sequence of finite-dimensional subspaces $\mathcal{H}_n$ of $\mathcal{H}$ such that $\mathcal{H}_n \to \mathcal{H}$ as $n \to \infty$. Let $(z^n, z_t^n) \in \mathcal{H}_n = H_n \times H_n$ where

$$z^n(x,t) = \sum_{i=0}^{n} a_i(t)\phi_i(x). \quad (4.2)$$

Also suppose that $\{\phi_i\}$, $i = 0, 1, \ldots, n$ are a basis for H_n. Let

$$a(t) = \begin{bmatrix} a_0(t) \\ a_1(t) \\ \vdots \\ a_n(t) \end{bmatrix}.$$

Substituting (4.2) into (4.1), setting $\psi(x) = \phi_j(s)$ for all $j = 0, 1, \ldots, n$ and rearranging we get,

$$\sum_{i=0}^{n} \ddot{a}(t)\int_0^L \phi_i(x)\phi_j(x)\,dx + Kc\phi_j(L)\sum_{i=0}^{n}\dot{a}_i(t)\phi_i(L) + c^2\sum_{i=0}^{n} a_i(t)\int_0^L \phi_i'(x)\phi_j'(x)\,dx = \frac{P_c(t)\phi_j(x_a)}{\rho} + \frac{P_d(t)\phi_j(x_d)}{\rho}, \qquad \text{for } j = 0, 1, \ldots, n. \quad (4.3)$$

Let $u(t) = P_c(t)$ be the control input, and $d(t) = P_d(t)$ be the disturbance. Then (4.3) may be written as

$$M\ddot{a}(t) + D\dot{a}(t) + Ga(t) = F_1 u(t) + F_2 d(t).$$

where

$$[M]_{ij} = \int_0^L \phi_i(x)\phi_j(x)\, dx,$$

$$[D]_{ij} = Kc\phi_i(L)\phi_j(L),$$

$$[G]_{ij} = c^2 \left(\int_0^L \phi_i'(x)\phi_j'(x)\, dx \right),$$

$$[F_1]_j = \frac{\phi_j(x_a)}{\rho},$$

and

$$[F_2]_j = \frac{\phi_j(x_d)}{\rho}.$$

Let

$$w_n(t) = \begin{bmatrix} a(t) \\ \dot{a}(t) \end{bmatrix}.$$

Thus, we may write

$$\dot{w}_n(t) = \begin{bmatrix} 0 & I \\ -M^{-1}G & -M^{-1}D \end{bmatrix} w_n(t) + \begin{bmatrix} 0 \\ M^{-1}F_1 \end{bmatrix} u(t) + \begin{bmatrix} 0 \\ M^{-1}F_2 \end{bmatrix} d(t) \quad (4.4)$$

or alternatively

$$\begin{aligned} M^{1/2}\dot{w}_n(t) = &\begin{bmatrix} 0 & I \\ -M^{-1/2}GM^{-1/2} & -M^{-1/2}DM^{-1/2} \end{bmatrix} M^{1/2} w_n(t) \\ &+ \begin{bmatrix} 0 \\ M^{-1/2}F_1 \end{bmatrix} u(t) + \begin{bmatrix} 0 \\ M^{-1/2}F_2 \end{bmatrix} d(t). \end{aligned} \quad (4.5)$$

The form given in (4.5) has the advantage in that it generally improves the condition number of the associated matrices. For $d(t) = 0$ in (4.4) we may write

$$\dot{w}_n(t) = A_n w_n(t) + B_n u(t)$$

where

$$A_n = \begin{bmatrix} 0 & I \\ -M^{-1}G & -M^{-1}D \end{bmatrix}$$

and

$$B_n = \begin{bmatrix} 0 \\ M^{-1}F_1 \end{bmatrix}.$$

If the pressure at $x \in \mathcal{X} = \{x_1, x_2, \ldots, x_m\}$ is observed (as in Problem 4 on page 27), then

$$\begin{aligned} y(t) &= -\rho c^2 \begin{bmatrix} \frac{\partial z}{\partial x}(x_1,t) & \frac{\partial z}{\partial x}(x_2,t) & \cdots & \frac{\partial z}{\partial x}(x_m,t) \end{bmatrix}^T \\ &= -\rho c^2 \begin{bmatrix} \sum_{i=0}^{n} a_i(t)\phi_i'(x_1) & \sum_{i=0}^{n} a_i(t)\phi_i'(x_2) & \cdots & \sum_{i=0}^{n} a_i(t)\phi_i'(x_m) \end{bmatrix}^T \\ &= -\rho c^2 \begin{bmatrix} \phi_0'(x_1) & \cdots & \phi_n'(x_1) \\ \phi_0'(x_2) & \cdots & \phi_n'(x_2) \\ \vdots & \vdots & \vdots \\ \phi_0'(x_m) & \cdots & \phi_n'(x_m) \end{bmatrix} \begin{bmatrix} a_0(t) \\ \vdots \\ a_n(t) \end{bmatrix}. \end{aligned}$$

Thus, the output equation has the form

$$y(t) = C_n w_n(t) = [\overline{C} \;\; 0_{m\times(n+1)}] w_n(t) \tag{4.6}$$

where $y(t) = P(x,t)$ for $x \in \mathcal{X}$, and

$$\overline{C} = -\rho c^2 \begin{bmatrix} \phi_0'(x_1) & \cdots & \phi_n'(x_1) \\ \phi_0'(x_2) & \cdots & \phi_n'(x_2) \\ \vdots & \vdots & \vdots \\ \phi_0'(x_m) & \cdots & \phi_n'(x_m) \end{bmatrix},$$

or alternatively

$$y(t) = -\rho c^2 [\overline{C} M^{-1/2} \;\; 0_{m\times(n+1)}] M^{1/2} w_n(t).$$

4.2 Method I: Legendre Polynomials

Consider the following set of Legendre polynomials,

$$P_0(x) = 1, \quad P_n(x) = \frac{1}{2^n n!}\frac{d^n}{dx^n}(x^2-1)^n, \quad n = 1, 2, \ldots,$$

for $x \in [-1, 1]$. Redefining these functions on $x \in [0, L]$ we obtain a set of orthogonal basis functions $\{\phi_i(x)\}$ for $i = 0, 1, \ldots, n$ whose first few terms are as follows (see Figure 4.1):

$$\begin{aligned} \phi_0(x) &= 1, \\ \phi_1(x) &= \tfrac{2}{L}x - 1, \\ \phi_2(x) &= \tfrac{3}{2}(\tfrac{2x}{L} - 1)^2 - \tfrac{1}{2}, \\ \phi_3(x) &= \tfrac{5}{2}(\tfrac{2x}{L} - 1)^3 - \tfrac{3}{2}(\tfrac{2x}{L} - 1), \quad \ldots, \ etc. \end{aligned} \tag{4.7}$$

Numerical simulations (see Table 4.1) indicate that this method yields approximations that have a uniform margin of stability. Therefore this scheme produces finite-dimensional approximations that are (trivially) uniformly stabilizable.

Figure 4.2(a)-(d) shows the poles and Figure 4.2(e)-(f) the zeros of the approximations for $n = 5$ and $n = 10$. We can clearly see that most of the poles lie on the vertical line $s = -\frac{c}{2L}[\ln|\alpha| + 2n\pi\jmath] = -71.7691 + 82.75n\pi\jmath$, for $n = 0, \pm1, \pm2, \ldots$, which is where exact poles of the system lie (see (2.10)). The inner factor of the original infinite-dimensional system is a pure delay. The zeros of $G(x, x_d)$ are solutions of

$$e^{\frac{2s}{c}(x-L)} - \alpha = 0.$$

This implies the zeros are

$$z_n = \frac{c}{2(x-L)}[\ln\alpha + 2n\pi\jmath], \quad n = 0, \pm1, \pm2, \ldots. \tag{4.8}$$

Thus, all the zeros of $G(x, x_d)$ lie in the left half plane. In the approximations, there are a number of zeros that lie on the vertical line $s = \frac{c}{2(x-L)}[\ln|\alpha| + 2n\pi\jmath] =$

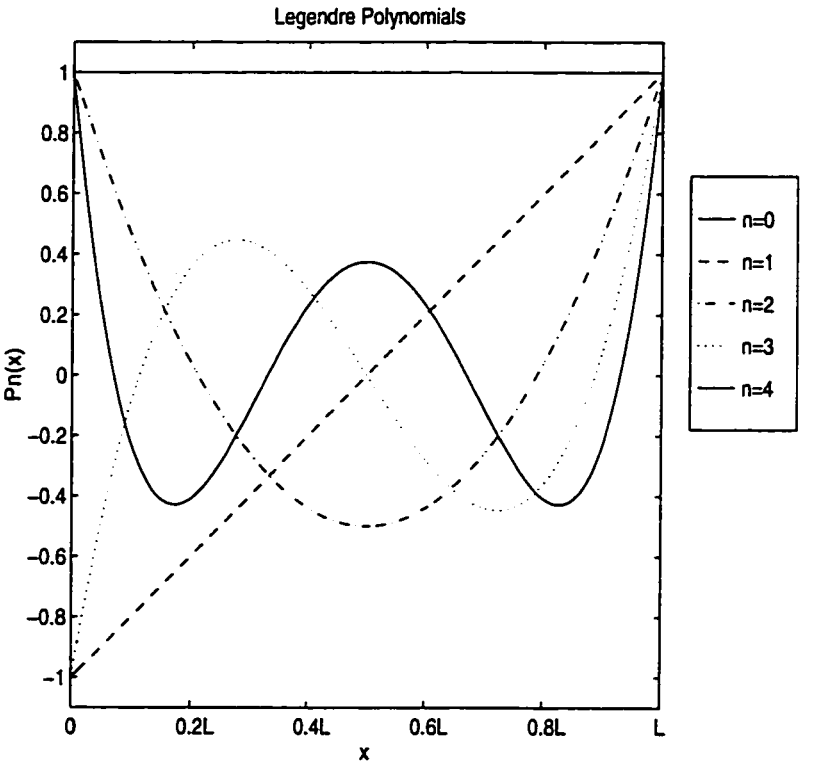

Figure 4.1: Legendre polynomials

n	$\dim(A_n)$	$\max\{\mathrm{Re}\lambda, \lambda \in \sigma(A_n)\}$
5	11	-71.7689
6	13	-71.7458
7	15	-71.6939
8	17	-71.7691
9	19	-71.7673
10	21	-71.7591
11	23	-71.7617
12	25	-71.7690
13	27	-71.7681
14	29	-71.7663
15	31	-71.7691
16	33	-71.7690
17	35	-71.7687
18	37	-71.7686
19	39	-71.7691
20	41	-71.7691
21	43	-71.7690
22	45	-71.7691
23	47	-71.7691
24	49	-71.7691
25	51	-71.7691
26	53	-71.7691
27	55	-71.7691
28	57	-71.7691
29	59	-71.7689
30	61	-71.7689

Table 4.1: Legendre polynomials: open loop margin of stability

$-143.5382 + 165.5n\pi\jmath$ for $n = 0, \pm 1, \pm 2, \ldots$, which is where exact zeros of the system lie. However, there are a number of zeros not on this line as seen in Figure 4.2(e)-(f). These are the zeros due to approximating the inner factor of the original infinite-dimensional system which is a pure delay.

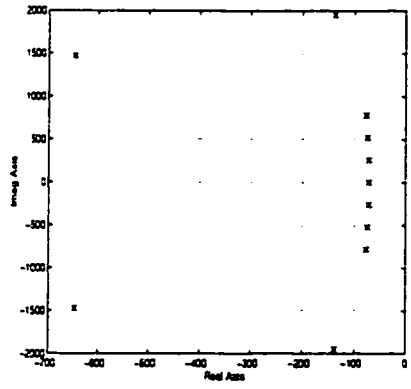

(a) poles for $n = 5$

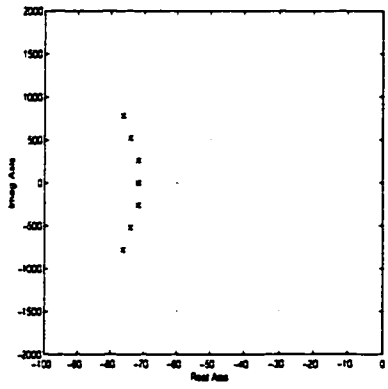

(b) poles for $n = 5$ (enhanced scale)

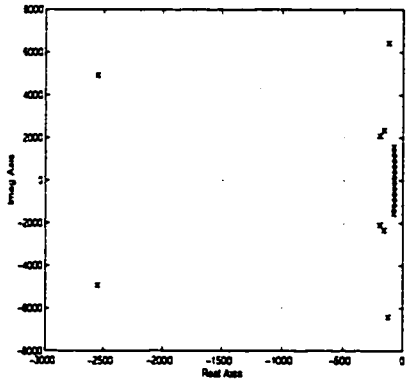

(c) poles for $n = 10$

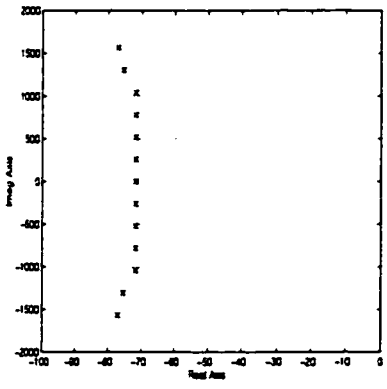

(d) poles for $n = 10$ (enhanced scale)

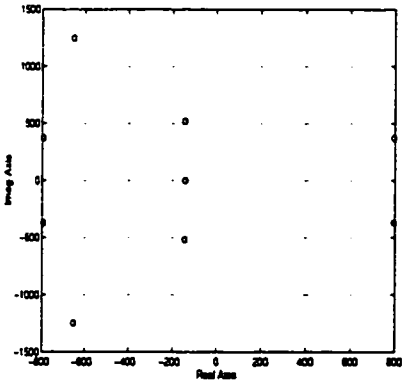

(e) zeros for $n = 5$

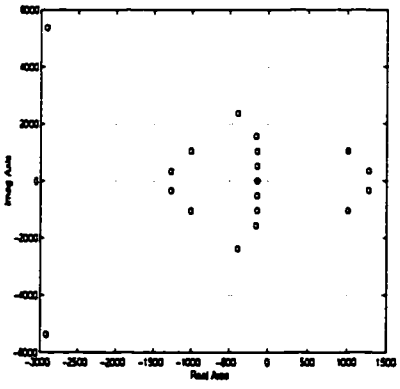

(f) zeros for $n = 10$

Figure 4.2: Legendre polynomials: poles and zeros for G_n (x=poles, o=zeros)

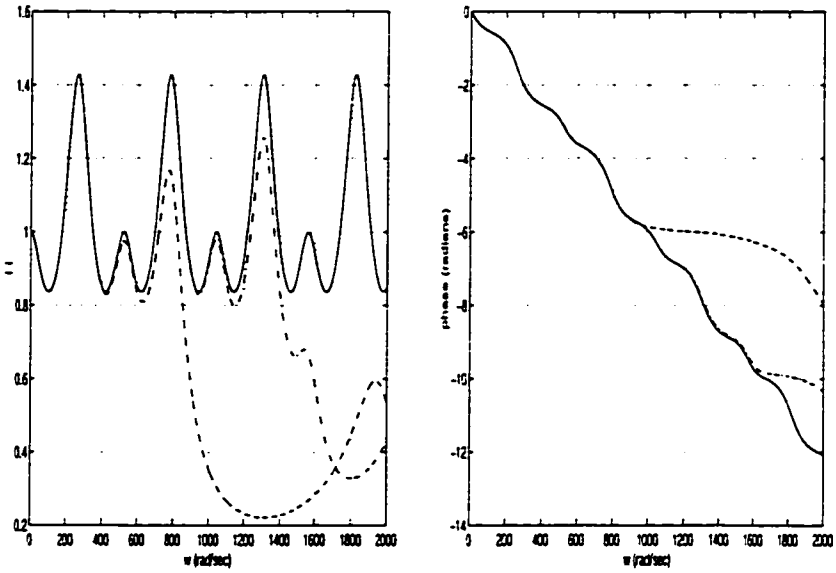

(a) magnitude (b) phase

Figure 4.3: Legendre polynomials: magnitude and phase for $G(jw)$ (solid) and $G_n(jw)$ ($n = 5$ (dashed), $n = 10$ (dash/dot))

4.2.1 Convergence of the Transfer Function

In this section, we examine the behaviour of $|G_n(jw) - G(jw)|$ over any compact interval Ω as n increases. Typical plots of the magnitude of the exact transfer function and the approximations are shown in Figure 4.3. From these plots, it is apparent that the approximating transfer functions for larger n are better representations of the exact transfer function over successively larger bandwidths.

Figure 4.4 shows the behaviour of $|G_n(jw) - G(jw)|$ for $0 \leq w \leq 2000$ rad/sec, for $n = 5$, 10, and 15. We can see that the error goes to zero very quickly. Figure 4.5 shows the maximum of $|G_n(jw) - G(jw)|$ over $0 \leq w \leq 2000$ rad/sec versus n. We can see that the error tends to zero as n increases.

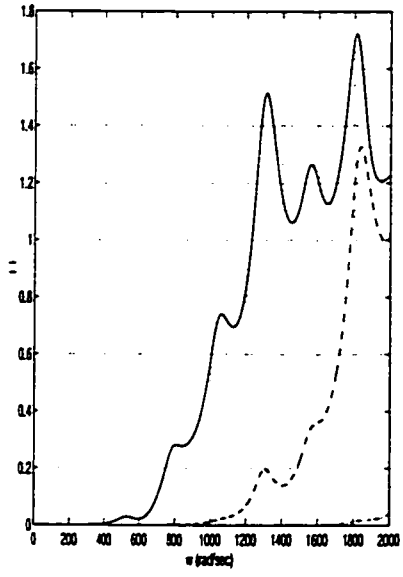

Figure 4.4: Legendre polynomials: $|G(jw) - G_n(jw)|$ ($n = 5$ (solid), $n = 10$ (dashed), $n = 15$ (dash/dot))

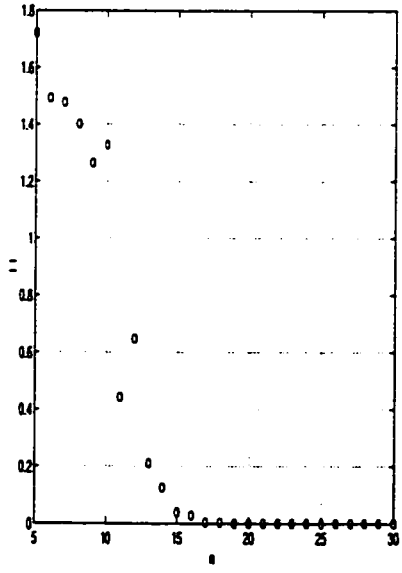

Figure 4.5: Legendre polynomials: $\max_{0 \leq w \leq 2000} |G(jw) - G_n(jw)|$ versus n

4.2.2 Convergence of the Inner Part of the Transfer Function

In this section, we examine the behaviour of $|W_1(jw)(G_{n_i}(jw) - G_i(jw))|$ over any compact interval Ω as n increases. We know the exact transfer function has inner factor (see (2.18))

$$G_i = e^{-\frac{s}{c}x}.$$

Because the magnitude of $G_{n_i}(jw)$ is effectively one for all frequencies, only the phase of $W_1(jw)(G_{n_i}(jw) - G_i(jw))$ was useful for determining convergence. Contributing to the phase are both the real and imaginary parts of $W_1(jw)(G_{n_i}(jw) - G_i(jw))$, with errors in these values occurring at all frequencies. Thus, we decided that it is easier to see the origin of errors by considering the real and imaginary parts of $W_1(jw)(G_{n_i}(jw) - G_i(jw))$. Figure 4.6 shows the behaviour of the magnitude of the real and imaginary parts of $W_1(jw)(G_{n_i}(jw) - G_i(jw))$ for $0 \leq w \leq 2000$ rad/sec. We can see from these plots that the errors are tending to zero although not as quickly as for the transfer function.

For $n = 5$, we find the right half plane zeros of the inner factor of the approximating transfer function are

$$z = \left[\begin{array}{c} 794.9385 \pm 372.6966j \end{array} \right]. \tag{4.9}$$

For $n = 10$, we find the right half plane zeros of the inner factor of the approximating transfer function are

$$z = \left[\begin{array}{c} 1009.6333 \pm 1050.2320j \\ 1274.0411 \pm 339.4994j \end{array} \right]. \tag{4.10}$$

We can clearly see the varied location of the right half plane zeros. This trend continues for larger n (see also Figure 4.2). The erratic behaviour of the right half

plane zeros is illustrated by the variation in the errors of the inner factors given in Figure 4.6.

4.2.3 Conclusion

As shown above, the numerical results obtained using Legendre polynomial based approximation method indicate the following:

1) $|G_n(jw) - G(jw)| \to 0$ as $n \to \infty$, for $0 \leq w \leq 2000$ rad/sec;
2) $|W_1(jw)(G_{n_i}(jw) - G_i(jw))| \to 0$ as $n \to \infty$, for $0 \leq w \leq 2000$ rad/sec; and
3) there is a uniform margin of stability for all approximations.

Thus, Legendre polynomials provide a suitable approximating scheme under which to study the H_∞ control problem.

The Legendre polynomials are what we may refer to as "global" basis functions since each basis function is defined for all $x \in [0, L]$ (see Figure 4.1). Any errors made in attempting to enforce the boundary condition at $x = L$ may be perpetuated along the rest of the duct. Thus, it is possible that a set of basis functions with compact support may be less sensitive to numerical errors. Using splines also leads to sparse matrices. This is advantageous for the three-dimensional case where computations are more intensive. For this reason, we also consider the linear spline based approximation method.

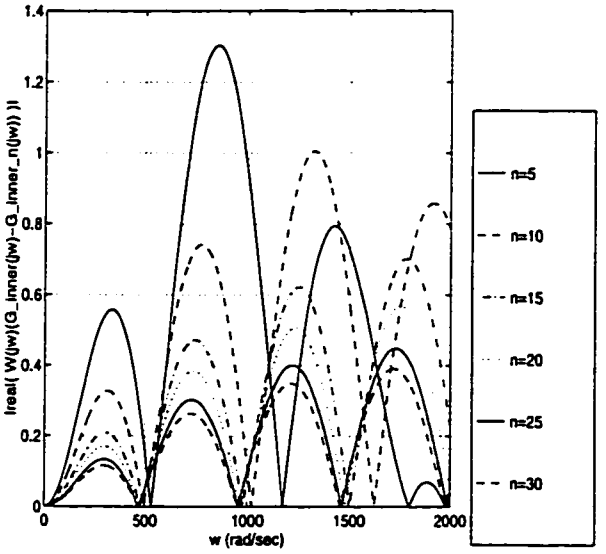

(a) $|\Re[W_1(jw)(G_i(jw) - G_{n_i}(jw))]|$

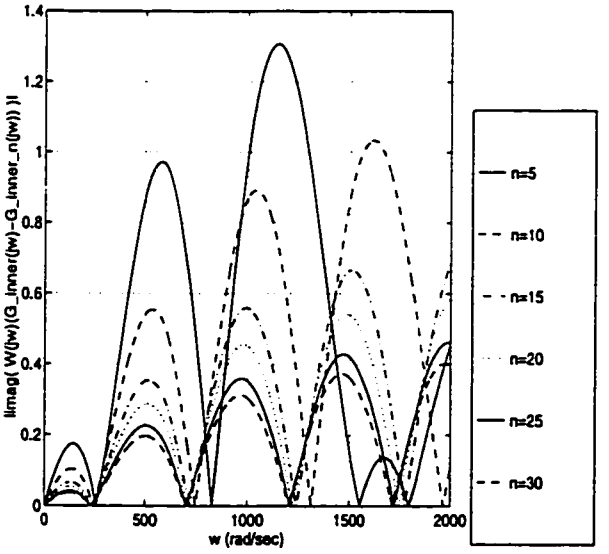

(a) $|\Im[W_1(jw)(G_i(jw) - G_{n_i}(jw))]|$

Figure 4.6: Legendre polynomials: magnitude of real and imaginary part of $W_1(jw)(G_i(jw) - G_{n_i}(jw))$

n	$\dim(A_n)$	$\max\{\mathrm{Re}\lambda, \lambda \in \sigma(A_n)\}$
5	11	-22.0314
6	13	-16.1294
7	15	-12.2373
8	17	-9.5679
9	19	-7.6698
10	21	-6.2773
11	23	-5.2279
12	25	-4.4186
13	27	-3.7822
14	29	-3.2730
15	31	-2.8595
16	33	-2.5193
17	35	-2.2361
18	37	-1.9978
19	39	-1.7956
20	41	-1.6225
21	43	-1.4732
22	45	-1.3435
23	47	-1.2302
24	49	-1.1306
25	51	-1.0426
26	53	-0.9644
27	55	-0.8947
28	57	-0.8323
29	59	-0.7762
30	61	-0.7256

Table 4.2: Linear splines: open loop margin of stability

4.3 Method II: Linear Splines

Consider the following set of linear splines:

$$\phi_i(x) = \begin{cases} \frac{n}{L}(x - \frac{(i-1)L}{n}), & \frac{(i-1)L}{n} \leq x \leq \frac{iL}{n} \\ \frac{n}{L}(\frac{(i+1)L}{n} - x), & \frac{iL}{n} \leq x \leq \frac{(i+1)L}{n} \\ 0, & \text{otherwise} \end{cases} \tag{4.11}$$

for $i = 0, 1, \ldots, n$. (These are commonly referred to as "hat" functions.)

Table 4.2 shows that all approximations are stable. However, there is no uniform margin of stability. Figure 4.7(a)-(d) shows the poles and Figure 4.7(e)-(f) the zeros

of the approximations for $n = 5$ and $n = 10$. As for the Legendre polynomials, we see that most of the poles lie on the vertical line $s = -71.7691 + 82.75n\pi\jmath$, for $n = 0, \pm1, \pm2, \ldots$, although it is much more difficult to see here than for Legendre polynomials. There are also a number of spurious poles, particularly a number that lie increasingly close to the imaginary axis (for larger imaginary parts) as evidenced in Table 4.2. In addition, there are a number of zeros that lie on the vertical line $s = -143.5382 + 165.5n\pi\jmath$ for $n = 0, \pm1, \pm2, \ldots$, although this is more difficult to see. However, there are also a number of zeros not on this line. Again, this is the recurring problem of wandering right half plane zeros which will affect the convergence of the inner factors. This is discussed further on page 100.

4.3.1 Convergence of the Transfer Function

In this section, we examine the behaviour of $|G_n(\jmath w) - G(\jmath w)|$ over any compact interval Ω as n increases. Plots comparing the magnitude and phase of the exact transfer function and the approximations are shown in Figure 4.8. We can see that the approximating transfer functions appear to converge to the exact transfer function as the number of basis functions is increased. However, the convergence is not as smooth as for Legendre polynomials.

Figure 4.9 shows the behaviour of $|G_n(\jmath w) - G(\jmath w)|$ for $0 \leq w \leq 2000$ rad/sec, for $n = 5$, 10, and 15. We can see that the error tends to zero, although convergence is apparently not uniform. This is perhaps more easily observed by looking at the maximum of $|G_n(\jmath w) - G(\jmath w)|$ versus n in Figure 4.10. We can see that the error is getting smaller although it oscillates for all larger values of n.

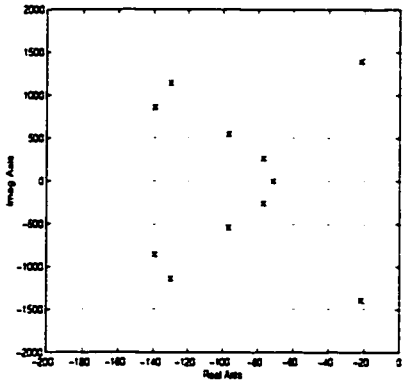

(a) poles for $n = 5$

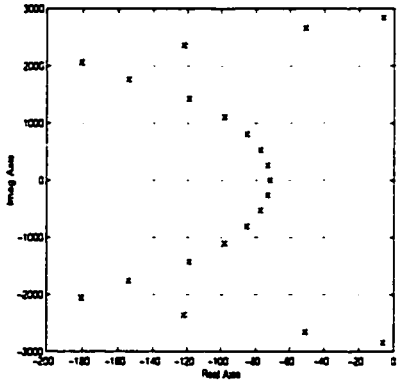

(b) poles for $n = 10$

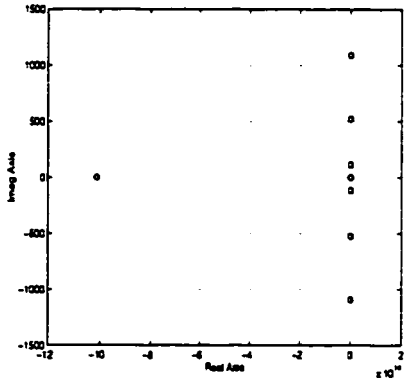

(c) zeros for $n = 5$

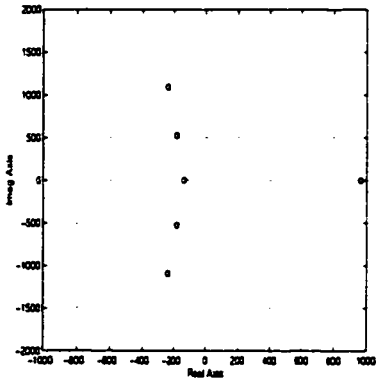

(d) zeros for $n = 5$ (enhanced scale)

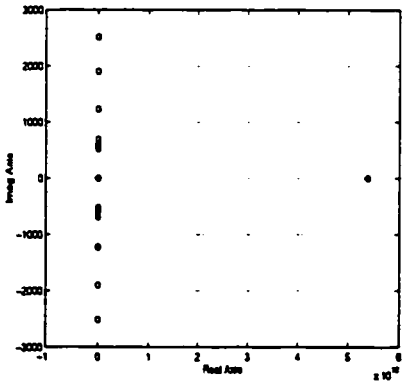

(c) zeros for $n = 10$

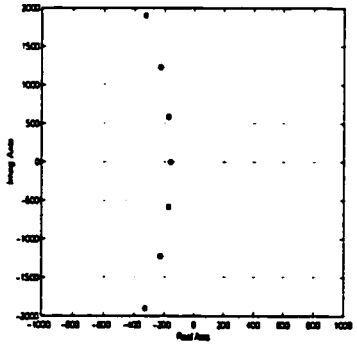

(d) zeros for $n = 10$ (enhanced scale)

Figure 4.7: Linear splines: poles and zeros for G_n (x=poles, o=zeros)

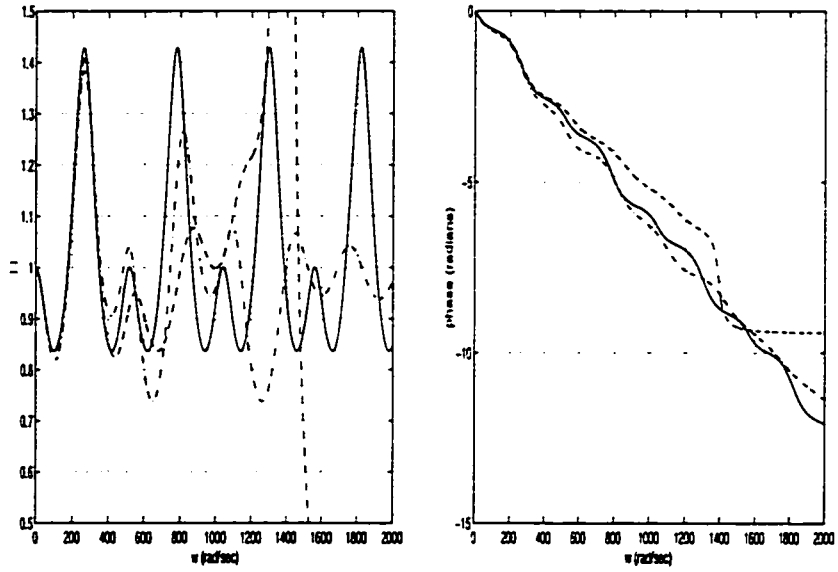

(a) magnitude (b) phase

Figure 4.8: Linear splines: magnitude and phase for $G(jw)$ (solid) and $G_n(jw)$ ($n = 5$ (dashed), $n = 10$ (dash/dot))

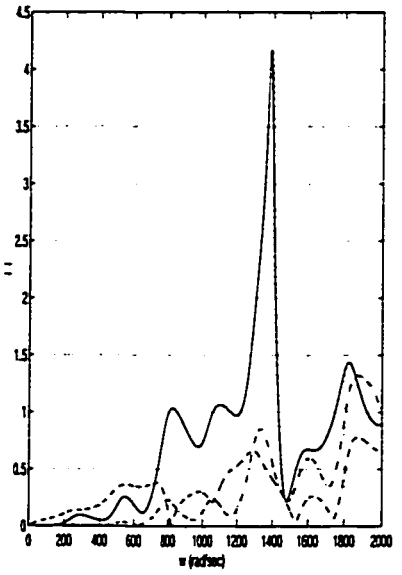

Figure 4.9: Linear splines: $|G(jw)-G_n(jw)|$ ($n = 5$ (solid), $n = 10$ (dashed), $n = 15$ (dash/dot))

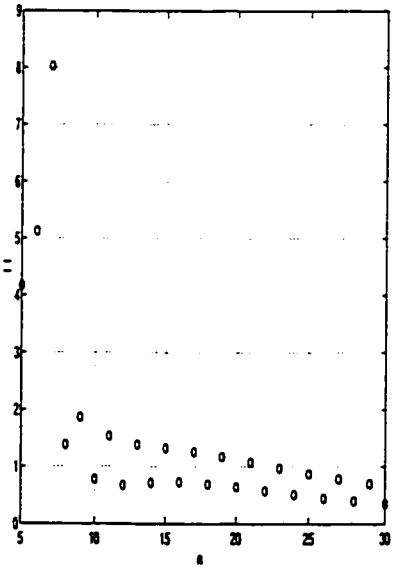

Figure 4.10: Linear splines: $\max_{0 \le w \le 2000} |G(jw) - G_n(jw)|$ versus n

4.3.2 Convergence of the Inner Part of the Transfer Function

Figure 4.11 shows the behaviour of the magnitude of the real and imaginary parts of $W_1(jw)(G_{n_i}(jw)-G_i(jw))$ for $0 \leq w \leq 2000$ rad/sec (see Section 4.2.2). We can see from these plots that the errors are tending smoothly to zero. In fact, convergence for the inner factors appears to be better than for the transfer function. This suggests that linear splines provide approximations that are suitable for controller design.

For $n = 5$, we find the right half plane zeros of the inner factor of the approximating transfer function are

$$z = \left[\begin{array}{c} 1013.4764 \pm 0.0013j \end{array} \right]. \tag{4.12}$$

For $n = 10$, we find the right half plane zeros of the inner factor of the approximating transfer function are

$$z = \left[\begin{array}{c} 2065.2172 \\ 2037.9170 \pm 36.0916j \\ 1996.8563 \pm 21.3390j \end{array} \right]. \tag{4.13}$$

Recall that for Legendre polynomials we had

$$z = \left[\begin{array}{c} 794.9385 \pm 372.6966j \end{array} \right]$$

for $n = 5$, and

$$z = \left[\begin{array}{c} 1009.6333 \pm 1050.2320j \\ 1274.0411 \pm 339.4994j \end{array} \right]$$

for $n = 10$. What is interesting to note here is the large difference in the location, magnitude and number of right half plane zeros for two different approximating schemes with the same dimension. This clearly will affect convergence of the inner

factors. If we compare Figure 4.6 with Figure 4.11, we see that the error for large n is smaller for Legendre polynomials than for linear splines. This suggests that Legendre polynomials better approximate the inner factor than do linear splines. Nevertheless, the inner factors determined using linear splines also appear to be converging.

4.3.3 Conclusion

As shown above, the numerical results obtained using the linear spline based approximation method indicate the following:

1) $|G_n(jw) - G(jw)| \to 0$ as $n \to \infty$, for $0 \leq w \leq 2000$ rad/sec (not smoothly);
2) $|W_1(jw)(G_{n_i}(jw) - G_i(jw))| \to 0$ as $n \to \infty$, for $0 \leq w \leq 2000$ rad/sec; and
3) there is no set margin of stability for successively larger approximations, although all approximations remain stable.

Thus, linear splines may provide a suitable approximating scheme. This will be further pursued in Chapter 7.

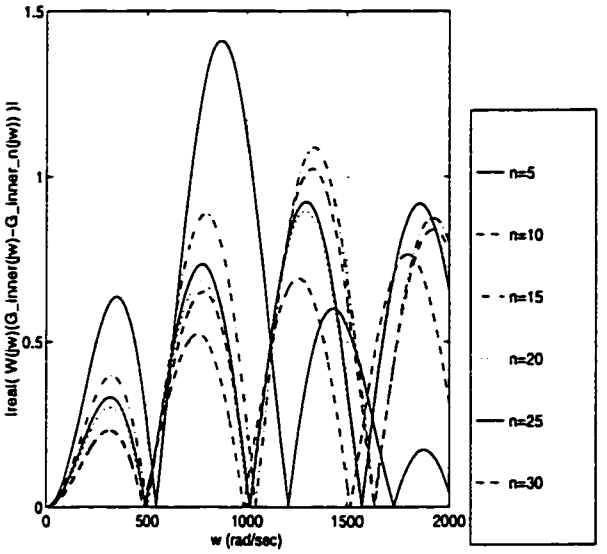

(a) $|\Re[W_1(jw)(G_i(jw) - G_{n_i}(jw))]|$

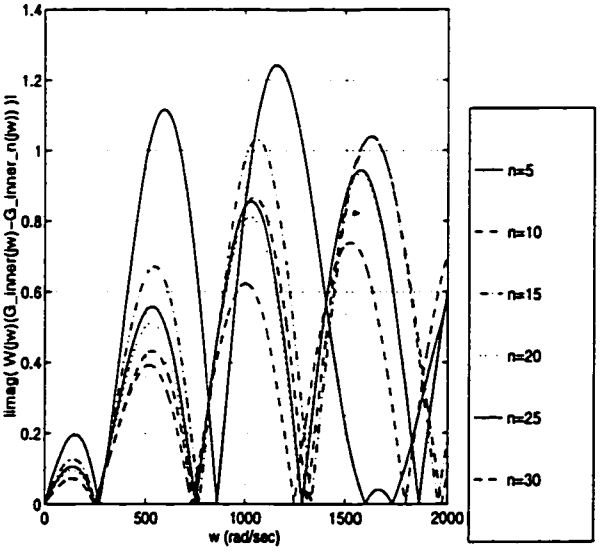

(a) $|\Im[W_1(jw)(G_i(jw) - G_{n_i}(jw))]|$

Figure 4.11: Linear splines: magnitude of real and imaginary part of $W_1(jw)(G_i(jw) - G_{n_i}(jw))$

4.4 Method III: Finite Differences

The finite difference method is generally used to compute the solution to a partial differential equation at nodes in the spatial domain. It is a common choice for simulating the dynamics of the one-dimensional wave equation and many other problems. Banks, Ito, and Wang [BIW91] show that a finite difference approximating scheme is not uniformly stable. For completeness, these results are verified in this section.

Suppose we have n equally spaced nodes x_i in $[0, L]$ where $\Delta x = \frac{L}{n-1}$ and

$$x_i = (i-1)\Delta x, \quad \text{for } i = 1, \ldots, n.$$

We will use central differences. Let $z_i(t)$ and $v_i(t)$ be the approximation of the solution values $z(t, x_i)$ and $z_t(t, x_i)$, respectively. Then the one-dimensional wave equation (2.1) is approximated by

$$\frac{d}{dt} z_i(t) = v_i(t)$$

and

$$\frac{d}{dt} v_i(t) = c^2 \left(\frac{z_{i+1}(t) - 2z_i(t) + z_{i-1}(t)}{\Delta x^2} \right) \tag{4.14}$$

for $i = 1, \ldots, n$. Suppose that a control $P_c(t)$ is applied at $x = 0$ so that the boundary condition becomes

$$\frac{\partial z}{\partial x}(0, t) = -\frac{P_c(t)}{\rho c^2}.$$

Discretizing and introducing an imaginary node at $i = 0$, we get

$$\frac{z_2 - z_0}{2\Delta x} = -\frac{P_c(t)}{\rho c^2}$$

which gives

$$z_0 = z_2 + \frac{P_c(t)}{\rho c^2}(2\Delta x).$$

Thus,

$$\frac{d}{dt}v_1(t) = \frac{c^2}{\Delta x^2}\left[2z_2 - 2z_1 + \frac{P_c(t)(2\Delta x)}{\rho c^2}\right]. \tag{4.15}$$

At $i = n$ (or $x = L$), the discretized boundary condition becomes

$$\frac{\partial z_n}{\partial x} = -\frac{K}{c}\frac{\partial z_n}{\partial t}.$$

Introducing an imaginary node at $i = n + 1$, this gives

$$z_{n+1} = z_{n-1} - \frac{K}{c}(2\Delta x)\frac{\partial z_n(t)}{\partial t}.$$

However,

$$v_n(t) = \frac{\partial z_n(t)}{\partial t}$$

so that

$$z_{n+1} = z_{n-1} - \frac{K}{c}(2\Delta x)v_n(t).$$

Thus

$$z_{n+1} = z_{n-1} - \frac{K}{c}(2\Delta x)v_n(t)$$

and

$$\frac{d}{dt}v_n(t) = \frac{c^2}{\Delta x^2}\left[2z_{n-1} - 2z_n - \frac{K}{c}(2\Delta x)v_n(t)\right]. \tag{4.16}$$

Collecting (4.14), (4.15), and (4.16), the state-space representation for the discretized form is

$$\begin{bmatrix} \dot{z}_1 \\ \dot{z}_2 \\ \vdots \\ \dot{z}_n \\ \dot{v}_1 \\ \dot{v}_2 \\ \vdots \\ \dot{v}_n \end{bmatrix} = \left[\begin{array}{c|c} A_{11} & A_{12} \\ \hline A_{21} & A_{22} \end{array}\right] \begin{bmatrix} z_1 \\ z_2 \\ \vdots \\ z_n \\ v_1 \\ v_2 \\ \vdots \\ v_n \end{bmatrix} + BP_c(t)$$

where

$$A_{11} = O_{n\times n},$$

$$A_{12} = I_{n\times n},$$

$$A_{21} = \frac{c^2}{\Delta x^2}\begin{bmatrix} -2 & 2 & 0 & 0 & \dots & 0 \\ 1 & -2 & 1 & 0 & \dots & 0 \\ 0 & 1 & -2 & 1 & \dots & 0 \\ \vdots & \vdots & \vdots & \vdots & \vdots & \vdots \\ 0 & 0 & \dots & 0 & 2 & -2 \end{bmatrix}_{n\times n},$$

$$A_{22} = \begin{bmatrix} 0 & 0 & \dots & 0 \\ 0 & 0 & \dots & 0 \\ \vdots & \vdots & \vdots & \vdots \\ 0 & 0 & \dots & -\frac{2Kc}{\Delta x} \end{bmatrix}_{n\times n},$$

and

$$B = \begin{bmatrix} 0_{n\times 1} \\ \frac{2}{\rho\Delta x} \\ 0 \\ \vdots \\ 0 \end{bmatrix}_{2n\times 1}.$$

If the pressure is observed at $x = x_s$, then

$$\begin{aligned} y(t) &= -\rho c^2 \frac{\partial z}{\partial x}(x_s, t) \\ &= -\rho c^2 \left[\frac{z_{i^*+1} - z_{i^*-1}}{2\Delta x}\right] \end{aligned}$$

where i^* is the $i^{*^{th}}$ cell closest to $x = x_s$. Thus,

$$y(t) = -\frac{\rho c^2}{2\Delta x}\begin{bmatrix} 0 & 0 & \dots & 0 & 1_{i^*-1} & 0 & 1_{i^*+1} & 0 & \dots & 0 \end{bmatrix}_{1\times 2n}\begin{bmatrix} z_1 \\ z_2 \\ \vdots \\ z_n \\ v_1 \\ v_2 \\ \vdots \\ v_n \end{bmatrix}.$$

Figure 4.12(a)-(b) shows the poles and zeros of the approximations for $n = 5$ and $n = 10$, respectively. We see that the poles with large imaginary part tend to the imaginary axis. As well, the margin of stability is very small (see Table 4.3). Banks, Ito, and Wang [BIW91] show that, for bounded control, a finite-difference method does not produce a uniform margin of stability, whereas, as illustrated in Table 4.1, Legendre polynomials do.

We attempted to test for the convergence of the transfer function but found that for both $n = 5$ and $n = 10$, $|G_n(jw)|$ was extremely large at low frequencies. In fact, the magnitude was of the order of 10^3. Aside from large values of $|G_n(jw) - G(jw)|$, poles with very small real part lead to numerical problems and no further analysis was made.

n	$\dim(A_n)$	$\max\{\mathrm{Re}\lambda, \lambda \in \sigma(A_n)\}$
5	9	-4.30794252539185
6	11	-2.81732506185543
7	13	-1.97835299062118
8	15	-1.46294421001218
9	17	-1.12469340564840
10	19	-0.89112563549924
11	21	-0.72323684934815
12	23	-0.59858278607953
13	25	-0.50352709711569
14	27	-0.42940516016569
15	29	-0.37050099967621
16	31	-0.32292186338634
17	33	-0.28394321877147
18	35	-0.2516123939166
19	37	-0.22450056032983
20	39	-0.20154278423252
21	41	-0.18193241332506
22	43	-0.16504924183261
23	45	-0.15041051546177
24	47	-0.13763546735322
25	49	-0.12642921429108
26	51	-0.11652296947000
27	53	-0.10774105478626
28	55	-0.09991773108766
29	57	-0.09291483303468
30	59	-0.08662286040794

Table 4.3: Finite differences: open loop margin of stability

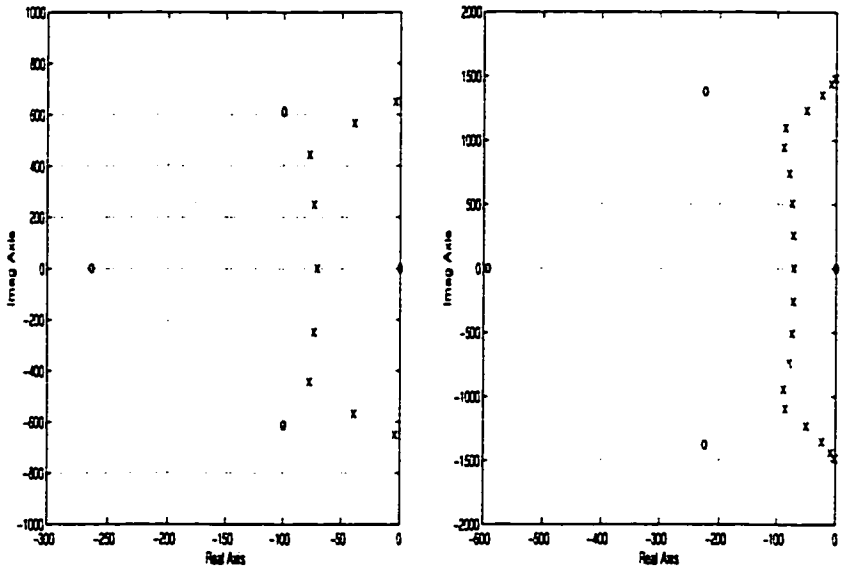

(a) $n = 5$ (b) $n = 10$

Figure 4.12: Finite differences: poles and zeros for G_n (x=poles, o=zeros)

4.5 Discussion

Banks, Ito, and Wang [BIW91] show that (Legendre) polynomial based Galerkin approximation methods provide a uniform margin of stability whereas polynomial (linear) spline based Galerkin approximation methods produce eigenvalues with large imaginary part that tend toward the imaginary axis. The eigenvalues found using Legendre polynomials also tend to the exact eigenvalues as the dimension of the approximating space tends to infinity.

Legendre polynomials appear to be the best choice of approximation scheme for control and simulation. This method exhibits smooth convergence of the transfer and inner functions, as well as a uniform margin of stability. Hence the approximations are (trivially) uniformly stabilizable. However, the numerical results produced using linear splines in Section 4.3 suggest that this method is also a practical choice. In Chapter 3, Section 3.6 we outlined some general conditions for the feasibility of an approximation scheme. Included in these conditions is the uniform stabilizability of the finite-dimensional approximations. In Section 4.3, we showed that linear splines produce finite-dimensional approximations that appear to not have a uniform margin of stability. The approximations may or may not be uniformly stabilizable. However, the approximations of the transfer and inner functions do appear to converge. This point will be further pursued in Chapter 7.

Chapter 5

Solving the H_∞ Optimal Control Problem

Consider the problem of determining

$$\gamma_{opt} = \inf_{Q \in RH_\infty} \|T_1 - T_2 Q\|_\infty \tag{5.1}$$

where T_1 and T_2 are tall matrices with one column. Since T_1 and T_2 have rational elements, there are a number of approaches to solve this problem. We will outline these methods below and end with the method of choice, Nevanlinna-Pick interpolation.

5.1 DGKF: State-Space Technique I

We describe here a state-space method for finding all stabilizing controllers such that

$$\|\mathcal{F}_l\|_\infty < \gamma,$$

where $\mathcal{F}_l$ is a closed loop transfer function. We then iterate to find the optimal solution γ_{opt} where $\gamma < \gamma_{opt}$. Consider the standard feedback system in Figure 5.1 where G is the transfer function of the plant we wish to control and C is the transfer function of the controller. Let

$$\begin{aligned} \dot{w}(t) &= Aw(t) + B_1 d(t) + B_2 u(t) \\ z(t) &= C_1 w(t) + D_{11} d(t) + D_{12} u(t) \\ y(t) &= C_2 w(t) + D_{21} d(t) + D_{22} u(t) \end{aligned}$$

where

$$\begin{aligned} d(t) &= \text{disturbance vector} \\ u(t) &= \text{control input vector} \\ z(t) &= \text{error vector} \\ y(t) &= \text{observation vector} \\ w(t) &= \text{state vector.} \end{aligned}$$

Also,

$$\begin{aligned} G(s) &:= \begin{bmatrix} G_{11} & G_{12} \\ G_{21} & G_{22} \end{bmatrix} \\ &= \begin{bmatrix} D_{11} & D_{12} \\ D_{21} & D_{22} \end{bmatrix} + \begin{bmatrix} C_1 \\ C_2 \end{bmatrix} (sI - A)^{-1} \begin{bmatrix} B_1 & B_2 \end{bmatrix}. \end{aligned} \tag{5.2}$$

From (5.2),

$$\begin{aligned} G_{11} &= C_1(sI - A)^{-1}B_1 + D_{11} \\ G_{12} &= C_1(sI - A)^{-1}B_2 + D_{12} \\ G_{21} &= C_2(sI - A)^{-1}B_1 + D_{21} \\ G_{22} &= C_2(sI - A)^{-1}B_2 + D_{22}. \end{aligned}$$

We assume that all frequency dependent weights are included in this model. The closed loop transfer function from d to z is

$$\mathcal{F}_l(G, C) := G_{11} + G_{12}C(I - G_{22}C)^{-1}G_{21}.$$

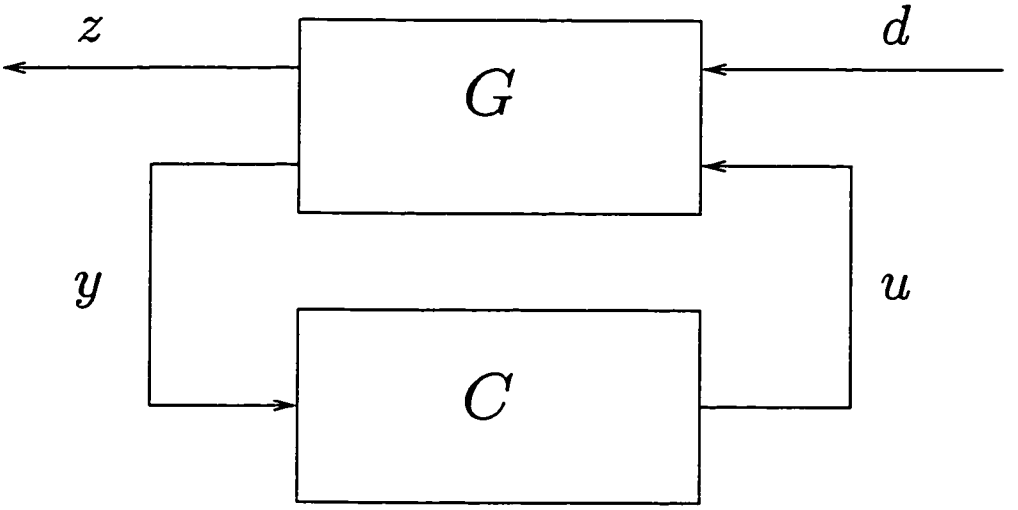

Figure 5.1: Basic feedback control system

We want to find a controller C so that the closed loop is stable and

$$\left\| \frac{\mathcal{F}_l}{\gamma} \right\|_\infty < 1 \tag{5.3}$$

for some given γ. The optimal performance γ_{opt} is the smallest γ for which (5.3) has a solution. Doyle and Glover [GD88] give a state-space parametrization of all controllers that satisfy (5.3). The solution involves solving two algebraic Riccati equations. The resulting algorithm is known as the DGKF algorithm, after the authors, Doyle, Glover, Khargonekar, and Francis, of the paper [DGKF89]. The following are required assumptions.

Assumptions:

(1) (A, B_1, C_1) must be stabilizable and detectable.

(2) (A, B_2, C_2) must be stabilizable and detectable.

(3) There must be a non-singular penalty on control, i.e., D_{12} must have full column rank.

(4) There must be a non-singular disturbance weighting, i.e., D_{21} must have full row rank.

(5a) $D_{11} = 0$, $D_{22} = 0$,

(5b) $D_{12}^T \begin{bmatrix} C_{12} & D_{12} \end{bmatrix} = \begin{bmatrix} 0 & I \end{bmatrix}$, and

(5c) $\begin{bmatrix} B_1 \\ D_{21} \end{bmatrix} D_{21}^T = \begin{bmatrix} 0 \\ I \end{bmatrix}$.

Theorem 5.1 *[DGKF89]*

Suppose that (1)-(5) hold. Then there exists a controller C such that

$$\left\| \frac{\mathcal{F}_l}{\gamma} \right\|_\infty < 1$$

if and only if the following conditions hold:

(a) *The Riccati equation*

$$A^T\Pi + \Pi A + \Pi(B_1B_1^T - B_2B_2^T)\Pi + C_1^TC_1 = 0$$

has a solution $\Pi = \Pi_1 = \Pi_1^T \geq 0$ and $A + (B_1B_1^T - B_2B_2^T)\Pi_1$ is Hurwitz.

(b) *The Riccati equation*

$$A\Pi + \Pi A^T + \Pi(C_1^TC_1 - C_2^TC_2)\Pi + B_1B_1^T = 0$$

has a solution $\Pi = \Pi_2 = \Pi_2^T \geq 0$ and $A + \Pi^2[C_1^TC_1 - C_2^TC_2]$ is Hurwitz.

(c) $\sigma_{max}(\Pi_1\Pi_2) < 1$.

Thus, given a choice for γ, we may iterate until we find a solution sufficiently close to γ_{opt}.

We now put the acoustic noise control problem into this standard framework. For simplicity, consider the SISO case, i.e., $m = 1$. Suitable choices for the above standard DGKF problem are then

$$\begin{aligned} G_{11} &= W_1 G_n(x, x_d), \\ G_{12} &= W_1 G_n(x, x_a), \\ G_{21} &= G_n(x_s, x_d), \\ G_{22} &= G_n(x_s, x_a), \\ C &= -K \end{aligned}$$

where K is some controller, and

$$Q = K(I - G_{22}K)^{-1} = K(I - G_n(x_s, x_a)K)^{-1}.$$

Since our approximations $G_n(x_1, x_2)$ are stable, assumptions (1) and (2) are trivially met. However these approximations are also strictly proper so that $D_{12} = D_{21} = 0$, and thus assumptions (3) and (4) are not met. Two possible ways of getting around this problem are as follows.

Method 1:

Let $D_{12} = D_{21} = \epsilon$, where ϵ is some "small" positive real number. The problem with this choice is that it changes some properties of the transfer function, such as the gain at low frequencies. Because of the complicated nature of the problem, we have no way of tracing the effects of ϵ on the optimal performance γ_{opt}.

Method 2:

We wish to solve

$$\left\| \frac{W_1}{\gamma} S \right\|_\infty < 1 \tag{5.4}$$

where $S = G_n(x, x_d) - G_n(x, x_a)G_n(x_s, x_d)Q(s)$. Suppose we instead solve

$$\left\| \begin{array}{c} \frac{W_1}{\gamma} S \\ W_2 T \end{array} \right\|_\infty < 1,$$

where $W_2 = \epsilon$, some small positive number, and $T = 1 - S$. Then

$$\begin{aligned} G_{11} &= \begin{bmatrix} W_1 G_n(x, x_d) \\ W_2(I - G_n(x, x_a)) \end{bmatrix}, \\ G_{12} &= \begin{bmatrix} W_1 G_n(x, x_a) \\ -W_2 G_n(x, x_a) \end{bmatrix}, \\ G_{21} &= G_n(x_s, x_d), \\ G_{22} &= G_n(x_s, x_a), \text{ and} \\ C &= -K. \end{aligned}$$

With these choices we can use the DGKF algorithm to find C. The solution is suboptimal since we are introducing an artificial weight W_2. This causes numerical problems since the problem is close to being singular. Also, the deviation from the optimal solution γ_{opt} is not known.

In the next two sections, we will discuss other methods that can be used to find the optimal solution to our problem. The first is another state-space technique.

5.2 Model-Matching: State-Space Technique II

Consider the following. Let T_1, $T_2 \in RH_\infty$. We perform an inner/outer factorization (see Definition 3.25) of T_2

$$T_2 = T_{2_i} T_{2_o}$$

where T_{2_i} is inner and T_{2_o} is outer. For any $Q \in H_\infty$

$$\begin{aligned} \|T_1 - T_2 Q\|_\infty &= \|T_1 - T_{2_i} T_{2_o} Q\|_\infty \\ &= \sup_w \left| T_{2_i}^{-1}(jw) T_1(jw) - T_{2_o}(jw) Q(jw) \right|. \end{aligned}$$

Let $R = T_{2_i}^{-1} T_1$ and $X = T_{2_o} Q$. Note that $R \notin H_\infty$.

Definition 5.1

The space L_∞ consists of all bounded functions $F(jw)$, $w \in \mathbb{R}$. The L_∞ norm of F is defined to be

$$\|F\|_\infty = \sup_w |F(jw)| < \infty.$$

Then

$$\inf_{X \in H_\infty} \|R - X\|_\infty = \inf_{X \in H_\infty} \sup_w |R(jw) - X(jw)|$$

where we are now looking at the L_∞ norm since $R \notin H_\infty$. Now factor R as

$$R = R_u + R_s$$

where $R_u \notin H_\infty$ and $R_s \in RH_\infty$. Then

$$\gamma = \inf_{X \in H_\infty} \|R_u + (R_s - X)\|_\infty.$$

From this last equation, we can see that we want to minimize the distance between a stable transfer function and an unstable transfer function, where distance is measured in the L_∞ norm. For R real-rational, by Nehari's Theorem (e.g., [Fra87]) we know that the optimal solution γ_{opt} exists where $\gamma < \gamma_{opt}$.

We may also show that γ_{opt} is the square root of the largest eigenvalue of the product of the observability and controllability gramians found using the state-space representation of R_u (e.g., [Fra87]). However, since we require that $X \in RH_\infty$ and $R \notin H_\infty$, there must be an *exact* cancellation of unstable poles in forming X. Because of this, computational difficulties often arise. This method is only suitable for lower order problems where Maple [Sof97] or hand calculations can be used. In addition, determining the stable and unstable parts of R is a numerically sensitive problem. Thus, it may be difficult to compute γ_{opt}.

As a result we consider an alternative approach, namely the Nevanlinna-Pick interpolation method for solving the minimal model-matching error problem.

5.3 Nevanlinna-Pick Interpolation

In this section, an interpolation method is considered because it is computationally more stable than the state-space techniques outlined in the previous two sections. Using an operator theoretical approach to interpolation, we will show how the results of Sarason [Sar67] imply the Nevanlinna-Pick interpolation method and how this method may be used to solve the above problem. After we review these results, we will show our acoustic noise reduction problem can be solved using Nevanlinna-Pick interpolation.

Recall that the problem we are solving is

$$\gamma_{opt} = \inf_{Q \in RH_\infty} \|T_1 - T_2 Q\|_\infty$$

where $T_1,\ T_2 \in RH_\infty^{m \times 1}$. For simplicity of exposition, let $m = 1$ at this point. Consider the following. Factor

$$T_2 = T_{2_i} T_{2_o}$$

where T_{2_i} is a finite Blashke product (see Definition 3.25) (i.e., T_{2_i} has all its zeros in the open right half plane) and T_{2_o} is outer. Then

$$\gamma_{opt} = \inf_{Q \in RH_\infty} \|T_1 - T_2 Q\|_\infty = \inf_{Q \in RH_\infty} \|T_1 - T_{2_i} T_{2_o} Q\|_\infty.$$

Now factor T_{2_o} as νu where ν has all of its zeros on the imaginary axis and u is a unit of RH_∞ (that is, $u, u^{-1} \in RH_\infty$). Thus,

$$\gamma_{opt} = \inf_{Q \in RH_\infty} \|T_1 - T_{2_i} \nu u Q\|_\infty = \inf_{Q \in RH_\infty} \|T_1 - T_{2_i} \nu Q\|_\infty \tag{5.5}$$

where u has been absorbed into the free parameter Q.

Consider the modified problem

$$\tilde{\gamma}_{opt} = \inf_{Q \in RH_\infty} \|T_1 - T_{2_i} Q\|_\infty. \tag{5.6}$$

Nevanlinna-Pick interpolation is a technique for solving (5.6). The following theorem gives conditions under which $\tilde{\gamma}_{opt} = \gamma_{opt}$.

Theorem 5.2 *[Vid85, Lemma 11, page 177]*

Let $jw_1, jw_2, \ldots, jw_l$ be the distinct zeros of ν on the imaginary axis. Also suppose that ν is strictly proper so that it has a zero as $s \to \infty$. Then $\gamma_{opt} = \tilde{\gamma}_{opt}$ if and only if $|T_1(jw_i)| \leq \tilde{\gamma}_{opt}$ for all i and $\lim_{s \to \infty} |T_1(s)| = 0$.

Proof:

"only if"

Since $\nu(jw_i) = 0$ for all i, $(T_{2_i} \nu Q)(jw_i) = 0$ for all i, for all $Q \in RH_\infty$. Hence $(T_1 - T_{2_i} \nu Q)(jw_i) = T_1(jw_i)$ for all i, and as a result

$$\begin{aligned} \|T_1 - T_{2_i} \nu Q\|_\infty &= \sup_{w \in \mathbf{R}} |(T_1 - T_{2_i} \nu Q)(jw)| \\ &\geq \max_i |(T_1 - T_{2_i} \nu Q)(jw_i)| \\ &= \max_i |T_1(jw_i)|, \quad \text{for all } Q \in RH_\infty. \end{aligned} \tag{5.7}$$

Thus,

$$\tilde{\gamma}_{opt} = \gamma_{opt} = \inf_{Q \in RH_\infty} \|T_1 - T_{2_i} \nu Q\|_\infty \geq \max_i |T_1(jw_i)|.$$

"if"

Select $Q_{opt} \in RH_\infty$ such that $\gamma_{opt} = \|T_1 - T_{2_i} Q_{opt}\|_\infty$. Define for $\epsilon > 0$ and $w \in \mathbb{R}$,

$$h_{w,\epsilon}(s) = \frac{s - jw}{s - (1+\epsilon)jw}$$

and

$$h_\epsilon(s) = \frac{1}{\epsilon s + (1+\epsilon)} \prod_{i=1}^{l} [h_{w_i,\epsilon}(s)]^{m_i}$$

where m_i is the multiplicity of jw_i as a zero of ν. Now observe that for each $\epsilon > 0$, h_ϵ/ν is a unit of RH_∞, and $h_\epsilon(jw) \to 1$ on all compact subsets of the imaginary axis that do not contain any of the w_i's, as $\epsilon \to 0^+$.

Consider the family $Q_\epsilon \in RH_\infty$ for $\epsilon > 0$ defined by $Q_\epsilon = Q_{opt} h_\epsilon/\nu$. Then by (5.5)

$$\|T_1 - T_{2_i} \nu Q_\epsilon\|_\infty \geq \gamma_{opt}, \quad \text{for each } \epsilon > 0. \tag{5.8}$$

Then

$$T_1 - T_{2_i} \nu Q_\epsilon = T_1 - T_{2_i} Q_{opt} h_\epsilon$$

so that

$$|(T_1 - T_{2_i} \nu Q_\epsilon)(jw)| \to |(T_1 - T_{2_i} Q_{opt})(jw)| \leq \tilde{\gamma}_{opt}$$

uniformly on all compact subsets of the imaginary axis that do not contain any of the w_i's. Also, by hypothesis,

$$|(T_1 - T_2 \nu Q_\epsilon)(jw_i)| = |T_1(jw_i)| \leq \tilde{\gamma}_{opt}.$$

Thus,

$$\limsup_{\epsilon \to 0^+} \|T_1 - T_{2_i} \nu Q_\epsilon\|_\infty \leq \tilde{\gamma}_{opt}. \tag{5.9}$$

Combining (5.8), (5.9), and the fact that $\gamma_{opt} \leq \tilde{\gamma}_{opt}$ leads to the conclusion that $\gamma_{opt} = \tilde{\gamma}_{opt}$ and that

$$\|T_1 - T_{2i}\nu Q_\epsilon\|_\infty \to \tilde{\gamma}_{opt} \quad \text{as } \epsilon \to 0^+.$$

□

We will show in the course of our numerical work that T_2 has no zeros on the imaginary axis except as $s \to \infty$. Thus, since $\lim_{s\to\infty} |T_1(s)| \to 0$, by Theorem 5.2, $\tilde{\gamma}_{opt} = \gamma_{opt}$.

Thus, we consider the equivalent problem

$$\gamma_{opt} = \inf_{Q \in RH_\infty} \|T_1 - T_{2i}Q\|_\infty.$$

This is the precise problem addressed by [Tan92], where Nevanlinna-Pick interpolation is used.

For simplicity of exposition, the results of this section are presented on the open unit disc. Let D be the open unit disc and $\overline{D}$ be the closed unit disc. The right half plane $\Re(s) > 0$ may be mapped to the open unit disc using a conformal mapping. For example, for s in the right half plane and $z \in D$, let

$$s = \frac{1+z}{1-z}$$

or equivalently,

$$z = \frac{s-1}{s+1}.$$

Thus, the imaginary axis as well as $s \to \infty$ is mapped to the unit circle $e^{j\theta}$, $\theta \in [0, 2\pi]$.

Let $F(s) = f(\frac{s-1}{s+1})$. If $F(s)$ is a bounded analytic function on $\Re(s) > 0$, then the conformal mapping preserves all important properties. That is, $f(z)$ is a bounded analytic function on D.

The basic Nevanlinna-Pick problem can be stated as follows.

> Find necessary and sufficient conditions for the existence of an analytic $\phi : D \to \overline{D}$ such that $\phi(\lambda_i) = b_i,\ i = 1, 2, \ldots, n$, for given points $\lambda_i \in D$ and $b_i \in \overline{D}$.

We assume the λ_i are distinct. If λ_i are the zeros of T_2 in the open unit disc, then $(T_1 - T_2Q)(\lambda_i) = T_1(\lambda_i) = b_i$, for all $i = 1, 2, \ldots, n$. Thus, ϕ "looks like" $T_1 - T_2Q$. That is, ϕ is an analytic function whose zeros match those of $T_1 - T_2Q$ in the right half plane.

Consider the model-matching problem

$$\|T_1 - T_{2_i}Q\|_\infty \leq 1. \tag{5.10}$$

Suppose we find $Q \in H_\infty(D)$ such that $\|\phi\|_\infty \leq 1$ and $\phi(\lambda_i) = b_i$. Write

$$\phi = T_1 - T_{2_i}Q$$

and solve for Q:

$$Q = \frac{T_1 - \phi}{T_{2_i}}.$$

Since $\phi(\lambda_i) = T_1(\lambda_i)$ at the zeros of T_{2_i}, $Q \in H_\infty(D)$. In other words, the model-matching problem can be solved by solving an interpolation problem. The technique for solving this interpolation problem is described below.

The explanation in this section is based largely on the tutorial paper of Tannenbaum [Tan92]. We first begin with some mathematical preliminaries.

Definition 5.2

A function $f(z)$, $z \in \mathbb{C}$, is in $H_2(D)$ if f is analytic in D and

$$\|f\|_2 = \sup_{r<1} \left(\frac{1}{2\pi} \int_0^{2\pi} \left| f(re^{j\theta}) \right|^2 \, d\theta \right)^{1/2} < \infty.$$

The inner product on $H_2(D)$ is defined by

$$\langle f, g \rangle := \frac{1}{2\pi} \int_0^{2\pi} f(e^{j\theta}) g(e^{j\theta})^* \, d\theta.$$

Let f be an analytic function in D. Then f may be written as

$$f(z) = \sum_{i=0}^{\infty} f_i z^i$$

where $z \in D$. Let $S : H_2(D) \to H_2(D)$ be the *right shift operator*, i.e., $Sf(z) = zf(z)$ for $z \in D$. That is, S shifts all coefficients of f to the right. The adjoint of the shift operator, denoted by S^*, shifts all coefficients to the left. That is, $S^* : H_2(D) \to H_2(D)$ is defined by

$$(S^* f)(z) = z^{-1}(f(z) - f_0) = f_1 + f_2 z + f_3 z^2 + \ldots$$

for all $f \in H_2(D)$. Let $P : H_2(D) \to H_2(D) \ominus UH_2(D)$ be the *orthogonal projection* where $U \in H_\infty$. Define the *orthogonal complement* of $\mathcal{H}_1$ in X by

$$X \ominus \mathcal{H}_1 := \left\{ h \in X \mid \langle h, h_1 \rangle = 0 \text{ for all } h_1 \in \mathcal{H}_1 \right\}.$$

Define the *compressed shift operator* by

$$T := PS|_{H_2(D) \ominus UH_2(D)}$$

where $U \in H_\infty$. The adjoint of T is $T^* = S^*$ restricted to $H_2(D) \ominus UH_2(D)$. Note that $TP = PS$.

Let $\phi \in H_\infty(D)$ be an arbitrary function. Let $M_\phi : H_2(D) \to H_2(D)$ denote the *multiplication operator* induced by ϕ. That is, $M_\phi f = \phi f$. Then we define

$$\phi(T) := PM_\phi|_{H_2(D) \ominus UH_2(D)}.$$

An operator $A : H_2(D) \to H_2(D)$ commutes with $S : H_2(D) \to H_2(D)$ if and only if $A = M_\phi$ for some $\phi \in H_\infty(D)$. That is, every time invariant input/output operator admits a transfer function. Thus, $\|A\| = \|\phi\|_\infty$ where $\|A\|$ is the operator norm of A [NS82]. Sarason's Theorem is a generalization of this idea.

Theorem 5.3 *(Sarason's Theorem, [Sar67])*

Let $U \in H_\infty$. Let $A : H_2(D) \ominus UH_2(D) \to H_2(D) \ominus UH_2(D)$ be any (bounded linear) operator such that $TA = AT$. Then there exists a function $\phi \in H_\infty(D)$ such that $A = \phi(T)$ and $\|A\| = \|\phi\|_\infty$.

We now put the Nevanlinna-Pick problem into the framework of Sarason's Theorem. For the Blashke product (see Definition 3.24)

$$B(z) = \prod_{i=1}^{n} \frac{z - \lambda_i}{1 - \bar{\lambda}_i z}$$

define $X = H_2 \ominus BH_2$. Every inner factor we consider is of this form. In particular, T_{2_i} is of this form. We also have the following result.

Lemma 5.1 *(e.g., [Tan92])*

X is a finite-dimensional vector space of dimension n. A basis of X consists of $\{g_1, g_2, \ldots, g_n\}$ where $g_i(z) = \frac{1}{1-\bar{\lambda}_i z}$ for $i = 1, 2, \ldots, n$.

Proof:

One can use Cauchy's Integral Theorem to show that for $h \in H_2$, $\langle h, g_i \rangle = h(\lambda_i)$,

for all i. So $q \in BH_2$ if and only if $\langle q, g_i \rangle = 0$ for all i. Thus $q \in BH_2$ if and only if $q \perp \{$ span of $g_i\}$ which is X. Linear independence can be shown by contradiction using the form of $B(z)$. □

It is easier to show how $T : X \to X$ acts on $\{g_i\}$ by considering $T^* : X \to X$.

Lemma 5.2 *(e.g., [Tan92])*

$$T^* g_i = \bar{\lambda}_i g_i, \quad \textit{for all } i = 1, 2, \ldots, n.$$

Thus, g_i are eigenvectors of T^*.

Proof:

Let z_0 be a point on the unit circle, i.e., $|z_0| = 1$. Then, for $g \in X$,

$$T^* g(z_0) = \overline{z_0}\Big(g(z_0) - g(0)\Big).$$

Also,

$$\overline{z_0}\Big(g_i(z_0) - g_i(0)\Big) = \overline{z_0}\left(\frac{1}{1 - \overline{\lambda_i} z_0} - 1\right) = \overline{\lambda_i} g_i(z_0).$$

□

An operator $A : X \to X$ commutes with T if and only if A^* commutes with T^*. From Sarason's Theorem, A commutes with T if and only if there exists a function $\phi \in H_\infty(D)$ such that $A = \phi(T)$. We then say that "ϕ interpolates A". This terminology is made clear by the following lemma.

Lemma 5.3 *[Tan92, Lemma 4]*

Let $A : X \to X$ be such that $A^* g_i = \bar{b}_i g_i$, for all i. A function $\phi \in H_\infty(D)$ satisfies $\phi(T) = A$ if and only if $\phi(\lambda_i) = b_i$, for all i. In this case, we say ϕ interpolates A.

Proof:

"only if"

Suppose $A = \phi(T)$. Then $Ag_i = \phi g_i - Bq_i$ for some $q_i \in H_2$, for all i. Thus,

$$(Ag_i)(\lambda_i) = \phi(\lambda_i)g_i(\lambda_i). \tag{5.11}$$

Also,

$$(A^* g_i)(\lambda_i) = \overline{b_i} g_i(\lambda_i).$$

But

$$\begin{aligned} (Ag_i)(\lambda_i) &= \langle Ag_i, g_i \rangle \\ &= \langle g_i, A^* g_i \rangle \\ &= \langle g_i, \overline{b_i} g_i \rangle \\ &= b_i g_i(\lambda_i). \end{aligned} \tag{5.12}$$

Thus, by (5.11) and (5.12), $\phi(\lambda_i) = b_i$.

"if"

Suppose that $\phi(\lambda_i) = b_i$, for all i. To show $\phi(T) = A$, we need only check the basis vector g_i. Hence, we must show that $\phi(T)^* g_i = \overline{b_i} g_i$, for all i. It is enough to show that

$$\langle \phi(T)^* g_i, g_j \rangle = \langle \overline{b_i} g_i, g_j \rangle, \quad \text{for all } i, j.$$

Observe that

$$\phi(T) g_i = \phi g_i - Bq_i$$

for some $q_i \in H_2(D)$, for all i. Also, since $g_i \perp BH_2(D)$,

$$\langle g_i, Bq_j \rangle = 0, \quad \text{for all } i, j.$$

Thus,

$$\begin{aligned}
\langle \phi(T)^* g_i, g_j \rangle &= \langle g_i, \phi(T) g_j \rangle \\
&= \langle g_i, \phi g_j - B q_j \rangle \\
&= \langle g_i, \phi g_j \rangle \\
&= \overline{\langle \phi g_j, g_i \rangle} \\
&= \overline{\phi(\lambda_i) g_j(\lambda_i)} \\
&= \overline{\phi(\lambda_i)} g_i(\lambda_j) \quad \text{since } g_i(\lambda_j) = \overline{g_j(\lambda_i)}.
\end{aligned}$$

Now since $\langle \overline{b_i} g_i, g_j \rangle = \overline{b_i} g_i(\lambda_i)$ and $\phi(\lambda_i) = b_i$, we are done. □

With the above results, we have the following main theorem.

Theorem 5.4 *(Nevanlinna-Pick Theorem)*

There exists an analytic function $\phi : D \to \bar{D}$ such that $\|\phi\| \leq 1$ and $\phi(\lambda_i) = b_i$, for all i if and only if the Pick matrix

$$\left[\frac{1 - \bar{b}_i b_j}{1 - \bar{\lambda}_i \lambda_j}\right] \geq 0.$$

Proof:

By Sarason's Theorem, there exists an interpolating function ϕ such that $\|\phi\|_\infty < 1$ (i.e., $\phi : D \to \bar{D}$) if and only if $\|A\| \leq 1$ where $A = \phi(T)$. By Lemma 5.3, we need necessary and sufficient conditions such that $A : X \to X$, $A^* g_i = \bar{b}_i g_i$, satisfies $\|A\| \leq 1$.

Now

$$\|A\| \leq 1$$

if and only if

$$\|A^*\| \leq 1$$

if and only if

$$\langle A^* g, A^* g \rangle \leq \langle g, g \rangle, \quad \text{for all } g \in X. \tag{5.13}$$

By Lemma 5.1, any $g \in X$ may be uniquely represented by

$$g = \sum_{i=1}^{n} \alpha_i g_i$$

for some $\{\alpha_i\}$. Now

$$\begin{aligned} \langle g, g \rangle &= \sum_{1 \le i,j \le n} \alpha_i \overline{\alpha_j} \langle g_i, g_j \rangle \\ &= \sum_{1 \le i,j \le n} \alpha_i \overline{\alpha_j} g_i(\lambda_j) \end{aligned}$$

so that

$$\langle g, g \rangle = \sum_{1 \le i,j \le n} \alpha_i \overline{\alpha_j} \frac{1}{1 - \bar{\lambda}_i \lambda_j}. \tag{5.14}$$

But

$$A^* g = \alpha_1 \bar{b}_1 g_1 + \ldots + \alpha_n \bar{b}_n g_n \tag{5.15}$$

and so

$$\langle A^* g, A^* g \rangle = \sum_{1 \le i,j \le n} \alpha_i \overline{\alpha_j} \bar{b}_i b_j \frac{1}{1 - \bar{\lambda}_i \lambda_j}.$$

Therefore (5.13) holds if and only if

$$\sum_{1 \le i,j \le n} \alpha_i \overline{\alpha_j} \bar{b}_i b_j \frac{1}{1 - \bar{\lambda}_i \lambda_j} \le \sum_{1 \le i,j \le n} \alpha_i \overline{\alpha_j} \frac{1}{1 - \bar{\lambda}_i \lambda_j}.$$

That is,

$$0 \le \sum_{1 \le i,j \le n} \alpha_i \bar{\alpha}_j \left(\frac{1 - \bar{b}_i b_j}{1 - \bar{\lambda}_i b_j} \right).$$

Since the α_i are arbitrary, the Pick matrix must be positive semi-definite. □

Thus, by the above results, we may solve the problem

$$\gamma_{opt} = \inf_{Q \in RH_\infty} \|T_1 - T_{2_i} Q\|_\infty$$

using Nevanlinna-Pick interpolation. Now suppose our "tall" problem (5.1) can be rewritten so that instead we are solving the *scalar* problem

$$J^* = \inf_{Q \in RH_\infty} \|F - BQ\|_\infty \tag{5.16}$$

where $F \in RH_\infty$ and B is inner. We shall show in Section 5.4 that our acoustic problem can in fact be rewritten this way. The following theorem and its corollary provide a simple method to compute this infimum.

Theorem 5.5 *[Vid85, page 197]*

Let $\lambda_1, \lambda_2, \ldots, \lambda_k$ *be the simple zeros of* B. *Suppose* $F \in RH_\infty$. *Define the following:*

$$\Omega = \textit{Block Diagonal}\Big\{ F^*(\lambda_1), \ldots, F^*(\lambda_k) \Big\}$$

and

$$\Gamma = [\Gamma]_{ij},\ i,j,= 1, \ldots, k$$

where

$$[\Gamma]_{ij} = \frac{1}{1 - \bar{\lambda}_j \lambda_i}$$

and $\Omega \in \mathbb{C}^{k \times k}$, $\Gamma \in \mathbb{C}^{k \times k}$. *Then*

$$\inf_{Q \in RH_\infty} \|F - BQ\|_\infty = \inf\Big\{ \gamma :\ \gamma^2 \Gamma - \Omega^* \Omega > 0 \Big\}. \tag{5.17}$$

Proof:

Examining the proof of Theorem 5.4 we see that the matrix representation of A^* with respect to the basis $\{g_i\}$ is the diagonal matrix Ω with entries $\overline{b_i}$ (see (5.15)). Let $\underline{\alpha}$ be the coordinates of some arbitrary element $g \in X$. Then

$$\|A^* g\|^2 = \|\Omega \underline{\alpha}\|^2 = \underline{\alpha}^* \Omega^* \Omega \underline{\alpha}.$$

Also by (5.14),

$$\|g\|^2 = \underline{\alpha}^* \Gamma \underline{\alpha}$$

where

$$[\Gamma]_{ij} = \frac{1}{1 - \bar{\lambda}_j \lambda_i}.$$

Thus,

$$\|A^*\| \leq \gamma$$

or,

$$\|A^* g\|^2 \leq \gamma^2 \|g\|^2$$

if and only if

$$\gamma^2 \Gamma - \Omega^* \Omega \geq 0.$$

□

From the proof of Theorem 5.5, both Γ and $\Omega^*\Omega$ are positive definite and Hermitian.

Corollary 5.6 *(e.g., [DFT92])*

Let $\sigma_{max}(M)$ denote the maximum eigenvalue of a symmetric matrix $M \in \mathbb{R}^{n \times n}$. Then,

$$\begin{aligned} J^* &= \inf\left\{\gamma : \gamma^2 \Gamma - \Omega^* \Omega > 0\right\} \\ &= \sqrt{\sigma_{max}\left(\Gamma^{-1/2} \Omega^* \Omega \Gamma^{-1/2}\right)}. \end{aligned}$$

Proof:

By simple manipulation we obtain

$$\begin{aligned} & \gamma^2 \Gamma - \Omega^* \Omega > 0 \\ \Leftrightarrow \quad & \gamma^2 \Gamma > \Omega^* \Omega \\ \Leftrightarrow \quad & \gamma^2 \Gamma \Gamma^{-1/2} > \Omega^* \Omega \Gamma^{-1/2} \\ \Leftrightarrow \quad & \gamma^2 I > \Gamma^{-1/2} \Omega^* \Omega \Gamma^{-1/2} \quad \text{since } \gamma \in \mathbb{C} \\ \Leftrightarrow \quad & \left\langle (\gamma^2 I - \Gamma^{-1/2} \Omega^* \Omega \Gamma^{-1/2}) x, x \right\rangle > 0. \end{aligned}$$

Therefore

$$\inf\Big\{\gamma:\ \gamma^2\Gamma - \Omega^*\Omega > 0\Big\} = \inf\Big\{\gamma:\ \Big\langle(\gamma^2 I - \Gamma^{-1/2}\Omega^*\Omega\Gamma^{-1/2})x, x\Big\rangle > 0\Big\}.$$

Now $\gamma^2\Gamma - \Omega^*\Omega > 0$ if and only if $\gamma^2 \geq \sigma_{max}\Big(\Gamma^{-1/2}\Omega^*\Omega\Gamma^{-1/2}\Big)$. Thus,

$$J^* = \sqrt{\sigma_{max}\Big(\Gamma^{-1/2}\Omega^*\Omega\Gamma^{-1/2}\Big)}.$$

□

These results hold for the scalar model-matching problem. In the next section, we shall see how these results may be used to solve the tall model-matching problem.

5.4 Solving the Tall Model-Matching Problem

Recall that

$$\gamma_{opt} = \inf_{Q\in RH_\infty} \|T_1 - T_2Q\|_\infty$$

where

$$\begin{aligned} T_1 &\in RH_\infty^{m\times 1} \\ T_2 &\in RH_\infty^{m\times 1} \end{aligned}$$

and m is the number of observation (performance) points. We need to rewrite this so that it is a scalar problem. Recall that T_1 and T_2 are strictly proper and assume T_2 has no zeros on the imaginary axis. We can then apply the results from the previous section. Factor

$$T_2 = T_{2_i}T_{2_o}$$

where $T_{2_i} \in RH_\infty^{m\times 1}$ is inner with no zeros on the imaginary axis except possibly as $s \to \infty$ and $T_{2_o} \in RH_\infty$ is outer. By Theorem 5.2, T_{2_o} may be absorbed into the free parameter Q.

Definition 5.3

A complementary inner factor (CIF) is defined to be a matrix $\Theta \in RH_\infty^{m\times(m-l)}$ *such that for* $M \in RH_\infty^{n\times l}$ *inner,* $\Phi \in RH_\infty^{m\times m}$ *given by*

$$\Phi = [M\ \Theta]$$

is square and inner.

By [Vid85, Lemma 7, page 213], we may construct a square inner matrix $\Phi \in RH_\infty^{m\times m}$ such that

$$T_2 = \Phi \begin{bmatrix} T_{2_o} \\ 0^{(m-1)\times l} \end{bmatrix}$$

and

$$\Phi = \begin{bmatrix} T_{2_i} & \Theta \end{bmatrix}$$

where $\Theta \in RH_\infty^{m\times(m-1)}$ is the complementary inner factor of T_2. Thus

$$\begin{aligned} \|T_1 - T_2Q\|_\infty &= \left\| T_1 - \Phi \begin{bmatrix} T_{2_o} \\ 0 \end{bmatrix} Q \right\|_\infty \\ &= \left\| \Phi^* T_1 - \begin{bmatrix} T_{2_o} \\ 0 \end{bmatrix} Q \right\|_\infty . \end{aligned}$$

Let

$$\begin{bmatrix} A \\ C \end{bmatrix} = \Phi^* T_1 \in M(L_\infty).$$

Therefore we may write

$$\|T_1 - T_2Q\|_\infty = \left\| \begin{bmatrix} A \\ C \end{bmatrix} - \begin{bmatrix} T_{2_o}Q \\ 0 \end{bmatrix} \right\|_\infty .$$

Let $\tilde{Q} = T_{2_*}Q$. Then

$$\|T_1 - T_2 Q\|_\infty = \left\| \begin{bmatrix} A - \tilde{Q} \\ C \end{bmatrix} \right\|_\infty . \tag{5.18}$$

Definition 5.4

If we can find M_l, where M_l, $M_l^{-1} \in M(RH_\infty)$, such that $M_l^* M_l = I - G^*G$, then M_l is a left spectral factor of $I - G^*G$.

Definition 5.5

If we can find M_r, where M_r, $M_r^{-1} \in M(RH_\infty)$, such that $M_r M_r^* = I - GG^*$, then M_r is a right spectral factor of $I - GG^*$.

The following lemma is needed to reduce (5.18) further to a scalar problem.

Lemma 5.4 *[Vid85, Lemma 27, page 216]*

Suppose $W = \begin{bmatrix} X \\ Y \end{bmatrix} \in M(L_\infty)$ *is rational. If* $\|Y\|_\infty < \gamma$, *then* $\|W\|_\infty \leq \gamma$ *if and only if* $\|X(\gamma^2 I - Y^*Y)^{-1/2}\|_\infty \leq 1$.

Note: $(\gamma^2 I - Y^*Y)^{-1/2}$ denotes the left spectral factor of $(\gamma^2 I - Y^*Y)^{-1}$.

Proof:

Clearly $\|W\|_\infty \geq \|Y\|_\infty$. Now $\|W\|_\infty \leq \gamma$ if and only if

$$\begin{aligned} & W(jw)W^*(jw) \leq \gamma^2 I, \quad \text{for all } w \\ \Leftrightarrow \quad & (XX^* + YY^*)(jw) \leq \gamma^2 I, \quad \text{for all } w \\ \Leftrightarrow \quad & (XX^*)(jw) \leq (\gamma^2 I - YY^*)(jw), \quad \text{for all } w. \end{aligned}$$

If $\gamma > \|Y\|_\infty$, $(\gamma^2 - Y^*Y)^{1/2}$ exists and has an inverse in $M(H_\infty)$ [Vid85]. The result now follows. □

Theorem 5.7

$$\inf_{\tilde{Q}\in M(RH_\infty)} \left\| \begin{bmatrix} A-\tilde{Q} \\ C \end{bmatrix} \right\|_\infty \leq \gamma$$

if and only if

$$\inf_{\tilde{Q}\in M(RH_\infty)} \|A(\gamma^2 I - C^*C)^{-1/2} - \tilde{Q}\|_\infty \leq 1.$$

Proof:

From Theorem 5.4 we know

$$\inf_{\tilde{Q}\in M(RH_\infty)} \left\| \begin{bmatrix} A-\tilde{Q} \\ C \end{bmatrix} \right\|_\infty \leq \gamma$$

if and only if

$$\inf_{\tilde{Q}\in M(RH_\infty)} \|(A-\tilde{Q})(\gamma^2 I - C^*C)^{-1/2}\|_\infty \leq 1$$

where $\|C\|_\infty < \gamma$. Now

$$\|(A-\tilde{Q})(\gamma^2 I - C^*C)^{-1/2}\|_\infty = \|A(\gamma^2 I - C^*C)^{-1/2} - \tilde{Q}(\gamma^2 I - C^*C)^{-1/2}\|_\infty$$

and $(\gamma^2 I - C^*C)^{-1/2} \in M(RH_\infty)$ since $\|C\|_\infty < \gamma$. Thus, let $\bar{Q} = \tilde{Q}(\gamma^2 I - C^*C)^{-1/2} \in M(RH_\infty)$ (another free parameter). □

Observe that $A(\gamma^2 I - C^*C)^{-1/2} \in M(L_\infty)$ (not necessarily stable) and $\bar{Q} \in M(H_\infty)$ (stable).

Definition 5.6

Suppose $\tilde{D}$, $\tilde{N} \in M(H_\infty)$. Then $\tilde{D}$ and $\tilde{N}$ are left coprime if and only if there exist X, $Y \in M(H_\infty)$ such that $X\tilde{D} + Y\tilde{N} = I$.

Definition 5.7

Let $G \in M(L_\infty)$. An ordered pair $(\tilde{D}, \tilde{N})$ where $\tilde{D}, \tilde{N} \in M(RH_\infty)$ is a left coprime factorization of G if

1) $\tilde{D}$ is square and $|\tilde{D}| \neq 0$,

2) $G = \tilde{D}^{-1}\tilde{N}$, and

3) $\tilde{D}$ and $\tilde{N}$ are left coprime.

Let $L = (\gamma^2 I - C^*C)^{-1/2}$. Since $AL \in M(L_\infty)$, it has a left coprime factorization $(\tilde{D}, \tilde{N})$ so that $AL = \tilde{D}^{-1}\tilde{N}$ where $\tilde{D}, \tilde{N} \in M(RH_\infty)$. Let $\tilde{D} = \tilde{D}_o\tilde{D}_i$ be an inner/outer factorization where $\tilde{D}_o$ is a unit (i.e., has an inverse in $M(RH_\infty)$). So

$$AL = \tilde{D}^{-1}\tilde{N} = \tilde{D}^{-1}\tilde{D}_o^{-1}\tilde{N} = \tilde{D}_i^{-1}V \tag{5.19}$$

where $V = \tilde{D}_o^{-1}\tilde{N} \in M(RH_\infty)$. Recall from properties of matrices that

$$A^{-1} = \frac{A^{adj}}{|A|}.$$

Thus,

$$\begin{aligned} \|AL - \bar{Q}\|_\infty &= \|\tilde{D}_i^{-1}V - \bar{Q}\|_\infty \\ &= \left\| \frac{\tilde{D}_i^{adj}V}{|\tilde{D}_i|} - \bar{Q} \right\|_\infty . \end{aligned}$$

Since $|\tilde{D}_i| = 1$ on the imaginary axis,

$$\|AL - \bar{Q}\|_\infty = \|F - B\bar{Q}\|_\infty \tag{5.20}$$

where $F = \tilde{D}_i^{adj}\tilde{D}^{-1}\tilde{N}$ and $B = |\tilde{D}_i|$. Details of how to find $\tilde{D}_i$ and V may be found in Appendix A, Section A.1.2.

This is now a scalar problem which can be solved using Corollary 5.6.

5.5 Implementation

The results of the previous section are summarized in the following algorithm. Some difficulties associated with computation are then discussed. Details of routine calculations, such as inner/outer factorizations, are in Appendix A.

Algorithm

Step (1) Calculate an inner/outer factorization of T_2,

$$T_2 = T_{2_i} T_{2_o}.$$

Step (2) Construct a square inner matrix Φ such that

$$T_2 = \Phi \begin{bmatrix} T_{2_o} \\ 0_{(m-l)\times l} \end{bmatrix}$$

where $\Phi = [\ T_{2_i} \quad \Theta\ ]$ and Θ is the complementary inner factor.

Step (3) Find A and C such that

$$\begin{bmatrix} A \\ C \end{bmatrix} = \Phi^* T_1.$$

Step (4) Choose $\gamma > \|C\|_\infty$.

Step (5) Calculate $L = (\gamma^2 I - C^*C)^{-1/2}$.

Step (6) Solve

$$J^* = \inf_{\bar{Q} \in M(RH_\infty)} \|AL - \bar{Q}\|_\infty \tag{5.21}$$

as follows.

6(a) Calculate a left coprime factorization $(\tilde{D}, \tilde{N})$ for AL: $AL = \tilde{D}^{-1}\tilde{N}$.

6(b) Calculate an inner/outer factorization for $\tilde{D}$: $\tilde{D} = \tilde{D}_o\tilde{D}_i$.

6(c) Let $F = \tilde{D}_i^{adj}\tilde{D}^{-1}\tilde{N}$ and $B = |\tilde{D}_i|$.

6(d) Find the (simple) zeros of B (call them $\{\lambda_1, \lambda_2, \ldots, \lambda_k\}$).

6(e) Form

(i) $\Omega = \text{Block Diagonal}\{F^*(\lambda_1), \ldots, F^*(\lambda_k)\}$,

(ii) $\Gamma = [\Gamma_{ij}]$ where

$$\Gamma_{ij} = \frac{1}{1 - \bar{\lambda}_j\lambda_i}.$$

6(f) Compute

$$J^* = \sqrt{\sigma_{max}\left(\Gamma^{-1/2}\Omega^*\Omega\Gamma^{-1/2}\right)}.$$

Step (7) If $J^* < 1$, decrease γ and go to Step (5). If $J^* > 1$, increase γ and go to Step (5). Stop when $J^* = 1$. The optimal γ is the current choice of γ.

In each step we must either determine a factorization or perform a numerical calculation such as determining zeros or computing the norm of a transfer matrix, for instance. Recall that we are solving a tall model-matching problem. That is,

$$\gamma_{opt} = \inf_{Q \in RH_\infty} \|T_1 - T_2Q\|_\infty$$

where $T_1,\ T_2 \in RH_\infty^{m\times 1}$. If we are to consider the problem of "global" noise reduction, then the number of rows of T_1 and T_2 (representing the number of performance points) must be allowed to increase. In addition, the elements of T_1 and T_2 are rational approximations with increasing dimension (see Problem 4 on page 27). Thus, the degree of each element is potentially very large, depending on the dimension n of the finite-dimensional approximating space used. We can see that the implementation of the algorithm becomes unwieldy very quickly.

Because of this, we found it necessary to be clever in the execution of each step of the algorithm. In particular, to prevent degree inflation and to circumvent the accumulation of numerical errors, it was essential that we employ model reduction techniques at every step. In the next section, we describe some approaches to model reduction.

5.5.1 Model Reduction

A realization which is both controllable and observable is called *minimal*. We may find a minimal realization by "removing" first any uncontrollable modes, and then any unobservable modes. For a single-input/single-output system, finding a minimal realization is essentially cancelling common poles and zeros in the transfer function. A numerically stable method is via balanced realizations.

Minimal and balanced realizations play a very important role in every aspect of the algorithm. They are used in every step that requires factorizations or the solution of a Riccati equation. Without these realizations, matrices become poorly conditioned and the degree of the transfer function in question inflates, causing the algorithm to fail.

Let us consider a strictly proper transfer function $G(s)$. A balanced realization of $G(s) = C(sI - A)^{-1}B := [A, B, C, 0]$ is one such that the Lyapunov equations

$$AP + PA^T + BB^T = 0 \tag{5.22}$$

and

$$A^TQ + QA + C^TC = 0 \tag{5.23}$$

have a common diagonal solution $X = P = Q$ such that

$$X = \begin{bmatrix} \sigma_1 I & 0 & \dots & 0 & 0 \\ 0 & \sigma_2 I & 0 & \dots & 0 \\ \vdots & 0 & \ddots & \dots & \vdots \\ 0 & 0 & \dots & 0 & \sigma_n I \end{bmatrix} \tag{5.24}$$

where σ_i are known as the system singular values. (e.g., [Mac89]). The solution P to (5.22) is called the *controllability gramian.* Similarly, the solution Q to (5.23) is called the *observability gramian.* In order to reduce the order of the model, we toss out the "small" σ_i, representing the unobservable and/or uncontrollable modes. The balanced realization of the original system is further reduced by discarding those states which are weakly coupled to the inputs and outputs.

One method for obtaining a balanced realization of the original system is given in [Moo81]. Suppose $P = Q = X$ as in (5.24). Let $G_k(s)$ is the k^{th} order reduced model, P the balanced controllability gramian, and Q the balanced observability gramian. Then

$$\|G(s) - G_k(s)\|_\infty \leq 2 \sum_{i=k+1}^{n} \sigma_i.$$

Thus, an error bound is easily obtained. A common criterion for order reduction is to choose k such that $\|G(s) - G_k(s)\|_\infty < \epsilon$ for some $\epsilon > 0$.

The question remains, how do we know which modes to discard? That is, at what point does a mode become essentially uncontrollable or unobservable? Unfortunately, the answer is more an art than a science. In the model reductions performed during the implementation of the algorithm, special care had to be taken not to move or remove any right half plane zeros of T_2 since this would alter the solution to the model-matching problem. In addition, care had to be given not to change the frequency response characteristics of the transfer function involved, since this

too would alter the solution to the problem. Thus, for n sufficiently large, the pattern of the right half plane zeros (the number and location) was observed before determining the most reasonable tolerance to be used in the model reduction.

5.5.2 Programming

The factorizations used in the implementation of the algorithm are discussed in Appendix A. These factorizations generally require the solution of either one or two algebraic Riccati equations. The factorizations are, for the most part, easily coded in Matlab [Mat94]. However, some of the methods to obtain these factorizations require that the state-space representations be non-strictly proper. Therefore, to alter the state-space form, a "relative degree" trick was used, the details of which may be found in Appendix A, Section A.2.

Finally, we would be remiss if we did not mention that all programs used in the course of this work were written in Matlab [Mat94]. Source code is listed in Appendix B. However, because of the size and complexity of the problem, most of the code had to be converted to C. This was done using the Matlab command *mcc*. Using this command was far from trivial. Unfortunately, the conversion was unreliable since *mcc* was unable to convert many of the more numerically intensive Matlab modules, such as the Riccati equation solver. Conversion had to be checked by hand.

Chapter 6

Achievable Acoustic Noise Reduction

In Chapter 5, we presented the algorithm required to solve Problem 4, the tall acoustic noise reduction problem with finite-dimensional approximations (see page 27). In Chapter 4, we showed that with an appropriate approximation scheme, the solution to Problem 4 converges to the solution of Problem 3, the infinite-dimensional acoustic noise reduction problem (see page 26). By increasing the number of observation points x_i and varying the location of the controller sensing point at x_s and controller actuating point at x_a, we will discuss the solution to the problem of achievable global noise reduction for a disturbance at x_d.

In the design of a controller, we may use either feedback or feedforward design. Recall that when the sensor location x_s is located to the right of the actuator location x_a so that $x_s > x_a$, we refer to this as a feedback system. Similarly, when $x_s < x_a$, we refer to this as a feedforward system. Both configurations are illustrated in Figure 2.3.

First, let us consider feedback design. There are a number of questions that we may pose. How does noise reduction with an increasing number m of observation points x_i located throughout the duct compare to the achievable level of noise reduction at a single point in the duct? Is it possible to reduce noise everywhere in the duct to a level comparable to that of reducing noise at a single point? How does the level of achievable noise reduction vary as x_s is varied? Similarly, how does the level of achievable noise reduction vary as x_a is varied? Finally, suppose that both x_a and x_s are fixed. How does the location of the observation points x_i about these fixed locations affect the achievable noise reduction?

Second, let us consider feedforward design. Suppose x_a and x_s are both fixed. How does an increasing number of observation points x_i between x_s and x_a affect the achievable level of acoustic noise reduction? What is the achievable level of noise reduction at observation points located to the right of x_a?

In the results that follow, we will try to answer these questions.

6.1 Numerical Preliminaries

Recall that we are solving an infinite-dimensional problem by approximating it on successively larger finite-dimensional subspaces using Legendre polynomials or linear splines. We know from Chapter 4 that our approximating plant transfer function G_n is converging to the exact transfer function G over any compact interval as n increases. We also know that the associated inner factors are also converging over any compact interval as n increases. Because of the computational intensity of the problem, we will determine a priori what value of n is sufficient for all further calculations. Recall the problem we are solving (see Problems 3 and 4 on pages 26 and 27, respectively). Let m be the number of observation (or performance) points

in the duct. Let $x \in \{x_1, x_2, \ldots, x_m\}$. Then

$$\begin{aligned}\gamma_n &= \inf_{Q \in RH_\infty} \left\| \begin{array}{c} W_1\Big(G_n(x_1,x_d) - G_n(x_1,x_a)G_n(x_s,x_d)Q\Big) \\ W_1\Big(G_n(x_2,x_d) - G_n(x_2,x_a)G_n(x_s,x_d)Q\Big) \\ \vdots \\ W_1\Big(G_n(x_m,x_d) - G_n(x_m,x_a)G_n(x_s,x_d)Q\Big) \end{array} \right\|_\infty \\ &= \inf_{Q \in RH_\infty} \|T_1 - T_2 Q\|_\infty. \end{aligned} \tag{6.1}$$

Let the length L of the duct be 4 metres. Let $W_1(s) = \frac{1}{\frac{s}{1000}+1}$ (so that low frequencies are weighted) and $K = 0.7$ (so that the boundary at $x = L$ is partially absorptive and reflective). Also, let the disturbance location x_d be fixed at zero.

We want to find n so that $\gamma_n \approx \gamma$ where

$$\gamma = \inf_{Q \in H_\infty} \left\| \begin{array}{c} W_1\Big(G(x_1,x_d) - G(x_1,x_a)G(x_s,x_d)Q\Big) \\ W_1\Big(G(x_2,x_d) - G(x_2,x_a)G(x_s,x_d)Q\Big) \\ \vdots \\ W_1\Big(G(x_m,x_d) - G(x_m,x_a)G(x_s,x_d)Q\Big) \end{array} \right\|_\infty .$$

Suppose Legendre polynomials are used in the approximation scheme. We will consider four cases: $m = 1$ (the SISO case), $m = 2$, $m = 3$, and $m = 4$, i.e., one, two, three, and four observation points. For the numerical computations, we let $x_s = 1$ and $x_a = 0$. The following observation points are used. For $m = 1$, $x = 2$; for $m = 2$, $x \in \{1.5,\ 2\}$; for $m = 3$, $x \in \{1.5,\ 2,\ 2.5\}$; and for $m = 4$, $x \in \{0,\ 1,\ 2,\ ,3\}$. The exact value for $m = 1$, where $x_s = 1$ and $x = 2$ is -2.21 dB [Mor97a]. The convergence results are shown in Figure 6.1. The solid line in Figure 6.1 is for $m = 1$. Comparing this achievable noise reduction at a single point with the exact solution of -2.21 dB we see that even for $n = 30$, that the sequence $\{\gamma_n\}$ has not yet converged to the exact value. However, the γ_n versus n results

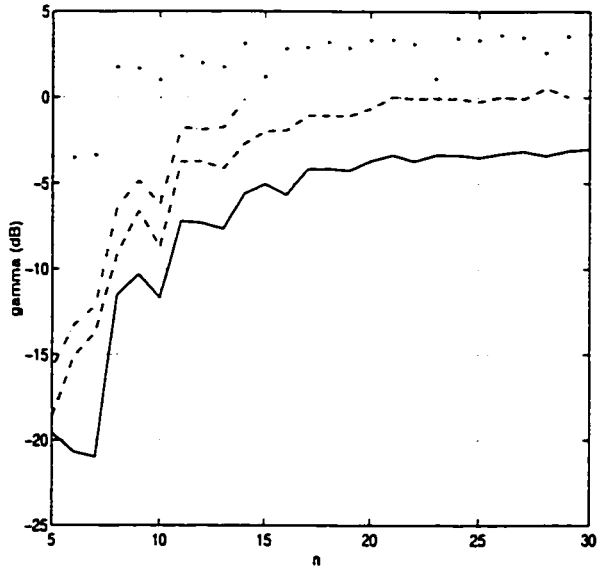

Figure 6.1: Legendre polynomials: determining n for convergence: γ_n versus dimension n for $m = 1$ (solid), $m = 2$ (dashed), $m = 3$ (dash/dot), and $m = 4$ (dot)

in Figure 6.1 for $m = 1, 2, 3$, and 4 appear to be converging for $n > 24$. Thus, we conclude that n at least 25 is adequate for all further calculations.

In Chapter 4, numerical results indicated that linear splines also provide a suitable approximation scheme. As for Legendre polynomials, we need to determine n such that $\gamma_n \approx \gamma$. Again we consider four cases: $m = 1$ (the SISO case), $m = 2$, $m = 3$, and $m = 4$. The same point locations used for Legendre polynomials are used here. Figure 6.2 shows the computed values of γ_n for increasing values of n. As for Legendre polynomials, we can see that the sequence $\{\gamma_n\}$ is converging as n gets large. In fact, it appears that $n = 15$ is sufficient for all further calculations. This is significantly smaller than the value of 25 determined earlier for Legendre polynomials.

In order to ensure that any further calculations of γ_n using linear splines are reasonable (in the sense that they are "close" to those determined using Legendre polynomials) we compared the computed values of γ_n versus n for $m = 1$, $m = 2$, $m = 3$, and $m = 4$ found using both Legendre polynomials and linear splines. These results are shown in Figure 6.3. We can see that γ_n for linear splines are slightly larger than γ_n for Legendre polynomials, although both appear to be converging to the same approximate value. Because we are solving a delicate numerical optimal sensitivity problem, we expect the jaggedness of the results given in Figure 6.3.

Recall that in Section 2.3.1 we reviewed the solution to the problem of achievable noise reduction at a single point through point control. The exact solution to this problem is known [Mor97a]. For $x_s = 2$, $x_d = 0$, and $x_a = 0$, the achievable noise reduction at $x = 1$ and at $x = 2.5$, for example, are identical. Figure 6.4 shows this exact solution (-0.8 dB) as well as the computed values for linear splines and Legendre polynomials. We can see that the computed solutions are very close to each other for all n and are in fact converging to the exact solution. Figure 6.5 illustrates the relative rate of convergence for linear splines and Legendre polynomials to the exact solution. As noted earlier, we see that linear splines do converge markedly faster.

Thus, in the results that follow, $n = 25$ is used for the Legendre polynomial based approximation scheme and $n = 15$ is used for linear splines. Because the Legendre polynomial approximations are uniformly stable, we shall use this scheme first. However, in some cases, linear spline based approximations prove to be more acceptable and versatile. Thus, in these cases, we use linear splines. Where not specified, we assume that Legendre polynomials are being used. In Chapter 7, we will discuss the differences in properties exhibited by these two schemes and study which properties affect controller design.

However, before proceeding, we first set a baseline for comparison of all future noise reduction results. Naturally, this choice is the uncontrolled level in the duct; that is, $\|T_1\|_\infty$. Using $n = 25$ basis functions and Legendre polynomials, we calculated the following. Consider three cases: $m = 1$ ($x = 2$), $m = 2$ ($x = \{1.5,\ 2\}$), and $m = 3$ ($x = \{1.5,\ 2,\ 2.5\}$). For $m = 1$, $\|T_1\|_\infty = 3.0980$ dB; for $m = 2$, $\|T_1\|_\infty = 5.9556$ dB; and for $m = 3$, $\|T_1\|_\infty = 7.6484$ dB. The norm could not be computed for $m = 4$ because of near singular matrices caused by the choice of x_i (see Section 6.2). From Figure 6.3 we see that introduction of the controller reduces the noise level in the duct anywhere from 3 to 6 dB.

In the remainder of this chapter, we focus on the question of achievable acoustic noise reduction. Results obtained will be compared relative to other noise reduction results, so that the effect of point location on the achievable noise reduction level may be determined.

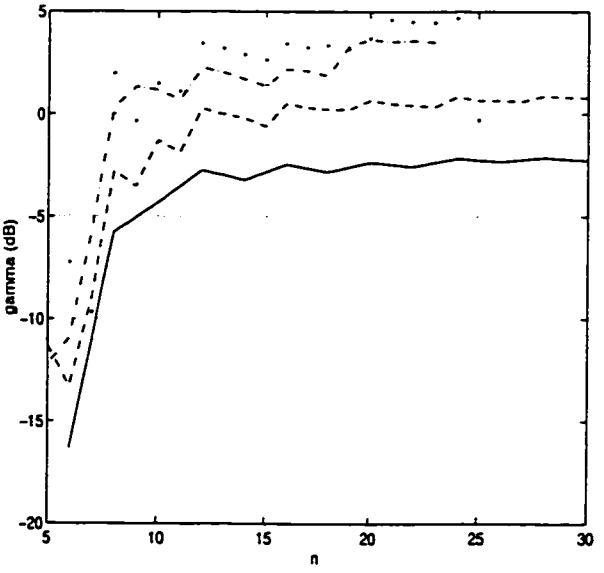

Figure 6.2: Linear splines: determining n for convergence: γ_n versus dimension n for $m = 1$ (solid), $m = 2$ (dashed), $m = 3$ (dash/dot), and $m = 4$ (dot)

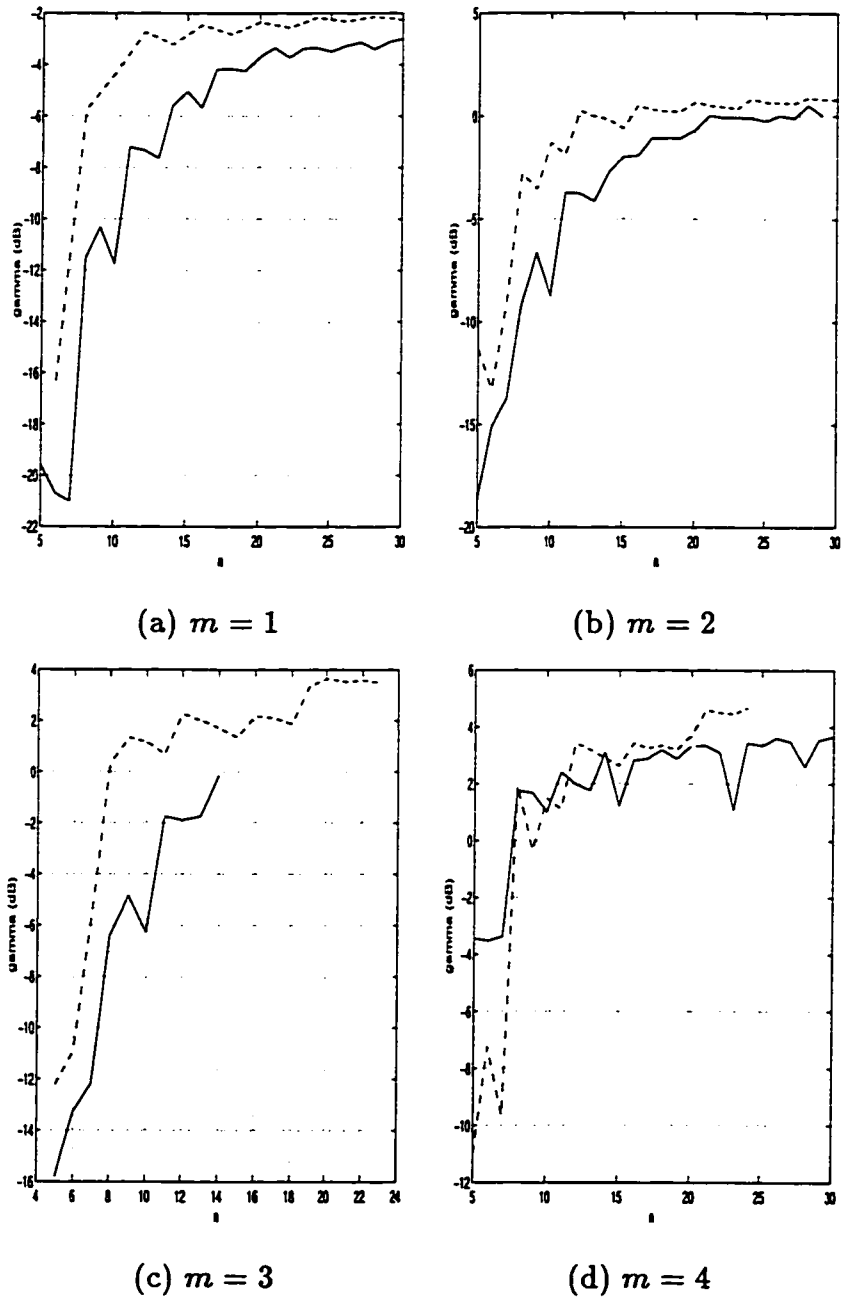

(a) $m = 1$ (b) $m = 2$

(c) $m = 3$ (d) $m = 4$

Figure 6.3: Comparison of n for convergence: Legendre polynomials (solid), linear splines (dashed)

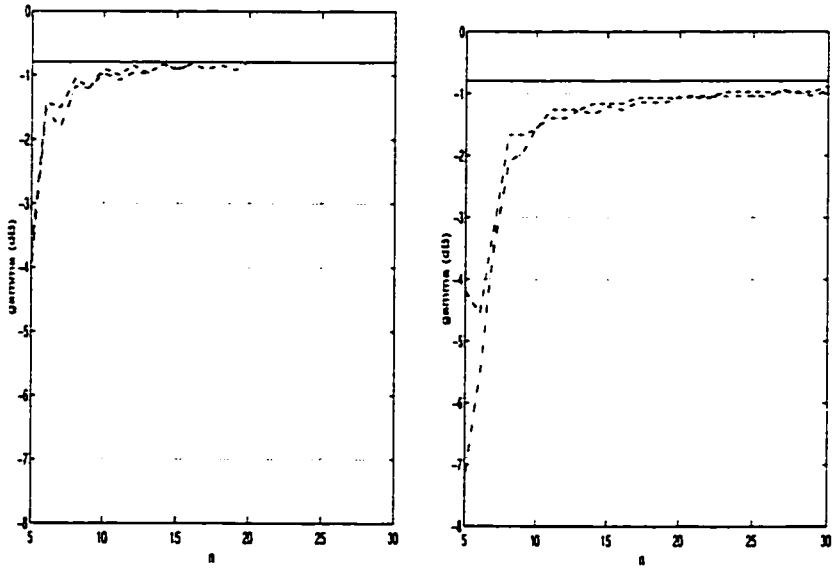

(a) Linear Splines (b) Legendre Polynomials

Figure 6.4: Determining n for convergence: exact solution (solid), $x = 1$ (dashed), $x = 2.5$ (dash/dot) ($x_s = 2$, $x_d = 0$, $x_a = 0$)

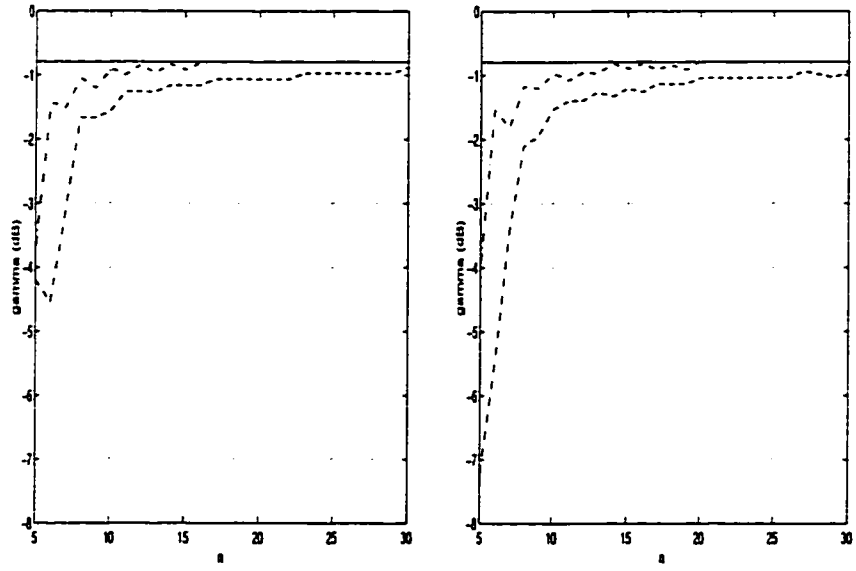

(a) $x = 1$ (b) $x = 2.5$

Figure 6.5: Comparison of n for convergence: exact solution (solid), linear splines (dash/dot), Legendre polynomials (dashed) ($x_s = 2$, $x_d = 0$, $x_a = 0$)

6.2 Feedback Design

In the study of the achievable level of acoustic noise reduction in the duct, there are three parameters that are allowed to vary. These are the sensor location x_s, the actuator location x_a, and the number and location of the observation or performance points x_i.

Analysis of the problem of achievable noise reduction at a point (see Section 2.3.1) showed that x_s should be as close as possible to the disturbance at x_d. In the feedback design case, this implies that x_a is as close as possible to the x_d (since $x_d < x_a < x_s$). However, we are still free to change the location x_s of the sensor and the number and location of the observation points x_i.

To help us in our choice of x_a, recall the following. The concept of "good" and "bad" x_a points was first introduced in the SISO feedforward case where $x_d = 0$, $x_a > x_s$, and $x > x_a$ (see Section 2.3.1). Recall that Morris [Mor97a] showed that the achievable noise reduction at a point is better at

$$x_a = \frac{L}{2k+1} \tag{6.2}$$

than at

$$x_a = \frac{L}{2k}, \tag{6.3}$$

where k is some positive integer. Thus, the points given in (6.2) are referred to as "good" points whereas the points in (6.3) are referred to as "bad" points. We will test some typical good and bad points in the feedback case. Since we know that the feedback sensor at x_s should be placed as close as possible to x_d for the best noise reduction results, we will generally restrict ourselves to x_a small, say $0 \leq x_a \leq 1$. For example, some good x_a points are $\{\frac{L}{41}, \frac{L}{21}, \frac{L}{11}\}$ and some bad x_a points are $\{\frac{L}{40}, \frac{L}{20}, \frac{L}{10}\}$. We will also consider $x_a = 0$ and $x_a = 1$ (good points).

In order to study the problem of global noise reduction, we consider an interval of the duct and increase the number of observation points in this interval. Let x_{min} and x_{max} be the minimum and maximum values of x, respectively. To avoid numerical difficulties when implementing the algorithm we must determine beforehand what values of x_{min} and x_{max} are possible.

The interpolation technique used is only valid for non-repeated open right half plane zeros in T_2 (see (6.1)). Thus, we must avoid the situation when $|x_i - x_a| = |x_s - x_d|$, for any $i = 1, 2, \ldots, m$ As well, for $x_d = 0$, we cannot have $|x_i - x_a| = |x_s|$, for any i. With x_a small (i.e., close to $x_d = 0$), we cannot have any $x_i \approx x_s$. In addition, we cannot have any x_i too close to x_d, since for $x_i \approx x_d$, we have $G(x_i, x_d) \approx G(x_i, x_i) = I$. Numerically for this to be true, we need an exact cancellation of poles and zeros, and attempting to do so leads to poorly conditioned and nearly singular matrices. Similarly, we also cannot have any x_i too close to x_a. Through numerical simulations and a trial and error approach, we found that $x_{min} = 0.25$ worked well as a minimum observation point.

According to the exact solution to the SISO feedback problem, γ is independent of x for $2(L - x) \geq x_s$ (see Section 2.3.1). For $K < 1$, γ decreases for $\frac{2L - x_s}{2} < x \leq L$. Thus, we let $x_{max} = \frac{2L - x_s}{2}$. Let m be the number of observation points and define

$$\Delta x = \frac{x_{max} - x_{min}}{m - 1}, \quad \text{for } m > 1.$$

The set of observation points $\{x_1, x_2, \ldots, x_m\}$ is chosen such that

$$x_i = x_{min} + (i - 1)\Delta x, \quad \text{for } i = 1, 2, \ldots, m$$

and $x_i \neq x_s$ for any i. For $m = 1$, $x = \frac{x_{min} + x_{max}}{2}$ (the midpoint of the interval considered). We will consider the cases $x_s = \{1, 2, 3\}$, $x_a = \{\frac{L}{41}, \frac{L}{21}, \frac{L}{11}\} = \{0.0976, 0.1905, 0.3636\}$ (good points), $x_a = \{\frac{L}{40}, \frac{L}{20}, \frac{L}{10}\} = \{0.1, 0.2, 0.4\}$ (bad points), $x_a = 0$, $x_a = 1$, and $m = 1, \ldots, 10$.

Global Noise Reduction

With these preliminaries, let us now determine how the achievable level of noise reduction in the duct with an increasing number of observation points compares to the achievable level of noise reduction at a single point. Suppose that instead of having m distinct observation points x_i we have m identical observation points $x_i = \bar{x}$. Defining $F_i = W_1 G_n(x_i, x_d) - W_1 G_n(x_i, x_a) G_n(x_s, x_d) Q$ for $i = 1, 2, \ldots, m$, the H_∞ optimal control problem of finding $Q \in RH_\infty$ such that

$$\left\| \begin{array}{c} F_1 \\ F_2 \\ \vdots \\ F_m \end{array} \right\|_\infty \leq \gamma$$

can be written as

$$\left\| \left[|F_1|^2 + |F_2|^2 + \ldots + |F_m|^2 \right]^{1/2} \right\|_\infty \leq \gamma.$$

So if $F_i = F_1$ for all $i = 1, 2, \ldots, m$, then

$$\|F_1\|_\infty \leq \frac{\gamma}{\sqrt{m}}.$$

Now, the achievable noise reduction γ for m distinct points can be no better than placing m observation points at one location in the duct. That is, if $\gamma^{(m)}$ is the achievable noise reduction for m distinct points, then

$$\gamma^{(m)} \geq \sqrt{m} \gamma^{(1)},$$

where $\gamma^{(1)}$ is the optimal noise reduction with any one point. In particular, let $\gamma^{(1)}$ be the noise reduction for $x = 2$ (at the centre of the duct).

Figures 6.6 – 6.11 show that $\gamma^{(m)}$, for $m = 1, 2, \ldots, 10$, is very close to $\gamma^{(1)}\sqrt{m}$. This implies that the minimum possible global (as m increases) acoustic noise reduction

$\gamma^{(m)}$ is attainable. Physically, this means that noise may be reduced everywhere in the duct to a level comparable to that of noise reduction at a single point.

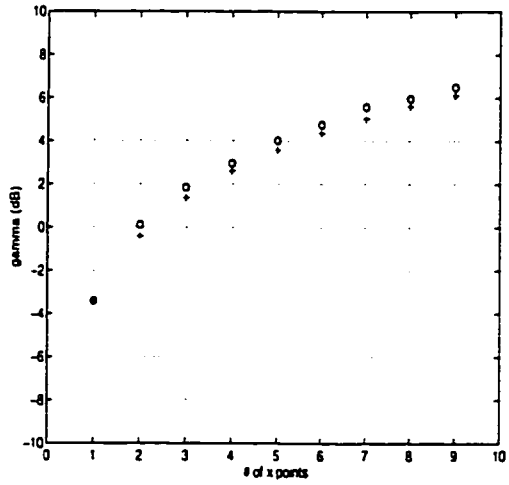

(a) $x_a = 0$

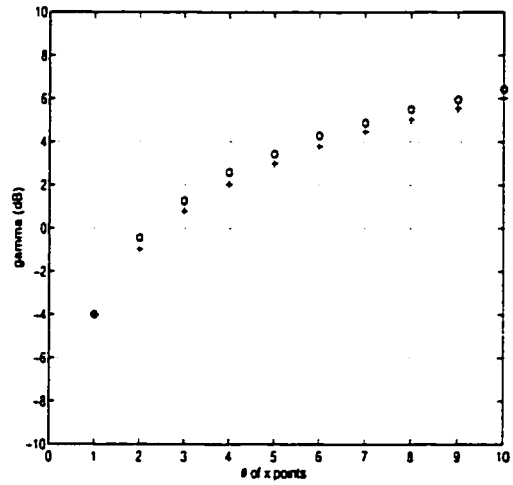

(b) $x_a = 0.0976$

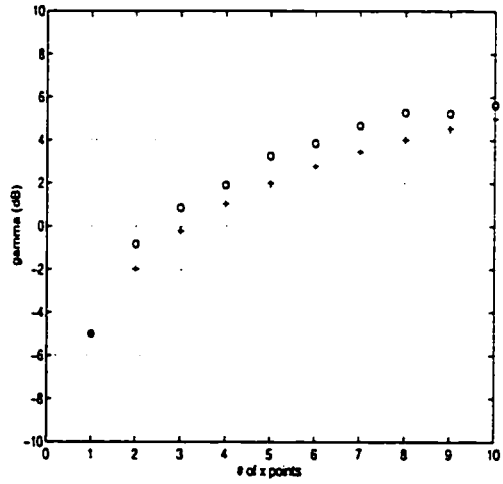

(c) $x_a = 0.1905$

Figure 6.6: Dependence on m: $x_s = 1$ and good x_a points (γ (o), $\gamma^{(1)}\sqrt{m}$ (+))

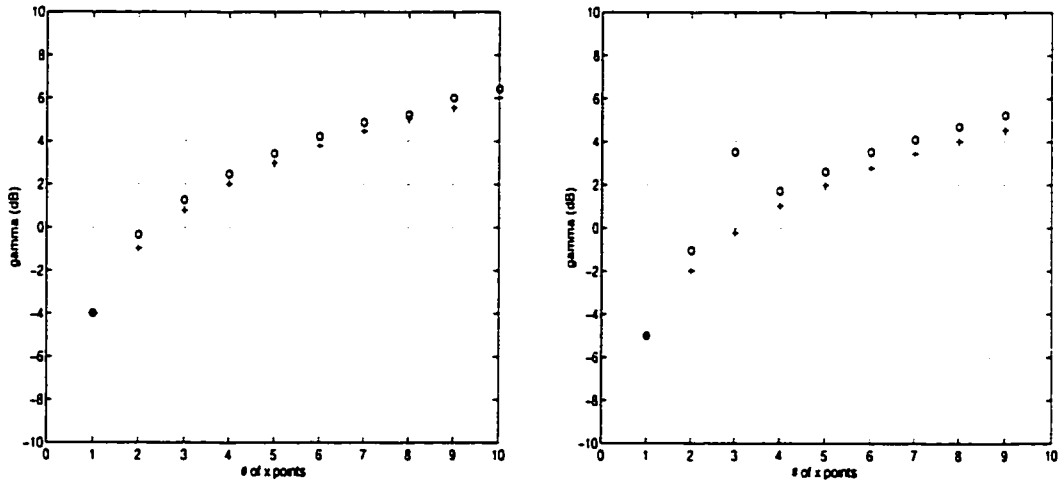

(a) $x_a = 0.1$ (b) $x_a = 0.2$

Figure 6.7: Dependence on m: $x_s = 1$ and bad x_a points (γ (o), $\gamma^{(1)}\sqrt{m}$ (+))

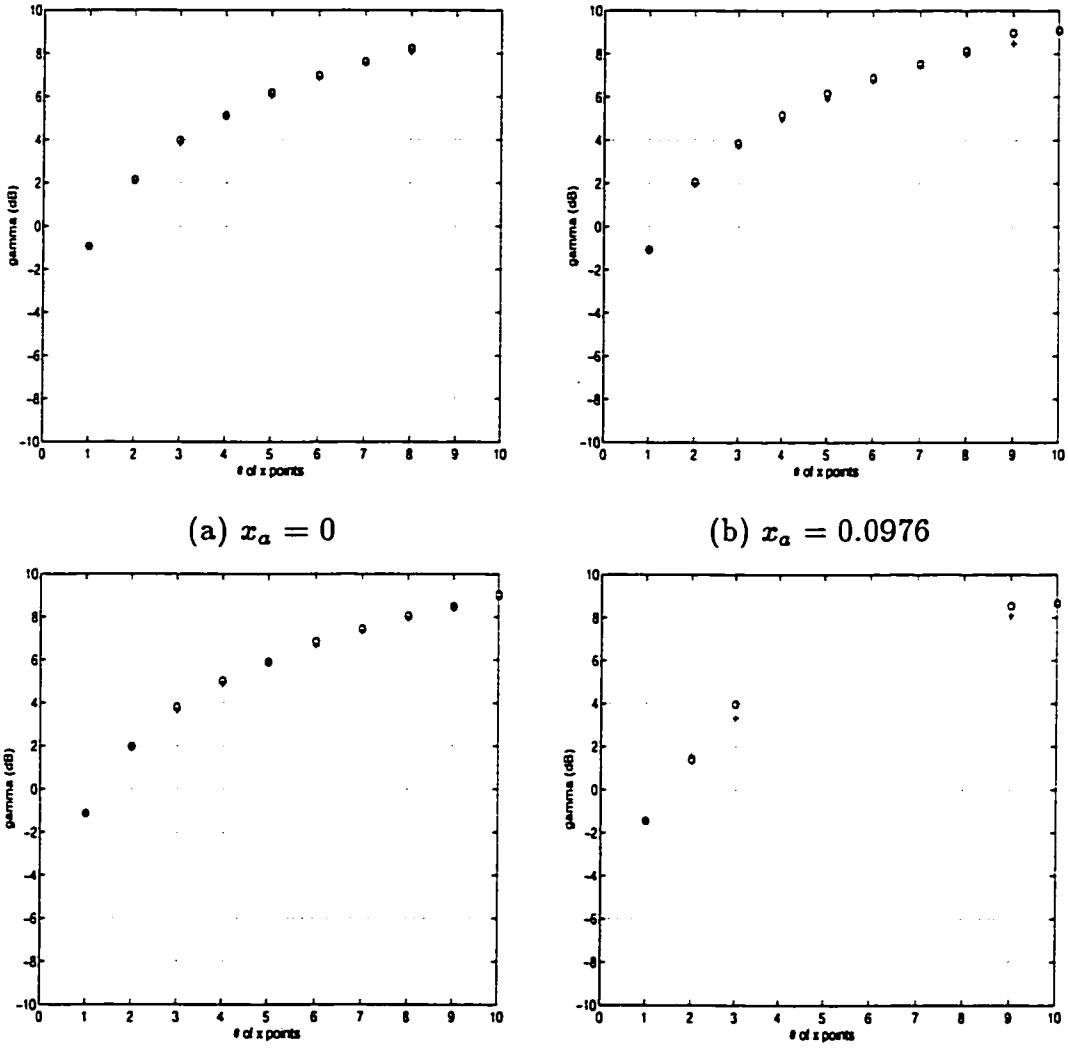

(a) $x_a = 0$ (b) $x_a = 0.0976$

(c) $x_a = 0.1905$ (d) $x_a = 0.3636$

Figure 6.8: Dependence on m: $x_s = 2$ and good x_a points (γ (o), $\gamma^{(1)}\sqrt{m}$ (+))

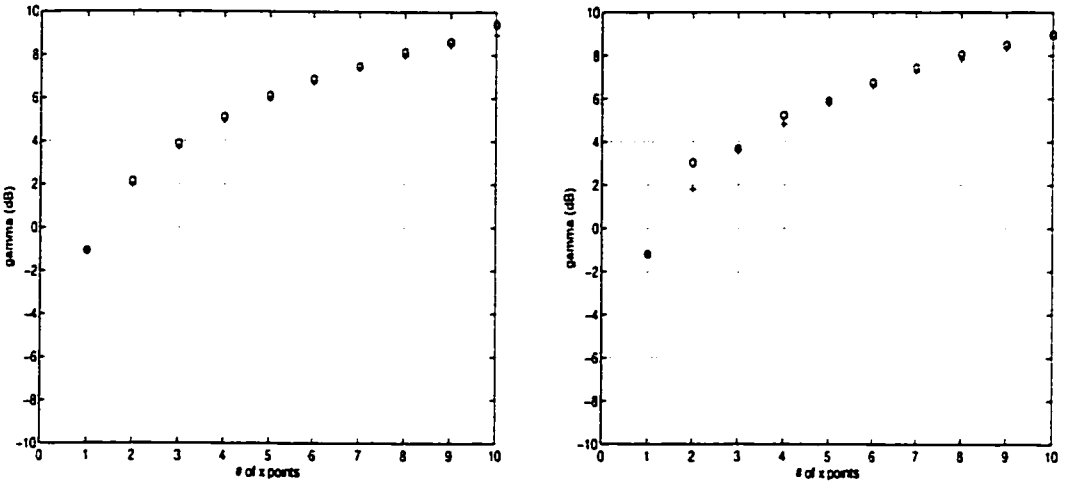

(a) $x_a = 0.1$ (b) $x_a = 0.2$

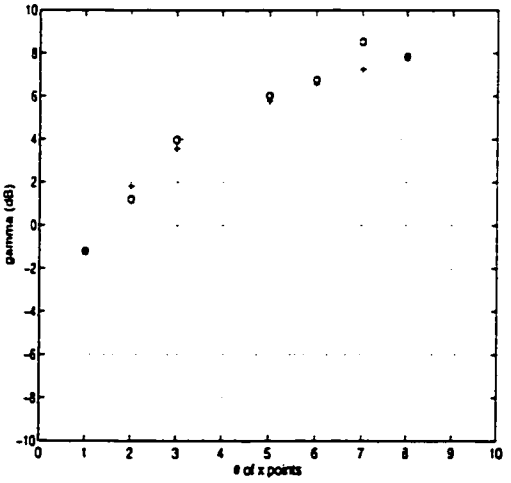

(c) $x_a = 0.4$

Figure 6.9: Dependence on m: $x_s = 2$ and bad x_a points (γ (o), $\gamma^{(1)}\sqrt{m}$ (+))

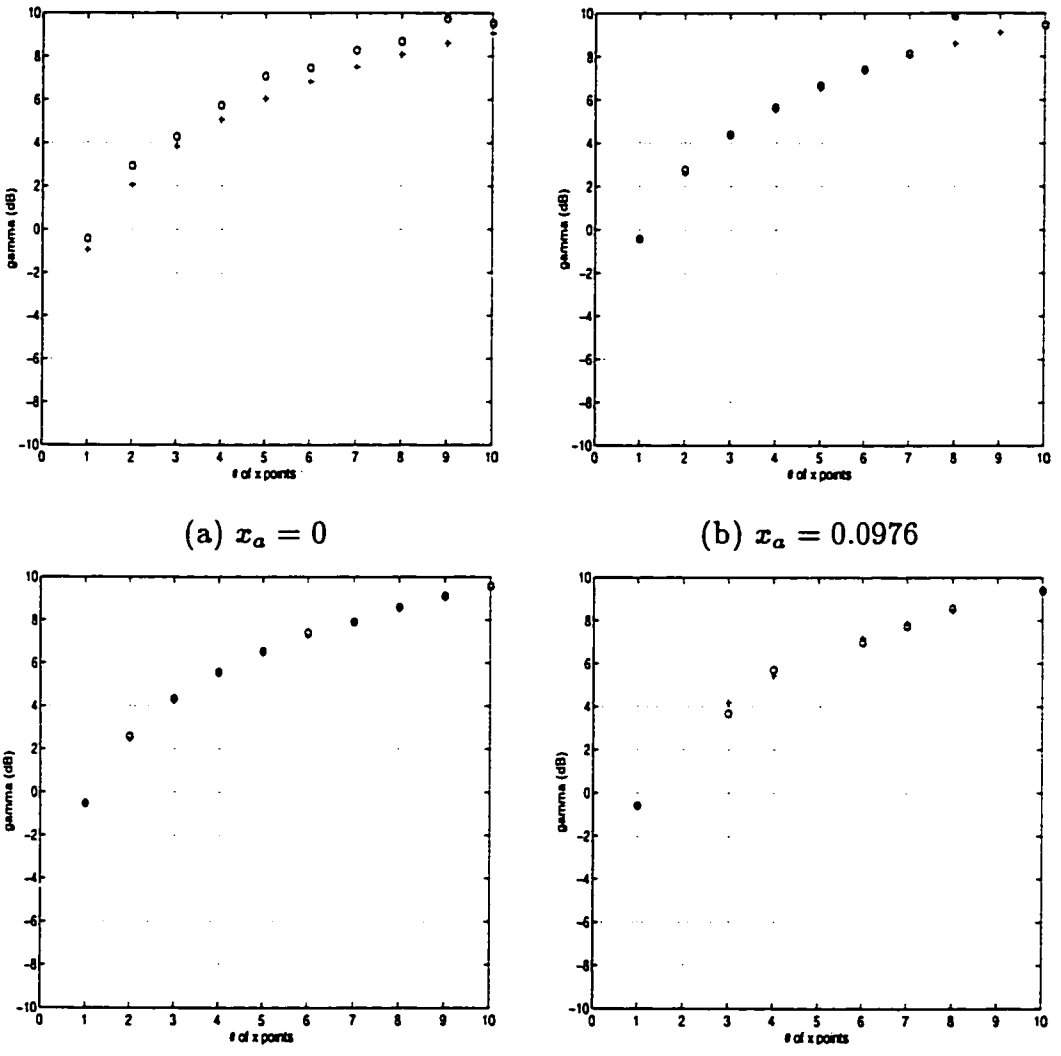

(a) $x_a = 0$ (b) $x_a = 0.0976$

(c) $x_a = 0.1905$ (d) $x_a = 0.3636$

Figure 6.10: Dependence on m: $x_s = 3$ and good x_a points (γ (o), $\gamma^{(1)}\sqrt{m}$ (+))

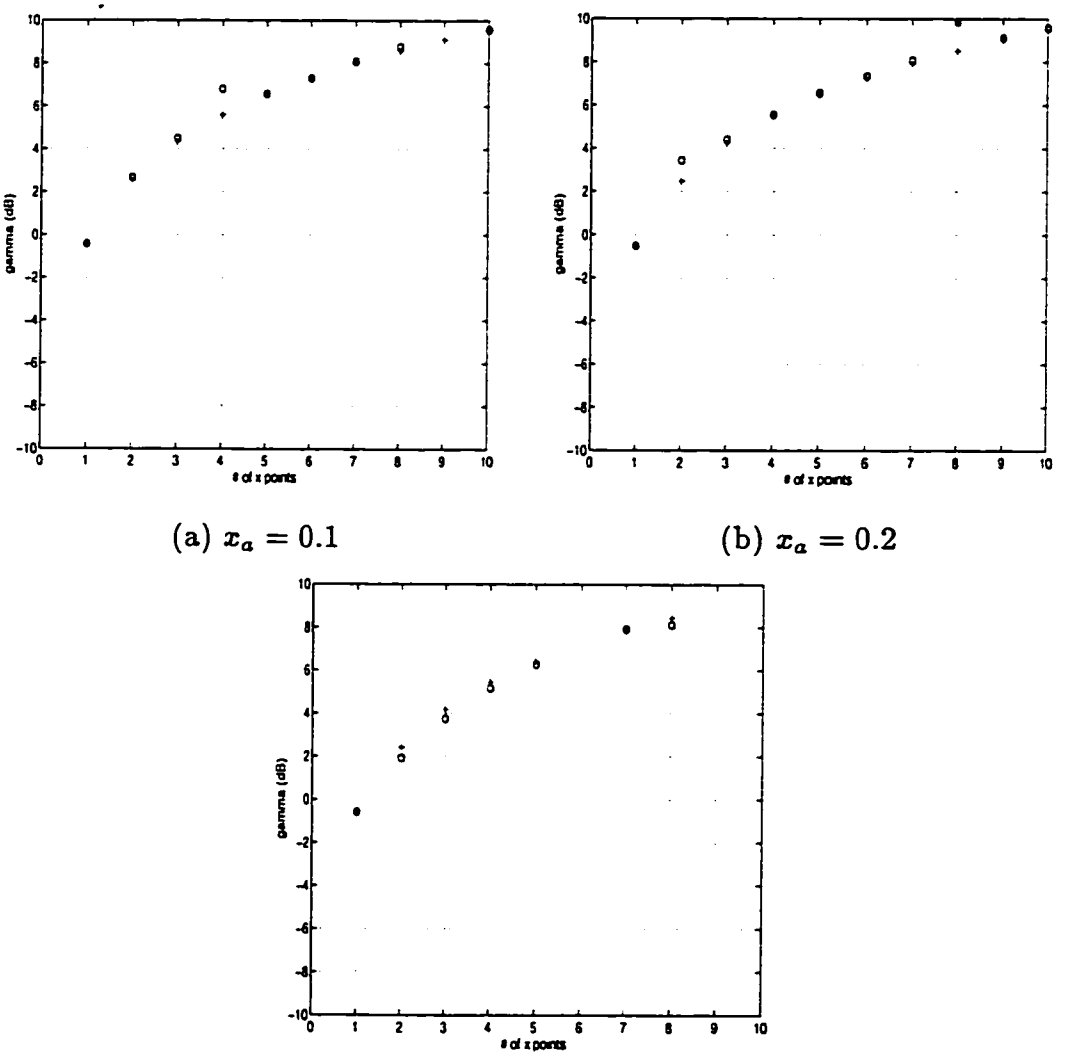

(a) $x_a = 0.1$ (b) $x_a = 0.2$

(c) $x_a = 0.4$

Figure 6.11: Dependence on m: $x_s = 3$, bad x_a points (γ (o), $\gamma^{(1)}\sqrt{m}$ (+))

Effect of sensor location x_s

Suppose that x_a is fixed. In particular, let $x_a = 0$. Figure 6.12 shows the dependence of γ on the location of the sensing point at x_s. In this figure, the relative location of x_s, x_a, and x_i are also illustrated. Each horizontal line in the figure represents the computed value of γ for some particular choice of x_a, x_d, x_s, and observation points x_i. These point locations are visually displayed on each horizontal line with the appropriate symbol. With several cases (γ determined for different points) displayed in each figure, we can easily see the effect of point location on achievable noise reduction. We find that the achievable noise reduction γ is better for x_s smaller (i.e., $x_s = 1$). Similar results for $x_a = \{0.0976,\ 0.1905,\ 0.3636\}$ and $x_a = \{0.1,\ 0.2,\ 0.4\}$ are also given in Figures 6.13 and 6.14.

The role of the sensor at x_s is to measure the effect of the disturbance at $x_d = 0$ and to use this information in the controller design. The closer x_s is to x_d, the smaller the delay in measurement of the actual disturbance. In this case, a controller is designed that acts almost immediately to try to cancel the disturbance seen in the duct. Thus, we expect the achievable noise reduction to be best for x_s small.

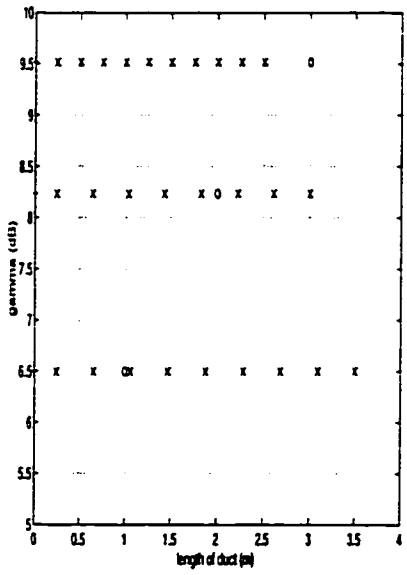

Figure 6.12: Feedback design (x_a fixed): γ versus locations ($x_a = 0$ (+), x_s (o), x_i (x))

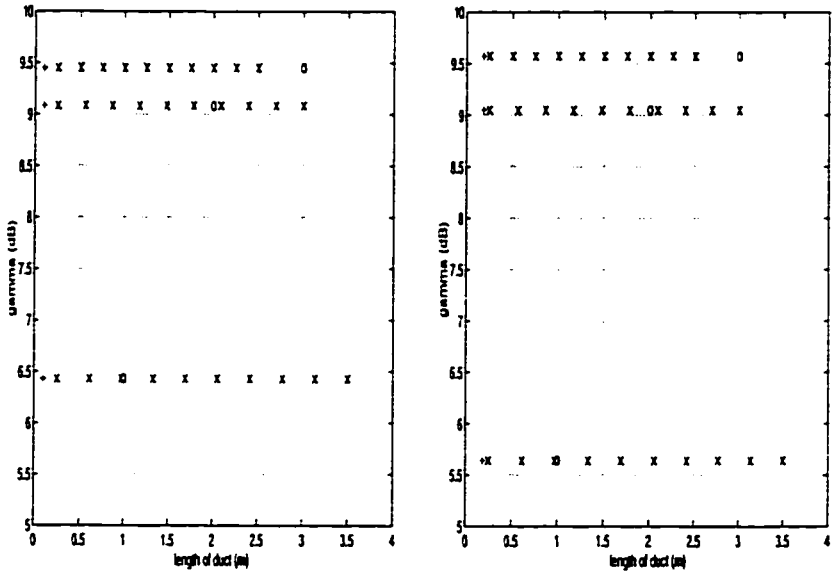

(a) $x_a = 0.0976$ (b) $x_a = 0.1905$

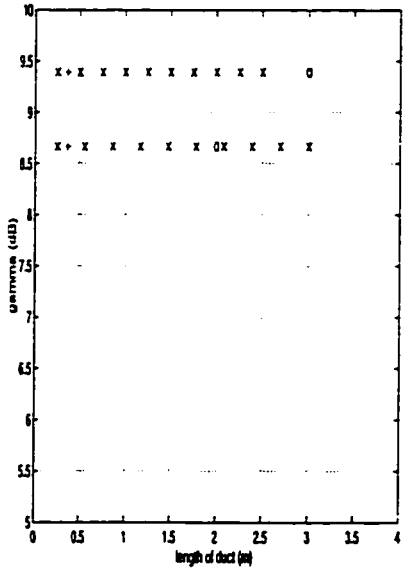

(c) $x_a = 0.3636$

Figure 6.13: Feedback design (x_a fixed (good points)): γ versus locations (x_a (+), x_s (o), x_i (x))

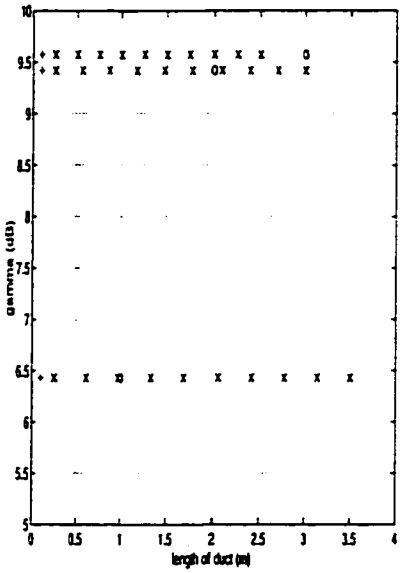

(a) $x_a = 0.1$

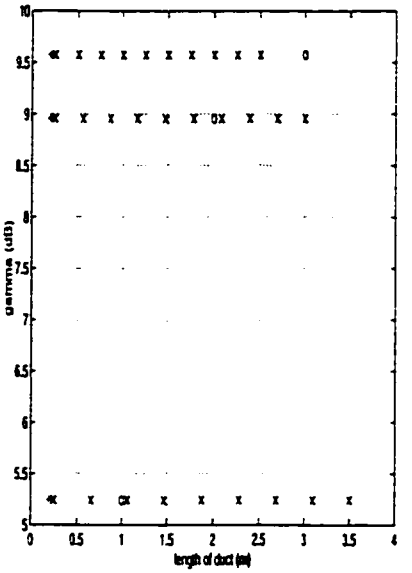

(b) $x_a = 0.2$

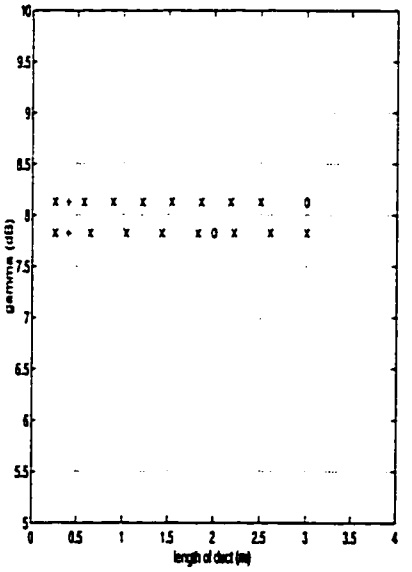

(c) $x_a = 0.4$

Figure 6.14: Feedback design (x_a fixed (bad points)): γ versus locations (x_a (+), x_s (o), x_i (x))

Effect of actuator location x_a

Suppose that x_s is fixed. Figures 6.15–6.17 show the dependence of γ on the location of the actuating point at x_a. For $x_s = 1$, $5 < \gamma < 6.5$. For $x_s = 2$, $8 < \gamma < 9.25$ (for good x_a points) and $7.5 < \gamma < 9.5$ (for bad x_a points). For $x_s = 3$, $9.25 < \gamma < 9.75$ (for good x_a points) and $8 < \gamma < 9.75$ (for bad x_a points). Thus, for each fixed location x_s considered, the variation in γ is no more than 2 dB. However, what is interesting to note is that, for fixed x_s, the achievable level of noise reduction is better for x_a larger. That is, the results are better for x_a closer to x_s rather than for x_a closer to $x_d = 0$. Recall that although the disturbance is introduced into the duct at x_d, it is actually measured at x_s. Thus, the closer x_a is to x_s, the more closely the control wave will be a mirror image of the disturbance seen by the controller so that the disturbance seen near x_a and x_s is reduced. Unfortunately, the disturbance at $x_d = 0$ is not directly cancelled. However, x_a and x_s are sufficiently close that the control wave acts to cancel all disturbances for performance points near $x = 0$.

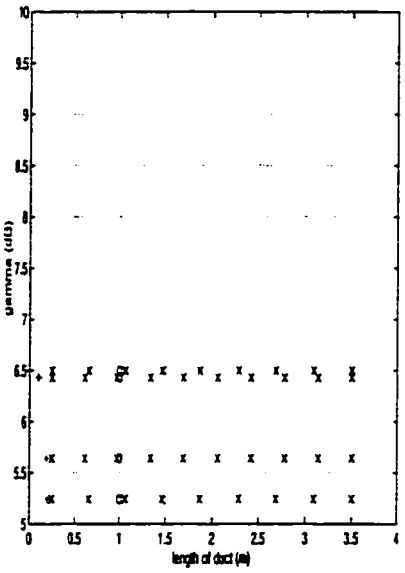

Figure 6.15: Feedback design ($x_s = 1$ fixed): γ versus locations ($x_s = 1$ (o), $x_a = \{0,\ 0.0976,\ 0.1,\ 0.1905\}$ (+), x_i (x))

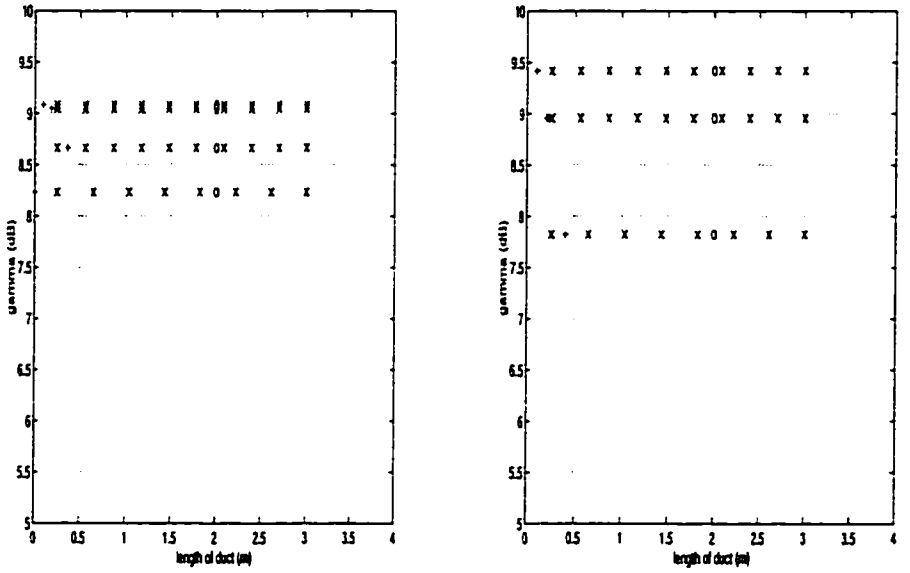

(a) $x_a = \{0,\ 0.0976,\ 0.1905,\ 0.3636\}$ (b) $x_a = \{0.1,\ 0.2,\ 0.4\}$

Figure 6.16: Feedback design ($x_s = 2$ fixed): γ versus locations ($x_s = 2$ (o), x_a (+), x_i (x))

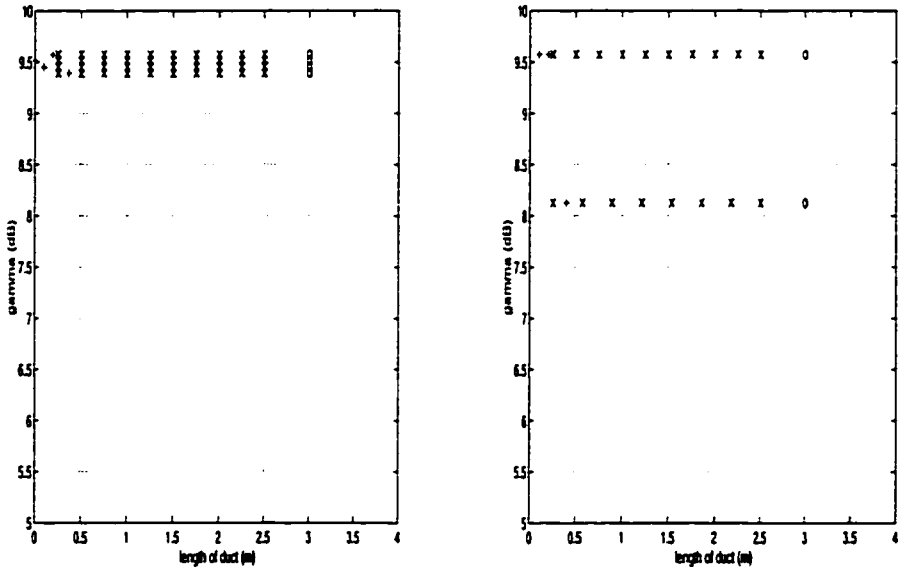

(a) $x_a = \{0,\ 0.0976,\ 0.1905,\ 0.3636\}$ (b) $x_a = \{0.1,\ 0.2,\ 0.4\}$

Figure 6.17: Feedback design ($x_s = 3$ fixed): γ versus locations ($x_s = 3$ (o), x_a (+), x_i (x))

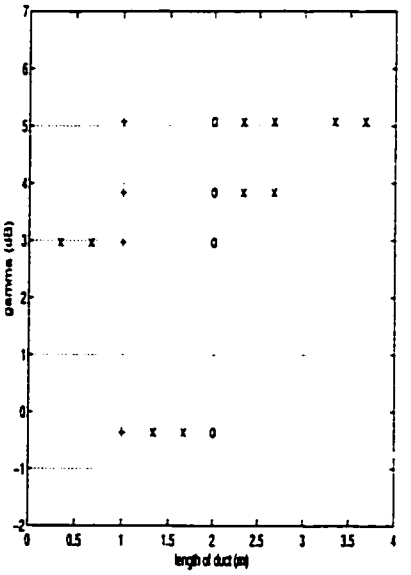

Figure 6.18: Feedback design ($x_a = 1$ and $x_s = 2$ fixed): γ versus locations ($x_s = 2$ (o), $x_a = 1$ (+), x_i (x))

Effect of observation point locations x_i

Again let us consider feedback design with $x_s > x_a$. In this case, we keep both the sensor location x_s and the actuator location x_a fixed, and move the observation points about x_s and x_a. Suppose $x_s = 2$ and $x_a = 1$. Figure 6.18 shows the value of γ for four different cases of multiple observation points: two observation points both located before x_a; two observation points located between x_a and x_s; two observation points located after x_s; and four observation points located after x_s. We observe the following. The achievable noise reduction is best for observation points located between the sensor and actuator. The achievable noise reduction is worst for observation points located after the sensing point.

Thus, the noise level at points located between the sensing point at x_s and the actuating point at x_a can be reduced more than at points outside this interval. In the next section, we compare this best case (x_i between x_s and x_a) in the feedback case to the analogous situation in the feedforward case (where $x_s < x_a$).

Consider now a linear spline based approximating scheme rather than Legendre polynomials. By using linear splines, we find that we have greater freedom in varying the location of the observation points x_i in relation to x_a and x_s. Suppose $x_s = 2$ and $x_a = 1$. Figure 6.19 shows the value of γ for several different cases of multiple observation points.

The relative location of each performance point is indicated by the appropriate symbol in Figure 6.19. We observe the following. The achievable noise reduction is best for observation points located close to the sensor at x_s. In this case, the controller is directly using these points (nearby the control point) to compute the noise cancellation signal. Points located at varying locations in the duct and more importantly further away from the sensing point at x_s do not greatly affect the determination of the control signal as those points located closer to x_s. For this same reason, the achievable noise reduction worsens when observation points are placed before the control point at x_a. As well, the achievable noise reduction is worst for observation points located over the entire duct, be they before x_a, between x_a and x_s, or after x_s.

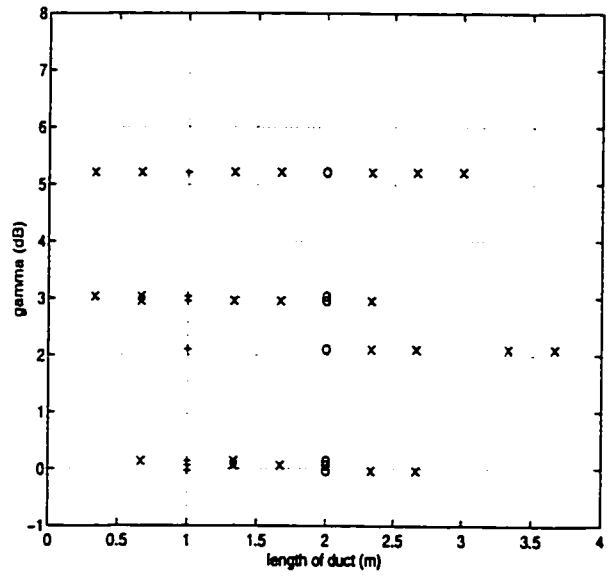

Figure 6.19: Feedback design (linear splines): γ versus locations (x_i (x), $x_s = 2$ (o), $x_a = 1$ (+))

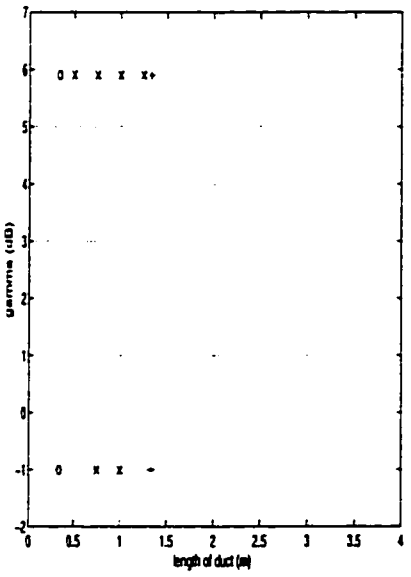

Figure 6.20: Feedforward design: γ versus locations ($x_s = 1/3$ (o), $x_a = 4/3$ (+), x_i (x))

6.3 Feedforward Design

Consider the feedforward case, $x_a > x_s$. Figure 6.20 shows the results for $m = 2$ and $m = 4$, where all observation points are located between x_a and x_s. We see that performance declines drastically with a larger number of observation points. Also if we compare Figure 6.18 with Figure 6.20 when the observation points are between x_a and x_s (and $m = 2$), we see that the feedforward design produces results which are only slightly better than the feedback case.

With both feedback and feedforward systems, we have the concern of reflected waves caused by the boundaries combining with the control wave. The net result is a disturbance that is not initially seen by the controller or used in the controller design. Thus, even feedforward control contains "feedback" due to these reflections.

Severe numerical difficulties were encountered for observation point locations $x_i < x_a$. In particular, we found that the algorithm failed when performing the inner/outer factorization (see Step (1) of the algorithm in Section 5.5). Thus far, considerable effort has been made to study the problem of achievable (global) noise reduction using Legendre polynomials in both feedback and feedforward design. However, this approximation scheme falls short in the case of feedforward design where we found great difficulties in varying the location of the observation points x_i in relation to the sensing point location x_s and the actuating point location x_a. For this reason, we used a linear spline based approximation scheme. In Chapter 7, we will study the approximations of the inner factors for both Legendre polynomials and linear splines.

Suppose $x_s = 1/3$ and $x_a = 4/3$. Figure 6.21 shows the value of γ for four different cases. We see that with multiple observation points located either 1) between the control point at x_a and the sensing point at x_s, or 2) between these points as well as after the control point, the achievable noise reduction only varies by 1 or 2 dB. Numerical results indicate that the achievable noise reduction decreases with an increasing number of observation points between x_a and x_s. Also we see that the feedback design produces results which are only slightly better than the feedforward case. In effect, the two cases illustrated in Figures 6.19 and 6.21 are duals of each other in that the locations of x_s and x_a have been switched. For x_a and x_s small enough, the reflective waves produced at the boundary $x = L$ do not pose any serious concerns, thereby giving the appearance that both cases (feedback and feedforward) do not significantly differ in their results.

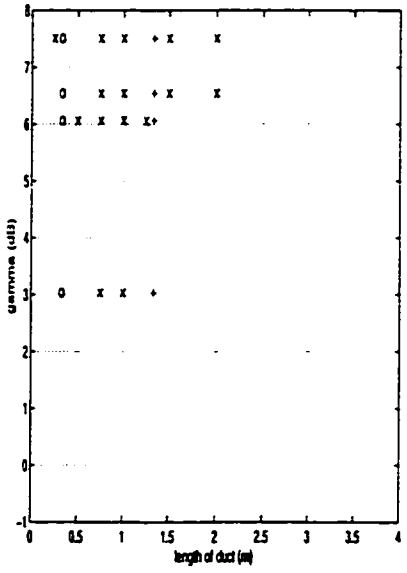

Figure 6.21: Feedforward (linear splines): γ versus locations (x_i (x), $x_s = 1/3$ (o), $x_a = 4/3$ (+))

6.4 Discussion

Figures 6.19 and 6.21 show the general picture of how feedback control compares to feedforward control. Consider each case in more detail. First consider feedback control. Figure 6.22(a)-(c) is Figure 6.19 expanded in more detail. Figure 6.22(a) shows the best noise reduction scenarios whereas Figure 6.22(c) shows the worst. We can see that as the number of performance or observation points x_i increases before the actuator at x_a and after the sensor at x_s, the achievable noise reduction worsens. The achievable noise reduction is best for performance points located near the actuator at x_a.

Now consider feedforward design. Figure 6.23(a)-(d) is Figure 6.21 expanded. In all cases, there are a number of observation points x_i between the sensor at x_s and the actuator at x_a. As expected, the achievable noise reduction worsens for an increasing number of points between x_s and x_a, and is worst for observation points located before x_s and after x_a. Performance or observation points located outside the interval $[x_s, x_a]$ (in the feedforward case) or $[x_a, x_s]$ (in the feedback case) places these points outside the "controller loop" where the controller has the most effect on the disturbance. Also, observation points located closer to the ends of the duct where either the disturbance is being introduced (at $x = 0$) or waves are being absorbed and reflected (at $x = 0$ and $x = L$) and further away from the control signal at x_a will have a greater level of noise measured.

Finally let us consider the variation in the achievable noise reduction for different scenarios presented in the feedback design case. Results in Figure 6.19 show that if the number of observation points increases in the duct, then the noise level changes from approximately 0 dB to just over 5 dB. Thus, there is a significant variation in results as the number of points increases. Similarly, we can consider the variation

in the achievable noise reduction for different scenarios in the feedforward design case. Figure 6.21 shows that the noise level varies from approximately 3 dB to around 7.5 dB.

In order to achieve the best level of acoustic noise reduction in the duct, the following point placements are recommended. In the feedback design case, the sensor at x_s should be placed as close as possible to the disturbance at x_d. In addition, the actuator at x_a should be placed as close as possible to the sensor. Not surprisingly, since $x_d < x_a < x_s$, these point placements suggest that x_s and x_a should be as close as possible to x_d. Feedforward design results indicate the same point placement. Numerical results with these point locations imply that the highest achievable noise reduction is for performance points situated between x_a and x_s, whereas the worst noise reduction observed is when performance points are located after x_s.

Results concerning the dependence of the achievable level of noise reduction on the number of observation points imply that noise can be reduced everywhere in the duct but not to some arbitrarily small level. Assuming a wide range of performance point locations throughout the duct, results also indicate that feedback design produces slightly better results than feedforward design.

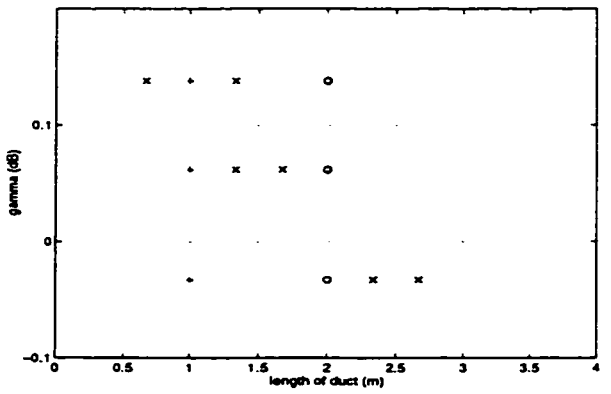

(a)

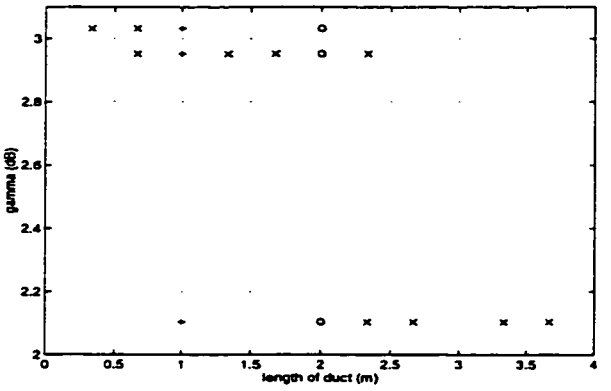

(b)

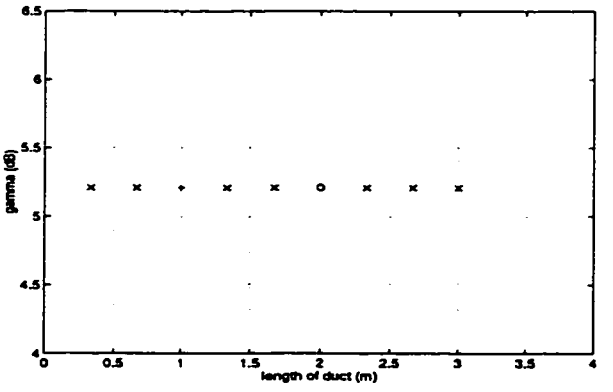

(c)

Figure 6.22: Feedback design (linear splines): γ versus locations (x_i (x), $x_s = 2$ (o), $x_a = 1$ (+))

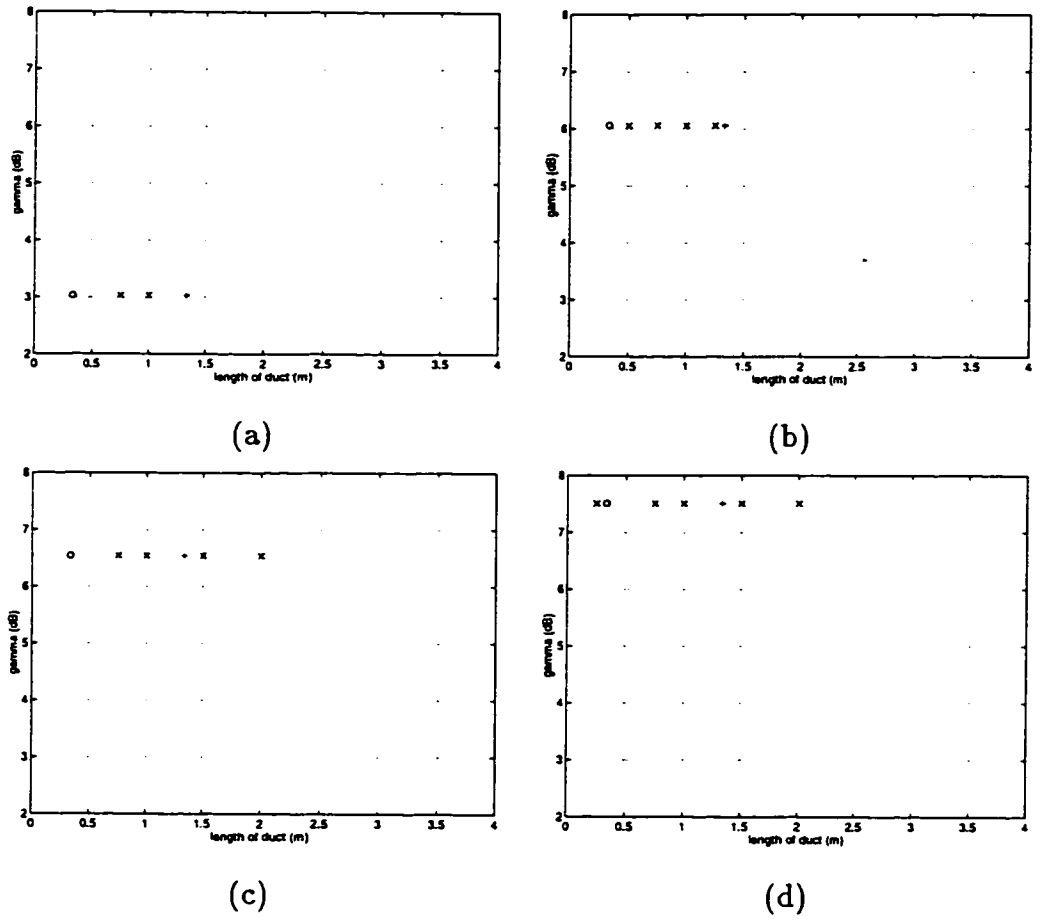

Figure 6.23: Feedforward design (linear splines): γ versus locations (x_i (x), $x_s = 1/3$ (o), $x_a = 4/3$ (+))

Chapter 7

Properties of Approximations for Control

In Chapter 4, we showed that Legendre polynomials provide a suitable approximation method for both simulation and control. A linear spline based approximation method was also considered. We showed that this method may be suitable for control since the approximating transfer functions and inner factors are converging.

Existing theorems indicate that an open loop convergent approximating scheme for a bounded control system is also closed loop convergent if the scheme is uniformly stabilizable and/or detectable. We saw in Chapter 3 that for certain classes of systems where results have been obtained, that uniform stabilizability is a sufficient condition for the convergence of the Riccati operator in the approximating LQR problem (see [BK84] for the bounded control case, [BI97] and [IT89] for results that apply to some unbounded control problems). In this chapter, we consider whether uniform stabilizability is a necessary condition for controller design for finite-dimensional approximations. In addition, we compare the ability of Legendre

polynomials and linear splines to approximate inner factors in both feedback and feedforward design and also discuss the symmetry properties exhibited in either case. We begin by considering the question of uniform stabilizability of approximations.

7.1 Uniform Stabilizability of Approximations

We consider three basic control systems. These are summarized as follows.

(1) **Infinite-dimensional operator control systems:** Let $w \in \mathcal{H}$ satisfy the equation

$$\dot{w}(t) = \mathcal{A}w(t) + \mathcal{B}u(t), \quad t > 0, \quad w(0) = w_0 \tag{7.1}$$

where $\mathcal{A} : D(\mathcal{A}) \subset \mathcal{H} \to \mathcal{H}$ and $\mathcal{B} \in \mathcal{L}(\mathcal{U}, \mathcal{H})$. We will assume, in general, that $\mathcal{U} = \mathbb{R}^p$. The operator $\mathcal{A}$ is an unbounded linear operator which generates a strongly continuous semigroup of bounded linear operators in $\mathcal{H}$.

(2) **Finite-dimensional operator control systems:** Let $\{\mathcal{H}_n\}_{n=1}^{\infty}$ be a sequence of finite-dimensional subspaces of $\mathcal{H}$. Let $\mathcal{A}_n \in \mathcal{L}(\mathcal{H}_n)$ and $\mathcal{B}_n \in \mathcal{L}(\mathcal{U}, \mathcal{H}_n)$ be approximations of $\mathcal{A}$ and $\mathcal{B} \in \mathcal{H}_n$, respectively. Let $w_n \in \mathcal{H}_n$ satisfy the equation

$$\dot{w}_n(t) = \mathcal{A}_n w_n(t) + \mathcal{B}_n u(t), \quad t > 0, \quad w_n(0) = w_{n_0}. \tag{7.2}$$

(3) **Finite-dimensional matrix representations:** Let $\{\phi_k\}_{k=1}^{n}$ be a basis for $\mathcal{H}_n$ and $\{\psi_k\}_{k=1}^{p}$ be a basis for $\mathcal{U}$. Then (2) can be represented by a linear system in $\mathbb{R}^n$. Namely, let $w_n \in \mathbb{R}^n$ satisfy the equation

$$\dot{w}_n(t) = A_n w_n(t) + B_n u(t), \quad t > 0, \quad w_n(0) = w_{n_0}. \tag{7.3}$$

The matrices A_n and B_n are the matrix representations of the operators $\mathcal{A}_n$ and $\mathcal{B}_n$.

Recall that the problem we are studying is an unbounded control problem. Unfortunately, well established results to determine whether or not a system is uniformly stabilizable exist only for bounded control systems. For example, Banks and Kunisch [BK84] describe a class of approximating systems that satisfy a condition they refer to as a *preservation of exponential stabilizability under approximation.* Peichl and Wang [PW97] give a necessary condition for the uniform stabilizability of the approximating systems for the wave equation with damping in the boundary conditions. Their main result may be summarized as follows. If the finite-dimensional approximating systems are uniformly stabilizable for all dimensions n and the choices of bases for the approximating state-space and control space satisfy a uniform norm equivalence condition, then the margin of stabilizability is uniformly bounded away from zero. Thus, if the margin of stabilizability tends to zero, then the approximating system is not uniformly stabilizable. It is interesting to note that one common scheme for approximating the one-dimensional wave equation (the one-dimensional duct problem) is to use finite differences. However, Peichl and Wang [PW97] show numerically that the finite difference approximation of the wave equation with bounded control is not uniformly exponentially stabilizable. Again this result is proven only for bounded control systems. In this chapter, we will look at the work of Peichl and Wang and assume, without proof, that their results extend to our unbounded control system.

7.1.1 Uniform Stabilizability and the Margin of Stabilizability

In this section, we present the results of Peichl and Wang which describe the connection between uniform stabilizability and the margin of stabilizability.

Consider the (possibly infinite-dimensional) system given in (7.1) and the approximations given in (7.2) and (7.3). We require the following definition.

Definition 7.1 *(Margin of Stabilizability for Matrix Representations [PW97])*

Let $A_n \in \mathbb{R}^{n\times n}$ *and* $B_n \in \mathbb{R}^{n\times p}$. *The margin of stabilizability of* (A_n, B_n) *is defined by*

$$\gamma_s(A_n, B_n) = \min\Big\{ \|[\delta A_n, \delta B_n]\|_2 \,,\ (A_n + \delta A_n, B_n + \delta B_n) \text{ is not stabilizable} \Big\}$$

where $\|\cdot\|_2$ *is the matrix norm induced by the Euclidean vector norm.*

The matrix representations A_n and B_n in the above definition are basis function dependent. If we consider instead the analogous case of approximating operators, we have a similar definition. Let $[\mathcal{A}_n, \mathcal{B}_n]$ be a linear operator in $\mathcal{L}(\mathcal{H}_n \times \mathcal{U}, \mathcal{H}_n)$ defined by

$$[\mathcal{A}_n, \mathcal{B}_n](w_n, u) = \mathcal{A}_n w_n + \mathcal{B}_n u, \quad (w_n, u) \in \mathcal{H}_n \times \mathcal{U}.$$

Then we have the following.

Definition 7.2 *(Margin of Stabilizability for Operator Representations [PW97])*

Let $\mathcal{A}_n \in \mathcal{L}(\mathcal{H}_n)$ *and* $\mathcal{B}_n \in \mathcal{L}(\mathcal{U}, \mathcal{H}_n)$. *The margin of stabilizability of* $(\mathcal{A}_n, \mathcal{B}_n)$ *is defined by*

$$\gamma_s(\mathcal{A}_n, \mathcal{B}_n) = \min\Big\{ \|[\delta\mathcal{A}_n, \delta\mathcal{B}_n]\|_{\mathcal{L}(\mathcal{H}_n\times\mathcal{U}, \mathcal{H}_n)} \,,\ (\mathcal{A}_n+\delta\mathcal{A}_n, \mathcal{B}_n+\delta\mathcal{B}_n) \text{ is not stabilizable} \Big\}.$$

The margin of stabilizability of operators is not easy to compute. Peichl and Wang given a condition under which the operator and matrix norms are equivalent.

Condition 7.1 *(Uniform Equivalence of the Operator Norms)*

A given choice of bases for the spaces $\mathcal{H}_n$ and $\mathcal{U}$ satisfies the uniform equivalence of the operator norms condition, if there exist positive constants c_1 and c_2 independent of n such that the matrix representations A_n and B_n of operators $\mathcal{A} \in \mathcal{L}(\mathcal{H}_n)$ and $\mathcal{B} \in \mathcal{L}(\mathcal{U}, \mathcal{H}_n)$ satisfy

$$c_1 \|[A_n, B_n]\|_2 \leq \|[\mathcal{A}_n, \mathcal{B}_n]\|_{\mathcal{L}(\mathcal{H}_n \times \mathcal{U}, \mathcal{H}_n)} \leq c_2 \|[A_n, B_n]\|_2 .$$

Let $\{\phi_k\}_{k=1}^n$ be a basis for $\mathcal{H}_n$ and $\{\psi_k\}_{k=1}^p$ be a basis for $\mathcal{U}$. Define the matrices

$$[M_n]_{ij} = \langle \phi_i, \phi_j \rangle_{\mathcal{H}}$$

for $i, j = 1, 2, \ldots, n$,

$$[V_n]_{ij} = \langle \psi_i, \psi_j \rangle_{\mathcal{U}}$$

for $i, j = 1, 2, \ldots, p$, and

$$G_n = \begin{bmatrix} M_n & 0 \\ 0 & V_n \end{bmatrix}.$$

Let $\{\lambda_k\}_{k=1}^n$ be the eigenvalues of M_n such that

$$\lambda_1 \geq \lambda_2 \geq \ldots \geq \lambda_n$$

and similarly let $\{\mu_k\}_{k=1}^{n+p}$ be the eigenvalues of G_n such that

$$\mu_1 \geq \mu_2 \geq \cdots \geq \mu_{n+p}.$$

We have the following result that is simpler to check than Condition 7.1.

Theorem 7.2 *[PW97]*

Condition 7.1 holds if and only if there exist positive constants τ_1 and τ_2 such that

$$\sqrt{\frac{\lambda_1}{\mu_{n+p}}} \leq \tau_1$$

and

$$\sqrt{\frac{\lambda_n}{\mu_1}} \leq \tau_2$$

for all n.

Peichl and Wang study the connection between stablizability and the margin of stabilizability. These authors give a necessary condition for the uniform stabilizability of approximate control systems.

Theorem 7.3 *[PW97, Corollary 3.1]*

Let $\mathcal{A} \in \mathcal{L}(\mathcal{H}_n)$ and $\mathcal{B} \in \mathcal{L}(\mathcal{U}, \mathcal{H}_n)$. If

(1) the approximating finite-dimensional control systems

$$\dot{w}_n(t) = \mathcal{A}_n w_n(t) + \mathcal{B}_n u(t), \quad t > 0,$$
$$w_n(0) = w_{n_0}$$

are uniformly stabilizable for all n, and

(2) the choice of bases for $\mathcal{H}_n$ and $\mathcal{U}$ satisfy the uniform equivalence of the operator norm condition,

then there exists a constant $\epsilon > 0$ such that for all n, $\gamma_s(A_n, B_n) \geq \epsilon$.

Thus, if the margin of stabilizability of (A_n, B_n) tends to zero as $n \to \infty$, then either $(\mathcal{A}_n, \mathcal{B}_n)$ is not uniformly stabilizable, or Condition 7.1 does not hold. For a given approximation method, if we can establish that Condition 7.1 holds and

show that the margin of stabilizability tends to zero, then we can conclude that $(\mathcal{A}_n, \mathcal{B}_n)$ is not uniformly stabilizable. This result is summarized in the following corollary of Theorem 7.3.

Corollary 7.4

Let $\mathcal{A} \in \mathcal{L}(\mathcal{H}_n)$ and $\mathcal{B} \in \mathcal{L}(\mathcal{U}, \mathcal{H}_n)$. If

(1) there exist positive constants τ_1 and τ_2 such that

$$\sqrt{\frac{\lambda_1}{\mu_{n+p}}} \leq \tau_1$$

and

$$\sqrt{\frac{\lambda_n}{\mu_1}} \leq \tau_2$$

for all n, and

(2) for any $\epsilon > 0$, there exists n such that $\gamma_s(A_n, B_n) < \epsilon$,

then $(\mathcal{A}_n, \mathcal{B}_n)$ is not uniformly stabilizable for all n.

In the following two sections, we consider (1) and (2) in Corollary 7.4.

7.1.2 Uniform Equivalence of Norms for Linear Splines

Recall, the inner product on $\mathcal{H} = \overline{H}_1 \times L_2$ is given by

$$\langle \zeta, \xi \rangle_{\mathcal{H}} = c^2 \int_0^L \frac{\partial \zeta_1}{\partial x} \overline{\frac{\partial \xi_1}{\partial x}}\, dx \; + \int_0^L \zeta_2 \overline{\xi_2}\, dx$$

where $\zeta = (\zeta_1, \zeta_2)$ and $\xi = (\xi_1, \xi_2)$. Let $\{\phi_k\}_{k=1}^n$ be the linear splines defined in (4.11). As in Chapter 4, we will assume that $\{\phi_k\}_{k=1}^n$ form a basis for H_n where $\mathcal{H}_n = H_n \times H_n$. Let Θ_n be the basis for $\mathcal{U} = \mathbb{R}$, i.e., one control input. In particular,

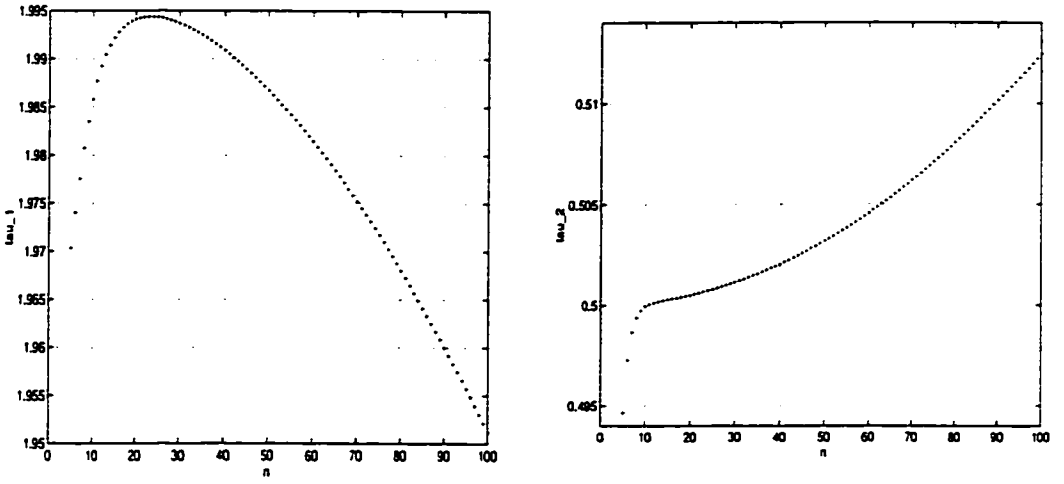

(a) $\sqrt{\frac{\lambda_1}{\mu_{n+p}}}$ vs n (b) $\sqrt{\frac{\lambda_n}{\mu_1}}$ vs n

Figure 7.1: Upper and lower bounds for equivalence of norms

let

$$\Theta_n = \frac{2c}{\sqrt{n}}$$

where $c = 331m/s$ is the speed of sound in air. Thus,

$$V_n = (\Theta_n)^2 = \frac{4c^2}{n}.$$

The computed values of $\sqrt{\frac{\lambda_1}{\mu_{n+p}}} \leq \tau_1$ and $\sqrt{\frac{\lambda_n}{\mu_1}} \leq \tau_2$ (from Theorem 7.2) are plotted in Figure 7.1. We find $\tau_1 \approx 2$ and $\tau_2 \approx 1/2$, i.e., $\tau_1 \approx 1/\tau_2$. Thus, Condition 7.1 holds.

7.1.3 The Margin of Stabilizability for Matrix Representations

In this section, we study the behaviour of the margin of stabilizability of the matrix representations $\gamma_s(A_n, B_n)$ as n gets large.

Let the approximating system (7.3) be determined using the semi-discrete Galerkin approach outlined in Chapter 4. Again we assume that $x_d = 0$, $x_a = 0$, $x_s = 1$, and $x = 2$. As well, $K = 0.7$ and $L = 4$. Numerical results in Chapter 4 indicate that the Legendre polynomial method is uniformly stable. Thus, the margin of stabilizability of this method is not in question. Instead, we consider a linear spline based scheme. As in Chapter 4, we consider the finite-dimensional transfer function $G_n(x, x_d)$. Let $[A_n, B_n, C_n, D_n]$ be the "natural" state-space representation of $G_n(x, x_d)$ given in (4.4) and (4.6).

Let $\sigma_{min}(M)$ denote the smallest singular value of a matrix $M \in \mathbb{R}^{n\times(n+m)}$. The minimal singular value $\sigma_{min}([A_n, B_n])$ provides an upper bound for $\gamma_s(A_n, B_n)$ [PW97] [BP89]. Figure 7.2(a) illustrates the computed minimum singular value $\sigma_{min}([A_n, B_n])$. We can see that $\sigma_{min}([A_n, B_n]) \to 0$ as n gets large. This suggests that $\gamma_s(A_n, B_n) \to 0$ as n gets large.

However, as mentioned in Section 5.5, balanced realizations are key to maintaining numerical stability of various state-space calculations (see Appendix A). In determining a balanced realization, a transformation $T_n \in \mathbb{R}^{n\times n}$ is found so that a balanced realization is $[\tilde{A}_n, \tilde{B}_n, \tilde{C}_n, \tilde{D}_n] = [T_n A_n T_n^{-1}, T_n B_n, C_n T_n^{-1}, D_n]$. In general, $\gamma_s(A_n, B_n) \neq \gamma_s(\tilde{A}_n, \tilde{B}_n)$ [BP89]. Figure 7.2(b) illustrates the computed minimum singular value $\sigma_{min}([\tilde{A}_n, \tilde{B}_n])$. We can see that $\sigma_{min}([\tilde{A}_n, \tilde{B}_n])$ is constant as n gets large. Thus, results in this case indicate that $\gamma_s(\tilde{A}_n, \tilde{B}_n)$ may or may not approach zero. However, balanced realizations, although generally numerically more stable, destroy any physical significance of the state variables. In addition, to obtain a balanced realization we need to employ the observation operator C_n. This introduces artificial weighting on the matrices A_n and B_n. Thus, in many respects, $\sigma_{min}([A_n, B_n])$ calculated using the "natural" realization provides a better representation of the true upper bound of the margin of stabilizability.

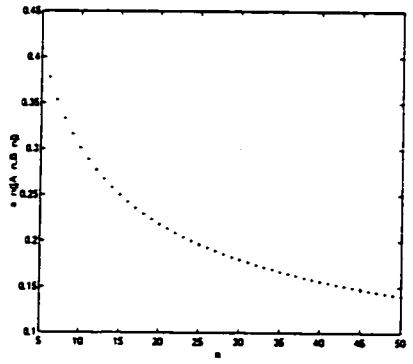

(a) $\sigma_{min}([A_n, B_n])$

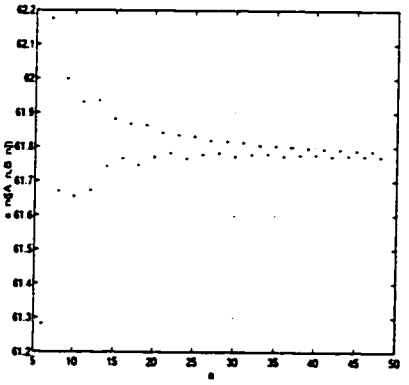

(b) $\sigma_{min}([\tilde{A}_n, \tilde{B}_n])$

Figure 7.2: Computed minimum singular values

7.1.4 LQR and LQE Design

Recall that in finite dimensions, two matrices A_n and B_n are stabilizable if there exists a constant matrix K_n such that $A_n - B_nK_n$ is stable. The matrix K_n can be found using standard LQR techniques. If we consider the margin of stability of $A_n - B_nK_n$, this will provide us with information similar to the margin of stabilizability of (A_n, B_n).

Thus, consider the control systems in (7.2). We need to find K_n such that $A_n - B_nK_n$ are stable. Let us consider the finite-dimensional system given in (7.3). Let the output equation be given by

$$y_n(t) = C_n w_n(t).$$

Suppose that all states are not detectable so that a state estimator is required. Let the estimator have the form

$$\dot{\hat{w}}_n(t) = A_n\hat{w}_n(t) + B_nu(t) + F_nC_n(w_n - \hat{w}_n) \tag{7.4}$$

where $\hat{w}$ are the estimated states and F_n is some constant vector. Combining (7.3) and (7.4) we get

$$\dot{e}_n(t) = (A_n - F_nC_n)e_n(t)$$

where $e_n = w_n - \hat{w}_n$. Thus, $\hat{w}_n$ tends to w_n provided that the eigenvalues of $A_n - F_nC_n$ have negative real parts. The control system with estimator and state feedback is shown in Figure 7.3. From this figure we have $u = r - K_nw_n$ (assuming a full state estimator) so that the realization of the feedback system is

$$\dot{w}_n(t) = (A_n - B_nK_n)w_n(t) + B_nr$$
$$y_n(t) = C_nw_n(t).$$

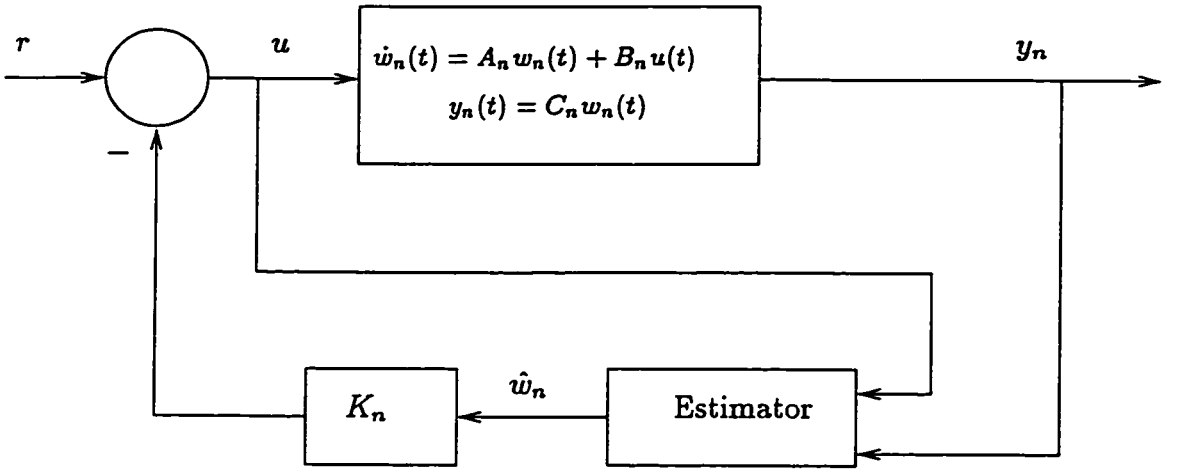

Figure 7.3: Estimator with state feedback

For closed loop stability, K_n is chosen so that the eigenvalues of $A_n - B_n K_n$ have negative real parts (which is possible if the system is stabilizable). A common way of choosing K_n and F_n is by solving the linear quadratic regulator (LQR) and linear quadratic estimator (LQE) problems, respectively. These are summarized as follows (e.g., [AM90]).

Consider the linear time-invariant stabilizable system

$$\dot{w}_n(t) = A_n w_n(t) + B_n u(t)$$
$$y_n(t) = C_n w_n(t).$$

Suppose (A_n, B_n) is stabilizable. Let D_n be any matrix such that $Q_n = D_n^T D_n \geq 0$ and (A_n, D_n) is detectable. Define the cost functional as

$$J(u) = \int_0^\infty \left[\langle w_n, Q_{r_n} w_n \rangle + \langle u, R_r u \rangle \right] dt.$$

The optimal solution of minimizing the above cost functional subject to

$$\dot{w}_n(t) = A_n w_n(t) + B_n u(t)$$

is given by state feedback $u(t) = -K_n w_n(t)$ where

$$K_n = R_r^{-1} B_n^T \Pi_{r_n}$$

where $\Pi_{r_n} = \Pi_{r_n}^T > 0$ satisfies the algebraic Riccati equation

$$\Pi_{r_n} A_n + A_n^T \Pi_{r_n} - \Pi_{r_n} B_n R_r^{-1} B_n^T \Pi_{r_n} + Q_{r_n} = 0.$$

If all states are not detectable, we require a state estimator. This may be determined by solving the linear quadratic estimator (LQE) problem (e.g., [Mac89]). Consider the system

$$\dot{w}_n(t) = A_n w_n(t) + B_n u(t) + \omega$$
$$y_n(t) = C_n w_n(t) + \nu$$

where ω is a random noise disturbance input and ν is a random measurement (sensor) noise. We assume that both of these variables are white Gaussian zero-mean with known covariances. The problem is to obtain an estimate $\hat{w}_n$ of the state w_n based on noise-corrupted measurements such that the variance of the error $w_n - \hat{w}_n$ is minimized. The following is assumed:

- (C_n, A_n) is detectable,
- $R_e > 0$, and
- there exists D_n such that $D_n D_n^T = Q_{e_n} \geq 0$ and (A_n, D_n) is stabilizable.

Under these assumptions, the optimal estimator is given by

$$\dot{\hat{w}}_n = A_n \hat{w}_n + B_n u + L_n(y_n - C_n \hat{w}_n)$$
$$L_n = \Pi_{e_n} C_n^T R_e^{-1}$$

where $\Pi_{e_n} = \Pi_{e_n}^T > 0$ solves the algebraic Riccati equation

$$A_n \Pi_{e_n} + \Pi_{e_n} A_n^T - \Pi_{e_n} C_n^T R_e^{-1} C_n \Pi_{e_n} + Q_{e_n} = 0.$$

Several authors have studied the convergence of the above Riccati operator Π_{r_n} (and likewise Π_{e_n}). These results were summarized in Chapter 3.

In the following two sections, we will consider two design cases: $Q = C^T C$ and $Q = I$. Because this latter case does not use the output equation $y_n = C_n w_n$, we avoid any special weighting incurred by this output equation.

Case 1: $Q_{r_n} = C_n^T C_n$

Let $Q_{r_n} = C_n^T C_n$ and $R_r = 1$. This choice for Q_{r_n} introduces the output in the cost function. Similarly, we may choose $R_e = 1$ and $Q_{e_n} = B_n B_n^T$ since (A_n, B_n) is stabilizable. Further examination of the LQR and LQE problems reveals that the two problems are duals of each other.

The state-space representation of the optimal feedback controller G_{c_n} is given by

$$\dot{\hat{w}}_n(t) = (A_n - B_n K_n - L_n C_n)\hat{w}_n(t) + L_n y_n(t)$$
$$\hat{u}(t) = K_n \hat{w}_n(t).$$

Figures 7.4 and 7.5 show the magnitude and phase of G_{c_n} for various increasing values of n, for both the Legendre polynomial and linear spline based approximation methods. Figure 7.6 shows the magnitude and phase of G_{c_n} for $n = 45$ for both approximation methods. We can see that the G_{c_n} computed by both methods are converging to the same controller. Figures 7.7 and 7.9 show the magnitude of the closed loop responses $\Delta(G, G_{c_n}) = y/r$ (with the exact plant) and $\Delta(G_n, G_{c_n}) = y/r$ (with the approximate plant) for both methods. The phase is shown in Figures 7.8 and 7.10. Again, we can see these are converging. Figures 7.11 and 7.12 show that the closed loop responses for both methods are in fact converging to the same response. For stable systems, convergence of the closed loop responses (i.e., $\Delta(G_n, G_{c_n}) \to \Delta(G, G_c)$) is equivalent to convergence of the plant $G_n \to G$ and the controller $G_{c_n} \to G_c$ in the *graph topology* [Vid85, Theorem 7.2.28]. This topology is a generalization of the H_∞ norm and so is an appropriate framework

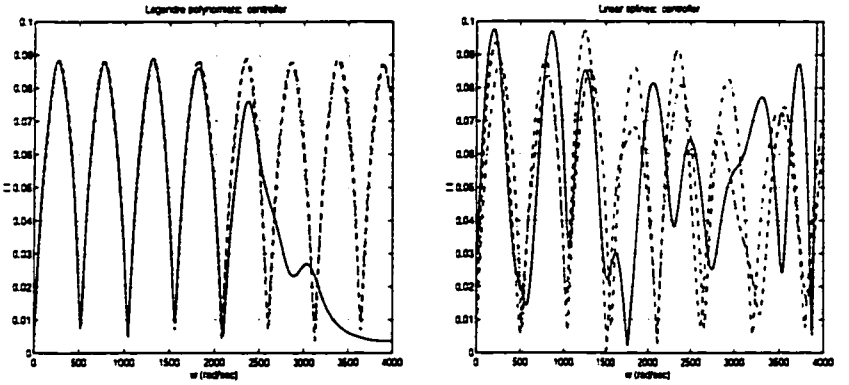

(a) Legendre polynomials (b) Linear splines

Figure 7.4: Case 1: magnitude of LQR controllers ($n = 15$ (solid), $n = 30$ (dashed), $n = 45$ (dash/dot))

in which to study convergence of approximations used in our controller design. Thus, convergence of the controllers and of the closed loop responses implies the applicability of the linear spline approximations for controller design.

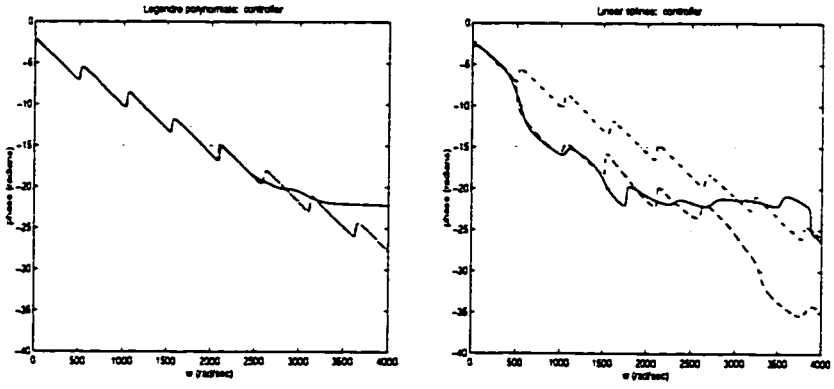

(a) Legendre polynomials (b) Linear splines

Figure 7.5: Case 1: phase of LQR controllers ($n = 15$ (solid), $n = 30$ (dashed), $n = 45$ (dash/dot))

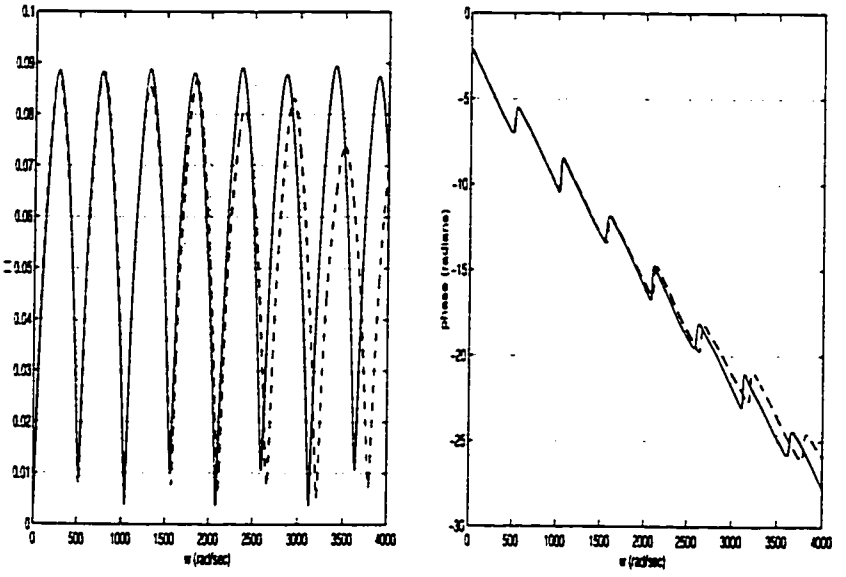

(a) Magnitude of controller (b) Phase of controller

Figure 7.6: Case 1: LQR controllers for Legendre polynomials and linear splines ($n = 45$, Legendre polynomials (solid), linear splines (dashed))

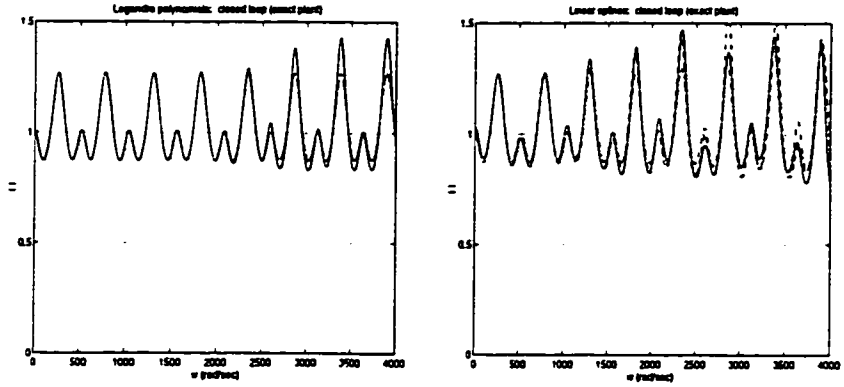

(a) Legendre polynomials (b) Linear splines

Figure 7.7: Case 1: magnitude of closed loop with exact plant and LQR controller ($n = 15$ (solid), $n = 30$ (dashed), $n = 45$ (dash/dot))

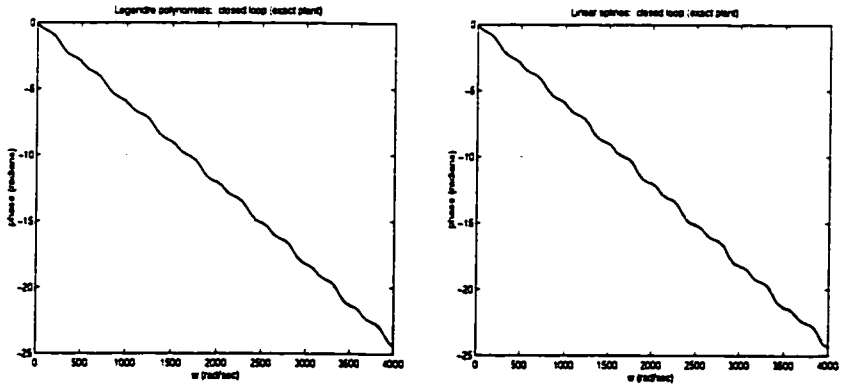

(a) Legendre polynomials (b) Linear splines

Figure 7.8: Case 1: phase of closed loop with exact plant and LQR controller ($n = 15$ (solid), $n = 30$ (dashed), $n = 45$ (dash/dot))

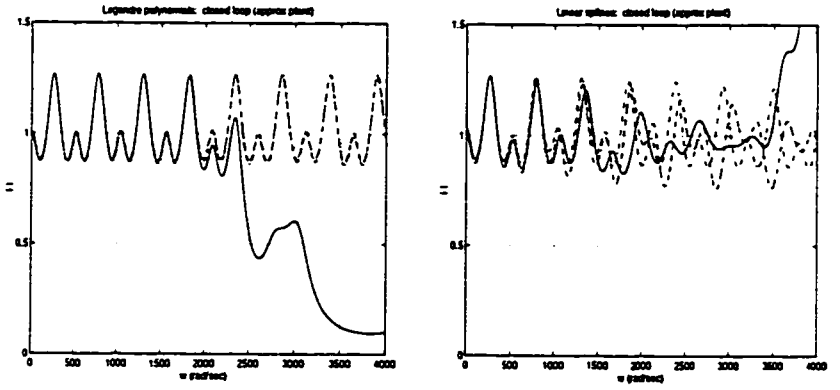

(a) Legendre polynomials (b) Linear splines

Figure 7.9: Case 1: magnitude of closed loop with approximate plant and LQR controller ($n = 15$ (solid), $n = 30$ (dashed), $n = 45$ (dash/dot))

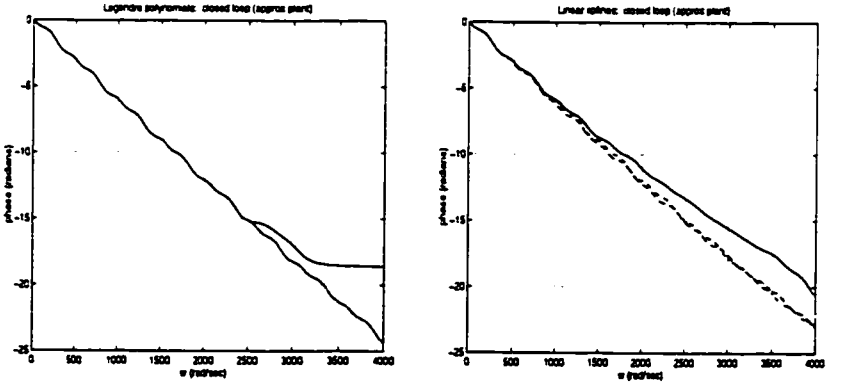

(a) Legendre polynomials (b) Linear splines

Figure 7.10: Case 1: phase of closed loop with approximate plant and LQR controller ($n = 15$ (solid), $n = 30$ (dashed), $n = 45$ (dash/dot))

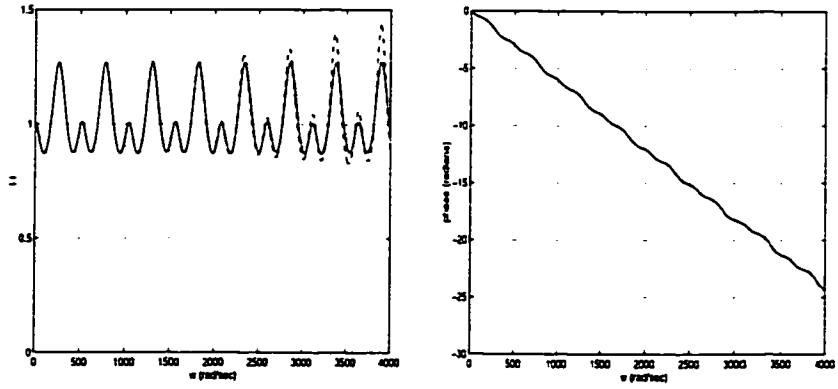

(a) Magnitude (b) Phase

Figure 7.11: Case 1: closed loop response with exact plant and LQR controllers for Legendre polynomials and linear splines ($n = 45$, Legendre polynomials (solid), linear splines (dashed))

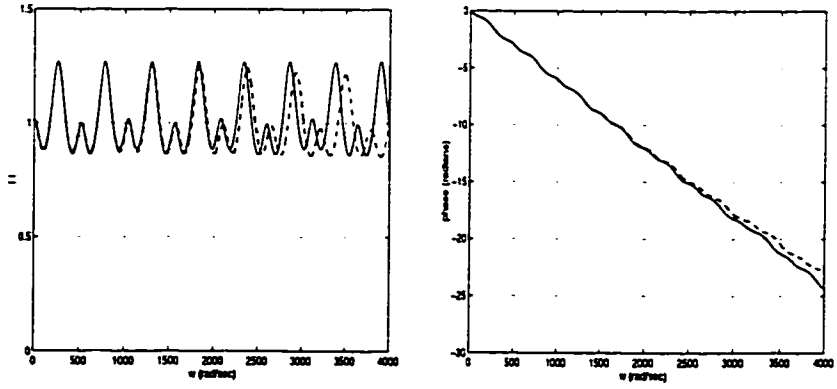

(a) Magnitude (b) Phase

Figure 7.12: Case 1: closed loop response with approximate plant and LQR controllers for Legendre polynomials and linear splines ($n = 45$, Legendre polynomials (solid), linear splines (dashed))

n	$\max\{\mathrm{Re}\lambda, \lambda \in \sigma(A_n - B_nK_n)\}$
5	-87.3613
10	-69.4325
15	-66.8039
20	-55.9816
25	-50.5908
30	-47.0653
35	-29.1101
40	-24.8533
45	-17.1784

Table 7.1: Case 1: linear splines - margin of stability of $A_n - B_nK_n$

The stability margin of $A_n - B_nK_n$ for linear splines controlled using LQR state feedback K_n is shown in Table 7.1. We can see from these results that this margin is tending to zero as n gets large.

Case 2: $Q = I$

In this section, we will only consider the solution to the LQR problem. Let $w \in \mathcal{H} = \overline{H}_1(0, L) \times L_2(0, L)$. Consider the infinite-dimensional state-space representation

$$\dot{w}(t) = \mathcal{A}w(t) + \mathcal{B}u(t)$$

and the associated cost functional

$$J(u) = \int_0^\infty \Big[\langle w, Qw\rangle + \langle u, Ru\rangle\Big]\, dt$$

where $Q > 0$ and $R > 0$ are symmetric. Let $Q_n = Q_{r_n}$ and $R_r = R$. The finite-dimensional matrix representation of the above system is

$$\dot{w}_n(t) = A_n w_n(t) + Bu(t)$$

for $w_n \in \mathcal{H}_n$ with the cost functional

$$J(u) = \int_0^\infty \Big[\langle w_n, Q_n w_n\rangle + \langle u, Ru\rangle\Big]\, dt.$$

Suppose $Q = I$. We need to determine the matrix representation of Q_n. Consider the inner product defined on $\mathcal{H}$ (see (3.4)). The state is $w = [z\ z_t]$. Then with $Q = I$ we have

$$\begin{aligned}\langle w, w\rangle_{\mathcal{H}} &= \left\langle \begin{bmatrix} z \\ z_t \end{bmatrix}, \begin{bmatrix} z \\ z_t \end{bmatrix} \right\rangle_{\mathcal{H}} \\ &= c^2 \int_0^L \nabla z \nabla z \, dx + \int_0^L z_t z_t \, dx.\end{aligned}$$

From (4.2),

$$\begin{aligned}z^n(x,t) &= \sum_{i=0}^{n} a_i(t)\phi_i(x) \\ &= \Phi V\end{aligned} \tag{7.5}$$

where

$$\Phi = [\phi_0(x)\ \phi_1(x)\ \ldots\ \phi_n(x)]$$

and

$$V = \begin{bmatrix} a_0(t) \\ a_1(t) \\ \vdots \\ a_n(t) \end{bmatrix}.$$

Thus,

$$\begin{aligned}\left\langle \begin{bmatrix} z_n \\ z_{n_t} \end{bmatrix}, \begin{bmatrix} z_n \\ z_{n_t} \end{bmatrix} \right\rangle_{\mathcal{H}_n} &= c^2 \int_0^L [\nabla(\Phi V)]^T \nabla (\Phi V)\, dx + \int_0^L [\Phi \dot{V}]^T \Phi \dot{V}\, dx \\ &= c^2 V^T \left[\int_0^L \nabla \Phi^T \nabla \Phi \, dx\right] V + \dot{V}^T \left[\int_0^L \Phi^T \Phi \, dx\right] \dot{V}.\end{aligned} \tag{7.6}$$

Now the "states" used in calculations are the coefficients $\{a_i(t)\}$, i.e., the vector V, so that we need to consider the inner product $\langle w_n, Q_n w_n\rangle_{\mathbf{R}}$ where $w_n = [V\ \dot{V}]$. Let

$$Q = \begin{bmatrix} Q_{n_1} & 0 \\ 0 & Q_{n_2} \end{bmatrix}.$$

Thus,

$$\begin{aligned} \langle w_n, Q_n w_n \rangle &= \left\langle \begin{bmatrix} V \\ \dot{V} \end{bmatrix}, \begin{bmatrix} Q_{n_1} V \\ Q_{n_2} \dot{V} \end{bmatrix} \right\rangle_{\mathbf{R}} \\ &= V^T Q_{n_1} V + \dot{V} Q_{n_2} \dot{V}. \end{aligned} \tag{7.7}$$

Comparing (7.6) and (7.7) we find

$$Q_{n_1} = c^2 \int_0^L \nabla \Phi^T \nabla \Phi \, dx$$

and

$$Q_{n_2} = \int_0^L \Phi^T \Phi \, dx.$$

That is,

$$[Q_{n_1}]_{ij} = c^2 \int_0^L \nabla \phi_i(x) \nabla \phi_j(x) \, dx$$

and

$$[Q_{n_2}]_{ij} = \int_0^L \phi_i(x) \phi_j(x) \, dx.$$

Table 7.2 shows the margin of stability of $A_n - B_n K_n$ with the above choice for Q_n and $R = 1$ with linear splines used as the basis functions. We clearly see that the margin is tending to zero as n gets large.

n	$\max\{\mathrm{Re}\lambda, \lambda \in \sigma(A_n - B_n K_n)\}$
5	-22.0421
6	-16.1439
7	-12.2564
8	-9.5921
9	-7.6999
10	-6.3138
11	-5.2715
12	-4.4701
13	-3.8421
14	-3.3419
15	-2.9380
16	-2.6079
17	-2.3354
18	-2.1083
19	-1.9177
20	-1.7566
21	-1.6196
22	-1.5026
23	-1.4021
24	-1.3155
25	-1.2407
26	-1.1757
27	-1.1192
28	-1.0699
29	-1.0268
30	-0.9891

Table 7.2: Case 2: linear splines – margin of stability of $A_n - B_n K_n$

7.1.5 Discussion

In this chapter, we have shown that (1) the approximating scheme using linear splines appears to have a margin of stabilizability that tends to zero as $n \to \infty$, and (2) the uniform equivalence of norms condition is satisfied. Thus, Corollary 7.4 suggests that this method is not uniformly stabilizable. In addition, LQR results for two separate cases indicate that the margin of stability of $A_n - B_n K_n$ is also tending to zero.

However, we make the following observations. In Chapter 4, we showed numerically that the approximating transfer function and inner factors using linear splines are converging. Figure 7.6 in Case 1 shows that the controller found for either Legendre polynomials or linear splines is converging to the same controller. As well, the closed loop responses in Figures 7.11 and 7.12 are also converging.

The convergence in the above mentioned situations is likely due to the feedback matrix C_n since this matrix plays a role in both the transfer function and in the state weighting $Q_{r_n} = C_n^T C_n$ in the LQR design. An observation is only made at a finite number of points. Hence, those modes which are tending towards the imaginary axis and as a result are difficult to uniformly stabilize, do not show up in the transfer function (since they are not observed and/or weighted).

If we compare the margin of stability in Table 7.1 or Table 7.2 with the open loop margin of stability in Table 4.2, we see that the addition of the controller does greatly improve the margin of stability of the system even though this margin is not uniform. In addition, both closed loop transfer functions $\Delta(G, G_{c_n})$ (closed loop with the exact plant and finite-dimensional controller) and $\Delta(G_n, G_{c_n})$ (closed loop with the approximate plant and finite-dimensional controller) are converging. Thus, the linear spline based method provides good results for both approximation

of the transfer function and design of a controller for closed loop stability. These results indicate that uniform stabilizability is not a necessary condition for controller design.

Recall also from Chapter 4 that (i) $|G_n(jw) - G(jw)| \to 0$ over all compact intervals as n increases, and (ii) $|W_1(jw)(G_{n_i}(jw) - G_i(jw))| \to 0$ over all compact intervals as n increases. Thus, besides convergence of the approximating transfer functions, we also have convergence of the inner factors of the approximating transfer functions. As discussed in Chapter 3, convergence of the inner factors is important for solving the optimal sensitivity problem. In the next section, we discuss the approximation of inner factors using different approximation schemes in an effort to understand why linear splines exhibit superior numerical properties to Legendre polynomials.

7.2 Approximation of Inner Functions

Consider the transfer function $G(x_1, x_2)$. Regardless of whether $x_1 > x_2$ or $x_1 < x_2$, the inner factor of $G(x_1, x_2)$ is given by (see (2.18))

$$G_i = e^{-\frac{s}{c}|x_1 - x_2|}.$$

Thus, approximations G_{n_i} to the inner factor G_i should also be the same regardless of whether the system is feedback or feedforward.

We will show here that although both Legendre polynomials and linear splines approximate the transfer function for a feedforward system "well", only linear splines approximate the inner factors such that

$$G_{n_i}(x_1, x_2) = G_{n_i}(x_2, x_1),$$

i.e.,

$$G_{n_i} \to e^{-\frac{s}{c}|x_1 - x_2|}.$$

We consider the transfer functions

(1) $G(x_1, x_2) = G(\frac{1}{2}, 2)$ (feedforward), and

(1) $G(x_2, x_1) = G(2, \frac{1}{2})$ (feedback).

Figure 7.13 shows a typical magnitude and phase of the approximating and exact transfer functions found using Legendre polynomials, for the feedforward and feedback cases, respectively. Figure 7.14 shows a typical magnitude and phase of the approximating and exact transfer functions found using linear splines, for the feedforward and feedback cases, respectively. We can see that both methods give good approximations. There is no offset visible for the linear spline method. Figure 7.15 shows the phase of the approximating inner factor G_{n_i} for the feedforward and feedback cases found using Legendre polynomials. The exact phase is also shown. The magnitudes in all cases are effectively unity for all frequencies and so are not shown. Figure 7.16 shows the phase for the approximating inner factor found using linear splines. Results for linear splines show that the phase for $G_{n_i}(\frac{1}{2}, 2)$ is exactly the same as that for $G_{n_i}(2, \frac{1}{2})$. This is not true for Legendre polynomials. Also, calculations carried out using Legendre polynomials are very sensitive to point locations (see Section 6.3). These problems do not appear to affect the linear spline based approximation method.

To explain this discrepancy between the two approximating methods, we hypothesize the following. Recall that in Chapter 4, we referred to Legendre polynomials as "global" basis function and linear splines as "local" basis functions or basis functions with "compact" support. The errors in approximating the inner factor of the transfer function are dependent on the choice of location for the output x_1 and the input x_2. The matrices which determine the control weights (see F_1 in (4.4)) and the observation weights (see $\bar{C}$ in (4.6)) depend on the basis functions and derivatives of the basis functions, respectively. For Legendre polynomials these matrices

are not sparse whereas for linear splines they are sparse. Thus, the points x_1 and x_2 and slight variations therein have a much wider and more far-reaching effect on these matrices when Legendre polynomials are used.

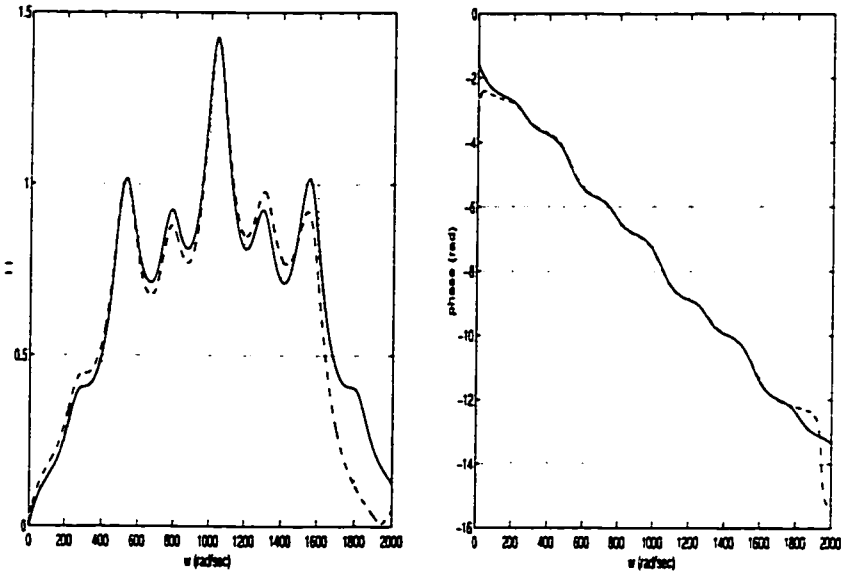

(a) Feedforward: magnitude (b) Feedforward: phase

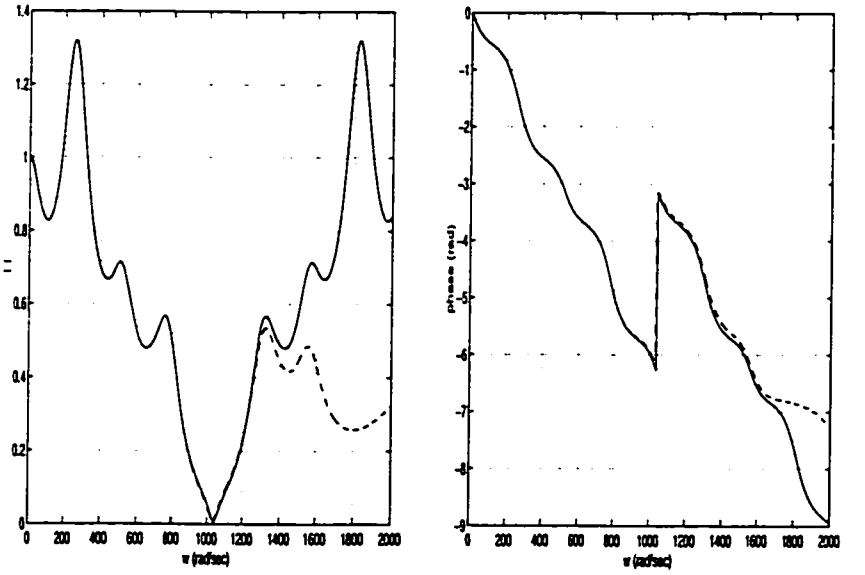

(c) Feedback: magnitude (d) Feedback: phase

Figure 7.13: Legendre polynomials: feedforward and feedback (exact solution (solid), approximate solution for $n = 10$ (dashed))

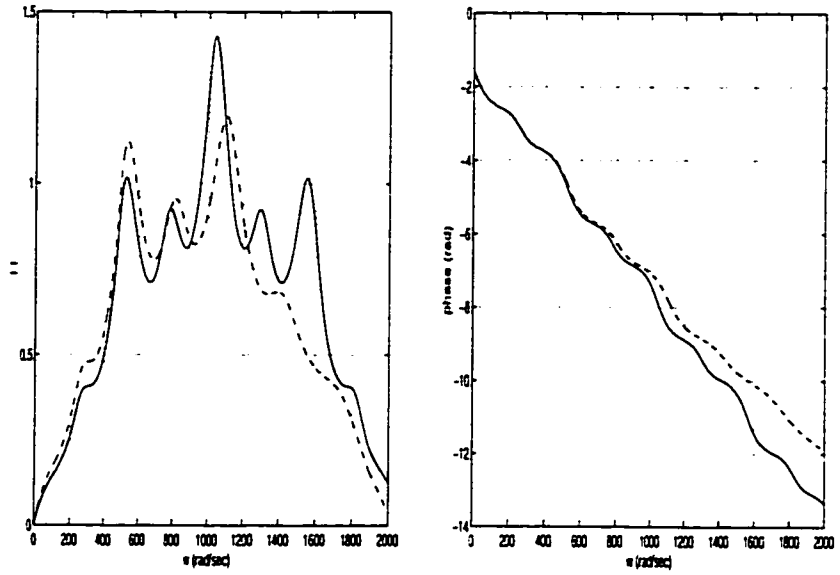

(a) Feedforward: magnitude (b) Feedforward: phase

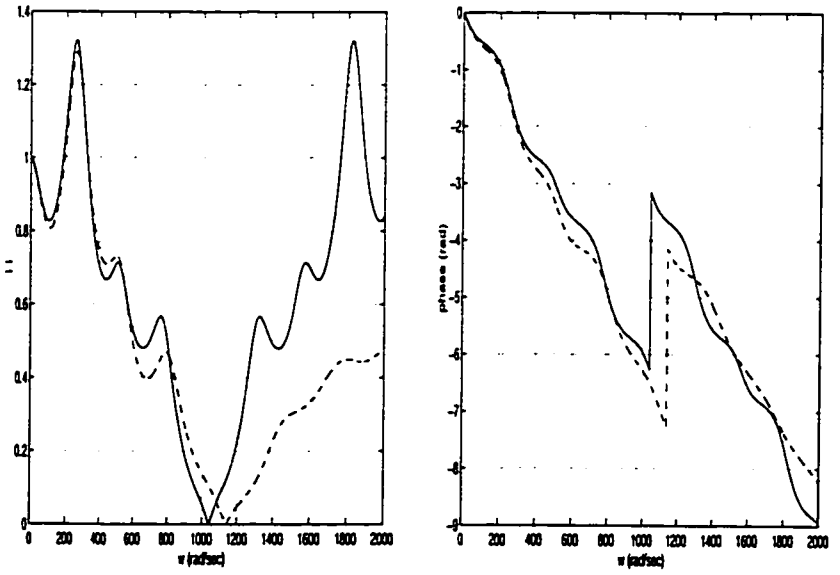

(c) Feedback: magnitude (d) Feedback: phase

Figure 7.14: Linear splines: feedforward and feedback (exact solution (solid), approximate solution for $n = 10$ (dashed))

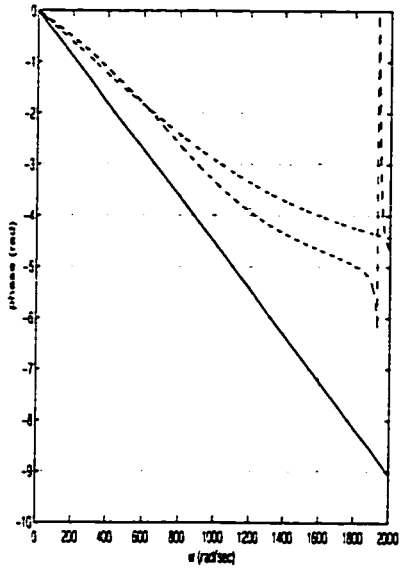

Figure 7.15: Legendre polynomials: inner factor for feedforward and feedback (exact solution (solid), approximate feedforward for $n = 10$ (dashed), approximate feedback for $n = 10$ (dash/dot))

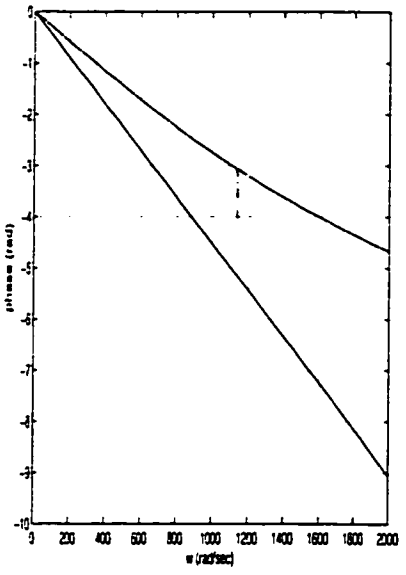

Figure 7.16: Linear splines: inner factor for feedforward and feedback (exact solution (solid), approximate feedforward for $n = 10$ (dashed), approximate feedback for $n = 10$ (dash/dot))

	Property	Legendre Polynomials	Linear Splines
1)*	$\|G_n(jw) - G(jw)\| \to 0$?	Yes	Yes
2)*	$\|W_1(jw)(G_{n_i}(jw) - G_i(jw)\| \to 0$?	Yes	Yes
3)*	$G_{n_i}(x_1, x_2) = G_{n_i}(x_2, x_1)$?	No	Yes
4)	uniform margin of stability?	Yes	No
5)	uniformly stabilizable?	Yes	No

Table 7.3: Properties of approximating schemes (* over compact intervals)

7.3 Summary

For completeness, we summarize the suitability of the two different schemes, Legendre polynomials and linear splines, for approximating our H_∞ control problem. Let G be the exact transfer function, G_n the n^{th}-dimensional approximation of G. Similarly, let G_i be the inner factor of G, and G_{n_i} the n^{th}-dimensional approximation of G_i. A summary of the relevant approximation results is given in Table 7.3. As seen in Chapter 6, the linear spline based approximation method allows us greater freedom in varying the location of performance points in the duct. These results indicate that points (1)–(3) of those listed in Table 7.3 are most important in the approximation and study of the acoustic noise reduction problem. Therefore, we suggest the following modification of Theorem 3.21.

Conjecture 7.1

Let $W_1(s) \in RH_\infty$. Let x_1 and x_2 be two control points, where a signal is measured and where a signal is applied. Suppose we are given an infinite-dimensional bounded or unbounded control system with transfer function $G(x_1, x_2)$ and inner

Approximating Scheme	γ_{opt} (dB)	CPU time (seconds)
Legendre polynomials	-3.6262	≈ 550
linear splines	-3.2811	≈ 185

Table 7.4: CPU time comparison

factor $G_i(x_1, x_2)$. *The finite-dimensional systems with transfer function* G_n *and inner factor* G_{n_i} *generated by the approximating scheme are suitable for* H_∞ *controller design if*

1) $|G_n(jw) - G(jw)| \to 0$ *over any compact interval as* $n \to \infty$,

2) $|W_1(jw)(G_{n_i}(jw) - G_i(jw))| \to 0$ *over any compact interval as* $n \to \infty$, *and*

3) $G_{n_i}(x_1, x_2) = G_{n_i}(x_2, x_1)$ *over any compact interval.*

Recall that when first considering approximation methods, our goal was to choose only those methods that are potentially applicable to the three-dimensional acoustic noise reduction problem. Results in this chapter as well as Chapter 4 suggest that linear splines satisfy the requirements of Conjecture 7.1. Also, it is well-known that linear splines generate sparse matrices when used to approximate partial differential equations. Thus, the above results indicate that linear splines would provide an appropriate as well as numerically feasible choice for the more complicated three-dimensional problem. To illustrate the difference in CPU time required for each approximating scheme, consider the following test case. Let $x_d = 0$, $x_a = 1$, $x_s = 2$, and $x = 3$. The results in Table 7.4 indicate that Legendre polynomials require approximately three times as much CPU time as linear splines to compute a solution in this simple SISO case. This difference will be very beneficial when studying the three-dimensional acoustic noise reduction problem.

Chapter 8

Conclusions and Future Research

The general aim of this thesis has been to study the problem of achievable global noise reduction in the one-dimensional duct. We formulated the problem of global noise reduction in the duct, considering the optimal placement of the sensor and the actuator. Through successive simplifications to this problem we arrived at (see Problem 3 on page 26)

$$\gamma_{opt} = \inf_{Q \in H_\infty} \left\| \tilde{T}_1 - \tilde{T}_2 Q \right\|_\infty \tag{8.1}$$

where $\tilde{T}_1$ and $\tilde{T}_2$ are non-rational transfer functions. We further simplied (8.1) by using an appropriate finite-dimensional approximation scheme to obtain (see Problem 4 on page 27)

$$\gamma_n = \inf_{Q \in RH_\infty} \left\| T_1 - T_2 Q \right\|_\infty \tag{8.2}$$

where T_1 and T_2 are rational transfer functions, and we stipulate that $\gamma_n \to \gamma_{opt}$.

The theory of both finite and infinite-dimensional control systems was presented in a uniform framework by describing the state-space dynamics of the model in terms of semigroup control systems. Several authors have studied conditions for the convergence of finite-dimensional approximations with respect to the LQR problem

for both bounded and unbounded control systems (e.g., [Gib79], [BK84], [IT89], [BI97]). These results were reviewed. Although none of these results directly applies to our problem, we saw that there is a common thread amongst all sufficient conditions. On the other hand, we saw in Chapters 4 and 7 that not all conditions are necessary. In particular, we illustrated that the common condition of uniform stabilizability of the approximations is not a necessary condition. We also considered conditions under which solutions to finite-dimensional approximations of the H_∞ optimal control problem converge to the solution of the infinite-dimensional H_∞ optimal control problem. We found that key are the convergence over compact intervals of both the transfer functions and the inner factors of the transfer functions [Smi90] [RD90].

Recall that one of our goals was to determine methods that are applicable to the three-dimensional acoustic noise reduction problem. Once the model is formulated in three dimensions, we must establish well-posedness of the system before any convergence results can be discussed. Wang [Wan95] considers the regularity of the wave equation with boundary damping and point control in two and three dimensions. These results provide insight into the question of well-posedness. Subsequently, in order to solve the three-dimensional problem via finite-dimensional approximations, we need an approximating method that will generate an appropriate as well as computationally feasible scheme. In this thesis, we showed that both Legendre polynomials and linear splines are suitable basis functions for approximating the one-dimensional duct model. It is well-known that linear splines generate matrices which are sparse. The local nature of the basis for linear splines may lead to better handling of the reflection of the waves in the duct at $x = 0$ and $x = L$. This suggests that linear splines would also be most appropriate in the three-dimensional case where reflection is caused by all boundaries. This clearly

is important in the three-dimensional problem where an effort must be made to reduce computation time. As well, because of the high degree of reflection present in a three-dimensional cavity, the achievable level of global acoustic noise reduction will most likely be significantly lower than in the one-dimensional duct.

Results in this thesis indicate that the stabilizability of approximations is not necessary for controller design. As well, the benefits of using linear splines to select sensor, actuator, and performance point locations in the duct were illustrated. These results indicate that again linear splines are the most suitable choice for approximating the global noise reduction problem. A formal derivation of necessary conditions for H_∞ state feedback controller design for bounded and unbounded control systems would provide a solid framework for all subsequent work on achievable global acoustic noise reduction.

Nevanlinna-Pick interpolation was explained and an algorithm to solve the tall model-matching problem was presented. An assumption of the algorithm is that T_2 not have any repeated right half plane zeros or finite imaginary axis zeros. As we saw in Chapter 6, this restricts our choices of sensor, actuator, and performance point locations. In addition, it is surprising that T_2 does not have any imaginary axis zeros since $\tilde{T}_2$ does. A logical extension of the algorithm would be to incorporate the two special cases: when there are imaginary axis zeros and when there are repeated right half plane zeros. This should make the algorithm less sensitive to point locations.

We studied the solution of the global noise reduction problem using feedback and feedforward design. Various configurations of the actuator, the sensor, and the observation points were considered, and recommendations for the optimal placement of the points were made. We found that noise may be reduced at a number of points in the duct to a level comparable to noise reduction at a single point. We also found

that linear splines allow for greater freedom in the placement of observation points with respect to the sensor and actuator locations.

It would be interesting to calculate the optimal controller and then to use this controller to determine if noise reduction at a number of points results in noise elevation between these points. If so, would it help to use more than one actuator and sensor to reduce noise everywhere in the duct to an arbitrarily small level?

In addition, there are several other point placements that would be interesting to investigate. For example, what is the effect of collocated sensor, actuator, and observation points on the achievable level of noise reduction? Rather than considering a uniform distribution of observation points throughout the duct, should these points be placed close together as well as close to the sensor to "block out" the disturbance wave past a certain point? The answer to these and other questions is the subject of future research.

Appendix A

State-Space Calculations

In this appendix, we consider the implementation of the algorithm given in Section 5.5. The problem is challenging numerically because of the complexity of the algorithm and because of the size of the problem, since we are considering a "tall" problem. A few of the most difficult numerical aspects of the algorithm will be considered in this appendix. We begin by looking at the various factorizations required and conclude with several useful numerical "tricks". All calculations are performed with the state-space realization

$$G(s) := [A, B, C, D] := \left[\begin{array}{c|c} A & B \\ \hline C & D \end{array}\right].$$

A.1 Factorizations

We will consider the cases where we need to perform one of the following factorizations:

(i) inner/outer factorization (IOF),

(ii) right and left coprime factorizations (RCF and LCF),

(iii) complementary inner factorization (CIF), and

(iv) spectral factorization (SF).

The details of these factorizations can be found in [CD84]. Let $G(s)$ have a stabilizable/detectable minimal realization. As we shall see in the following sections, the algebraic Riccati equation plays a crucial role in obtaining each of the above named factorizations. Each of these factorizations requires the solution of either one or two algebraic Riccati equations.

A.1.1 Inner/Outer Factorizations (IOF)

An inner/outer factorization for $G(s)$ is

$$G(s) = N(s)M^{-1}(s)$$

where M is outer and a unit (i.e., $M,\ M^{-1} \in H_\infty$), $N(s)$ is inner, and

$$N(s) := \left[\begin{array}{c|c} A_{in} & B_{in} \\ \hline C_{in} & D_{in} \end{array}\right] := \left[\begin{array}{c|c} A - BK & BR^{-1/2} \\ \hline C - DK & DR^{-1/2} \end{array}\right], \tag{A.1}$$

$$M(s) := \left[\begin{array}{c|c} A_{out} & B_{out} \\ \hline C_{out} & D_{out} \end{array}\right] := \left[\begin{array}{c|c} A - BK & BR^{-1/2} \\ \hline -K & R^{-1/2} \end{array}\right]. \tag{A.2}$$

Here $R = D^TD > 0$, $K = R^{-1}(B^T\Pi_{iof} + D^TC)$ and $\Pi_{iof} \geq 0$ solves the Riccati equation

$$(A - BR^{-1}D^TC)^T\Pi_{iof} + \Pi_{iof}(A - BR^{-1}D^TC) - \Pi_{iof}BR^{-1}B^T\Pi_{iof} + C^TD_\perp D_\perp^TC = 0 \tag{A.3}$$

where $D_\perp$ is the orthogonal complement of D. This method only applies to non-strictly proper transfer functions. However, in the algorithm, we need an IOF of T_2, where T_2 is strictly proper. Thus, we must use the "relative degree" trick, i.e., find k such that $\hat{T}_2 = T_2(s+a)^k$ is proper. To preserve equality, $(s+a)^{-k}$, is absorbed into the Youla parameter. The details are in Section A.2.

A.1.2 Right and Left Coprime Factorizations (RCF and LCF)

A right coprime factorization for $G(s)$ is

$$G(s) = N(s)M^{-1}(s)$$

where

$$N(s) := \left[\begin{array}{c|c} A-BK & B \\ \hline C-DK & D \end{array}\right]$$

and

$$M(s) := \left[\begin{array}{c|c} A-BK & B \\ \hline -K & I \end{array}\right].$$

The gain K is chosen so that $A-BK$ is Hurwitz. Finding the left coprime factorization is the dual problem of finding the right coprime factorization.

To find $\tilde{D}_i$ and V in (5.19), we use the following result.

Theorem A.1 *[Mac89, p.320]*

Suppose that G has a minimal realization $G := [A, B, C, D]$. If $\tilde{N}$ and $\tilde{M}$ have realizations

$$\tilde{N} := [A+HC, B+HD, C, D]$$
$$\tilde{M} := [A+HC, -H, C, -I]$$

where $H = -XC^T$ *and* X *is the stabilizing solution of the Riccati equation*

$$AX + XA^T - XC^TCX = 0.$$

Then $G = \tilde{M}^{-1}\tilde{N}$ *and* $\tilde{M}\tilde{M}^* = I$ *(i.e.,* $\tilde{M}$ *is inner).*

Thus, in the above factorizations, we make the substitutions,

$$\tilde{M} \to \tilde{D}_i$$
$$\tilde{N} \to V.$$

That is, to find the LCF and IOF of AL, consider the following. We know from Theorem A.1 that $AL = \tilde{M}^{-1}\tilde{N}$ where $\tilde{M}$ is inner. So,

$$\begin{aligned} \|AL - Q\|_\infty &= \|\tilde{M}^{-1}\tilde{N} - Q\|_\infty \\ &= \|\tilde{M}(\tilde{M}^{-1}\tilde{N} - Q)\|_\infty \\ &= \|\tilde{N} - \tilde{M}Q\|_\infty \end{aligned}$$

since AL is SISO and $\tilde{M}$ is inner.

A.1.3 Complementary Inner Factorizations (CIF)

Recall from Definition 5.3 that a CIF is defined to be a matrix $\Theta \in RH_\infty^{m\times(m-l)}$ such that for $T_{2_i} \in RH_\infty^{m\times l}$ inner,

$$\Phi = \begin{bmatrix} T_{2_i} & \Theta \end{bmatrix}$$

is square and inner. Thus, using the above state-space representation for the inner factor (see (A.1)) we have the following.

Let Π_p be a pseudo-left inverse of Π_{iof} where Π_{iof} is the solution to (A.3). Then a CIF for $G(s)$ is given by

$$G_{cif}(s) = \left[\begin{array}{c|c} A_{in} & -\Pi_p C^T D_\perp \\ \hline C_{in} & D_\perp \end{array}\right] \tag{A.4}$$

where A_{in} and B_{in} are given in (A.1). Thus, to find a CIF for T_{2_i} we need a state-space representation for T_{2_i}

$$T_{2_i} = [A_{in}, B_{in}, C_{in}, D_{in}].$$

Then Θ is given by (A.4).

A.1.4 Spectral Factorizations (SF)

Let

$$G(s) := [A, B, C, D]$$

be a stabilizable realization of $G(s) \in RL_\infty^{p\times m}$. We would like to compute a left spectral factor $M(s)$ such that

$$M^*(s)M(s) = \mu^2 - G^*(s)G(s)$$

where $\|G\|_\infty < \mu$ and

$$M(s) := [A_m, B_m, C_m, D_m]$$

is a unit in $RH_\infty^{m\times m}$. A realization is

$$M(s) := \left[\begin{array}{c|c} A - K_f K_c & B - K_f \\ \hline R^{1/2}K_c & R^{1/2} \end{array}\right]$$

where

$$\begin{aligned} R &= \mu^2 I - D^T D > 0, \\ K_c &= R^{-1}(B^T\Pi_1 - D^T D), \\ K_f &= \Pi_2 K_c^T R, \end{aligned}$$

Π_1 is the solution to the Riccati equation

$$(A+BR^{-1}D^TC)^T\Pi_1+\Pi_1(A+BR^{-1}D^TC)-\Pi_1(BR^{-1}B^T)\Pi_1+C^T(I+DR^{-1}D^T)C = 0,$$

and Π_2 is the solution to the Riccati equation

$$A^T\Pi_2 + \Pi_2 A - \Pi_2 K_c^T R K_c = 0.$$

A.2 Relative Degree

To find the IOF and CIF of T_2 using the Riccati solution (see Section A.1.1), T_2 must be proper, not strictly. However, T_2 is strictly proper. To circumvent this problem, we find a positive integer k such that $\hat{T}_2 = T_2(s+a)^k$, where $a > 0$, is non-strictly proper. This k is called the *relative degree*. Let $\hat{T}_2 = \hat{T}_{2_i}\hat{T}_{2_o}$ be an IOF. Then

$$\begin{aligned} T_2 &= \hat{T}_2(s+a)^{-k} \\ &= \hat{T}_{2_i}\hat{T}_{2_o}(s+a)^{-k} \\ &= T_{2_i}T_{2_o} \end{aligned}$$

where

$$\begin{aligned} T_{2_i} &= \hat{T}_{2_i} \\ T_{2_o} &= \hat{T}_{2_o}(s+a)^{-k} \end{aligned}$$

and

$$\begin{aligned} T_1T_2Q &= T_1 - T_{2_i}T_{2_o}Q \\ &= T_1 - T_{2_i}\bar{Q} \end{aligned}$$

where $\bar{Q} = T_{2_o}Q \in H_\infty$. We, however, also need the state-space representation of $\hat{T}_2$.

Let the following be a minimal realization of a strictly proper transfer function $F(s)$:

$$\begin{aligned} F(s) &= C(sI-A)^{-1}B \\ &:= [A,B,C,0]. \end{aligned}$$

Then

$$\begin{aligned} sF(s) &= CsI(sI-A)^{-1}B \\ &= C(sI-A)(sI-A)^{-1}B + CA(sI-A)^{-1}B \\ &= CB + CA(sI-A)^{-1}B \end{aligned}$$

and

$$aF(s) = Ca(sI-A)^{-1}B.$$

So,

$$\begin{aligned} F(s)(s+a) &= C(A+aI)(sI-A)^{-1}B + CB \\ &:= [A, B, C(A+aI), CB] \end{aligned}$$

which is non-strictly proper if $CB \neq 0$. In this case, the relative degree is one. If $CB = 0$, we continue. Assume $CB = 0$. We need to determine what the state-space representation for $F(s)(s+a)^2$ is. Thus,

$$\begin{aligned} F(s)(s+a)s &= C(A+aI)s(sI-a)^{-1}B \\ &= C(A+aI)(sI-A)(sI-A)^{-1}B + C(A+aI)A(sI-A)^{-1}B \\ &= C(A+aI)B + C(A+aI)A(sI-A)^{-1}B \end{aligned}$$

and

$$F(s)(s+a)a = Ca(A+aI)(sI-A)^{-1}B.$$

So

$$\begin{aligned} F(s)(s+a)^2 &= C(A+aI)^2(sI-A)^{-1}B + C(A+aI)B \\ &:= [A, B, C(A+aI)^2, C(A+aI)B]. \end{aligned}$$

Hence, if $C(A+aI)B \neq 0$, the relative degree is two. In general, we have the following result which can be proven by induction.

Theorem A.2

Let

$$F(s) := [A, B, C, 0]$$

be a minimal state-space realization. Let $n \in \mathbb{N}$ and $a \in \mathbb{R}$. Then if F has relative degree $N \geq n$,

$$F(s)(s+a)^n := [A, B, C(A+aI)^n, C(A+aI)^{n-1}B]. \tag{A.5}$$

A.3 Computing $\|G\|_\infty$

In the algorithm, the H_∞ norm (or L_∞ norm) provides an upper and lower bound on the achievable noise reduction. For this reason, we must have a reliable method for computing these values.

Let $G := [A, B, C, D]$. If A is Hurwitz,

$$\|G\|_\infty = \sup_{Re(s)>0} \sigma_{max}(G(s))$$

where σ_{max} is the maximum singular value, i.e.,

$$\sigma_{max}(G) = \lambda_{max}^{1/2}(G^*G).$$

If $G \in L_\infty$,

$$\|G\|_\infty = \sup_{w\in\mathbf{R}} \sigma_{max}(G(jw)).$$

So in particular, if A is Hurwitz, the L_∞ norm is the H_∞ norm. Let

$$H_\gamma := \begin{bmatrix} A - BR^{-1}D^TC & -\gamma BR^{-1}B^T \\ \gamma C^TS^{-1}C & -A^T + C^TDR^{-1}B^T \end{bmatrix}$$

where $R = D^TD - \gamma^2 I$, $S = DD^T - \gamma^2 I$ and H_γ is the Hamiltonian matrix, i.e.,

$$J^{-1}H_\gamma J = -H_\gamma^T$$

where

$$J = \begin{bmatrix} 0 & I \\ -I & 0 \end{bmatrix}.$$

Theorem A.3 *[BBK89]*

Assume A has no imaginary axis eigenvalues, $\gamma > 0$ is not a singular value of D, and $w_0 \in \mathbb{R}$. Then γ is a singular value of $G(jw_0)$ if and only if $(H_\gamma - jw_0 I)$ is singular.

Theorem A.4 *[BBK89]*

Let A be Hurwitz and $\gamma > \sigma_{max}(D)$. Then $\|G\|_\infty \geq \gamma$ if and only if H_γ has imaginary axis eigenvalues, i.e., $\|G\|_\infty < \gamma$ if and only if H_γ has no eigenvalues on the imaginary axis.

Remarks:

(1) Theorem A.4 suggests a bisection method for computing $\|G\|_\infty$.

(2) If A is not Hurwitz, but has no $jw-$axis eigenvalues, then Theorem A.4 remains true with the H_∞ norm replaced by the L_∞ norm:

$$\|G\|_{L_\infty} = \sup_{w \in \mathbf{R}} \sigma_{max}(G(jw)).$$

Appendix B

Program Listings

In this appendix, the Matlab routines used to solve the acoustic noise reduction problem in the one-dimensional duct are given.

B.1 Main Source Code

B.1.1 Legendre Polynomials

```
function [gamma_opt,x,xs,xa,xd,nn]=mimo(x,xs,xa,xd);
%  function [gamma_opt,x,xs,xa,xd,nn]=mimo(x,xs,xa,xd);
%  October, 1997
%  Janet R. Grad
%  Matlab code to run the frequency domain algorithm on the
%  MIMO system.
%  x is varied over all values between 0 and L
% (global noise reduction).
%  gamma_opt = \inf_{Q \in {\cal H}_{\infty} } \| T1 - T2*Q \| where
%  T1=W1*G(x,xd)
%  T2=W1*G(x,xa)*G(xs,xd)
%  xs = sensor location
%  xa = actuator location
%  xd = disturbance location
%  x = global location
```

```
%  n = number of Legendre polynomials used in approximation
format long
tcpu=cputime;
value=now;
disp('the time of day is....')
date
[hour(value) minute(value) second(value)]
%  input standards
disp('standards:  input standards (L,c,rho,...)')
[L,c,rho,K,alpha,Aw,Bw,Cw,Dw]=standards(1);
n=25;
j_star_tol=0.01
gam_tol=0.005
%  ************************************************************
%  ************************************************************
disp('t1t2_mimo:  form ss reps for T1 and T2')
[At1,Bt1,Ct1,Dt1,At2,Bt2,Ct2,Dt2]=...
   t1t2_mimo_x(n,x,xs,xa,xd,c,L,rho,K,Aw,Bw,Cw,Dw);
%  the relative degree should be the same for all n
%  given some set of x
if norm(Dt2)<0.1,
   a=10;
%  determine the relative degree of T2 (strictly proper)
   disp('relative_degree:  determine the relative degree of T2')
   [rel_deg]=relative_degree(At2,Bt2,Ct2,Dt2,a)
   [At2_hat,Bt2_hat,Ct2_hat,Dt2_hat,scale]=T2_hat(At2,Bt2,Ct2,...
      Dt2,a,rel_deg);
else
   At2_hat=At2;
   Bt2_hat=Bt2;
   Ct2_hat=Ct2;
   Dt2_hat=Dt2;
   rel_deg=0;
end
%  perform the IOF/CIF of T2_hat
%  (s+a)^(reg_deg) is absorbed into the outer part
disp('iof:  find the IOF and CIF of T2_hat')
[At2_hat_in,Bt2_hat_in,Ct2_hat_in,Dt2_hat_in,...
     At2_hat_cif,Bt2_hat_cif,Ct2_hat_cif,Dt2_hat_cif,junk,...
     junk,junk,junk]=iof(At2_hat,Bt2_hat,Ct2_hat,Dt2_hat);
%  find Phi
disp('phi:  find Phi and Phi^*')
[Aphi,Bphi,Cphi,Dphi,Aphi_star,Bphi_star,Cphi_star,Dphi_star]=...
     phi(At2_hat_in,Bt2_hat_in,Ct2_hat_in,Dt2_hat_in,...
         At2_hat_cif,Bt2_hat_cif,Ct2_hat_cif,Dt2_hat_cif);
```

```
% find (Phi^*)(T1)
disp('phi_star_t1:  find (Phi^*)(T1)')
[Ap,Bp,Cp,Dp]=phi_star_t1(Aphi_star,Bphi_star,...
                          Cphi_star,Dphi_star,...
                          At1,Bt1,Ct1,Dt1);

% find A and C
disp('A_C:  find A and C')
[AA,BA,CA,DA,AC,BC,CC,DC]=A_C(Ap,Bp,Cp,Dp);

disp('norm_infty:  find infinity norm of C (lower bound)')
gam_lower=norm_infty_bis(AC,BC,CC,DC);
disp('norm_infty:  find infinity norm of T1 (upper bound)')
gam_upper=norm_infty_bis(At1,Bt1,Ct1,Dt1);

gam=(gam_lower+gam_upper)/2;
iflag=0;
icount=0;
max_count=20;
counter=zeros(max_count,1);
gam_cur=zeros(max_count,1);
j_star_cur=zeros(max_count,1);

% ************************************************************
while iflag==0 & icount<max_count,

icount=icount+1
gam_lower
gam_upper
gam

% find L
disp('L_function:  find L')
[AL,BL,CL,DL]=L_function(AC,BC,CC,DC,gam);

% find (A)(L)
disp('A_L:  find AL')
[A_al,B_al,C_al,D_al]=A_L(AA,BA,CA,DA,AL,BL,CL,DL);

% find j_star
disp('j_star:  find j_star')
[j_star_val]=j_star(A_al,B_al,C_al,D_al);

gam_cur(icount,:)=gam;

if j_star_val==[],
   iflag=1;
   j_star_opt=999;
   gamma_opt=gam_upper;
end
if iflag==0,
   disp('gam_upper-gam_lower')
   gam_upper-gam_lower
   if ((gam_upper-gam_lower)/gam)<gam_tol | ...
       ( j_star_val<1 & (1-j_star_val)<j_star_tol),
      gamma_opt_upper=gam_upper;
      gamma_opt_lower=gam_lower;
```

```
      if j_star_val<=1,
         gamma_opt=gam;
      else
         gamma_opt=gam_upper;
      end
      j_star_opt=j_star_val;
      iflag=1
   else
      if j_star_val>1,
         disp('go bigger')
         gam_lower=gam;
         gam=(gam_upper+gam)/2;
      elseif j_star_val<1,
         disp('go smaller')
         gam_upper=gam;
         gam=(gam+gam_lower)/2;
      end
   end
end

if abs(j_star_val-gam)<0.05 & iflag<1,
   disp('offset the gamma to make it different from j_star')
   gam=gam+(gam_upper-gam)/4;
end

counter(icount,:)=icount;
j_star_cur(icount,:)=j_star_val;

disp(' *** counter *** gamma *** j_star *** ')
[counter(1:icount,:) gam_cur(1:icount,:) j_star_cur(1:icount,:)]
disp('*************************************************************')

end
%  ****************************************************************

if icount==max_count,
   gamma_opt_upper=gam_upper;
   gamma_opt_lower=gam_lower;
   if j_star_val<=1,
      gamma_opt=gam;
   else
      gamma_opt=gam_upper;
   end
end
clear counter gam_cur j_star_cur
counter=zeros(max_count,1);
gam_cur=zeros(max_count,1);
j_star_cur=zeros(max_count,1);

gu=gamma_opt_upper;
gl=gamma_opt_lower;

%  ****************************************************************
%  ****************************************************************

value=now;
disp('the time of day is....')
date
```

```
[hour(value) minute(value) second(value)]
Tcpu=cputime-tcpu
```

B.1.2 Linear Splines

```
function [gamma_opt,x,xs,xa,xd,nn]=mimo(x,xs,xa,xd);
%  function [gamma_opt,x,xs,xa,xd,nn]=mimo(x,xs,xa,xd);
%  October, 1997
%  Janet R. Grad
%  Matlab code to run the frequency domain algorithm
%  on the MIMO system.
%  x is varied over all values between 0 and L
%  (global noise reduction).
%  gamma_opt = \inf_{Q \in {\cal H}_{\infty} } \| T1 - T2*Q \|
%  where
%  T1=W1*G(x,xd)
%  T2=W1*G(x,xa)*G(xs,xd)
%  xs = sensor location
%  xa = actuator location
%  xd = disturbance location
%  x = global location
%  n = number of linear splines used in approximation
format long
tcpu=cputime;
value=now;
disp('the time of day is....')
date
[hour(value) minute(value) second(value)]
%  input standards
disp('standards:  input standards (L,c,rho,...)')
[L,c,rho,K,alpha,Aw,Bw,Cw,Dw]=standards(1);
n=15;
j_star_tol=0.01
gam_tol=0.005
%  ************************************************************
%  ************************************************************
disp('t1t2_mimo:  form ss reps for T1 and T2')
[At1,Bt1,Ct1,Dt1,At2,Bt2,Ct2,Dt2]=...
   t1t2_mimo_x_linspl(n,x,xs,xa,xd,c,L,rho,K,Aw,Bw,Cw,Dw);
%  the relative degree should be the same for all n
%  given some set of x
if norm(Dt2)<0.1,
```

```
   a=10;
%  determine the relative degree of T2 (strictly proper)
   disp('relative_degree:  determine the relative degree of T2')
   [rel_deg]=relative_degree(At2,Bt2,Ct2,Dt2,a)
   disp('T2_hat:  form a 4pts_a non-strictly proper T2')
   [At2_hat,Bt2_hat,Ct2_hat,Dt2_hat,scale]=...
      T2_hat_linspl(At2,Bt2,Ct2,Dt2,a,rel_deg);
   else
      At2_hat=At2;
      Bt2_hat=Bt2;
      Ct2_hat=Ct2;
      Dt2_hat=Dt2;
      rel_deg=0;
   end

%  perform the IOF/CIF of T2_hat
%  (s+a)^(reg_deg) is absorbed into the outer part
disp('iof:  find the IOF and CIF of T2_hat')
[At2_hat_in,Bt2_hat_in,Ct2_hat_in,Dt2_hat_in,...
     At2_hat_cif,Bt2_hat_cif,Ct2_hat_cif,Dt2_hat_cif,junk,...
     junk,junk,junk]=iof_linspl(At2_hat,Bt2_hat,Ct2_hat,Dt2_hat);

%  find Phi
disp('phi:  find Phi and Phi^*')
[Aphi,Bphi,Cphi,Dphi,Aphi_star,Bphi_star,Cphi_star,Dphi_star]=...
     phi(At2_hat_in,Bt2_hat_in,Ct2_hat_in,Dt2_hat_in,...
         At2_hat_cif,Bt2_hat_cif,Ct2_hat_cif,Dt2_hat_cif);

%  find (Phi^*)(T1)
disp('phi_star_t1:  find (Phi^*)(T1)')
[Ap,Bp,Cp,Dp]=phi_star_t1(Aphi_star,Bphi_star,...
                          Cphi_star,Dphi_star,...
                          At1,Bt1,Ct1,Dt1);

%  find A and C
disp('A_C:  find A and C')
[AA,BA,CA,DA,AC,BC,CC,DC]=A_C(Ap,Bp,Cp,Dp);

disp('norm_infty:  find infinity norm of C (lower bound)')
gam_lower=norm_infty_bis(AC,BC,CC,DC);
disp('norm_infty:  find infinity norm of T1 (upper bound)')
gam_upper=norm_infty_bis(At1,Bt1,Ct1,Dt1);

gam=(gam_lower+gam_upper)/2;
iflag=0;
icount=0;
max_count=20;
counter=zeros(max_count,1);
gam_cur=zeros(max_count,1);
j_star_cur=zeros(max_count,1);

%  ***************************************************************
while iflag==0 & icount<max_count,

icount=icount+1
```

```
gam_lower
gam_upper
gam

%  find L
disp('L_function:  find L')
[AL,BL,CL,DL]=L_function(AC,BC,CC,DC,gam);

%  find (A)(L)
disp('A_L:  find AL')
[A_al,B_al,C_al,D_al]=A_L(AA,BA,CA,DA,AL,BL,CL,DL);

%  find j_star
disp('j_star:  find j_star')
[j_star_val]=j_star(A_al,B_al,C_al,D_al);

gam_cur(icount,:)=gam;

if j_star_val==[],
   iflag=1;
   j_star_opt=999;
   gamma_opt=gam_upper;
end
if iflag==0,
   disp('gam_upper-gam_lower')
   gam_upper-gam_lower
   if ((gam_upper-gam_lower)/gam)<gam_tol | ...
       ( j_star_val<1 & (1-j_star_val)<j_star_tol),
      gamma_opt_upper=gam_upper;
      gamma_opt_lower=gam_lower;
      if j_star_val<=1,
         gamma_opt=gam;
      else
         gamma_opt=gam_upper;
      end
      j_star_opt=j_star_val;
      iflag=1
   else
      if j_star_val>1,
         disp('go bigger')
         gam_lower=gam;
         gam=(gam_upper+gam)/2;
      elseif j_star_val<1,
         disp('go smaller')
         gam_upper=gam;
         gam=(gam+gam_lower)/2;
      end
   end
end

if abs(j_star_val-gam)<0.05 & iflag<1,
   disp('offset the gamma to make it different from j_star')
   gam=gam+(gam_upper-gam)/4;
end

counter(icount,:)=icount;
```

```
j_star_cur(icount,:)=j_star_val;
disp(' *** counter *** gamma *** j_star *** ')
[counter(1:icount,:) gam_cur(1:icount,:) j_star_cur(1:icount,:)]
disp('*****************************************************')
end
%  ****************************************************************
if icount==max_count,
   gamma_opt_upper=gam_upper;
   gamma_opt_lower=gam_lower;
   if j_star_val<=1,
      gamma_opt=gam;
   else
      gamma_opt=gam_upper;
   end
end
clear counter gam_cur j_star_cur
counter=zeros(max_count,1);
gam_cur=zeros(max_count,1);
j_star_cur=zeros(max_count,1);
gu=gamma_opt_upper;
gl=gamma_opt_lower;
%  ************************************************************
%  ************************************************************
value=now;
disp('the time of day is....')
date
[hour(value) minute(value) second(value)]
Tcpu=cputime-tcpu
```

B.2 Sub-Routines

B.2.1 standards.m

```
function [L,c,rho,K,alpha,Aw,Bw,Cw,Dw]=standards(dummy);
%  function [L,c,rho,K,alpha,num_w,den_w]=standards(dummy);
%  standard values
%  October, 1997
%  Janet R. Grad
%  constants are for dry air (see Tipler)
L=4;  % length of duct
c=331;  %  speed of sound
rho=1.29;  %  density of air
%  set up the range of frequencies we wish to consider
w_last=6300;
```

```
w=[0.000001:1:w_last];
w_size=max(size(w));
K=0.7;  % impedence for boundary condition at x=L
alpha=(1+K)/(1-K);
num_w=1;  % numerator of the weight
den_w=[1/1000 1];  % denominator of the weight
[Aw,Bw,Cw,Dw]=tf2ss(num_w,den_w);
```

B.2.2 t1t2_mimo_x.m

```
function [AT1,BT1,CT1,DT1,AT2,BT2,CT2,DT2]=...
   t1t2_mimo_x(n,x,xs,xa,xd,c,L,rho,K,Aw,Bw,Cw,Dw);
%function [AT1,BT1,CT1,DT1,AT2,BT2,CT2,DT2]=...
%   t1t2_mimo(n,x,xs,xa,xd,c,L,rho,K,Aw,Bw,Cw,Dw);
%  October, 1997
%  Janet  R. Grad
%  form the statespace representation of T1 and T2
%  x-pts: ... output/input
%  x varies over some set;  xs, xd, and xa are constant
AT1=[];
BT1=[];
CT1=[];
DT1=[];
AT2=[];
BT2=[];
CT2=[];
DT2=[];
x_len=length(x);
xs_len=length(xs);
xd_len=length(xd);
xa_len=length(xa);
%  ********************************************************
%  form T1
for ii=1:x_len,
   [At1,Bt1,Ct1,Dt1]=ss(n,L,c,K,rho,x(ii),xd);
   CT1(ii,:)=Ct1;
   DT1(ii,1)=Dt1;
end
AT1=At1;
BT1=Bt1;
%  put W1 in series with G(x,xd)
[n1,n2]=size(AT1);
[n3,n4]=size(Aw);
```

```
AT1=[AT1 BT1*Cw; zeros(n3,n2) Aw];
BT1=[BT1*Dw; Bw];
CT1=[CT1 DT1*Cw];
DT1=DT1*Dw;

%  ********************************************************
%  form T2

[A,B,C,D]=ss(n,L,c,K,rho,xs,xd);
[A,B,C,D]=series(Aw,Bw,Cw,Dw,A,B,C,D);

%  x changes the output C (and D)
%  B stays the same

for ii=1:x_len,
   [At2,Bt2,Ct2,Dt2]=ss(n,L,c,K,rho,x(ii),xa);
   CT2(ii,:)=Ct2;
   DT2(ii,1)=Dt2;
end
AT2=At2;
BT2=Bt2;

% put in series
[n1,n2]=size(AT2);
[n3,n4]=size(A);

AT2=[AT2 BT2*C; zeros(n3,n2) A];
BT2=[BT2*D; B];
CT2=[CT2 DT2*C];
DT2=DT2*D;

[AT1,BT1,CT1,DT1]=mymodred(AT1,BT1,CT1,DT1,10^(-5));
[AT2,BT2,CT2,DT2]=mymodred(AT2,BT2,CT2,DT2,10^(-5));
if norm(DT1)<10^(-5),
  DT1=zeros(size(DT1));
end
if norm(DT2)<10^(-5),
  DT2=zeros(size(DT2));
end
```

B.2.3 t1t2_mimo_x_linspl.m

```
function [AT1,BT1,CT1,DT1,AT2,BT2,CT2,DT2]=...
   t1t2_mimo_x_linspl(n,x,xs,xa,xd,c,L,rho,K,Aw,Bw,Cw,Dw);
%function [AT1,BT1,CT1,DT1,AT2,BT2,CT2,DT2]=...
%   t1t2_mimo(n,x,xs,xa,xd,c,L,rho,K,Aw,Bw,Cw,Dw);

%  October, 1997
%  Janet R. Grad

%  form the statespace representation of T1 and T2
%  x-pts: ... output/input

%  x varies over some set;  xs, xd, and xa are constant
```

```
AT1=[];
BT1=[];
CT1=[];
DT1=[];
AT2=[];
BT2=[];
CT2=[];
DT2=[];
x_len=length(x);
xs_len=length(xs);
xd_len=length(xd);
xa_len=length(xa);
%  ********************************************************
%  form T1
for ii=1:x_len,
   [At1,Bt1,Ct1,Dt1]=ss_splines(n,L,c,K,rho,x(ii),xd);
   CT1(ii,:)=Ct1;
   DT1(ii,1)=Dt1;
end
AT1=At1;
BT1=Bt1;
%  put W1 in series with G(x,xd)
[n1,n2]=size(AT1);
[n3,n4]=size(Aw);
AT1=[AT1 BT1*Cw; zeros(n3,n2) Aw];
BT1=[BT1*Dw; Bw];
CT1=[CT1 DT1*Cw];
DT1=DT1*Dw;
%  ********************************************************
%  form T2
[A,B,C,D]=ss_splines(n,L,c,K,rho,xs,xd);
[A,B,C,D]=series(Aw,Bw,Cw,Dw,A,B,C,D);
%  x changes the output C (and D)
%  B stays the same
for ii=1:x_len,
   [At2,Bt2,Ct2,Dt2]=ss_splines(n,L,c,K,rho,x(ii),xa);
   CT2(ii,:)=Ct2;
   DT2(ii,1)=Dt2;
end
AT2=At2;
BT2=Bt2;
% put in series
[n1,n2]=size(AT2);
[n3,n4]=size(A);
AT2=[AT2 BT2*C; zeros(n3,n2) A];
BT2=[BT2*D; B];
```

```
CT2=[CT2 DT2*C];
DT2=DT2*D;

[AT1,BT1,CT1,DT1]=mymodred(AT1,BT1,CT1,DT1,10^(-5));
[AT2,BT2,CT2,DT2]=mymodred(AT2,BT2,CT2,DT2,10^(-5));
if norm(DT1)<10^(-5),
  DT1=zeros(size(DT1));
end
if norm(DT2)<10^(-5),
  DT2=zeros(size(DT2));
end
```

B.2.4 ss.m (Legendre)

```
function [aa,bb,cc,dd]=ss(n,L,c,K,rho,x1,x2);
%function [aa,bb,cc,dd]=ss(n,L,c,K,rho,x1,x2);

%  October, 1997
%  Janet R. Grad

%  Form the state-space reps using Legendre polynomials.

m=n+1;

M=zeros(m,m);
for i=1:m,
   M(i,i)=L/(2*i-1);
end
G1_test=zeros(n,n);
s=0;
for i=1:n,
   s=s+i;
   G1_test(i,i)=s;
end
stuff=diag(G1_test);
for i=3:2:n,
count=0;
for j=1:n-i+1,
   G1_test(i+count,j)=stuff(j);
   count=count+1;
end
end
G1_test=G1_test+G1_test.'-diag(diag(G1_test));
G1=zeros(1:m,1:m);
G1(2:m,2:m)=G1_test;

D1=ones(m,m);

for i=1:m,
   F2(i)=leg(i-1,x2,L);
end
F2=F2.';

for i=1:m,
   C1(i)=leg_diff(i-1,x1,L);
```

```
end

aa=zeros(2*m,2*m);
aa(1:m,m+1:2*m)=eye(m,m);

aa(m+1:2*m,1:m)=-c^2*M^(-1/2)*G1*M^(-1/2);
aa(m+1:2*m,m+1:2*m)=-K*c*M^(-1/2)*D1*M^(-1/2);

bb=zeros(2*m,1);
cc=zeros(1,2*m);

bb(m+1:2*m,1)=M^(-1/2)*F2/rho;

cc(1,1:m)=-rho*c^2*C1*M^(-1/2);
dd=0;

%  Find the stable part only since we know the
%  approximations are stable.
%  This gets rid of the unstable pole/zero at s=0.
[aa,bb,cc,dd,junk,junk,junk,junk,junk]=stabproj(aa,bb,cc,dd);
```

B.2.5 ss_splines.m (linear splines)

```
function [AA,BB,CC,DD]=ss_splines(n,L,c,K,rho,x1,x2);
%function [AA,BB,CC,DD]=ss_splines(n,L,c,K,rho,x1,x2);

%  October, 1997
%  Janet R. Grad

%  Form the state-space reps using linear splines.
format long

[M,G,D]= mats_linspl(n,L);

G2=c^2*G;
D2=c*K*D;

procread('Bmatrix_linear.src');
maple('Bmatrix_linear',n,L,x2);
F=numeric(ans);
F2=(1/rho)*F;
F2=F2';

aa=zeros(2*(n+1),2*(n+1));
aa(1:n+1,n+2:2*(n+1))=eye(n+1,n+1);
aa(n+2:2*(n+1),1:n+1)=-inv(M)*G2;
aa(n+2:2*(n+1),n+2:2*(n+1))=-inv(M)*D2;

bb=zeros(2*(n+1),1);
bb(n+2:2*(n+1),1)=inv(M)*F2;

procread('Cmatrix_linear.src');
maple('Cmatrix_linear',n,L,x1);
C_tilde=-rho*c^2*numeric(ans);
```

```
C_tilde(1,n+2:2*(n+1))=zeros(1,n+1);
cc=C_tilde;
dd=0;
[AA,BB,CC,DD]=minreal(aa,bb,cc,dd);
if any(real(eig(AA))>0),
   disp('A is unstable')
   max(real(eig(AA)))
else
   disp('A is stable')
end
```

B.2.6 mats_linspl.m (linear splines)

```
function [m,g,d]=mats_linspl(n,L);
%function [m,g,d]=mats_linspl(n,L);
%  October, 1997
%  Janet R. Grad
%  Form the matrices used in the state-space rep
%  for linear splines.
m=zeros(n+1,n+1);
m=diag(2/3*ones(1,n+1))+...
  diag(1/6*ones(1,n),-1)+...
  diag(1/6*ones(1,n),1);
m(1,1)=1/3;
m(n+1,n+1)=1/3;
m=(L/n)*m;
g=zeros(n+1,n+1);
g=diag(2*ones(1,n+1))+diag(-ones(1,n),-1)+diag(-ones(1,n),1);
g(1,1)=1;
g(n+1,n+1)=1;
g=g*(n/L);
d=zeros(n+1,n+1);
d(n+1,n+1)=1;
```

B.2.7 relative_degree.m

```
function [rel_deg]=relative_degree(At2,Bt2,Ct2,Dt2,a,tol);
%  function [rel_deg]=relative_degree(At2,Bt2,Ct2,Dt2,a);
%  determine the relative degree
%  October, 1997
%  Janet R. Grad
```

```
count=0;
iflag=0;
if nargin==5,
   tol=0.01;
end
while iflag==0,
count=count+1;
norm(Ct2*(At2+a*eye(length(At2)))^(count-1)*Bt2)
if norm(Ct2*(At2+a*eye(length(At2)))^(count-1)*Bt2)>tol,
   rel_deg=count;
   iflag=1;
end
end
```

B.2.8 T2_hat.m

```
function [At2_hat,Bt2_hat,Ct2_hat,Dt2_hat,scale]=...
      T2_hat(At2,Bt2,Ct2,Dt2,a,rel_deg);
%  function [At2_hat,Bt2_hat,Ct2_hat,Dt2_hat]=...
%       T2_hat(At2,Bt2,Ct2,Dt2,a,rel_deg);
%  October, 1997
%  Janet R. Grad
At2_hat=At2;
Bt2_hat=Bt2;
Ct2_hat=Ct2*( ( At2+a*eye(length(At2)) )^rel_deg );
Dt2_hat=Ct2*( ( At2+a*eye(length(At2)) )^(rel_deg-1))*Bt2;
%  make sure the new system has the same dcgain as the old system
disp('T2_hat:  scaling')
scale=mean(dcgain(At2,Bt2,Ct2,Dt2))/...
      mean(dcgain(At2_hat,Bt2_hat,Ct2_hat,Dt2_hat))
Ct2_hat=Ct2_hat*scale;
Dt2_hat=Dt2_hat*scale;
[At2_hat,Bt2_hat,Ct2_hat,Dt2_hat]=...
   mymodred(At2_hat,Bt2_hat,Ct2_hat,Dt2_hat);
```

B.2.9 T2_hat_linspl.m

```
function [At2_hat,Bt2_hat,Ct2_hat,Dt2_hat,scale]=...
      T2_hat_linspl(At2,Bt2,Ct2,Dt2,a,rel_deg);
%  function [At2_hat,Bt2_hat,Ct2_hat,Dt2_hat]=...
%       T2_hat(At2,Bt2,Ct2,Dt2,a,rel_deg);
```

```
% October, 1997
% Janet R. Grad
At2_hat=At2;
Bt2_hat=Bt2;
Ct2_hat=Ct2*( ( At2+a*eye(length(At2)) )^rel_deg );
Dt2_hat=Ct2*( ( At2+a*eye(length(At2)) )^(rel_deg-1))*Bt2;
% make sure the new system has the same dcgain as the old system
disp('T2_hat:  scaling')
scale=mean(dcgain(At2,Bt2,Ct2,Dt2))/...
      mean(dcgain(At2_hat,Bt2_hat,Ct2_hat,Dt2_hat))
Ct2_hat=Ct2_hat*scale;
Dt2_hat=Dt2_hat*scale;
[At2_hat,Bt2_hat,Ct2_hat,Dt2_hat]=...
   mymodred_linspl(At2_hat,Bt2_hat,Ct2_hat,Dt2_hat);
```

B.2.10 phi.m

```
function [Aphi,Bphi,Cphi,Dphi,Aphi_star,Bphi_star,Cphi_star,...
   Dphi_star]=phi(At2_hat_in,Bt2_hat_in,Ct2_hat_in,Dt2_hat_in,...
   At2_hat_cif,Bt2_hat_cif,Ct2_hat_cif,Dt2_hat_cif);
%function [Aphi,Bphi,Cphi,Dphi,Aphi_star,Bphi_star,Cphi_star,...
%   Dphi_star]=phi(At2_hat_in,Bt2_hat_in,Ct2_hat_in,Dt2_hat_in,...
%   At2_hat_cif,Bt2_hat_cif,Ct2_hat_cif,Dt2_hat_cif);
% October, 1997
% Janet R. Grad
% siso
if (norm(sum(Bt2_hat_cif))<0.001 & ...
    norm(sum(Dt2_hat_cif))<0.001 ) | ...
   (norm(sum(Ct2_hat_cif))<0.001 & ...
    norm(sum(Dt2_hat_cif))<0.001 ),
   Aphi=At2_hat_in;
   Bphi=Bt2_hat_in;
   Cphi=Ct2_hat_in;
   Dphi=Dt2_hat_in;
% mimo
else
   Aphi=At2_hat_in;
   Bphi=[Bt2_hat_in Bt2_hat_cif];
   Cphi=[Ct2_hat_in];
   Dphi=[Dt2_hat_in Dt2_hat_cif];
end
[Aphi,Bphi,Cphi,Dphi]=mymodred(Aphi,Bphi,Cphi,Dphi,10^(-8));
```

```
%  find Phi^*
Aphi_star=-Aphi';
Bphi_star=-Cphi';
Cphi_star=Bphi';
Dphi_star=Dphi';
```

B.2.11 phi_star_t1.m

```
function [AA,BB,CC,DD]=phi_star_t1(Aphi_star,Bphi_star,...
                Cphi_star,Dphi_star,At1,Bt1,Ct1,Dt1);
%function [AA,BB,CC,DD]=phi_star_t1(Aphi_star,Bphi_star,...
%                 Cphi_star,Dphi_star,At1,Bt1,Ct1,Dt1);
%  October, 1997
%  Janet R. Grad
[n1,n2]=size(Aphi_star);
[n3,n4]=size(At1);
AA=[Aphi_star Bphi_star*Ct1; zeros(n3,n2) At1];
BB=[Bphi_star*Dt1; Bt1];
CC=[Cphi_star Dphi_star*Ct1];
DD=Dphi_star*Dt1;
[AA,BB,CC,DD]=mymodred(AA,BB,CC,DD,10^(-8));
```

B.2.12 A_C.m

```
function [a1,b1,c1,d1,a2,b2,c2,d2]=A_C(Ap,Bp,Cp,Dp);
%function [a1,b1,c1,d1,a2,b2,c2,d2]=A_C(Ap,Bp,Cp,Dp);
%  October, 1997
%  Janet R. Grad
%  A is the first row of [Ap Bp Cp Dp]
%  (i.e., the first output and the first input)
%  C is the rest
[m1,m2]=size(Cp);
%  siso
if m1==1,
   a1j=Ap;
   b1j=Bp;
   c1j=Cp;
   d1j=Dp;
   a1=a1j;
   b1=b1j;
   c1=c1j;
```

```
   d1=d1j;

   a2=0;
   b2=0;
   c2=0;
   d2=0;

[a1,b1,c1,d1]=mymodred(a1,b1,c1,d1,10^(-8));

%  mimo
else
   a1j=Ap;
   b1j=Bp;
   c1j=Cp(1,:);
   d1j=Dp(1,:);

   a1=a1j;
   b1=b1j;
   c1=c1j;
   d1=d1j;

   a2j=Ap;
   b2j=Bp;
   [n1,n2]=size(Cp);
   c2j=Cp(2:n1,:);
   [n1,n2]=size(Dp);
   d2j=Dp(2:n1,:);

   a2=a2j;
   b2=b2j;
   c2=c2j;
   d2=d2j;

[a1,b1,c1,d1]=mymodred(a1,b1,c1,d1,10^(-8));
[a2,b2,c2,d2]=mymodred(a2,b2,c2,d2,10^(-8));
end
```

B.2.13 norm_infty_bis.m

```
function [norm_val]=norm_infty_bis(a,b,c,d);
%function [norm_val]=norm_infty_bis(a,b,c,d);

%  October, 1997
%  Janet R. Grad

%  Compute the infinity norm of statespace rep [a b c d].
%  We require a minimal realization.

[a,b,c,d]=myminreal(a,b,c,d);
[n1,n2]=size(a);
if  n1==1 & n2==1 & a==0,
   norm_val=abs(d);
else
```

```
gamma_upper=100;
gamma_lower=0;
gamma_diff=abs(gamma_upper-gamma_lower);
tol=10^(-6);
%  ***************
while gamma_diff>tol,
   gam=(gamma_upper+gamma_lower)/2;
   r=d'*d-gam^2*eye(length(d'*d));
   s=d*d'-gam^2*eye(length(d*d'));
   H=[a-b*inv(r)*d'*c -gam*b*inv(r)*b' ;...
      gam*c'*inv(s)*c  -a'+c'*d*inv(r)*b'];
   ee=eig(H);
   ind=find(abs(real(ee))<10^(-6));
   if isempty(ind)==1,  % no eigenvalues on the imaginary axis
      gamma_upper=gam;
   else                 % eigenvalues on the imaginary axis
      gamma_lower=gam;
   end
   gamma_diff=abs(gamma_upper-gamma_lower);
end
%  ***************
norm_val=gam + (gamma_upper-gamma_lower)/2;
end
```

B.2.14 L_function.m

```
function [AL,BL,CL,DL]=L_function(AC,BC,CC,DC,gam);
%function [AL,BL,CL,DL]=L_function(AC,BC,CC,DC,gam);
%  October, 1997
%  Janet R. Grad
%  siso
[n1,n2]=size(AC);
if n1==1 & n2==1,
   AL=0;
   BL=0;
   CL=0;
   DL=(gam^2-DC^2)^(-1/2);
%  mimo
else
   CC=CC/gam;
   DC=DC/gam;
   [AC,BC,CC,DC]=mymodred(AC,BC,CC,DC,10^(-8));
   [AL,BL,CL,DL]=matlabsfl(AC,BC,CC,DC);
```

```
   CL=CL/gam;
   DL=DL/gam;
end
```

B.2.15 A_L.m

```
function [aa,bb,cc,dd]=A_L(AA,BA,CA,DA,AL,BL,CL,DL);
%function [aa,bb,cc,dd]=A_L(AA,BA,CA,DA,AL,BL,CL,DL);
%  October, 1997
%  Janet R. Grad
[n1,n2]=size(AA);
[n3,n4]=size(AL);
A=[AA BA*CL; zeros(n3,n2) AL];
B=[BA*DL; BL];
C=[CA DA*CL];
D=DA*DL;
[aa,bb,cc,dd]=mymodred(A,B,C,D);
```

B.2.16 j_star.m

```
function [j_star_val]=j_star(a,b,c,d,icount);
%function [j_star_val]=j_star(a,b,c,d);
%  October, 1997
%  Janet R. Grad
%  Compute j_star.m
aric=a;
wric=c'*c;
qric=zeros(length(a));
[P1,P2,lamp,perr,wellposed,x]=myriccati(aric',qric,wric,'schur');
resx=aric*x+x*aric'-x*wric*x+qric;
if norm(resx)>10,
   disp('Warning:  residual of riccati equation in j_star')
   norm(resx)
end
H=-x*c';
An=a+H*c;
Bn=b+H*d;
Cn=c;
Dn=d;
Am=a+H*c;
Bm=-H;
Cm=c;
```

```
Dm=-1;

% In the standard configuration,
% \| AL - Q \| _{\infty} = \| M * ( M^(-1)*N - Q  ) \| _{\infty}
%     = \| N - MQ \| _{\infty}
%  where M is inner  (AL is siso).
flag3=0;
ai=Am;
bi=Bm;
ci=Cm;
di=Dm;
ao=An;
bo=Bn;
co=Cn;
do=Dn;
[ai,bi,ci,di]=mymodred(ai,bi,ci,di);
[ao,bo,co,do]=mymodred(ao,bo,co,do);
%  set up Omega
%  ******************
if length(ai)==0,
   p=0;
   z=0;
   flag2=1;  %  no rhp zeros
   flag3=1;
else
   [p,z]=inner(ai,bi,ci,di);
%  get rid of the repeated rhp zeros case
   z=sort(z);
   ij_count=0;
   for ij=1:length(z),
      if imag(z)>=0,
         ij_count=ij_count+1;
         z_test(ij_count)=z(ij);
      end
   end
   diff_z_test=diff(z_test);
   for ij=1:length(diff_z_test),
      if abs(diff_z_test(ij))<10^(-2),
         flag3=1;
      end
   end
   if flag3==1,
      j_star_val=999;
   end
end
%  ******************
%  ***************************************************************
```

```
if flag3==0,  %  there are no repeated roots
   nz=length(z);
%  check to see if there are any rhp zeros
   if nz==0,
      flag2=1;
      disp('no RHP zeros!')
   else
      flag2=0;  %  go on
   end
%  ************************************************************
   if flag2==0,  %  there are RHP zeros so continue
%  {a} is the rhp zeros of T2
%  enforce what nz is since this tends to get lost somehow
      nz=length(z);
%  evaluate T1 at the rhp zeros of T2 to determine {b}
      size_ao=max(size(ao));
      for i=1:nz,
            b(i)=co*inv(z(i)*eye(size_ao,size_ao)-ao)*bo+do;
      end
%  ************************************************
%  find the Pick matrix
      for i=1:nz,
      for j=1:nz,
         A_tilde(i,j)=(1/(z(i)+conj(z(j))));
         B_tilde(i,j)=((b(i)*conj(b(j)))/(z(i)+conj(z(j))));
      end
      end
      q=diag(schur(A_tilde^(-1/2)*B_tilde*A_tilde^(-1/2)));
      j_star_val=real(sqrt(max(q)));
      P=A_tilde-realpow(j_star_val,-2)*B_tilde;
      if any((real(eig(P))<-0.0001)),
         disp('P is NOT positive semi-definite!')
         j_star_val=999;
      end
   end  % end of flag2
%  ************************************************************
end  % end of flag3
%  ************************************************************
```

B.2.17 mymodred.m

```
function [aa,bb,cc,dd]=mymodred(AA,BB,CC,DD,tol);
%function [aa,bb,cc,dd]=mymodred(AA,BB,CC,DD,tol);
%  October, 1997
```

```
%  Janet R. Grad
%  function to eliminate unobservable/uncontrollable states
%  using obalreal
[n1,n2]=size(CC);
[n3,n4]=size(DD);
%  siso
if n1==1 & n4==1,
   [AA,BB,CC,DD]=myminreal(AA,BB,CC,DD);
end
if nargin==4,
   tol=0.0001;
end
[AA_bal,BB_bal,CC_bal,g,p]=obalreal(AA,BB,CC);
gg=g/max(abs(g));
elim=find( abs(gg)<tol );
if elim==[],
   aa=AA_bal;  bb=BB_bal;  cc=CC_bal;  dd=DD;
else
   [aa,bb,cc,dd]=modred(AA_bal,BB_bal,CC_bal,DD,elim);
end
error_obalreal=2*sum(g(elim));
if error_obalreal>10,
   disp('Warning:  error_obalreal in mymodred')
   error_obalreal
end
```

B.2.18 myminreal.m

```
function [am,bm,cm,dm] = myminreal(a,b,c,d,tol)
%function [am,bm,cm,dm] = myminreal(a,b,c,d,tol)
%  Matlab function call minreal.m
[ns,nu] = size(b);
if nargin == 4
   tol = 10*ns*norm(a,1)*eps;
end
[am,bm,cm,t,k] = ctrbf(a,b,c,tol);
kk = sum(k);
nu = ns - kk;
nn = nu;
am = am(nu+1:ns,nu+1:ns);
bm = bm(nu+1:ns,:);
cm = cm(:,nu+1:ns);
ns = ns - nu;
if ns
   [am,bm,cm,t,k] = obsvf(am,bm,cm,tol);
   kk = sum(k);
   nu = ns - kk;
   nn = nn + nu;
```

```
   am = am(nu+1:ns,nu+1:ns);
   bm = bm(nu+1:ns,:);
   cm = cm(:,nu+1:ns);
end
dm = d;
```

Bibliography

[AM90] B.D.O. Anderson and J.B. Moore. *Optimal Control Linear Quadratic Methods*. Prentice-Hall, Inc., 1990.

[BBK89] S. Boyd, V. Balagrishnan, and P. Kabamba. A bisection method for computing the H_∞ norm of a transfer matrix and related problems. *Mathematics of Control, Signals, and Systems*, 2:207–219, 1989.

[BDS97] H.T. Banks, M.A. Demetriou, and R.C. Smith. Utilization of coupling effects in compensator design for structural acoustic systems. Preprint, 1997.

[BFSS91] H.T. Banks, W. Fang, R.J. Silcox, and R.C. Smith. Approximation methods for control of acoustic/structure models with piezoceramic actuators. *ICASE Report No. 91-88, Nasa Langley Research Center, Hampton, Virginia*, 1991.

[BI97] H.T. Banks and K. Ito. Approximation in LQR problems for infinite dimensional systems with unbounded input operators. *Journal of Mathematical Systems, Estimation, and Control*, 7(1):1–34, 1997.

[BIW91] H.T. Banks, K. Ito, and C. Wang. Exponentially stable approximations of weakly damped wave equations. *International Series of Numerical Mathematics, Birkhauser Verlag Basel*, 100:1–33, 1991.

[BK84] H.T. Banks and K. Kunisch. The linear regulator problem for parabolic systems. *SIAM Journal of Control and Optimization*, 22:684–698, 1984.

[BP89] J.A. Burns and G.H. Peichl. Open questions concerning approximation and control of infinite dimensional systems. Preprint, 1989.

[CD84] C-C. Chu and J.C. Doyle. On inner-outer and spectral factorizations. In *Proceeding of 23rd Conference on Decision and Control, Las Vegas, NV*, pages 1764–1765, December 1984.

[CP78] R.F. Curtain and A.J. Pritchard. *Infinite Dimensional Linear Systems Theory.* Springer-Verlag, 1978.

[Cur88] R.F. Curtain. Equivalence of input-output stability and exponential stability for infinite-dimensional systems. *Mathematical Systems Theory*, 21:19–48, 1988.

[CW89] R.F. Curtain and G. Weiss. Well-posedness of triples of operators (in the sense of linear systems theory). *International Series of Numerical Mathematics*, 91:41–59, 1989.

[CZ95] R.F. Curtain and H.J. Zwart. *An Introduction to Infinite-Dimensional Linear Systems Theory.* Springer-Verlag, 1995.

[DFT92] J.C. Doyle, B.A. Francis, and A.R. Tannenbaum. *Feedback Control Theory.* Maxwell Macmillan Canada, Toronto, 1992.

[DGKF89] J.C. Doyle, K. Glover, P.P. Khargonekar, and B.A. Francis. State-space solutions to standard H_2 and H_∞ control problems. *IEEE Transactions on Automatic Control*, 34(9):831–847, August 1989.

[Doa73a] P.E. Doak. Excitation, transmission and radiation of sound from source distributions in hard-walled ducts of finite length (I): The effects of duct cross-section geometry and source distribution space-time pattern. *Journal of Sound and Vibration*, 31(1):1–72, 1973.

[Doa73b] P.E. Doak. Excitation, transmission and radiation of sound from source distributions in hard-walled ducts of finite length (II): The effects of duct length. *Journal of Sound and Vibration*, 31(2):137–174, 1973.

[EN93] S.J. Elliott and P.A. Nelson. Active noise control. *IEEE Signal Processing Magazine*, 10(4):12–34, October 1993.

[Fra87] B.A. Francis. *A Course in H_∞ Control Theory, Lecture Notes in Control and Information Sciences.* Springer Verlag, 1987.

[FTZ86] C. Foias, A. Tannenbaum, and G Zames. Weighted sensitivity minimization for delay systems. *IEEE Transactions on Automatic Control*, 31(8):763–766, August 1986.

[FTZ87] C. Foias, A. Tannenbaum, and G. Zames. Sensitivity minimization for arbitrary SISO distributed plants. *Systems and Control Letters*, 8:189–195, 1987.

[GD88] K. Glover and J.C. Doyle. State-space formulae for all stabilizing controllers that satisfy an H_∞-norm bound and relations to risk sensitivity. *Systems and Control Letters*, 11:167–172, 1988.

[Gib79] J.S. Gibson. The Riccati integral equations for optimal control problems on Hilbert spaces. *SIAM J. Control Optim.*, 17:537–565, 1979.

[Gib83] J.S. Gibson. Linear quadratic optimal control of hereditary differential systems: Infinite dimensional Riccati equations and numerical approximations. *SIAM J. Control Optim.*, 21:95–139, 1983.

[HAV+96] J. Hong, J.C. Akers, R. Venugopal, M. Lee, A.G. Sparks, P.D. Washabaugh, and S. Bernstein. Modeling, identification, and feedback control of noise in an acoustic duct. *IEEE Transactions of Control Systems Technology*, 4(3):283–291, 1996.

[HB95] J. Hong and D.S. Bernstein. A comparison of fundamental properties of feedback and feedforward control: Bode integral constraints and spillover. In *Proceedings of Active 1995, Newport Beach, CA, USA*, pages 929–940, 1995.

[HR92] A.J. Hull and C.J. Radcliffe. Experimental verification of the nonself-adjoint state space duct model. *Transactions of the ASME*, 114:404–408, July 1992.

[HRMM90] A.J. Hull, C.J. Radcliffe, M. Miklavcic, and C.R. MacCluer. State space representation of the nonself-adjoint acoustic duct system. *Journal of Vibration and Acoustics*, 112:483–488, October 1990.

[HRS93] A.J. Hull, C.J. Radcliffe, and S.C. Southward. Global active noise control of a one-dimensional acoustic duct using a feedback controller. *Transactions of the ASME*, 115:488–494, September 1993.

[Hu95] J. Hu. Active sound attenuation in finite-length ducts using close-form transfer function models. *Journal of Dynamic Systems, Measurement, and Control*, 117:143–154, 1995.

[Hu96] J. Hu. Active noise cancellation in ducts using internal model-based control algorithms. *IEEE Transactions on Automatic Control*, 4(2), March 1996.

[IM98] K. Ito and K.A. Morris. An approximation theory of solutions to operator Riccati equations for H_∞ control. To appear, SIAM Journal on Control and Optimization, 1998.

[IT89] K. Ito and H.T. Tran. Linear quadratic optimal control problem for linear systems with unbounded input and output operators: numerical approximations. *International Series of Numerical Mathematics*, 91:171–195, 1989.

[Ito87] K. Ito. Strong convergence and convergence rates of approximating solutions for algebraic equations in Hilbert spaces. *Distributed Parameter Systems, Lecture Notes in Control and Information Sciences (F. Kappel, et al., eds), Berlin, Springer-Verlag*, 102:153–166, 1987.

[LRT93] D.K. Lindner, K.M. Reichard, and L.M. Tarkenton. Zeros of modal models of flexible structures. *IEEE Transactions on Automatic Control*, 38(9):1384–1388, September 1993.

[LST88] T.A. Lypchuk, M.C. Smith, and A. Tannenbaum. Weighted sensitivity minimization: General plants in H_∞ and rational weights. *Linear Algebra and Its Applications*, 109:71–90, 1988.

[Mac89] J.M. Maciejowski. *Multivariable Feedback Design.* Addison-Wesley Publishers Ltd., 1989.

[Mat94] The MathWorks. Matlab, Version 4.2c, 1994.

[Moo81] B.C. Moore. Principal component analysis in linear system: controllability, observability, and model reduction. *IEEE Transactions on Automatic Control*, 26:17–31, September 1981.

[Mor96] K.A. Morris. Design of finite-dimensional controllers for infinite-dimensional systems by approximation. *Journal of Mathematical Systems, Estimation, and Control*, 6(2):151–180, 1996.

[Mor97a] K.A. Morris. Noise reduction achievable by point control. To appear, ASME Journal of Dynamic Systems, Measurement, and Control, 1997.

[Mor97b] K.A. Morris. Personal communication with, 1997.

[MRH91] C.R. MacCluer, C.J. Radcliffe, and A.J. Hull. Diagonalizing acoustic models. *SIAM Journal of Applied Mathematics*, 51(4):1006–1010, August 1991.

[NE92] P.A. Nelson and S.J. Elliott. *Active Control of Sound.* Academic Press, 1992.

[NS82] A.W. Naylor and G.R. Sell. *Linear Operator Theory in Engineering and Science.* Springer-Verlag, 1982.

[Ö93] H. Özbay. H_∞ optimal controller design for a class of distributed parameter systems. *International Journal of Control*, 58(4):739–782, 1993.

[Paz83] A. Pazy. *Semigroups of Linear Operators and Applications to Partial Differential Equations.* Springer-Verlag, 1983.

[PS87] A.J. Pritchard and D. Salamon. The linear quadratic optimal control problem for infinite dimensional systems with unbounded input and output operators. *SIAM J. Control Optim.*, 25:121–144, 1987.

[PW97] G.H. Peichl and C. Wang. On uniform stabilizability and the margin of stabilizability. *Journal of Mathematical Systems, Estimation, and Control*, 7(3):277–304, 1997.

[RD90] A.A. Rodriguez and M.A. Dahleh. Weighted H_∞ optimization for stable infinite dimensional systems using finite dimensional techniques. In *Proceeding of 29th Conference on Decision and Control, Honolulu, Hawaii*, pages 1814–1820, December 1990.

[Rou85] A. Roure. Self-adaptive broadband active sound control system. *Journal of Sound and Vibration*, 101(3):429–441, 1985.

[Sal84] D. Salamon. *Control and Observation of Neutral Systems.* Pitman, Boston, 1984.

[Sal87] D. Salamon. Infinite-dimensional linear systems with unbounded control and observation: A functional analytic approach. *Transactions of the American Mathematical Society*, 300:383–431, 1987.

[Sar67] D. Sarason. Generalized interpolation in H_∞. *Transactions of the American Mathematical Society*, 127:179–203, 1967.

[Set71] W.W. Seto. *Theory and Problems of Acoustics.* McGraw-Hill, 1971.

[Smi90] M.C. Smith. Well-posedness of H_∞ optimal control problems. *SIAM Journal of Control and Optimization*, 28:342–358, 1990.

[Sof97] Waterloo Maple Software. Maple V, Release 3, 1997.

[SR88] C.E. Spiekermann and C.J. Radcliffe. Decomposing one-dimensional acoustic pressure response into propagating and standing waves. *Journal of the Acoustic Society of America*, 84(4):1536–1541, October 1988.

[Tan92] A. Tannenbaum. Frequency domain methods for the H_∞-optimization of distributed systems. In *Analysis and Optimization of Systems: State and Frequency Domain Approaches for Infinite-Dimensional Systems. Lecture Notes in Control and Information Sciences*, pages 242–278. Proceedings of the 10th International Conference, Sophia-Antipolis, France, June 1992.

[TL92] M.O. Tokhi and R.R. Leitch. *Active Noise Control.* Oxford University Press, 1992.

[Vid85] M. Vidyasagar. *Control System Synthesis.* The MIT Press, 1985.

[Wan95] C. Wang. Linear quadratic optimal control of a wave equation with boundary damping and pointwise control input. *Journal of Mathematical Analysis and Applications*, 192(2):562–578, 1995.

[YT92] B. Yang and C.A. Tan. Transfer functions of one-dimensional distributed parameter systems. *Journal of Applied Mechanics*, 59:1009–1014, 1992.

[Zab92] J. Zabczyk. *Mathematical Control Theory: An Introduction.* Birkhäuser, 1992.

[ZK87] K. Zhou and P.P. Khargonekar. On the weighted sensitivity minimization problem for delay systems. *Systems and Control Letters*, 8:307–312, 1987.

IMAGE EVALUATION
TEST TARGET (QA-3)

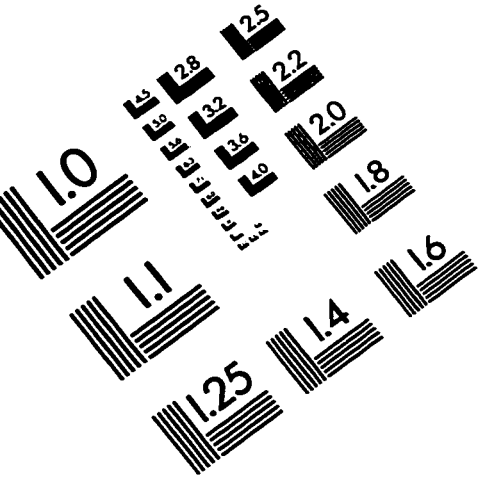

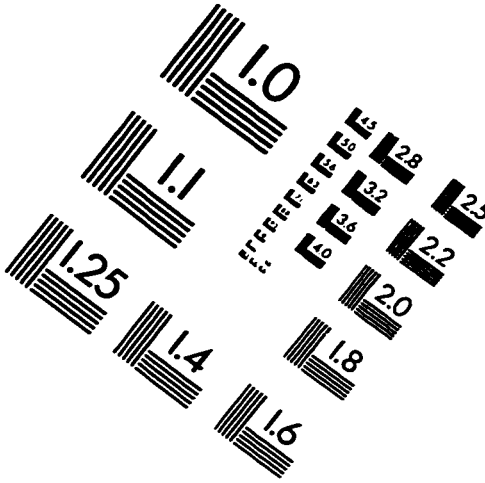

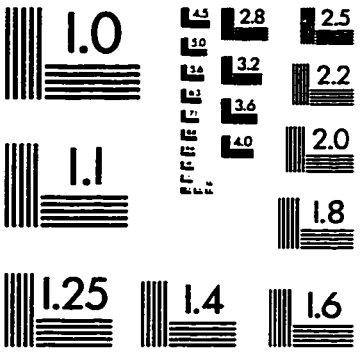

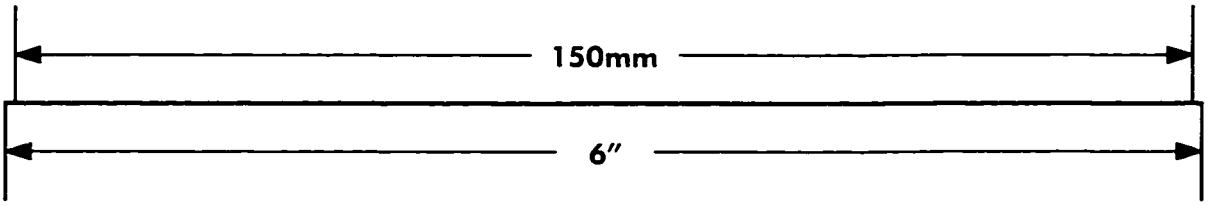

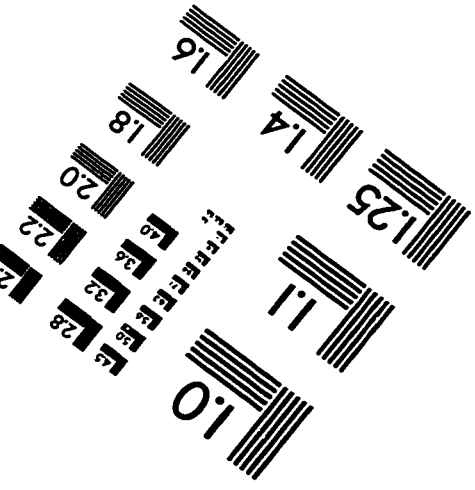

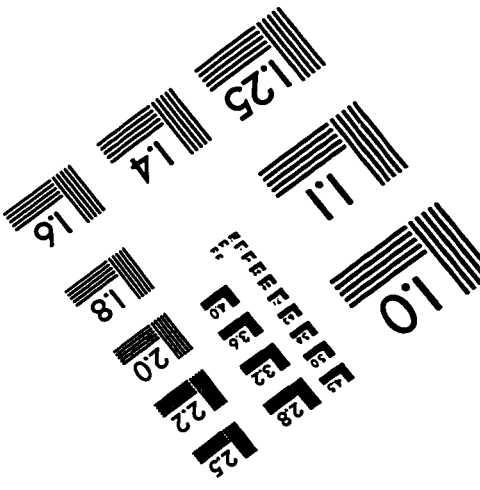

APPLIED IMAGE, Inc
1653 East Main Street
Rochester, NY 14609 USA
Phone: 716/482-0300
Fax: 716/288-5989